



Chaitanya R. Tabib, MSc

Biochemical studies on the mechanism of bacterial
bioluminescence *in vivo* and *in vitro*

DOCTORAL THESIS

to achieve the university degree of

Doktor der Naturwissenschaften

submitted to

Graz University of Technology

Supervisor

Univ.-Prof. Mag. rer nat. Dr. rer. nat. Peter Macheroux

Institute of Biochemistry

Graz, December 2016

AFFIDAVIT

I declare that I have authored this thesis independently, that I have not used other than the declared sources/resources, and that I have explicitly indicated all material which has been quoted either literally or by content from the sources used. The text document uploaded to TUGRAZonline is identical to the present doctoral thesis.

Date

Signature

Dedicated to

My Grandparents... I miss you

Acknowledgements

First and foremost, I would like to thank my supervisor Prof. Dr. Peter Macheroux for the trust he had in me, encouraging me to conduct this study and giving his expert advises at all times needed. He has been very nice to me and I appreciate his attempts trying to understand and help the students both professionally and personally.

My thesis committee members Prof. Dr. Karl Gruber, Prof. Dr. Rolf Breinbauer and Prof. Dr. Ellen Zechner deserve special thanks for taking their time to talk to me, every time I wanted their advice. Their constant guidance, knowledge and support kept me going through the ups and downs of this project.

I would like to express my grateful appreciation to Dr. Karin Athenstaedt for her time, to be the chair person for my PhD defense.

At some part of my stay in the institute, I've interacted with each and every faculty member of this institute (Prof. Daum, Prof. Hermetter, Prof. Murkovic, Asst. Prof. Winkler and Dr. Straganz) and I sincerely thank each one of them for their inspiration and good wishes.

My stay in Graz wouldn't have been so meaningful unless I had met this person. My 1st friend from Graz, also 1st from the AGM group and the best mentor I have ever met, Dr. Silvia Wallner. I'm deeply indebted to you for grooming me in the best possible way. It is probably impossible to enumerate all the things which I should thank you for. I would also like to thank your whole family for making me feel so welcomed whenever we met.

I have been very lucky to be part of AGM group. I have no words to thank all my past and present lab mates... Alexandra, Venu, Domen, Thomas, Tanja, Pez, Bastian, Johannes, Majd, Sami, Chanakan, Barbara, Stefan and Geoffrey for their valuable discussions and providing nice atmosphere to work in our lab (I know coffee time is 2 pm Majd.. I will be there.. :P).

I want to thank my "best friends for life" Emilia, Karin, Shalinee and Wolfi whose company and support will be cherished throughout my life. 2016 is the best year I have ever had and it's all because of you guys 😊 😊 .. Special thanks to Marina and her mother for the wonderful evenings together.. (I know how to make a cake now.. he he)

I would like to thank Eveline, for all the work done together and for being such a nice friend. I also wish you a very good success ($\text{Career}_{\text{max}} = \text{goodluck} * 490 \text{ nm}$) in the upcoming Bioluminescence project.

I would also like to thank people from AGD group, Martina, Isa, Heinz, Birgit, Ariane, Andreas, Claudia and Lisa for the wonderful time spent together like at Institute cookie party or at International lunch or a hello with a smile whenever we met in the corridors.

Like a torch cannot run without the batteries, similarly the lab cannot run without Rosemarie, Eva and Elfi.. You need very special thanks for taking care of the lab matters. Your ever-approachable and cool nature is deeply appreciated.

Thank you Annemarie and Kristina for managing every paper work concerning DK selection, my VISA, contracts, course registrations and making it possible for me to be a part of DK. I would also like to thank the “DK Molecular Enzymology PhD program” for giving me the opportunity to pursue my PhD.

I would like to thank both my super motivated students: Andrea and Corina. It was a pleasure to supervise you both and I wish you both great luck for your future endeavors.

I would also like to thank my previous supervisor Prof. D N Rao, my Master thesis supervisor Dr. Sunil Morey, my Bachelors mentor Dr. Anuradha Bhat and my friend Dr. Leelaram for their friendly email chats throughout my PhD. Thank you for keeping in touch.

Many thanks to Vinod, Nitesh, Raj, Govind, Akshada, Priya and Rajni for keeping the Indian spirits alive and calling me on all Indian festival occasions. It was great time spent together with you guys. Thanks to Dr. Lingaraju for helping me settle in Graz in my beginning days here.

Some people are always first when I want to share my feelings. Thanks to my best buddies of life Govindkumar, Farooq, Jere, Dindur and Sachin. Thanks for tolerating me at all time (actually u guys deserve me.. ha ha).

Thanks to my loving brother Chinmaya and his fiancée Shwetha for your love and support at all times. Thanks for being a “best friend” cum brother always.

Heartfelt gratitude to my brother-in-law Yogesh and his wife Vasundhara for being so lovely and supportive from the time I have known you. Waiting to see you soon.

Thanks to all Kurandwads and adjoining family members for your love and affection from my childhood till today and thanks for nourishing me like a little boy.. :P

My dearest appreciation goes to my beloved family (Tabib pariwar) and in-laws (the Kumbhakonams) for being so passionate, supportive and understanding. Without you all, it would have been impossible for me to finish this journey. My mom actually thought I would never pass out of school.. he he

Last but the best, Savitri – A friend, roommate and companion. I’m not sure if my stay in Graz would be so cheerful if I hadn’t married you and spent these 4 years here with you. I’m not sure if achieving my PhD would be so exciting if you were not here beside me to celebrate it. Thank you for being so lovely and making these years memorable forever.

Chai...

Abstract

Bioluminescence is the production of light by living organisms using enzyme-catalyzed reactions as a key factor to release the energy. Generally, the bioluminescent reaction in bacteria is catalyzed by a luciferase, an enzyme employing FMN as a redox cofactor to drive the mono-oxygenation of an aldehyde substrate to its corresponding acid product. The free energy released during the oxidation of the aldehyde gives rise to an excited state FMN-4a-hydroxide, which in turn serves as the light emitting molecule luciferin.

The genes responsible for the light production are present as an operon, *luxCDABEG*: *luxA* and *luxB* encode the α and β subunits of luciferase; *luxC*, *luxD*, and *luxE* specify the enzymatic components of a fatty acid reductase complex; and *luxG* encodes a flavin reductase. Many strains of *Photobacterium* also carry an extra gene, termed *luxF*, having a lux operon gene order of *luxCDABFEG*. Sequence similarity to *luxB* suggests that *luxF* has evolved by gene duplication, however, its role in bacterial bioluminescence is obscure. The hypothesized function of LuxF is to bind 6-(3'-(*R*)-myristyl)-FMN (myrFMN, a possible side product of the luciferase reaction), which otherwise is thought to bind the active site of luciferase sufficiently tight thus leading to inhibition of the bioluminescence reaction.

The generation of myrFMN in the *Photobacterium* is a largely unexplored phenomenon. In the present study, we have developed a method to isolate myrFMN from *Photobacterium leiognathi* S1. Using isolated and purified myrFMN we could show that binding to apo-LuxF ($K_d = 80$ nM) was fifty times tighter than to luciferase ($K_d = 4$ μ M) by using isothermal titration calorimetry. In addition, we exploited this tight binding of myrFMN to recombinant apo-LuxF, to explore the occurrence of myrFMN in various bioluminescent bacterial strains (*luxF*⁺ and *luxF*⁻) in *Photobacterium*. This analysis showed that myrFMN is present in all photobacterial strains tested, suggesting that myrFMN production is independent of the occurrence of *luxF*. Similarly, finding of trace amounts of myrFMN in *Vibrio* and *Aliivibrio* indicates that myrFMN generation is not restricted only to *Photobacterium*.

To study the effect of myrFMN on the bioluminescence yield, an inhibition assay was performed using single turnover reactions. With increasing myrFMN concentration the total light yield went down dramatically. Addition of LuxF helped in scavenging the myrFMN to

substantial levels bringing back the lost activity of luciferase, thereby confirming our hypothesis that LuxF serves as a scavenger of myrFMN in bioluminescent bacteria. The creation of *luxF*, presumably by gene duplication of *luxB*, was an important evolutionary invention that provided an enormous advantage over other bioluminescent bacteria. Finally, in order to investigate the formation of myrFMN and to analyze the role of luciferase and LuxF in this process, we established a cofactor regeneration enzyme-catalyzed cascade reaction that supports the luciferase reaction for up to 72 hours. This approach enabled to unambiguously demonstrate by UV-Vis absorption spectroscopy and mass spectrometry that myrFMN is generated in the bacterial bioluminescent reaction. Based on this finding we have postulated a reaction mechanism for myrFMN generation that is compatible with the proposed radical mechanism for the luciferase reaction (CIEEL mechanism).

Zusammenfassung

Biolumineszenz ist die Produktion von Licht durch lebende Organismen. In Bakterien ist in die Biolumineszenzreaktion eine Luziferase, ein FMN abhängiges Enzym, involviert, welches die Monooxygenierung eines Aldehyds zur entsprechenden Säure katalysiert. Die während der Oxidation freiwerdende Energie führt zur Bildung eines angeregten FMN-4a-Hydroxids, das sogenannte Luziferin, welches bei Relaxation Licht emittiert.

Die Gene, die für die Biolumineszenz verantwortlich sind, finden sich auf einem Operon, *luxCDABEG*. *luxA* und *luxB* stehen dabei für die α und β Untereinheiten der Luziferase. *luxC*, *luxD*, und *luxE* bilden die Komponenten eines Fettsäurereduktasekomplexes und *luxG* codiert für eine Flavinreduktase. In vielen Vertretern der Gattung *Photobacterium* findet sich außerdem ein zusätzliches Gen, *luxF*, mit einer Operonanordnung von *luxCDABFEG*. Sequenzähnlichkeiten zu *luxB* deuten darauf hin, dass *luxF* durch Genduplizierung entstanden ist, dessen Rolle für die bakterielle Lumineszenz ist jedoch weitgehend unklar. Vermutet wird, dass LuxF 6-(3'-(R)-myristyl)-FMN (myrFMN, ein Nebenprodukt und Inhibitor der Luziferasereaktion) bindet und so von der Active Site der Luziferase fernhält.

Die Bildung von myrFMN in Photobakterien ist ein großteils unerforschtes Phänomen. In dieser Studie wurde eine Methode zur Isolierung von myrFMN aus *Photobacterium leiognathi* S1 entwickelt. Die Bindung von isoliertem und gereinigtem myrFMN zu apo-LuxF ($K_d = 80$ nM) war in Bindungsstudien ca. 50 Mal stärker als zur Luziferase ($K_d = 4$ μ M). Diese starke Bindung wurde ausgenutzt um das Vorkommen von myrFMN in verschiedenen biolumineszenten Photobakterienstämmen (*luxF*⁺ and *luxF*⁻) zu untersuchen. Dabei wurde myrFMN in allen getesteten Stämmen gefunden, was nahe legt, dass die Produktion von myrFMN nicht mit dem Vorhandensein von *luxF* gekoppelt ist. Außerdem wurden Spuren von myrFMN auch in *Vibrio* und *Aliivibrio* festgestellt, was darauf hinweist, dass die myrFMN Bildung kein alleiniges Phänomen der Gattung *Photobacterium* darstellt.

Um den Einfluss von myrFMN auf die Biolumineszenzausbeute zu untersuchen wurde ein Inhibitionsassay mit Single Turnover Reaktionen entwickelt. Dabei ging die totale Lichtausbeute mit steigender myrFMN-Konzentration drastisch zurück. Die Zugabe von LuxF zu den Reaktionsansätzen führte zur Bindung von myrFMN an LuxF und zur Wiederherstellung der Luziferaseaktivität, was die von uns vorgeschlagene Funktion von LuxF als „Fänger“ von myrFMN in biolumineszenten Bakterien bestätigt. Die Bildung von *luxF* durch Genduplizierung

war eine wichtige evolutionäre Erfindung, die den Trägern einen enormen Vorteil gegenüber anderen biolumineszenten Bakterien verschaffte.

Um die Bildung von myrFMN und die Rollen von Luziferase und LuxF in diesem Prozess genauer zu untersuchen, wurde ein Multiturnover Assay mit Kofaktorregenerierung entwickelt bei dem die Luziferasereaktion für bis zu 72 Stunden aufrecht gehalten werden konnte. Diese Experimente zeigten eindeutig, dass myrFMN während der bakteriellen Biolumineszenzreaktion gebildet wird. Basierend auf diesen Ergebnissen schlagen wir einen Mechanismus zur Bildung von myrFMN vor, welcher mit dem radikalischen Mechanismus für die Luziferasereaktion (CIEEL Mechanismus) vereinbar ist.

Table of Contents

Affidavit.....	II
Acknowledgements.....	IV
Abstract.....	VI
Zusammenfassung.....	VIII
Introduction.....	1
1. Bioluminescence.....	2
1.1. History.....	2
1.2. Evolution and Distribution.....	2
1.3. Function.....	3
1.4. Application.....	3
1.5. Basic chemical reaction.....	5
1.6. The luciferin.....	5
1.7. Flavin reactivity.....	7
2. Bacterial Bioluminescence.....	8
2.1. Genetic organization.....	8
2.2. Reaction mechanism.....	11
2.3. Bacterial luciferase – the enzyme that catalyzes the light production.....	13
2.3.1. Analysis of the <i>Vibrio</i> luciferase structure.....	14
2.3.2. Comparative analysis of different luciferases (based on the data from this thesis)	18
3. Supplementary data.....	19
4. References.....	21
5. Aim of the thesis.....	24
6. Thesis briefing.....	24
7. Presentations.....	26
Chapter 1.....	27
Structural and biochemical properties of LuxF from <i>Photobacterial leiognathi</i>	28
Chapter 2.....	38
Synthesis of α , β -unsaturated aldehydes as potential substrates for bacterial luciferases.....	39
2.1 Abstract.....	40
2.2 Introduction.....	40
2.3 Materials and methods.....	43
2.3.1 General experimental information.....	43
2.3.2 General procedure GP-1 (Synthesis of α , β -unsaturated ethyl esters).....	44
2.3.3 General procedure GP-2 (Synthesis of allyl alcohols).....	45

2.3.4	General procedure GP-3 (Synthesis of α , β -unsaturated aldehydes).....	45
2.3.5	Ethyl (<i>E</i>)-oct-2-enoate (3d).....	45
2.3.6	Ethyl (<i>E</i>)-dec-2-enoate (3c).....	46
2.3.7	Ethyl (<i>E</i>)-dodec-2-enoate (3b)	46
2.3.8	Ethyl (<i>E</i>)-tetradec-2-enoate (3a)	47
2.3.9	(<i>E</i>)-Oct-2-en-1-ol (4d)	47
2.3.10	(<i>E</i>)-Dec-2-en-1-ol (4c)	48
2.3.11	(<i>E</i>)-Dodec-2-en-1-ol (4b)	48
2.3.12	(<i>E</i>)-Tetradec-2-en-1-ol (4a)	48
2.3.13	(<i>E</i>)-Oct-2-enal (5d)	49
2.3.14	(<i>E</i>)-Dec-2-enal (5c)	49
2.3.15	(<i>E</i>)-Dodec-2-enal (5b)	50
2.3.16	(<i>E</i>)-tetradec-2-enal (5a)	50
2.3.17	Instrumentation.....	51
2.3.18	Design, expression and purification of recombinant His-tagged proteins.....	51
2.3.19	<i>In vitro</i> assay.....	52
2.3.20	Molecular docking.....	53
2.4	Results.....	54
2.5	Discussion.....	58
2.6	Conclusion.....	61
2.7	Acknowledgements.....	61
2.8	References.....	62
2.9	Highlights.....	63
2.10	Supplementary data.....	64
2.11	Graphical abstract.....	80
Chapter 3	81
	Generation of myristylated FMN by luciferase supports a radical mechanism for bacterial bioluminescence.....	82
3.1	Abstract.....	83
3.2	Introduction.....	83
3.3	Experimental procedures.....	85
3.3.1	Chemicals.....	85
3.3.2	Instrumentation.....	85
3.3.3	Bioluminescent bacterial strains.....	87
3.3.4	Cloning, expression and purification of various proteins.....	87
3.3.5	Analysis of bacterial strains for light emission vs myrFMN content.....	88
3.3.6	Inhibition assay.....	88
3.3.7	<i>In vitro</i> multiple turnover reaction.....	89
3.4	Results.....	91
3.4.1	Analysis of bacterial strains for light emission and myrFMN content.....	91

3.4.2	Inhibition of luciferase by myrFMN.....	92
3.4.3	<i>In vitro</i> multiple turnover reaction.....	92
3.5	Discussion.....	94
3.5.1	Proposed mechanism for myrFMN formation.....	95
3.6	References.....	97
3.7	Acknowledgements.....	99
3.8	Author contributions.....	99
3.9	Figure legends.....	100
3.10	Scheme legends.....	101
3.11	Figures.....	103
3.12	Schemes.....	107
3.13	Supplementary data.....	109
3.14	Graphical abstract.....	115
Chapter 4	116
	Mutagenic study of cysteine residues on the structural stability and enzymatic behavior of bacterial luciferase.....	117
4.1	Abstract.....	118
4.2	Introduction.....	119
4.2.1	Homology model.....	120
4.3	Materials and methods.....	121
4.3.1	Cloning and expression of luciferase variants.....	121
4.3.2	Matrix-assisted laser desorption/ionization time-of-flight mass spectrometry (MALDI-TOF MS)	122
4.3.3	Thermofluor stability check.....	122
4.3.4	Enzyme activity assay.....	123
4.4	Results and discussion.....	123
4.4.1	Cloning and expression of luciferase variants.....	123
4.4.2	Verification of the luciferases with MALDI-TOF MS.....	125
4.4.3	Determination of the T _m of LuxAB WT and variant LuxAB with Thermofluor experiments.....	125
4.4.4	Determining the activity of LuxAB WT and variants by measuring the bioluminescence.....	129
4.5	Conclusions.....	130
4.6	Supplementary data.....	131
4.7	References.....	135
Chapter 5	136
	Generation of <i>luxAB</i> , <i>luxF</i> and <i>luxABF</i> knockouts in photobacterial strains.....	137
5.1	Introduction.....	138
5.1.1	Type IV secretion system (T4SSs)	139

5.2 Aim of the study.....	140
5.3 Experiments and setups.....	141
5.3.1 Preparation of constructs in conjugative plasmids.....	141
5.3.2 Plasmids and strains used.....	142
5.3.3 Principle underlying usage of these plasmid/strains.....	142
5.4 Results.....	144
5.4.1 Different conditions tested.....	144
5.5 Conclusion.....	145
5.5.1 Possible reasons for DNA not being taken up by <i>Photobacteria</i>	145
5.5.2 Alternative experimental approaches to investigate production of myrFMN....	145
5.6 References.....	154
5.7 Supplementary figures.....	155
Appendix.....	157
Curriculum Vitae.....	160

Introduction

1. Bioluminescence

1.1 History

It has been 100 years since “Bioluminescence” was described in the scientific literature for the first time; it was then called “The mechanism of light production by animals” by E N Harvey in 1916 (Harvey, 1916). In this paper, Harvey points out that an organic catalyst, “an enzyme”, is involved in the light production when supplied with water containing oxygen. He gave the credit of discovering the luciferase/luciferin system to Professor Raphael Dubois at the University of Lyon in France, for a work conducted as early as 1884, whom he called the author of the “luciferin-luciferase theory”. The exact chemical nature of the luciferin was still unknown, however, a concept on how to tackle the problem had been outlined. At that time it was unclear whether the luciferin and luciferase of all forms of bioluminescence found in nature are identical or different. In order to analyse the chemical nature of these components, methods to extract a sufficient quantity of the luminescent material were required. Harvey believed that the problem of bioluminescence was solved in a broader scenario, however the minute details would take some time to be resolved satisfactorily. As anticipated by Harvey, scientists across the globe are still trying to understand the system and its mechanism. The fact that “bioluminescence” is the production of “cold-light” by living organisms without the requirement of any external energy stimuli, makes this natural process a very interesting chemical reaction from a scientific perspective.

1.2 Evolution and Distribution

Bioluminescence has evolved several times in many distinct species, ranging from terrestrial to aquatic systems, but the major of light producing organisms live in a marine environment. Examples of bioluminescent organisms in a terrestrial environment comprise insect larvae, limpets, fireflies, beetles, insects, fungi, centipedes, millipedes, snails and earthworms; and a large range of marine organisms from bacteria (+ symbionts), protists, squids to fishes. Interestingly, one species in a genus may be luminous but another closely related one is not, suggesting that apparently there is no easy explanation for the distribution of luminescence. It is also noteworthy to observe that bioluminescence has not evolved or spread to higher eukaryotic systems like plants, birds, amphibians and mammals. The occurrence of

bioluminescent species in marine environment can be rationalized in part by the permanent darkness in the deep sea (below ca. 500 m) in the resulting utility of light production for a plethora of ecological functions, such as communication and predation (Haddock *et al.*, 2010; Lee, 1989).

1.3 Function

The functions of bioluminescence range from communication to predator-prey interactions and reproduction (Figure 1). In some cases like fungi, research is ongoing to deduce the role of bioluminescence. The concept of “quorum sensing” is an excellent example for bacterial communication via chemical auto-induction. Bioluminescence is also exploited by a wide range of higher order animals like fish and squid in a symbiotic manner. The light production is either controlled by the host nervous system (produced on stimulation as flashes, typically of 0.1-1 second duration) or could be continuously emitted (like in bacteria), depending on the requirement of the organism to perform the specific function (Haddock *et al.*, 2010). Therefore, bioluminescence adapted to acquire and evolve to functions in ways advantageous to the species that possesses it.

1.4 Application

The property of production of “cold-light” during bioluminescence has been exploited by researchers for analytical tools in various scientific applications. For example, the firefly luciferase requires adenosine-5'-triphosphate (ATP) for bioluminescence and thus this reaction is used for the detection of ATP in various systems (Thore *et al.*, 1983). Similarly, luminescent dinoflagellates are sensitive to toxins and thus are used as biosensors (Lapota *et al.*, 2007). Finally the fluorescence of photoproteins, such as the ‘aequorins’ are used to track the localization and behaviour of any partner protein (Shimomura *et al.*, 1962). The outstanding stability and fluorescent properties of the green fluorescent protein (GFP) makes it a popular tool for studying cell and sub-cellular processes without any requirement of external substrate feeding (Zimmer, 2002).

DEFENSE		Startle	Dinoflagellates, squid, stern-chaser myctophid
		Counterillumination	Many: crustaceans, fish, squid
		Misdirection: smoke screen	Many: crustaceans, polychaetes, scyphozoans, chaetognaths, squids, tube-shoulder fishes, ctenophores, siphonophores, larvaceans?
		Distractive body parts	<i>Octopoteuthis</i> squid, brittle stars, polychaetes, siphonophores
		Burglar alarm	Dinoflagellates, jellies, others?
		Sacrificial tag	Pelagic sea cucumbers, jellies, polychaetes
		Warning coloration (deter settlers)	Jellies, brittle stars? (tube worms, clams)
OFFENSE		Lure prey or attract host (bacteria)	Anglerfishes, siphonophores, cookie cutter shark, squid?
		Lure with external light (evaluate habitat?)	Sperm whale? megamouth shark?
		Stun or confuse prey	Squid, headlamp myctophid?
		Illuminate prey	Flashlight fish, dragonfishes
		Mate attraction/recognition (swarming cue)	Ostracods, <i>Japetella</i> octopus? lanternfish, flashlight fish, anglerfish? syllid polychaetes, others?
	 Flash  Glow  Prey  Predator  2° Predator		

*Figure and legend adapted from: Haddock, *et al.*, 2010.

Figure 1: Schematic diagram showing the functions of bioluminescence. Marine luminescence can be used for defence (blue), offense (magenta), and intraspecific communication (grey). The organisms thought to benefit from these functions are listed to the right. Some animals are known to use their luminescence in two, three, or even four different roles.

1.5 Basic chemical reaction

Bioluminescence is being studied since over a century and many aspects were determined on the molecular level of the reaction mechanism and the intermediates involved in different bioluminescent systems were characterised. One thing common to all bioluminescent reactions is the requirement of a substrate or cofactor that acts as the so called “luciferin” (Latin *Lucifer* means "light-bearer"), which typically contains an organic aromatic compound. This luciferin undergoes an enzyme-catalysed oxidation leading to the population of an excited state intermediate, which then emits light in order to relax to its ground state. Accordingly, the enzyme that catalyses this reaction is called the “luciferase”. Bacterial bioluminescence is one of the well-studied examples (Bergner *et al.*, 2015).

1.6 The luciferin

Luciferin can be described as an organic molecule that is present in all luminous organisms. A variety of molecules can serve as luciferin. Thus far, nine luciferins (for different luciferases) have been characterised as shown in Figure 2 (Kaskova, *et al.*, 2016). The luciferins may also be produced by nonluminous organisms maybe as a part of their regular metabolic pathways. Thus luciferins are relatively easy to obtain exogenously (Haddock *et al.*, 2010).

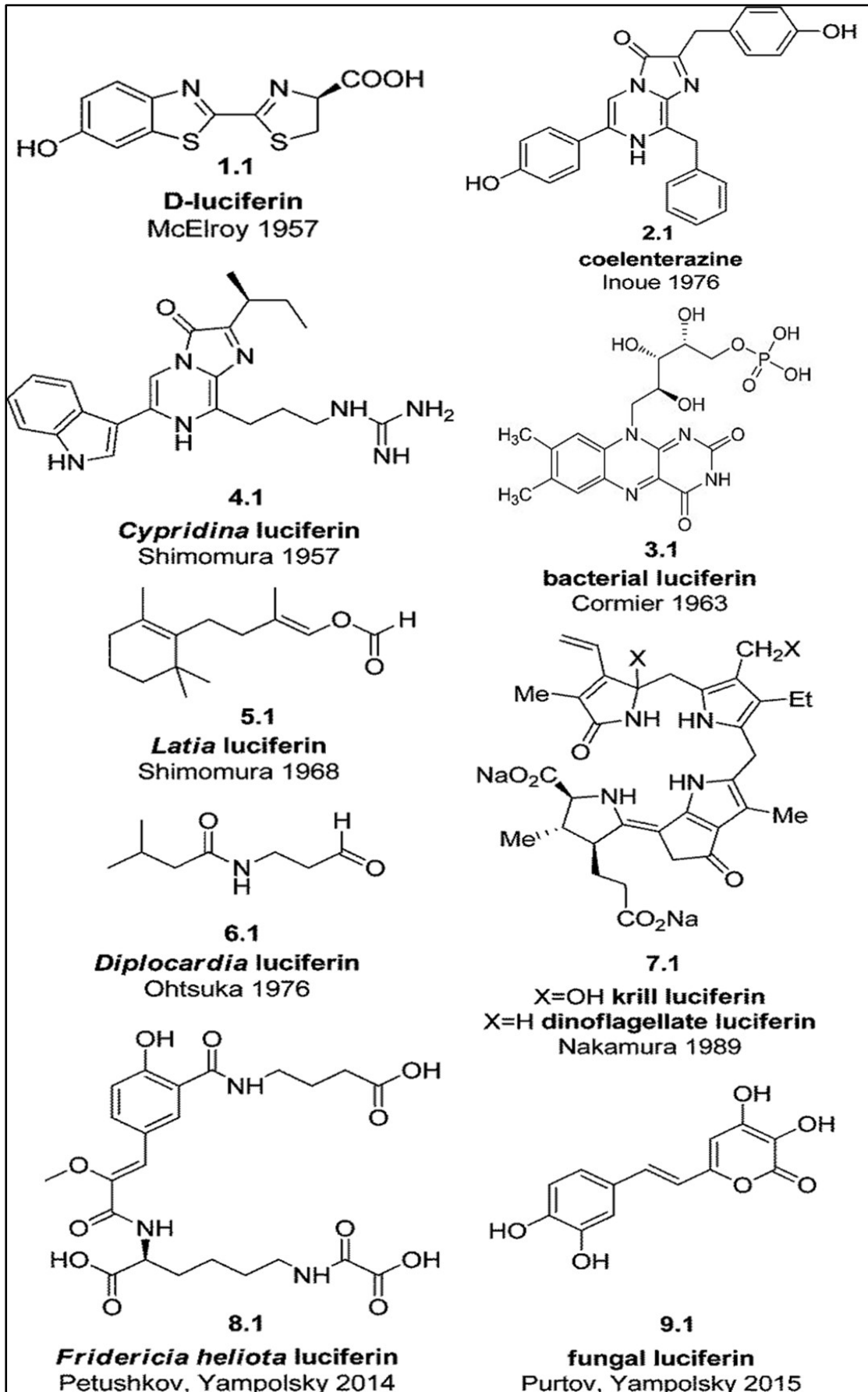


*figure and legend adapted and modified from Kaskova, *et al.*, 2016

Figure 2: Diversity, discovery and chemical structures of nine known natural luciferins.

1.7 Flavin reactivity

The latin word *flavus* means yellow, and thus the name flavin. Vitamin B2 or riboflavin synthesized by bacteria and plants, acts as the main precursor for the production of two cofactor units, flavin mononucleotide (FMN) and flavin adenine dinucleotide (FAD). The basic structure contains the 7,8-dimethylisoalloxazine ring as shown in Figure 3. In flavin catalyzed reactions, FAD is utilised 75% of times and FMN the rest 25%, riboflavin as such has never been reported acting directly in catalysis (Macheroux *et al.*, 2011).

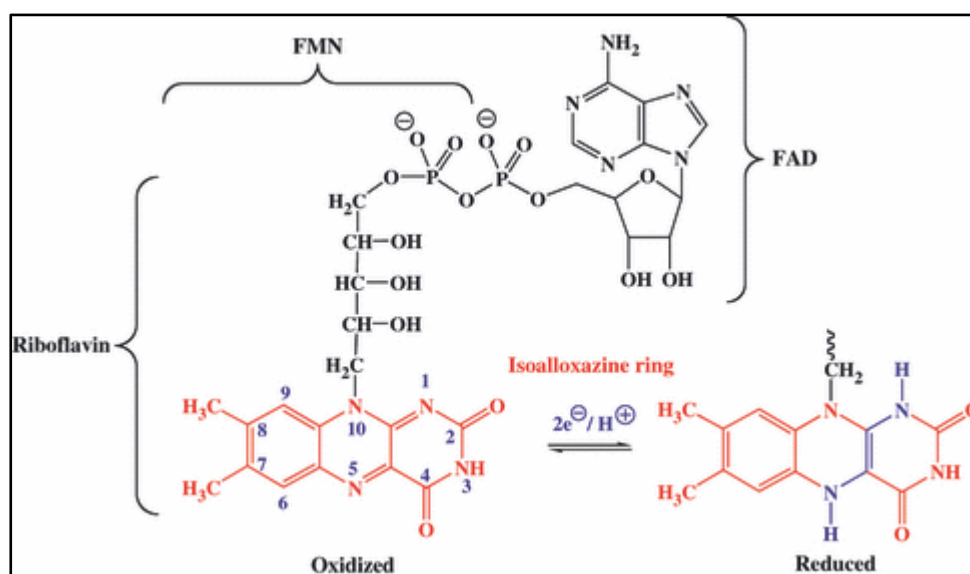


*figure and legend adapted from: Macheroux, *et al.*, 2011.

Figure 3: Structure of riboflavin and its derivatives FMN and FAD. The numbering of the redox-active isoalloxazine ring and the corresponding oxidized and fully reduced form of the ring system is shown.

The tricyclic heteronuclear organic ring acts as the main functional moiety when catalysing the redox reactions. The N5-C4a locus of the isoalloxazine ring, not only acts as the hot spot position for the electron exchange but also plays a role in covalent adduct formation. This property is crucial for the unique reactivity and versatile redox chemistry of the flavin cofactor. Under anoxic conditions (in the absence of oxygen), flavins can be reduced to either the semiquinone (one electron reduced) or hydroquinone (two electron reduced) redox state (Teufel *et al.*, 2016). These redox states also exist in different protonation forms depending on the existing pH environment.

2. Bacterial Bioluminescence

The luminous bacteria are not so different from non-luminescent bacteria, except for their capacity to produce light. Bacterial bioluminescence has been known as early as 1875, when Pflüger and Boyle realised that bacteria are responsible for the light emission by certain marine fish. Equally, they concluded that this process requires oxygen (air) (Dunlap, 2014). All known luminous bacterial species studied so far use the same “luciferase-luciferin” enzymatic pathway for light production. Bioluminescent bacteria, which carry the genes for luminescence (the *lux* genes), are all known to be gram-negative and belong to the group of *Gammaproteobacteria*. The most studied genera of luminous bacteria are *Aliivibrio*, *Vibrio*, *Photobacterium* and *Shewanella*, all of them being marine bacteria. The species of these bacteria are distributed from free-floating to surface associated or symbionts (Dunlap, 2014).

2.1 Genetic organization

The genetic loci, regulation and involvement of various proteins responsible in this reaction have been studied since 1991 (Meighen, 1991). The proteins involved in bacterial bioluminescence are encoded by the so called ‘*lux*’ genes. Different bacterial strains have between 5 – 8 genes, organised as a single operon called the ‘*lux* operon’. The core *lux* genes are encoded in the operon in the order *luxCDABEG*. Figure 4 provides an overview of the different organization of *lux* operons in various bacterial strains.

The *luxI* gene encodes an autoinducer protein. This protein produces a basal level of an inducer molecule, 3-oxohexanoyl-L-homoserine lactone. With increasing cell density, the inducer molecule accumulates until a certain threshold is reached. Once the threshold concentration is reached, this inducer molecule binds to LuxR (encoded by *luxR* as a transcriptional regulator protein). This complex directly induces high levels of transcription for the *lux* operon (downstream to *luxR/luxI*) (Dunlap, 1999).

The *lux* operon typically consists of 6 genes, *luxCDABEG*, except for *Photobacterial* species, where an extra gene (*luxF*) is added to the *lux* operon exhibiting the gene organization, *luxCDABFEG* (Meighen, 1991; Lee *et al.*, 1991; Dunlap, 2009; Bergner *et al.*, 2015). The *luxAB* encodes the luciferase (detailed description will follow below). The genes *luxCDE* encode for a multi enzyme complex (~500 kDa with the stoichiometry $r_4s_4t_{2-4}$, where ‘r’ represents

reductase, 's' represents synthetase and 't' represents transferase subunits), which is responsible for the synthesis of the aldehyde substrate for the bioluminescence reaction. The LuxC (NADPH-dependent acyl reductase) and LuxE (ATP-dependent acyl protein synthetase) are essential for the reduction of the fatty acid to aldehyde and LuxD (acyl transferase) is supposedly involved in its delivery to the luciferase (Boylan *et al.*, 1985). LuxG (encoded by *luxG*) is not directly essential for luminescence but catalyses the reduction of FMN, which is then supplied to the luciferase as the co-substrate (Nijvipakul *et al.*, 2008). The exact role of LuxF was unknown until recently, where, in our group we have shown that LuxF binds myrFMN (myristylated FMN - an inhibitor of luciferase) very tightly and scavenges it from inhibiting the luciferase (Bergner *et al.*, 2015; Tabib *et al.*, manuscript in preparation). The study of 'LuxF, luciferase and myrFMN' is a part of this thesis and will be described in detail in the next chapters.

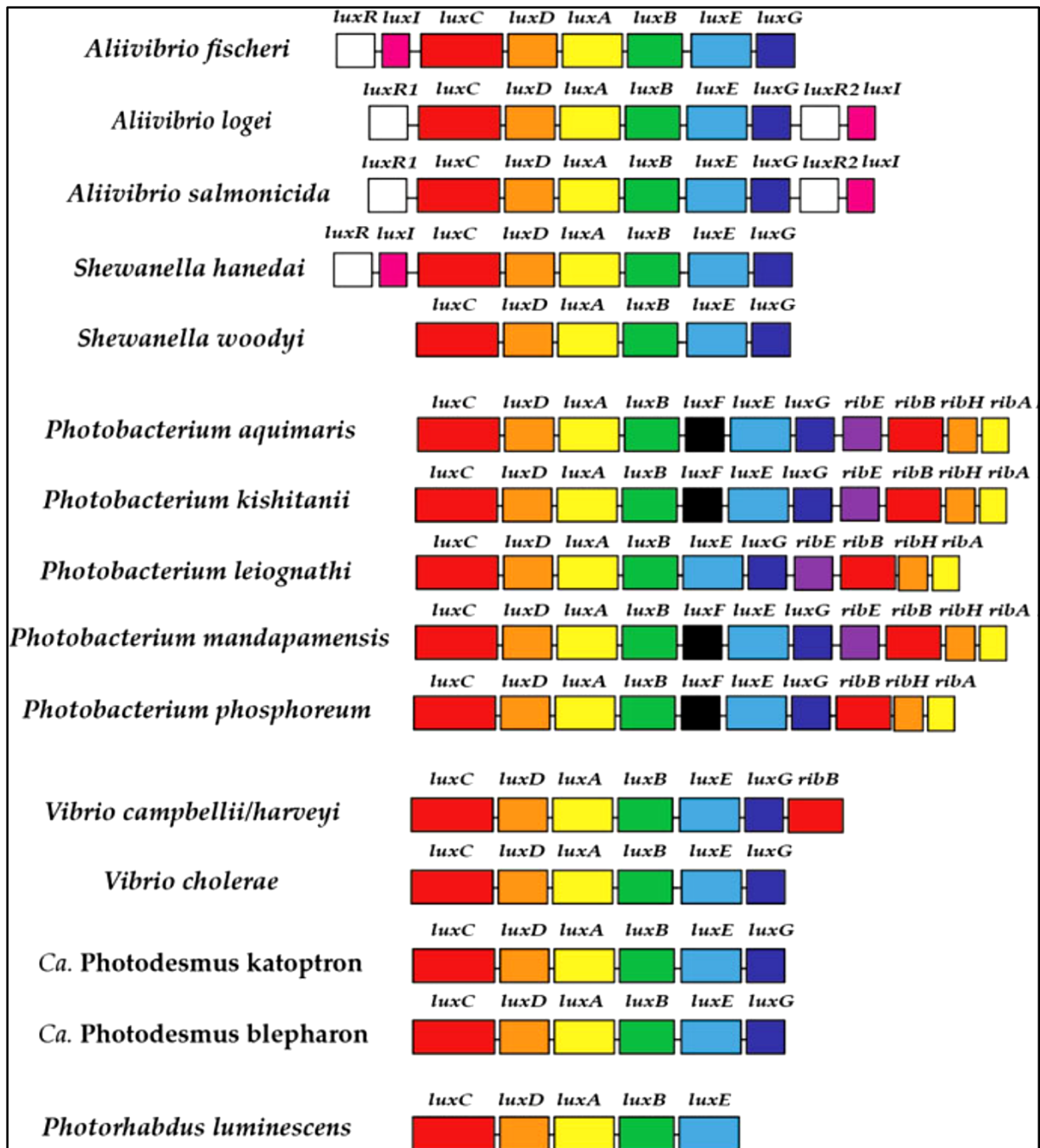
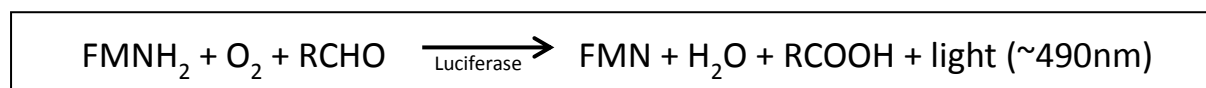


*figure and legend adapted from Dunlap, 2014.

Figure 4: Bacterial luminescence (*lux*) genes. Shown are the gene content and gene order of *lux* operons for those bacteria for which complete *lux* operon sequence data are available. Contiguous genes of the *lux* operons are aligned to highlight similarities and differences. Four distinct types of *lux* operons are evident based on commonalities of gene content, organization, and sequence similarity: (1) *Aliivibrio/Shewanella* type, with *luxI/luxR* regulatory genes; (2) *Photobacterium* type, with *ribEBHA* genes forming a *lux-rib* operon; (3) *Vibrio/Candidatus Photodesmus* type, without linked regulatory genes; and (4) *Photorhabdus* type, composed of just five core *lux* genes, *luxCDABE*.

2.2 Reaction mechanism

Generally, the bioluminescent reaction in bacteria is catalyzed by the luciferase, an enzyme employing FMN as a redox cofactor to drive the mono-oxygenation of an aldehyde substrate to its corresponding acid product. The free energy released during the oxidation of the aldehyde gives rise to an excited state FMN-4a-hydroxide, which in turn serves as the light emitting molecule luciferin, as shown in the reaction below:



Scheme 1: General reaction of bacterial bioluminescence, where RCHO can be any aldehyde with chain length C8-C14.

The above scheme can be broken down into two steps:

a) The reaction of O₂ to the luciferase FMNH₂ complex:

According to previous reports, FMNH[•] is the first substrate that binds to the luciferase. Then the O₂ molecule approaches the FMNH[•], triggering a charge transfer to the O₂ and giving rise to a radical pair on the neutral FMNH and a superoxide (O₂^{•-}) molecule forming FMN-4a-hydroperoxide (FMNHOO[•]). (Hou *et al.*, 2014).

b) The reaction of the aldehyde with the FMN-4a-hydroperoxide intermediate:

The FMN-4a-peroxyhemiacetal adduct is supposedly formed by a nucleophilic attack of the C4a-peroxyflavin on the aldehyde substrate (Eberhard *et al.*, 1972). The decomposition of this intermediate is the most critical step because it eventually leads to the population of the excited state of the FMN-4a-hydroxide intermediate (Scheme 2). Two possible mechanisms were predicted for the further conversion of the FMN-4a-peroxyhemiacetal *viz.* the CIEEL mechanism (chemically initiated electron exchange luminescence, Eckstein *et al.*, 1993) and the “dioxirane” mechanism (Raushel *et al.*, 1989). The CIEEL mechanism suggests an one-electron rearrangement from the N5 position of the flavin to the distal oxygen of the peroxide moiety, triggering the cleavage of the O-O bond and leading to the formation of a radical intermediate, which after hydrogen abstraction forms a carboxyl anion radical. Internal rearrangement of this radical triggers the back-transfer of the electron to the flavin moiety resulting in an excited state species and in the process the acid product is formed that is then released from the luciferase. On the contrary the “dioxirane” mechanism states that the reaction continues from the

peroxyflavin with the attack of the carbonyl oxygen on the distal oxygen of the peroxide leading to the cleavage of the O-O bond and to the formation of a dioxirane state. This then takes up an electron from the flavin hydroxide donor to form a dioxirane radical. Rearrangement of this dioxirane radical leads to the formation of a carboxyl radical, which then donates one electron back to the flavin moiety thus resulting in an excited state flavin. The current preferred model is however based on the radical mechanism, such as the CIEEL process discussed above.

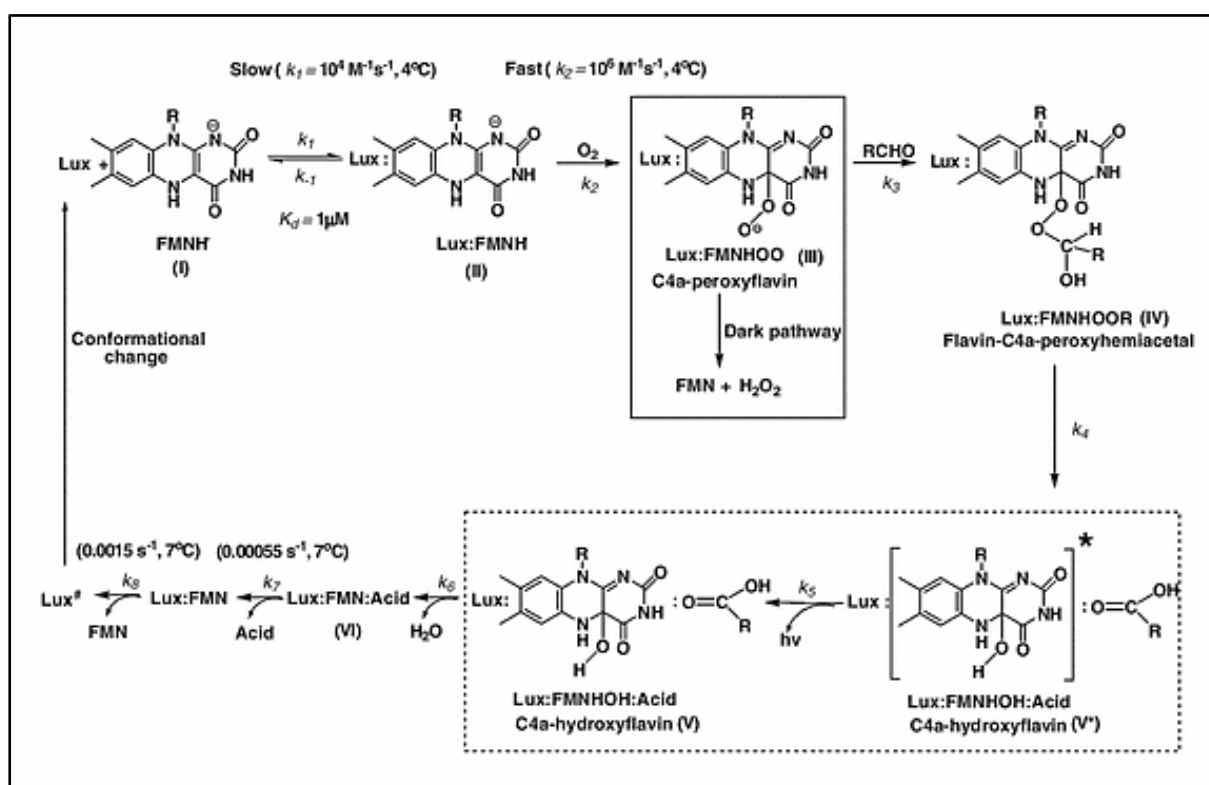


*Figure adapted from Tinikul *et al.*, 2016

Scheme 2: Overall catalytic mechanism and intermediates of the bacterial luciferase reaction.

2.3 Bacterial luciferase – the enzyme that catalyzes the light production

Bacterial luciferase is a flavin-dependent heterodimeric enzyme (as shown in Figure 5), of molecular mass ~78-80 kDa (α -subunit is ~40-42 kDa and β -subunit is ~36-38 kDa) that catalyses the monooxygenation of a long chain aldehyde to its corresponding acid and in this process FMNH₂ is oxidised and visible luminescence is emitted ($\lambda_{\text{max}} = 490 \text{ nm}$). The catalytic function and the reaction mechanism of the luciferase have been extensively studied for more than half a century. The crystal structures for the $\alpha\beta$ heterodimer and β homodimer of luciferase from *Vibrio harveyi* were solved and it was evidently shown that only the heterodimeric enzyme harbours one binding site each for FMNH₂ as well as the aldehyde substrate (Meighen *et al.*, 1971; Becvar *et al.*, 1975; Lei *et al.*, 1994; Fisher *et al.*, 1996; Tanner *et al.*, 1997; Thoden *et al.*, 1997).

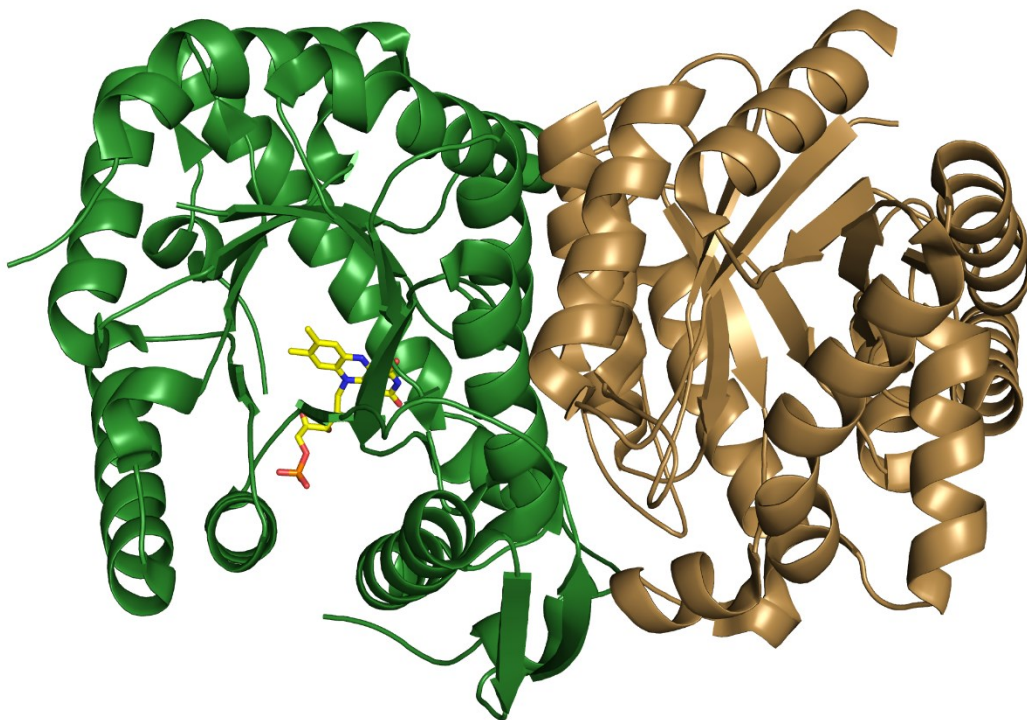


Figure 5: Structure of the bacterial luciferase with FMN bound (3FCG). The α -subunit is represented in green and the β -subunit in gold. The FMN is represented as a stick model.

2.3.1 Analysis of the *Vibrio luciferase* structure

A closer look at the two subunits (α and β) of the *Vibrio* luciferases shows that they share around 30-32 % sequence identity with 95 of 350 amino acids conserved, clearly indicating that LuxB may have arisen by gene duplication from LuxA. Also, both subunits feature a structurally conserved TIM ($\alpha\beta$)8 barrel supporting the notion that they have a common ancestor. Compared to the luciferases of other genera like *Photobacteria* and *Aliivibrio*, a high degree of sequence identity (50-90 %) is observed. A detailed comparison of these luciferases is shown in Supplementary Figure S1 and sequence identities are summarized in Table 1 (Baldwin *et al.*, 1995; Fisher *et al.*, 1996; Sparks *et al.*, 2001).

Table 1: Identity between luciferases from different bacterial strains (%)

Bacterial strains	VH_ATCC_14126	AF_ATCC_7744	PL_ATCC_27561	PL_TH1	PL_ATCC_25521
VH_ATCC_14126	100%	58%	56%	51%	50%
AF_ATCC_7744	-	100%	71%	63%	61%
PL_ATCC_27561	-	-	100%	74%	75%
PL_TH1	-	-	-	100%	92%
PL_ATCC_25521	-	-	-	-	100%

*VH – *Vibrio harveyi*; AF – *Aliivibrio fischeri*; PL – *Photobacterium leiognathi*

The active site is known to reside on the α -subunit of the heterodimer, however it was also shown that the β -subunit is essential for the stabilization and activity of the enzyme (Campbell *et al.*, 2009^b). Homodimers of α_2 or β_2 showed very low or no activity compared to the $\alpha\beta$ heterodimer (Choi *et al.*, 1995). In 2009, a crystal structure of luciferase in complex with FMN was solved, which clearly showed that the flavin binding site is located on the α -subunit (Campbell *et al.*, 2009^b). The flavin binds in the active site pocket with the isoalloxazine ring having a planar conformation. Amino acids Cys106, Val173, Ile191 and the *cis*-peptide Ala74-Ala75 are found on the *re*-face of the isoalloxazine ring whereas Trp194, Phe6 and Ser227 form a hydrophobic patch on the *si*-face of the isoalloxazine ring (Figure 6). The *cis*-peptide was shown to play an important role in the luciferase reaction and the hydrophobic patch was proposed to be an aldehyde binding site. Furthermore, side chains of residues like Arg107, Arg125, Ser176 and Glu175 surround the 5' phosphate group of the FMN, where Arg107 was shown to be crucial for flavin binding. Assembly of the two subunits is mediated by formation of hydrogen bonds between amino acids of the subunits. For example, Tyr151 of the β -subunit

was shown to interact with Phe272 residue located in the loop region of the α -subunit. Site-directed mutagenesis experiments carried out with luciferase in order to deduce the catalytic function of the amino acids in and around the active site provided many insights of the possible role of these amino acids. For example, substitution of α -His44 to Ala resulted in an inactive protein and α -Cys106 to Val showed decreased aldehyde utilization and reduced intermediate stability. Furthermore, amino acid replacements such as β -Tyr151 to Lys or Trp resulted in a dramatic decrease of the quantum yield indicating the importance of the α - β subunit heterodimer formation (Campbell *et al.*, 2009^a; Baldwin *et al.*, 1995; Fisher *et al.*, 1996).

The exclusive difference between the two subunits is the presence of a protease-labile loop inserted between Lys259 and Asn289 of the α -subunit, which is highly conserved in various luciferases. It is believed that this loop region is important for intermediate stabilization involving a lid-gating mechanism. Deletion of the mobile loop between β strand 7 and α strand 7 of the α -subunit resulted in a 10% smaller protein. The truncated protein still folded, however its total quantum yield decreased by two orders of magnitude. Binding of FMNH₂ should be able to fix the loop as this protein complex is not protease-labile anymore (Campbell *et al.*, 2009^a; Campbell *et al.*, 2010; Sparks *et al.*, 2001).

A summary of the key amino acids in the active site is given in Table 2. The key amino acids in the active site are displayed in Figure 6.

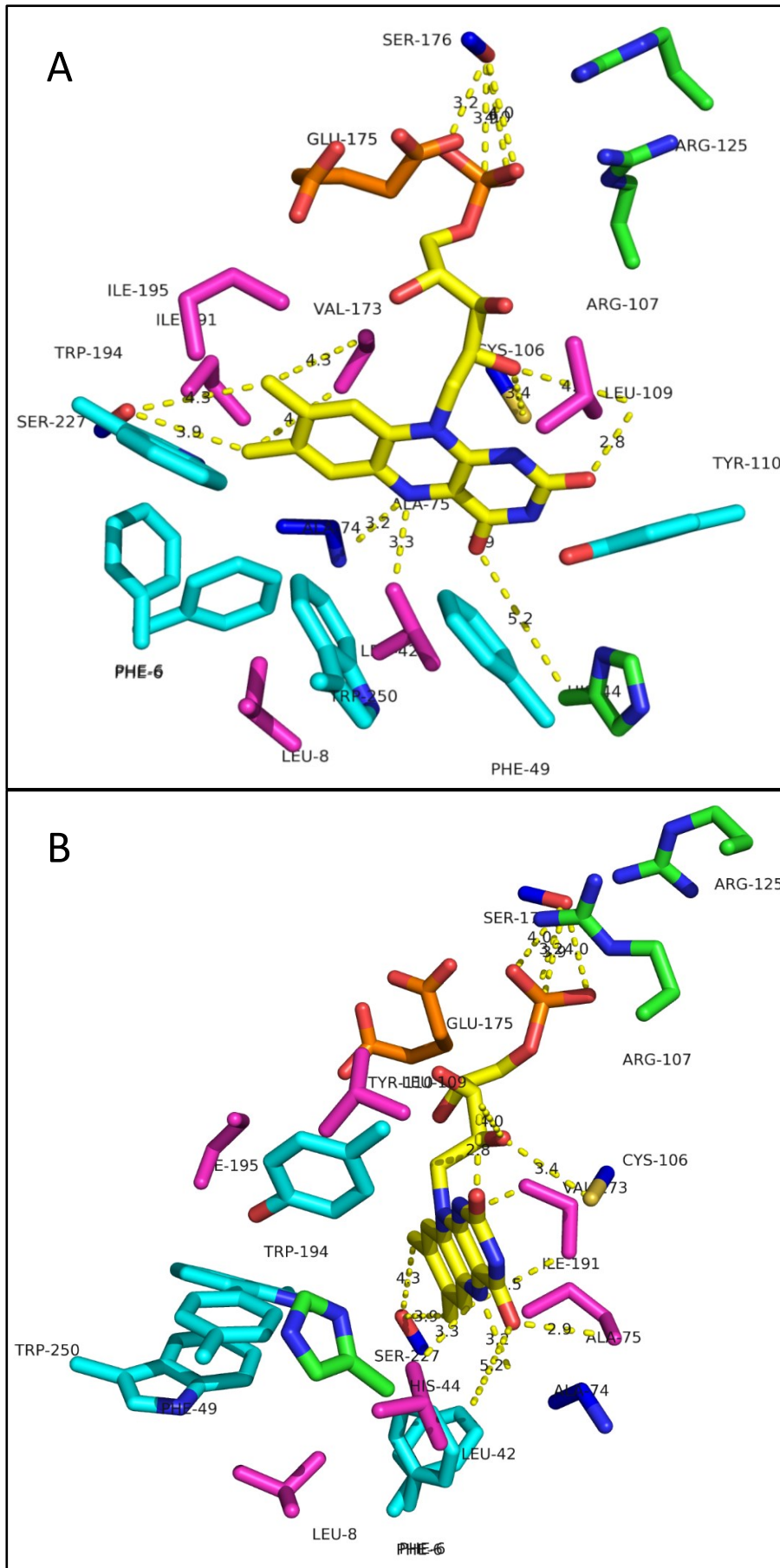


Figure 6: Active site composition of *Vibrio harveyi* luciferase (pdb: 3FGC). **Blue:** nucleophilic amino acids; **Magenta:** hydrophobic amino acids; **Green:** basic amino acids; **Cyan:** aromatic amino acids; **Orange:** acidic amino acids

Table 2: Comparison of the amino acids present at crucial positions in different luciferases

Luciferases	VH_ATCC_14126	AF_ATCC_7744	PL_ATCC_27561	PL_TH1	PL_ATCC_25521
Position					
α-44	His	His	His	His	His
α-74	Ala	Met	Met	Met	Met
α-75	Ala	Gly	Gly	Gly	Gly
α-106	Cys	Val	Val	Val	Val
α-173	Val	Thr	Thr	Thr	Thr
α-191	Ile	Val	Val	Val	Val
α-194	Trp	Trp	Trp	Trp	Trp
α-6	Phe	Ile	Ile	Ile	Ile
α-227	Ser	Thr	Thr	Thr	Thr
α-107	Arg	Arg	Arg	Arg	Arg
α-125	Arg	Arg	Arg	Arg	Arg
α-175	Glu	Glu	Glu	Glu	Glu
α-176	Ser	Ser	Ser	Ser	Ser
α-272	Phe	Tyr	Tyr	Tyr	Tyr
β-151	Tyr	Tyr	Tyr	Phe	Phe
Other amino acids in close vicinity to the active site					
α-250	Trp	Trp	Trp	Trp	Trp
α-49	Phe	Phe	Phe	Phe	Phe
α-42	Leu	Leu	Leu	Leu	Leu
α-8	Leu	Phe	Phe	Phe	Phe
α-110	Tyr	Tyr	Tyr	Tyr	Tyr
α-109	Leu	Leu	Leu	Leu	Leu
α-195	Ile	Ile	Ile	Ile	Ile
α-179	Thr	Thr	Thr	Thr	Thr

*VH – *Vibrio harveyi*; AF – *Aliivibrio fischeri*; PL – *Photobacterium leiognathi*

2.3.2 Comparative analysis of different luciferases (based on the data from this thesis):

The activity of luciferases is typically analyzed by measuring the number of photons produced by the luciferase in a certain amount of time. A comparison of *in vivo* light production and *in vitro* activity suggests that the light emission maxima and the decay kinetics vary drastically between luciferases of different origins. For example, *Photobacterium leiognathi*, strain TH1 emits more light compared to any other strains from different genera.

When the luciferases from four different strains were compared to the structurally studied *Vibrio* luciferase, the results were quite interesting. Though the sequence identity between these luciferases is between 50-55 %, many key amino acids, which are responsible for the luciferase activity are highly conserved or replaced by a functionally similar amino acid (as shown in the Table 2). For example, His44, Arg107, Arg125, Glu175 and Ser176 are few amino acids, which are highly conserved among luciferases of all genera of bacteria.

On the contrary, residues like Cys106, Val173 and Ser227, which play an important role in the *Vibrio* luciferase, are seen to be replaced by other amino acids in *Aliivibrio* and *Photobacterial* proteins. Interestingly, all these 'variants' show either equal or several orders of magnitude more activity than the *Vibrio* luciferase. Therefore, it would be interesting to make site-directed mutations at these positions to pin down the role of these amino acids in these luciferases. For example, in the photobacterial strain TH1, with 51 % identity and Val at position 106, it would be quite an interesting to create variants and compare their effects on the activity.

3. Supplementary data

VH_14126	MKFGN FL LTYPPELSQTEVMKRLVNLGKASEGCGFDTVWLE EH HFTEFGLLGPNPVAAA	60
AF_7744	MKFGNICFSYQPPGETHKQVMDRFVRLGIASEEVGFDTYWTE EH HFTEFGLTG NL FVAAA	60
ATCC_27561	MKFGNICFSYQPPGESHKEVMDRFVRLGVASEELNFDTFWTE EH HFTEFGLTG NL VACA	60
TH1	MKISNICFSYQPPGESHQEVMERFVRLGVASEELNFDGFYTE EH HFTEFGITGNLYVACA	60
ATCC_25521	MKISNICFSYQPPGESHQEVMERFIRLGVASEELNFDGFYTE EH HFTEFGITGNLYIACA	60
	:* : :** : : **:* : ** ** * : ***** : * : :.*	
VH_14126	HLLGATETLNVGTAAIVLPTAHPVRQAEDVNLLDQMSKGRFRFGICRGLYDKDFRVFGTD	120
AF_7744	NLLGRTKTLNVGTMGVVIPTAHPVRQLEDVLLLDQMSKGRFNFGTVRGLYHKDFRVFGVD	120
ATCC_27561	NILGRTKKLVNVTMGIVLPTAHPARQMEDLLLDQMSKGRFNFGVVRGLYHKDFRVFGVT	120
TH1	NILGRTKRIKVGTMGIVIPTAHPARHVESLLVLDQLSKGRFNFGTVRGLYHKDFRVFGTS	120
ATCC_25521	NILGRTKRIQVGTMGIVLPTAHPARHVESLLVLDQLSKGRFNFGTVRGLYHKDFRVFGTS	120
	:** * : : :**** : : **:* **:* : * : : ***** : * : *****	
VH_14126	MDNSRALMDCWYDLMKEGFNEGYIAADNEHIKFPKIQLNPSAYTQGGAPVYVAESASTT	180
AF_7744	MEESRAITQNFYQMIMESLQGTGVSSDSYIQFPNVDVYPKVYSK-NVPTCMAESASTT	179
ATCC_27561	MEDSRSITEDEFHKMIMDGSKSGVLHTDGNIEFPD VN VYPEAYLD-KIPTCMAESAATT	179
TH1	QEDSRAIAENFYDMIMDASKTGILHTDGEQVDFPDVSVYPEAYSK-KVPTCMAESSETI	179
ATCC_25521	QEDSRKTAENFYSMILDASKTGVLHTDGEVVEFPD VN VYPEAYSK-KQPTCMAESSETI	179
	:** : : : : : : * : : * . . . ** . . . : * . * . * . : ** : *	
VH_14126	EWAAERGLPML SWI INTHEKKAQLDLYNEVATEHGYDVTKIDHCLSYITSVDHDSNRAK	240
AF_7744	EWLAIQGLPML SWI IGTNEKKAQMELYNEIATEYGHDISKIDHCMTYICSVDDDAQKAQ	239
ATCC_27561	TWLAERGLPML SWI IITSEKKAQMELYNEIAAEHGHDIHNIDHSMTFICSVNEDPEKAE	239
TH1	IYLAARGYPM LSWI IVPISEKVAQIELYNEVAEAEHGHDIHNIEHILTFICSVNEDAEDAD	239
ATCC_25521	TYLAERGLPML LSWI IVPSEKVSQMELYNEVAEAEHGHDIHNIEHILTFICSVNEDGEKAD	239
	: * : * ** : **** : ** : : : **** : * : * : * : : * : : * : * : * : *	
MOBILE LOOP		
VH_14126	DICRNFLGH WY DSYVNATKIFDSDQTKGYDFNKGQWRDFVLK GH KDNTNRRIDYSYEINP	300
AF_7744	DVCREFLKN WY DSYVNATNIFDSDNQTRGYDYHKGQWRDFVLQ GH TNTNRRVDYSNGINP	299
ATCC_27561	SVCRDFLSN WY ESYTNATNIFKDSNQTRGYDYHKGQWRDFVLQ GH TDTRRRLDYSNNLNP	299
TH1	RVCRNFLN WY DSYK NATQ IFDSDQTKGYDYLKAQWREWVMKGLADPRRLDYSNELNP	299
ATCC_25521	SVCRNFLN WY DSYK NATN IFDSDNQTRGYDYLKAQWREWVMKGLADPRRLDYSNELNP	299
	:**:* : **:* **:* **:* **:* **:* : * . ***** : : : * : **:* **:*	
VH_14126	VGTPEECIAIIQQDIDATGIDNICGFEANGSEEEIIASMKLFQSDVMPYLKEKQ-MKFG	359
AF_7744	VGTPEQCIEIIQRDIDATGITNITCGFEANGTEDEIIASMRFRMTQVAPFLKEPK-MKFG	358
ATCC_27561	VGTPEKCIEIIQRDIDATGINNITLGFEANGSEQEIIASMERFMTQVAPYLKDPK-MNFG	358
TH1	VGTPERCIEIIQNNIDATGIKHITVGFANGSEHEIRESMELFMEKVAPHLKDPQ-MNFG	358
ATCC_25521	VGTPERCIEIIQSNIDATGIKHIIVGFANGSEQEIRESMELFMEKVAPHLKDPQ-MNFG	358
	***** ** * : ***** : * ***** : * ** * . * * . * : **:*	
VH_14126	LFFLNFMNSKRSSDQVIEEMLDTAHYVDQL--KFDTLAVYENHFSNNGVVGAPLTVAGFL	417
AF_7744	LFFLNQKDGITSEETLDNMVKTVTLIDSTKYHFNTAFVNEHHFSKNGIVGAPITAAGFL	418
ATCC_27561	LFFLNQKLGMTSEAVLDNMIDTIALVDKDEYHFKTAFVNEHHFSKNGIVGAPMTAASFL	418
TH1	LFFLNQPEGMTSEMVL DN MVDTVALVDKDDYHYNRVLVSEHHFSKNGIIGEPLTAVSFL	418
ATCC_25521	LFFLNQPEGMTSEMVL DN MVDTVALVDKDDYHFKRVLVSEHHFSKNGIIGEPLTAISFL	418
	***** . : * : : : * : * : * . : : * * : * : * : * : * : * . . **	
VH_14126	LGMTKNAKVASLNHVITTHHPVRVAAEACL LD QMSSEGRFAFGFSDCEKSADMRFFNRPTD	477
AF_7744	LGLTNKLHIGSLNQVITTHHPVRVAAEASLLDQMSSEGRFILGFSDCESDFEMEFFKRHIP	478
ATCC_27561	LGLTERLHIGSLNQVITTHHPVRIAAEASLLDQMSDGRFILGLSDCVSDFEMDFKQRD	478
TH1	LGLTKRLKIGSLNQVITTHHPVRI GE QTGLLDQMSYGRFILGLSDCVNDFEMDFKQRD	478
ATCC_25521	LGLTKRIEIGSLNQVITTHHPVRI GE QTGLLDQMSYGRFVGLSDCVNDFEMDFKQRD	478
	:* . . . : **:* *** : : : ***** ** * : * : * . . . : * * : *	
VH_14126	SQFQLFSECHKIINDAFTTGYCHPNND FS FPKISVNPHAFTEGGPAQFVNATSKEVVEW	537
AF_7744	SRQQQFEACYEINDALTGYCHPNND FS FPKVSINPHCYSDNGPKQYVSATSKEVVMW	538
ATCC_27561	SQQQQFEACYEILNDGITTNYCYANND FS FPKISINPHCISKENLKQYILATSMGVVEW	538
TH1	SQQQKFEACYEILNEALTTNYCHADDD FS FPFRISVNPHCIN--EIKQYILASSMEVVEW	536
ATCC_25521	SQQQQFEACYEILNEALTTNYCQADDD FS FPFRISVNPHCIS--EVKQYILASSMGVVEW	536
	* : : * . : **:* **:* **:* **:* **:* : * : * : * : * : * : * : * : * : *	

VH_14126	AAKLG LPLVFRWDDSNAQRKEYAGLYHEVAQAHGVDVSQVRHKLTLNQNVDGEAARAE	597
AF_7744	AAKKALPLTFKWEDNLETKERYAILYNKTAQQYGVDISDQVHQLTVIANLNSDRSTAQEE	598
ATCC_27561	AAKKGLPLTYRWSDTLAEKENYQRYLTVAEENNVDTIHDVDFPPLLNVINPDRDIKQE	598
TH1	AAKKGLPLTYRWSDKLAEKEKYYQRYLAVAKENNVDSNVDHQFPLLNVINENRRVARDE	596
ATCC_25521	AARKGLPLTYRWSDSLAEKEKYYQRYLAVAKENNIDVSNIDHQFPLLNVINENRRIARDE	596
	** : .*** .:.*.* . :.* * .* .:***: * : :.* * : * : *	
VH_14126	ARVYLEEFVRESYSNTD-FEQKMGELLSENAIGTYEESTQAARVAIECCGAADLLMSFES	656
AF_7744	VREYLKDYITETYPQMD-RDEKINCIIEENAVGSHDDYYESIKLAVEKTGSKNILLSFES	657
ATCC_27561	MRDYIRGYIAEAYPNTD-QEEKIEELIKQHAVGTEDEYYESSKYALEKTGSKNVLLSFES	657
TH1	VRKYIESYVAEAYPTDPNIELRIELLEQHAVGKMDYYDPTMHAVKVTGSKNVLLSFES	656
ATCC_25521	VREYIQSYVSEAYPTDPNIELRVEELIEQHAVGKVDEYYDSTMHAVKVTGSKNILLSFES	656
	* *:. : : *:* : : : : : : *:* * : : : * : : : * : * : * : *	
VH_14126	MEDKAQQRAVIDVNVANIVKYHSRPNLYFQG	688
AF_7744	MADFKGVKEIIDMLNQKIEKNLSPENLYFQG	689
ATCC_27561	MKNKAAVIDLINMVNEKIKKNL-----	671
TH1	MKNKDDVTKLINMFNQKIKDNLIK-----	672
ATCC_25521	MKNKDDVTKLINMFNQKIKDNLIK-----	672
	* : : : * : * .	

Figure S1: Multiple sequence alignment. Sequence alignment of luciferase sequences from three different genera. (VH_14126 - *Vibrio harveyi* ATCC 14126; AF_7744 - *Aliivibrio fischeri* ATCC 7744; ATCC_27561 - *Photobacterium leiognathi* ATCC 27561; TH1 - *Photobacterium leiognathi* TH1; ATCC_25521 - *Photobacterium leiognathi* ATCC 25521)

4. References

- Baldwin, T.O., Christopher, J.A., Raushel, F.M., Sinclair, J.F., Ziegler, M.M., Fisher, A.J., and Rayment, I., (1995) Structure of bacterial luciferase. *Curr Opin Struct Biol* **5**:798-809.
- Becvar, J.E., and Hastings, J.W., (1975) Bacterial luciferase requires one reduced flavin for light emission. *Proc Natl Acad Sci U S A* **72**:3374-6.
- Bergner, T., Tabib, C.R., Winkler, A., Stipsits, S., Kayer, H., Lee, J., et al., (2015) Structural and biochemical properties of LuxF from *Photobacterium leiognathi*. *Biochim Biophys Acta*, **1854**:1466-1475.
- Boylan, M., Graham, A.F., and Meighen, E.A., (1985) Functional identification of the fatty acid reductase components encoded in the luminescence operon of *Vibrio fischeri*. *J Bacteriol* **163**:1186-90.
- ^aCampbell, Z.T., and Baldwin, T.O., (2009) Two lysine residues in the bacterial luciferase mobile loop stabilize reaction intermediates. *J Biol Chem* **284**:32827–32834
- Campbell, Z.T., Baldwin, T.O., and Miyashita, O., (2010) Analysis of the bacterial luciferase mobile loop by replica-exchange molecular dynamics. *Biophys J* **99**:4012–4019
- ^bCampbell, Z.T., Weichsel, A., Montfort, W.R., and Baldwin, T.O., (2009) Crystal structure of the bacterial luciferase/flavin complex provides insight into the function of the β subunit. *Biochemistry* **48**:6085–6094
- Choi, H., Tang, C-K., and Tu, S-C., (1995) Catalytically active forms of the individual subunits of *Vibrio harveyi* luciferase and their kinetic and binding properties. *J Biol Chem* **270**:16813–16819
- Dunlap, P.V., (1999) Quorum regulation of luminescence in *Vibrio fischeri*. *J Mol Microbiol Biotechnol* **1**:5-12.
- Dunlap, P.V., (2009) Bioluminescence, microbial, In M. Schaechter (ed.), *Encyclopedia of Microbiology*, 3rd edition. Elsevier, Oxford, pp 45-61.
- Dunlap, P.V., (2014) Biochemistry and genetics of bacterial bioluminescence. In G. Thouand and R. Marks (ed.), *Bioluminescence: fundamentals and applications in biotechnology*. Springer-Verlag, Berlin, Germany.
- Eberhard, A., and Hastings, J. W., (1972) A postulated mechanism for the bioluminescent oxidation of reduced flavin mononucleotide. *Biochem Biophys Res Commun* **47**, 348-353.
- Eckstein, J. W., Hastings, J. W., and Ghisla, S., (1993) Mechanism of bacterial bioluminescence: 4a,5-dihydroflavin analogs as models for luciferase hydroperoxide intermediates and the effect of substituents at the 8-position of flavin on luciferase kinetics. *Biochemistry* **32**, 404-411.

- Fisher, A.J., Thompson, T.B., Thoden, J.B., Baldwin, T.O., and Rayment, I., (1996) The 1.5-Å resolution crystal structure of bacterial luciferase in low salt conditions. *J Biol Chem* **271**:21956-68.
- Harvey, E.N., (1916) The mechanism of light production in animals. *Science* **44**:208-209
- Haddock, S.N.D., Moline, M.A., and Case, J.F., (2010) Bioluminescence in the sea. *Ann Rev Mar Sci* **2**:443-93.
- Hou, C., Liu, Y.J., Ferré, N., and Fang, W.H., (2014) Understanding bacterial bioluminescence: a theoretical study of the entire process, from reduced flavin to light emission. *Chemistry* **20**:7979-86.
- Kaskova, Z.M., Tsarkova, A.S., and Yampolsky, I.V., (2016) 1001 lights: luciferins, luciferases, their mechanisms of action and applications in chemical analysis, biology and medicine. *Chem Soc Rev* **45**:6048-6077.
- Lapota, D., Osorio, A.R., Liao, C., and Bjorndal, B., (2007) The use of bioluminescent dinoflagellates as an environmental risk assessment tool. *Mar Pollut Bull* **54**:1857-67.
- Lee, C. Y., Szittner R. B., and Meighen E. A., (1991) The lux genes of the luminous bacterial symbiont, *Photobacterium leiognathi*, of the ponyfish. Nucleotide sequence, difference in gene organization, and high expression in mutant *Escherichia coli*. *Eur J Biochem* **201**: 161-167.
- Lee, J., (1989) Bioluminescence. In Kendrick C. Smith (ed.), *The Science of Photobiology*. pp 391-417
- Lei, B., Cho, K.W., and Tu, S.C., (1994) Mechanism of aldehyde inhibition of *Vibrio harveyi* luciferase. Identification of two aldehyde sites and relationship between aldehyde and flavin binding. *J Biol Chem* **269**:5612-8.
- Macheroux, P., Kappes, B., and Ealick, S. E, (2011). Flavogenomics - A genomic and structural view of flavin-dependent proteins. *FEBS J* **278**, 2625-2634.
- Meighen, E.A., and Hastings, J.W., (1971) Binding site determination from kinetic data. Reduced flavin mononucleotide binding to bacterial luciferase. *J Biol Chem* **246**:7666-74.
- Meighen, E. A., (1991) Molecular biology of bacterial bioluminescence. *Microbiol Rev* **55**, 123-142.
- Nijvipakul, S., Wongratana J., Suadee C., Entsch B., Ballou D. P., and Chaiyen P., (2008) LuxG is a functioning flavin reductase for bacterial luminescence. *J Bacteriol* **190**: 1531- 1538.
- Raushel, F. M., and Baldwin, T. O., (1989) Proposed mechanism for the bacterial bioluminescence reaction involving a dioxirane intermediate. *Biochem Biophys Res Commun* **164**, 1137-1142.

Shimomura, O., Johnson, F.H., and Saiga, Y. (1962) Extraction, purification and properties of aequorin, a bioluminescent protein from the luminous hydromedusan, *Aequorea*. *J Cell Comp Physiol* **59**:223-39.

Sparks, J.M., and Baldwin, T.O., (2001) Functional implications of the unstructured loop in the (beta/alpha)₈ barrel structure of the bacterial luciferase alpha subunit. *Biochemistry* **18**:15436-43.

Tabib, C.R., Brodl, E., and Macheroux, P., (2016) Generation of myristylated FMN by luciferase supports a radical mechanism for bacterial bioluminescence. (*Manuscript under preparation*)

Tanner, J.J., Miller, M.D., Wilson, K.S., Tu, S.C., and Krause, K.L., (1997) Structure of bacterial luciferase beta 2 homodimer: implications for flavin binding. *Biochemistry* **36**:665-72.

Teufel, R., Agarwal, V., and Moore, B.S., (2016) Unusual flavoenzyme catalysis in marine bacteria. *Curr Opin Chem Biol* **31**:31-9.

Tinikul, R., and Chaiyen, P., (2016) Structure, Mechanism, and Mutation of Bacterial Luciferase. In *Bioluminescence: Fundamentals and Applications in Biotechnology* - Volume **3**. Gérald Thouand, Robert Marks (ed.) pp: 47-74

Thoden, J.B., Holden, H.M., Fisher, A.J., Sinclair, J.F., Wesenberg, G., Baldwin, T.O., and Rayment, I., (1997) Structure of the beta 2 homodimer of bacterial luciferase from *Vibrio harveyi*: X-ray analysis of a kinetic protein folding trap. *Protein Sci* **6**:13-23.

Thore, A., Lundin, A., and Anséhn, S., (1983) Firefly luciferase ATP assay as a screening method for bacteriuria. *J Clin Microbiol* **17**:218-24.

Zimmer, M., (2002) Green fluorescent protein (GFP): applications, structure, and related photophysical behavior. *Chem Rev* **102**:759-81.

5. Aim of the thesis

Since the first observation of bacterial bioluminescence, the visible light phenomena has been studied extensively and more organisms have been added to this class of luminescence. The natural production of light, catalyzed by enzymes, exhibits a highly sophisticated energy efficiency system for a bacterial cell, thus a better understanding of these systems can be advantageous. Although the enzymes responsible for the light production and intermediates of bacterial bioluminescence system have been discovered, an extensive study of the protein involvement and the quantified data on luminescence is still missing.

- The main aim of this work lies on investigating the role of LuxF and luciferase in the formation of myrFMN. It also emphasizes on a detailed study of *Photobacterial* luminescence system in comparison to *Vibrio* and *Aliivibrio* systems.

6. Thesis briefing

This thesis includes 5 chapters:

Chapter 1: Investigation of the structural and biochemical properties of LuxF from *Photobacterium leiognathi*.

In this chapter, I have investigated for the presence of *luxF* in different bacterial strains, and examined its role in the production of myrFMN (6-(3'-(R)-myristyl)-FMN). I have also studied the binding affinities of LuxF and luciferase to purified myrFMN using isothermal titration calorimetry (ITC).

I was successful to establish a method to isolate myrFMN from bacterial cells. I also showed that binding to apo-LuxF ($K_d = 80 \text{ nM}$) to pure myrFMN was fifty times tighter than to luciferase ($K_d = 4.0 \text{ }\mu\text{M}$). In addition, I exploited this tight binding of myrFMN to recombinant apo-LuxF, to reveal that myrFMN is present in all photobacterial strains tested suggesting that myrFMN production is independent of the occurrence of *luxF*.

This chapter was published as:

Bergner T*, Tabib CR*, Winkler A, Stipsits S, Kayer H, Lee J, Malthouse JP, Mayhew S, Müller F, Gruber K, Macheroux P (2015): Structural and biochemical properties of LuxF from *Photobacterium leiognathi*; *Biochim-Biophys Acta*, **1854**, 1466-1475.

Chapter 2: Investigation of different substrates and their efficiencies for the bacterial luciferase.

In this chapter, we (Myself, Eveline Brodl and Jakov Ivkovic) have synthesized and tested different chain lengths of aldehydes (C8-C14) as substrates for luciferase. In addition we also synthesized and tested their analogs having a double bond at α , β -position.

We could successfully synthesize all the seven aldehydes (C8-C12 saturated and C8-C12 unsaturated) to test them as luciferase substrates. C14 saturated was commercially purchased. We also showed that, for both saturated and unsaturated aldehydes, the longer chain lengths had higher activity in terms of bioluminescence. A difference in the luminescence kinetics was also observed.

This chapter is currently under preparation for submission.

Chapter 3: This chapter exclusively deals with the study of myrFMN generation and the possible mechanism.

In this chapter, I have tested seven different bacterial strains for a correlation between the bioluminescence and the myrFMN production. I have also tested for the inhibition effect of myrFMN on the luciferase and the scavenging effect of LuxF. With strong indications of a direct link light production and myrFMN production, we (Myself and Eveline Brodl) tested *in vitro* multi-enzyme cascade with cofactor turnover system.

I could successfully show a correlation between light production and myrFMN content in bacterial strains. The inhibition assay also was quite evident with loss of 90 % of activity with excess of myrFMN and scavenging effect of LuxF rescuing the activity back. Finally, we were successful to collect enough material with the *in vitro* assay to confirm myrFMN via HPLC and HPLC-MS.

This chapter is currently under preparation for submission.

Chapter 4: Mutagenic study of cysteine residues on the structural stability and enzymatic behavior of bacterial luciferase.

This chapter was performed as a thesis by a bachelor student, Andrea Marianne Friedrich under my supervision. Here we mutated six cysteines to test for its possible effect on the protein, with an aim to stabilize the enzyme.

We were successful in creating all the six variants of the luciferase. We further purified the proteins, estimated their yields, confirmed the proteins using MALDI and performed Thermofluor experiments to test their melting temperatures. None of the variants were more stable than the wildtype protein. On the contrary, the variants lost upto 95 % activity with a single mutation.

Chapter 5: The aim of this chapter was to create bacterial knock-outs to study the role of different enzymes from the *lux* operon.

Several methods; like type IV secretion system, electroporation and chemical transformation; were tried to insert DNA into the photobacterial strains to allow it to recombine and form genetic knockouts.

None of the system worked to transfer DNA into the photobacterial cells, possibly due to the presence of R plasmids or other unknown factors.

This chapter is a documentation of all the tested conditions and methodologies.

7. Presentations

The work in this thesis was presented in part as oral contributions (2) or poster presentations (10) at conferences, congresses and meetings.

Chapter 1



Structural and biochemical properties of LuxF from *Photobacterium leiognathi*



Thomas Bergner^{a,1}, Chaitanya R. Tabib^{a,1}, Andreas Winkler^a, Steve Stipsits^a, Heidemarie Kayer^a, John Lee^b, J. Paul Malthouse^c, Stephen Mayhew^c, Franz Müller^d, Karl Gruber^e, Peter Macheroux^{a,*}

^a Graz University of Technology, Institute of Biochemistry, Graz, Austria

^b University of Georgia, Department of Biochemistry and Molecular Biology, Athens, GA 30602, USA

^c Conway Institute, University College Dublin, Dublin, Ireland

^d Wylstrasse 13, CH-6052 Hergiswil (Formerly Novartis AG, Basel), Switzerland

^e University of Graz, Institute of Molecular Biosciences, Graz, Austria

ARTICLE INFO

Article history:

Received 8 May 2015

Received in revised form 1 July 2015

Accepted 19 July 2015

Available online 21 July 2015

Keywords:

Bioluminescence
Isothermal calorimetry
Luciferase
Marine bacteria
UV-Vis absorption spectroscopy
X-ray crystallography

ABSTRACT

The *lux*-operon of bioluminescent bacteria contains the genes coding for the enzymes required for light emission. Some species of *Photobacteria* feature an additional gene, *luxF*, which shows similarity to *luxA* and *luxB*, the genes encoding the heterodimeric luciferase. Isolated dimeric LuxF binds four molecules of an unusually derivatized flavin, i.e., 6-(3'-(*R*)-myristyl)-FMN (myrFMN). In the present study we have heterologously expressed LuxF in *Escherichia coli* BL21 in order to advance our understanding of the protein's binding properties and its role in photobacterial bioluminescence. Structure determination by X-ray crystallography confirmed that apo-LuxF possesses four preorganized binding sites, which are further optimized by adjusting the orientation of amino acid side chains. To investigate the binding properties of recombinant LuxF we have isolated myrFMN from *Photobacterium leiognathi* S1. We found that LuxF binds myrFMN tightly with a dissociation constant of 80 ± 20 nM demonstrating that the purified apo-form of LuxF is fully competent in myrFMN binding. In contrast to LuxF, binding of myrFMN to luciferase is much weaker ($K_d = 4.0 \pm 0.4$ μ M) enabling LuxF to prevent inhibition of the enzyme by scavenging myrFMN. Moreover, we have used apo-LuxF to demonstrate that myrFMN occurs in all *Photobacteria* tested, irrespective of the presence of *luxF* indicating that LuxF is not required for myrFMN biosynthesis.

© 2015 Elsevier B.V. All rights reserved.

1. Introduction

Bacterial bioluminescence results from the oxidation of a long-chain fatty aldehyde, such as myristic aldehyde, to the corresponding long-chain fatty acid (e.g., myristic acid [1,2]). The bioluminescent reaction is catalyzed by luciferase, an enzyme employing FMN as a redox cofactor to drive the monoxygenation of the aldehyde substrate to the acid product. The free energy released during the oxidation of the aldehyde gives rise to an excited state FMN-4a-hydroxide serving as the luciferin in bacterial bioluminescence [3]. Bacterial luciferase is a heterodimeric protein encoded by *luxA* and *luxB* in the so-called *lux*-operon of bioluminescent bacteria. In addition, the *lux*-operon contains three genes, *luxC*,

luxD and *luxE*, encoding enzymes for the generation of the aldehyde substrate. Finally, a nicotinamide nucleotide dependent enzyme that produces reduced FMN for bacterial luciferase is encoded by *luxG* [4,5]. Generally, these genes occur in the order CDABEG in most bioluminescent bacteria with the exception of some species in the genera *Photobacterium*, such as *Photobacterium leiognathi* and *Photobacterium phosphoreum* [6]. These bacteria have an additional gene termed *luxF* inserted into the *lux*-operon between *luxB* and *luxE* [7–9]. Sequence similarity to *luxB* suggests that *luxF* has arisen by gene duplication, however, its role in bacterial bioluminescence is obscure especially because only free-living but not symbiotic *Photobacteria* appear to exhibit the *luxF* insertion in their *lux*-operon [7]. To shed more light on the role of *luxF*, James and colleagues have solved the structure of the protein isolated from *P. leiognathi* [10,11]. Interestingly, X-ray crystallographic analysis revealed the presence of four flavin derivatives in the homodimeric protein. The flavins occupy two types of symmetry related binding sites, two at the interface and two at the N-termini. In all four flavins the C-6 carbon of the isoalloxazine ring system is linked to C-3 of myristic acid, i.e., 6-(3'-(*R*)-myristyl)-FMN (myrFMN) [12]. Because of its lower fluorescence efficiency (ca. 10–13% compared to FMN, [13])

* Corresponding author at: Graz University of Technology, Institute of Biochemistry, Petersgasse 12/II, A-8010 Graz, Austria.

E-mail address: peter.macheroux@tugraz.at (P. Macheroux).

¹ The first two authors have contributed equally to this publication.

² This work was supported by the Austrian "Fonds zur Förderung der wissenschaftlichen Forschung" (FWF) through grant P24189-B17 and the PhD program "Molecular Enzymology" (W901).

the protein was also referred to as non-fluorescent protein (NFP). The discovery of myrFMN raised the question of its origin, especially since an unusual carbon–carbon bond is formed in a stereospecific fashion [14]. Since luciferase uses FMN as a co-substrate and myristic acid is the product of the light-producing reaction, it was speculated that myrFMN might be generated as a by-product in this reaction [11,15]. A summary of the reactions catalyzed by bacterial luciferase and the proposed role of LuxF is shown in Scheme 1.

According to this model, LuxF scavenges myrFMN and thus prevents inhibition of luciferase by the side product. In fact, Tu and coworkers could demonstrate that myrFMN inhibits luciferase from *Vibrio harveyi* [16]. Its role as a “molecular sponge” of myrFMN is also supported by the large amounts of LuxF produced by *P. phosphoreum* and *P. leiognathi*. However, production of myrFMN in the luciferase reaction has never been demonstrated and remains to be shown. To better understand the binding of myrFMN to LuxF and luciferase, we have developed a heterologous expression system for *luxF* and *luxAB* in *Escherichia coli*. Here we present the X-ray crystallographic structure of recombinant LuxF as well as a study of the interaction of isolated myrFMN with recombinant LuxF and luciferase (LuxAB). Furthermore, we have employed recombinant LuxF to investigate the relationship of myrFMN production and the presence of *luxF* in the *lux*-operon in various bioluminescent *Photobacteria*.

2. Materials & methods

2.1. Photobacterial strains

The following *P. leiognathi* strains were selected for our study: ATCC 25521, ATCC 25587, ATCC 27561, S1, TH1 and svers.1.1. The first two

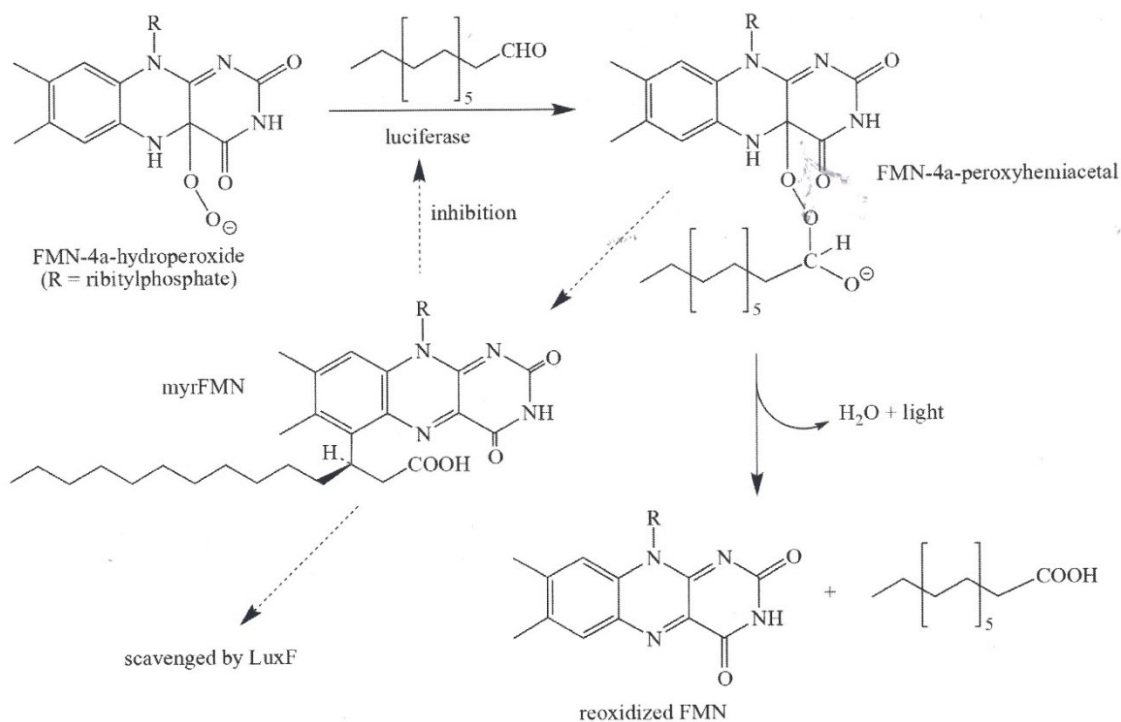
strains were reported to lack *luxF* (*luxF*⁻) whereas ATCC 27561, S1 and svers.1.1 possess *luxF* in the *lux*-operon (*luxF*⁺). The presence of *luxF* in TH1 was not reported prior to our study.

2.2. Instrumentation

UV/Vis absorption spectra were recorded with a Specord 205/210 spectrophotometer (Analytic Jena, Jena, Germany). Difference absorption spectra were recorded using tandem cuvettes. Isothermal calorimetry titrations were performed with a VP-ITC system (MicroCal, Northampton, MA, USA). ³¹P-NMR spectra at 11.75 T were recorded with a Bruker Avance DRX 500 standard-bore spectrometer operating at 202.45631 MHz for ³¹P nuclei. 10 mm-diameter sample tubes were used. The spectral conditions for the samples at 11.75 T were: 8192 time-domain data points; spectral width 40 ppm; acquisition time 1.0 s; 3 s relaxation delay time; 90° pulse angle; 256 transients were recorded per spectrum. Spectra were transformed using an exponential weighting factor of 5 Hz. ³¹P chemical shifts were referenced to external 85% phosphoric acid (=0.00 ppm).

2.3. Construction of expression plasmids for LuxF, LuxAB and LuxB

Based on the reported amino acid sequence of LuxF [17,18] a synthetic gene was designed and optimized for expression in *E. coli*. The synthetic DNA was integrated into the vector pET-21a(+) using the restriction sites *Nde*I and *Xho*I, allowing the use of the C-terminal hexa-histidine tag of the vector, if required, for facilitated protein purification by Ni-NTA affinity chromatography. Furthermore a synthetic gene for *LuxAB* was designed corresponding to the DNA-sequence of *P. leiognathi* S1, with a C-terminal octa-histidine tag and optimized for



Scheme 1. The reaction of the FMN-4a-hydroperoxide with a long-chain fatty aldehyde results in the formation of the FMN-4a-peroxyhemiacetal intermediate. The decay of this species produces the products water, light, FMN and the corresponding long-chain fatty acid. The mechanism for the generation of myrFMN from the FMN-4a-peroxyhemiacetal is unknown.

expression in *E. coli* (DNA 2.0, CA, USA). *E. coli* BL21 (DE3) strain was used for heterologous expression. The expression plasmid for *luxB* was constructed by introducing a *NdeI* restriction site at the 5'-end of the *luxB* gene. Further cloning steps were performed as described before for *luxF* and *luxAB*.

2.4. Expression and purification of recombinant His-tagged proteins

E. coli BL21 (DE3) cells harboring the expression plasmids were grown at 37 °C in LB broth containing ampicillin (100 µg/ml) as selection marker. The cells were induced with 0.5 mM IPTG at $OD_{600} = 0.6$. After induction the cells were further grown for 4 h at 37 °C (*LuxF*) or 16 h at 20 °C (*LuxAB* and *LuxB*). Cells were harvested by centrifugation (7000 g, 10 min, at 4 °C) and the wet cell pellet was stored at –20 °C for further use.

Recombinant protein was purified by resuspension of wet cell paste in lysis buffer pH 8 (50 mM NaH_2PO_4 , 300 mM NaCl and 10 mM imidazole) and lysed by sonication. To remove cell debris the resulting suspension was centrifuged at 30,000 g for 45 min at 4 °C, followed by an additional filtration step. The cleared solution was then loaded onto a pre-equilibrated 5 ml HisTrap FF column (GE Healthcare), washed with about 10 column volumes of wash buffer (50 mM NaH_2PO_4 , 300 mM NaCl and 20 mM imidazole) and finally eluted with elution buffer (50 mM NaH_2PO_4 , 300 mM NaCl and 300 mM imidazole). Protein containing fractions were pooled. In the case of *LuxF*, the protein was dialyzed against 20 mM Tris buffer containing 100 mM NaCl, pH 8. For *LuxAB* and *LuxB* a 45 mM Tris-buffer and 40 mM MES containing 20 mM L-malic acid, pH 8 was used for dialysis. After concentration the proteins were further purified using a Superdex-200 gel filtration column equilibrated with dialysis buffer. The purified protein was further concentrated and stored at –20 °C. The concentrations were determined spectrophotometrically at 280 nm using a molar extinction coefficient employing ProtParam at the ExPASy site following the method of Gill and von Hippel [19]. The extinction coefficients calculated for *LuxF*, *LuxAB* and *LuxB* were 26,025 M⁻¹ cm⁻¹, 83,825 M⁻¹ cm⁻¹ and 36,580 M⁻¹ cm⁻¹, respectively. From 1 l of culture we obtained 40 mg, 35 mg and 45 mg of *LuxF*, *LuxAB* and *LuxB*, respectively.

2.5. Crystallization and X-ray structure determination

For crystallization trials purified, recombinant *LuxF* was used at a concentration of 16 mg/ml. Drops of 1 µl were set up using the microbatch method employing an Oryx 7 crystallization robot (Douglas Instruments Ltd.). After mixing equal volumes of protein and precipitant solution (0.15 M malic acid, 20% w/v polyethylene glycol 3350, pH 7.0) tetragonal *LuxF* crystals grew to full size within 1–2 weeks at 289 K. Crystals were harvested directly from their mother liquor and flash-frozen in liquid nitrogen.

Data from diffraction quality crystals were collected at beamline X06DA (PX-III) of the Swiss Light Source (Paul Scherrer Institute, Villigen, Switzerland). The dataset was integrated and scaled using the XDS suite [20]. Initial phases were obtained by molecular replacement using Phaser [21] with the holo-*LuxF* structure (pdb-code: 1NFP [12]) as search model. The initial model was further refined against reflection data in alternating cycles of real-space refinement against σ_A -weighted 2FO-FC and FO-FC electron density maps and likelihood-based reciprocal space optimisation (including five TLS groups [21]) using the programs Coot [22] and PHENIX [23], respectively. R_{free} values were computed from 5% randomly chosen reflections, which were not used throughout the refinement [24].

No electron density was observed for the 8 C-terminal residues originating from the cloning strategy with a hexa-His tag and its two amino acid linker. In addition, weak electron density was observed for one loop region and amino acids 56–59 were therefore omitted from the final model. Coordinates and structure factors were deposited in the Protein Data Bank (PDB) under accession number 4J2P.

2.6. Isolation and purification of *LuxF* from *P. leiognathi* S1

The isolation and purification of *LuxF* from *P. leiognathi* was described only briefly previously [25]. In the present study, 1 kg (wet weight) of frozen cell paste was suspended in 500 ml 100 mM Tris/HCl, pH 7.5, containing 1 mM dithiothreitol (DDT) and NaN_3 (in the following called "buffer"). The cells were disintegrated at 4 °C using a French press. The resulting suspension was centrifuged at 27,000 g for 1 h at 4 °C. The supernatant was treated with 80% ammonium sulfate (AS) and centrifuged. The precipitate was dissolved in and dialyzed against 4 l of buffer, with two changes in 24 h, centrifuged 10 min at 39,000 g and 4 °C to remove insoluble material. The clear supernatant was loaded onto a Sepharose Q (11 × 2 cm) column equilibrated with buffer, then washed with 200 ml of buffer, followed by washing with 400 ml buffer containing 0.2 M NaCl and then buffer containing 0.5 M NaCl. Fractions showing absorption at 450 nm were collected and pooled. The pooled fractions were dialyzed against 4 l of buffer, with one change in 24 h. The lemon yellow dialysate was loaded again onto a Sepharose Q column, washed with 200 ml buffer, followed by 400 ml buffer containing 0.05 M NaCl, 200 ml buffer containing 0.1 M NaCl, 200 ml buffer containing 0.15 M NaCl and 400 ml buffer containing 0.2 M NaCl. Finally, a gradient of 0.2 M–0.4 M NaCl in buffer (300 ml) was used to elute a brightly yellow protein. The fractions exhibiting a ratio of A_{280}/A_{442} between 7 and 10 were pooled, concentrated to about 20 ml in an ultrafiltration device (Amicon, 10 kDa cut-off filter), and applied to a Sephadex G75 column (90 × 2.5 cm diameter), equilibrated with buffer. Fractions showing a ratio of $A_{280}/A_{442} < 4$ were collected and combined. The yield of *LuxF* was about 200 mg and exhibited a single band on SDS-PAGE.

2.7. Isolation of 6-(3'-*R*)-myristyl)-FMN (*myrFMN*) from *P. leiognathi* S1 using recombinant *LuxF*

For isolation of *myrFMN*, frozen cell paste (~250 g) was allowed to thaw before the cells were suspended in 250 ml of a 0.1 M potassium phosphate buffer, pH 7. To improve cell lysis, the cell suspension was

Table 1
Data collection and refinement statistics.

	Apo- <i>LuxF</i> , PDB-code 4J2P
Data collection	
Space group	I422
Cell dimensions	
<i>a</i> , <i>b</i> , <i>c</i> (Å)	93.2, 93.2, 115.4
α , β , γ (°)	90.0, 90.0, 90.0
Resolution (Å)	50–1.85 (1.95–1.85)
No. unique reflections	22,033
R_{merge}	0.044 (0.66)
<i>I</i> / σ <i>I</i>	41.0 (3.14)
Completeness (%)	99.9 (99.7)
Redundancy	13.4 (8.4)
Wilson B (Å ²)	27.9
Refinement	
Molecules per a.u.	1
Resolution (Å)	39.2–1.85
No. unique reflections	22,031
R_{work}/R_{free}	0.1706/0.2040
No. atoms	2001
Protein	1828
Water	173
β -factors	41.0
Protein	40.6
Water	45.1
R.m.s. deviations	
Bond lengths (Å)	0.007
Bond angles (°)	1.01
Ramachandran	
Favored (%)	99.1
Outliers (%)	0.0
Clashscore	4.4

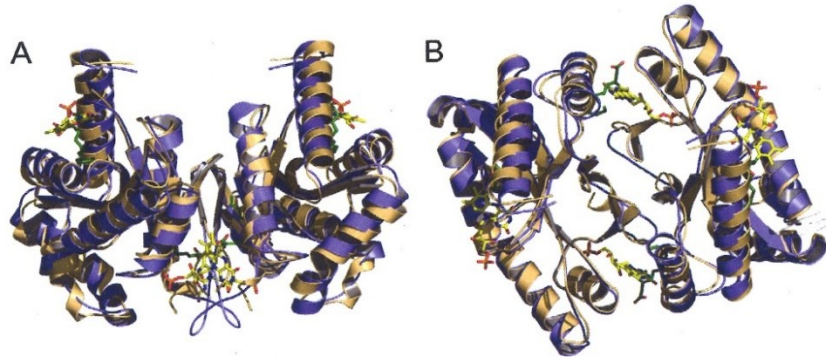


Fig. 1. Structure alignment of recombinant apo-LuxF with holo-LuxF. Both structures are shown as cartoon models. The myrFMN bound LuxF (pdb 1NFP) is shown in blue and apo-LuxF in light brown. The myristylated flavin derivative is shown as a stick model with the FMN moiety in yellow and the myristyl chain in green. (A) The homodimer features two sets of equivalent myrFMN binding sites: two at the interface (lower central part) and two at the N-termini (upper left and right). (B) View into the LuxF barrel (90° rotated with respect to the structure shown in panel A).

incubated with lysozyme for 30 min and further sonicated for 10 min. The lysate was further centrifuged at 30,000 g for 45 min at 4 °C to remove cell debris and the supernatant was filtrated through a Whatman filter (No.1). The supernatant contained free myrFMN as well as protein-bound myrFMN (mostly LuxF).

To retrieve free myrFMN, the supernatant was incubated for 30 min with recombinant histidine-tagged apo-LuxF, which binds four molecules of myrFMN per dimer. Apo-LuxF was then collected by Ni-NTA affinity chromatography and purified as described above. The eluent

fractions were yellow in color, suggesting the presence of myrFMN, pooled and stored at 4 °C for further use.

For the isolation of myrFMN from LuxF, the flow-through was treated with 4 M guanidinium hydrochloride and adjusted to pH 2 with concentrated HCl to release myrFMN. It was then extracted from the aqueous solution by adding 50–100 ml of 1-butanol:ethylacetate (1:1 v/v) solution. The organic phase was separated by centrifugation (4000 g for 10 min at 4 °C) and removed from the aqueous phase. This procedure was repeated until no yellow color was seen in the

PL_ATCC_27561_luxF	VTKNNGVFFLNFXHVGQEQEPLTMSNALETLRIIDEDTSYDVAASEHHIDKSYN---DETKLAPF---VSLGKQIH	73
PL_1NFP	VTKNNGVFFLNFXHVGQEQEPLTMSNALETLRIIDEDTSYDVAASEHHIDKSYN---DETKLAPF---VSLGKQIH	73
PL_TH1_luxF	VTKNNGVFFLNFXHVGQEQEPLTMSNALETLRIMDEEDTSYDVAASEHHIDKSYN---DETKLAPF---VSLGKQIH	73
PL_svers.1.1_luxF	VTKNNGVFFLNFXHVGQEQEPLTMSNALETLRIMDEEDTSYDVAASEHHIDKSYN---DETKLAPF---VSLGNHVV	73
PA_NBRC_104633_luxF	VTKNNGVFFLNFXHVGQEQEPLTMSNALETLRINEDTSYDVTIIEQHIIDKSYN---NETKLAPF---VSLGNHVV	73
PP_NBRC_104104_luxF	VTKNNGVFFLNFXHVGQEQEPLTMSNALETLRIIDEDTSYDVTIIEQHIIDKSYN---NETKLAPF---VSLGNHVV	73
PK_FS-8.1_luxF	VTKNNGVFFLNFXHVGQEQEPLTMSNALETLRIIDEDTSYDVTIIEQHIIDKSYN---NETKLAPF---VSLGNHVV	73
PK_FS-1.1_luxF	VTKNNGVFFLNFXHVGQEQEPLTMSNALETLRIIDEDTSYDVTIIEQHIIDKSYN---NETKLAPF---VSLGNHVV	73
PL_ATCC_27561_LuxB	--MNFGLFFLNFKLGMTSE-AVLDNMIDTIALVDKDEYHFKTAFVNEHHFSSKNGI-96-NDFYNEPK-8-SKENLKQY	174
PL_ATCC_27561_luxF	VLATSPETVVAARYGMPLLFKWDDSQQRRIELLNHYQAAAAAFNVDIAGVRHRLMLFNVNDFPTQAKAELSIYLEDYL	153
PL_1NFP	VLATSPETVVAARYGMPLLFKWDDSQQRRIELLNHYQAAAAAFNVDIAGVRHRLMLFNVNDFPTQAKAELSIYLEDYL	153
PL_TH1_luxF	VLATSPETVVAARYGMPLLFKWDDSQQRRIELLNHYQAAAAAFNVDITGVRHRLMLFNVNDFPTQAKAELSIYLEDYL	153
PL_svers.1.1_luxF	VLATSPETVVAARYGMPLLFKWDDSQQRRIELLNHYQAAAAAFNVDITDVRHRLMLFNVNDFPTQAKAELSIYLEDYL	153
PA_NBRC_104633_luxF	VLATSPETVVAARYGMPLLFKWDDSQQRRIELLNHYQAAAAAFNVDITDVRHRLMLFNVNDFPTQAKAELSIYLEDYL	153
PP_NBRC_104104_luxF	VLATSENTVDSAAKYALPLVFKWDDTNEERLKLSSYNASASKYKRNIDLVRHQMLMLNVNEAETVAKEELKSYFENVV	153
PK_FS-8.1_luxF	VLATSENTVDSAAKYALPLVFKWDDTNEERLKLSSYNASASKYKRNIDLVRHQMLMLNVNEAETVAKEELKSYFENVV	153
PK_FS-1.1_luxF	VLATSENTVDSAAKYALPLVFKWDDTNEERLKLSSYNASASKYKRNIDLVRHQMLMLNVNEAETVAKEELKSYFENVV	153
PL_ATCC_27561_LuxB	ILATSMGVVWAAKGLPLTYRNSDTLAEKENYQRYLTVAAENNVDTIHDVDFPFLVNIINPDRDIAQEMRDYIRGYI	254
PL_ATCC_27561_luxF	SYTQA---ETSIDEIINSNAAGNDTGLHHEAEMAQGLNKKVDFLCEESMKDQENKKSIMINIDKRVINRKEHNLN	228
PL_1NFP	SYTQA---ETSIDEIINSNAAGNDTGLHHEAEMAQGLNKKVDFLCEESMKDQENKKSIMINIDKRVINRKEHNLN	228
PL_TH1_luxF	SYTQA---ETSIDEIINSN'TAGNDTGLHHEAEMAQGLNKKVDFLCEESMKDQENKKSIMINIDKRVINRKEHNLN	228
PL_svers.1.1_luxF	SYTQA---EASIDEIINSNAAGNDTGLHHEAEMAQGLNKKVDFLCEESIKLQDNKKSIMINIDKRVINRKRHQLK	228
PA_NBRC_104633_luxF	SYTKI---EAPIDDIINRNAAGNDTGLHHEAEMAQGLNKKVDFLCEESMKDQENKKSIMINIDKRVINRKEHNLN	228
PP_NBRC_104104_luxF	ACTQPS-NFNGSIDSIQSNVTGSKKDCSYANLAGKFDNTVDFLCEESMQDQNKKKSIMIDNNVIVIKRQDNNLI	231
PK_FS-8.1_luxF	ACTQPS-NFNGSIDSIQSNVTGSKKDCSYANLAGKFDNTVDFLCEESMQDQNKKKSIMIDNNVIVIKRQDNNLI	231
PK_FS-1.1_luxF	ACTQPS-NFNGSIDSIQSNVTGSKKDCSYANLAGKFDNTVDFLCEESMQDQNKKKSIMIDNNVIVIKRQDNNLI	231
PL_ATCC_27561_LuxB	AEAYPNTDQEEKIEELIKQHAVGTEDYEYSSKYLEKTKGSKVLLSFEESMKNAAVIDLINMVEKI----KKNL-	327

Fig. 2. Multiple sequence alignment of LuxF proteins from different photobacterial strains compared to the LuxB protein from *Photobacterium leiognathi*. PL – *Photobacterium leiognathi*; PA – *Photobacterium aquimaris*; PP – *Photobacterium phosphoreum* and PK – *Photobacterium kishitani*. GenInfo Identifier numbers: PL_ATCC_27561_luxF – GI 37812030; PL_1NFP – GI 157832107; PL_svers.1.1_luxF – GI 111380328; PA_NBRC_104633_luxF – GI 388892190; PP_NBRC_104104_luxF – GI 159576916; PK_FS-8.1_luxF – GI 61661674; PP_FP390 – GI 119116590; PP_FS-1.1_luxF – GI 61661594; PL_ATCC_27561_LuxB – GI 37812029. Color code: yellow – amino acids accommodating the myristic acid in the hydrophobic patch at the interface binding site; orange – amino acids involved in the polar interactions with the ribitylphosphate side chain at the interface binding site; light green – amino acids accommodating the myristic acid in the hydrophobic patch at the N-terminal binding site; dark green – amino acids involved in the polar interactions with the ribitylphosphate side chain at the N-terminal binding site; bold letters – conserved amino acids in LuxF.

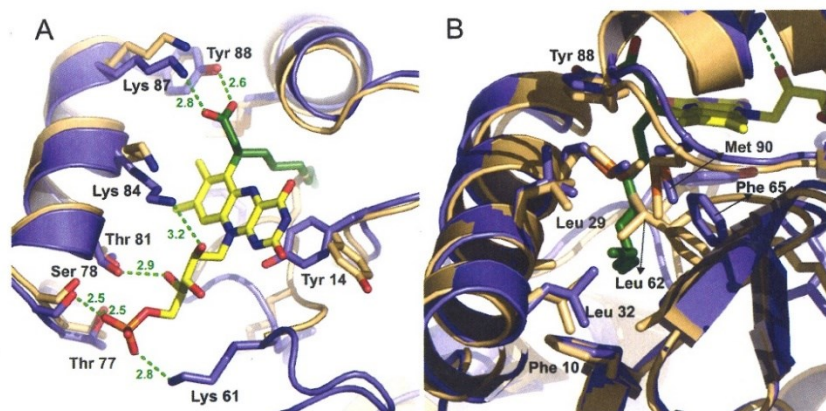


Fig. 3. Detailed view of the LuxF-dimer interface binding site of myrFMN. (A) Interactions between amino acids and polar regions of myrFMN. myrFMN and selected amino acids are shown as stick models using the same color-coding as in Fig. 1. One salt bridge and two inter-atom distances between the flavin methyl groups and surrounding amino acids are indicated as dashed green lines and distances are provided in Å. (B) Rendition of the hydrophobic channel accommodating the myristyl chain.

precipitate at the phase interface. The organic solvent was then dried in a vacuum evaporator at 50 °C under reduced pressure. The residual powder was dissolved in potassium phosphate buffer.

Free myrFMN captured by recombinant apo-LuxF was released from the protein and extracted as described in the previous section. Desalting of isolated myrFMN was achieved by dissolving the yellow powder in 100 mM potassium phosphate buffer pH 7 and loading onto a C18-sepak column, and was washed with 20 ml of water. The yellow organic eluent was further dried by evaporation and the yellow powder was stored at –20 °C. The purity of myrFMN was evaluated by HPLC.

2.8. Detection of luxF in Photobacteria

In order to analyze the presence of luxF in the lux operon colony PCR was conducted using the following primers: 5'-GGAATTCCATATGACA AAATGGAATTATGGCGTCTCTTC CTTAATTTTACC-3' (forward) and 5'-CCGCTCGAGGTTAAGGTTGTCTTCTTCTA TAATTAATAACGCG-3' (reverse).

2.9. Detection of myrFMN by HPLC

HPLC analysis was performed with a Dionex UltiMate 3000 HPLC using an Atlantis® dC18 5 μM (4.6 × 250 mm) column. Separation was achieved using a linear gradient of 0.1% TFA in water and 0.1% TFA in acetonitrile (20 min, 25 °C) from 0% to 95% at a flow rate of 1 ml/min. Peak detection was at 280, 370 and 450 nm, respectively. Under these conditions FAD, FMN and riboflavin elute at around 10 ml whereas myrFMN elutes at 19 ml.

3. Results

3.1. Expression and purification of recombinant LuxF

Heterologously expressed LuxF was purified using a C-terminal hexa-histidine tag by means of Ni-NTA affinity chromatography. From 1 l of bacterial culture 35 mg of purified protein was obtained. The concentrated protein (ca. 20 mg/ml) was colorless with no absorption

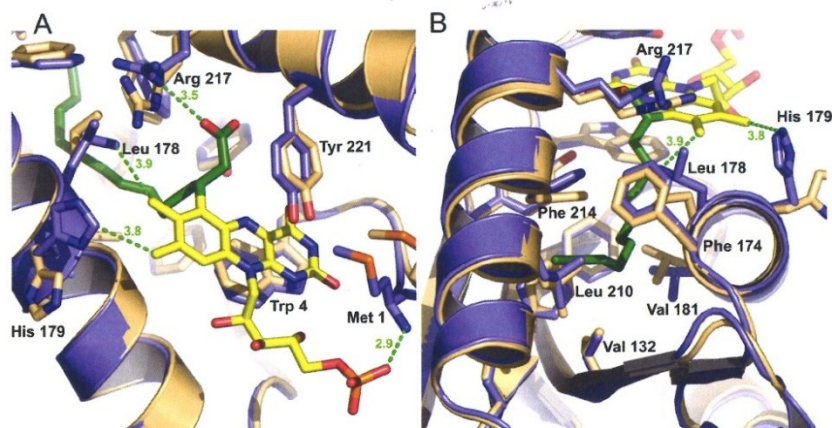


Fig. 4. Detailed view of the N-terminal binding site of myrFMN. For clarity, only the protomers of the holo- and apo-structures were aligned for this representation. myrFMN and selected amino acids are shown as stick models using the same color-coding as in Fig. 1. Two salt bridges and two inter-atom distances between the flavin methyl groups and surrounding amino acids are indicated as dashed green lines and distances are provided in Å. (A) In contrast to the interface binding site, only relatively few polar interactions are observed between amino acids and myrFMN (e.g., Met1 and Arg217). Note, however, the similar position of Tyr221 and Trp4 in the apo- and holo-structures between which the isoalloxazine ring system is stacked. (B) View into the preformed hydrophobic tunnel that accommodates the apolar part of the myristyl moiety.

in the visible range (350–800 nm). This result was not unexpected as the myristylated flavin derivative (myrFMN) is thought to be a side product of the luciferase reaction and the expression host lacks the enzymes responsible for light production (see introduction). Obviously LuxF has a low affinity to other naturally occurring flavin molecules, such as riboflavin, FMN and FAD and hence is isolated as an apoprotein.

3.2. Crystal structure of apo-LuxF

The high affinity of LuxF to myrFMN suggested that the recombinant protein adopts a native structure, which is fully competent to scavenge the derivatised flavin. To get more insight into the apo-structure of LuxF and the changes occurring upon myrFMN binding we analyzed our colorless LuxF crystals by X-ray crystallography. Data sets diffracting to 1.85 Å resolution were collected using synchrotron radiation at the Swiss-Light-Source (SLS) in Villigen, Switzerland and the structure was solved by molecular replacement using the holo-structure of LuxF [12] as template (Table 1):

The tetragonal crystal form (space group *I*422) contained one protein chain in the asymmetric unit which forms a dimer with a symmetry equivalent molecule according to a PISA (Proteins, Interfaces, Structures and Assemblies) analysis [26]. As shown in Fig. 1, the overall structure of recombinant LuxF is very similar to the one determined earlier for the holo-protein. The dimeric structures could be aligned with an overall RMSD of 1.2 Å using the protein structure alignment tool in PyMol. The largest differences between apo- and holo-structure were found at the interface of the homodimer, where two myrFMN binding sites are located near a loop region that is reorganized upon ligand binding. Interestingly, this region, connecting residues Ile52 and Pro64, corresponds to the structural element that substitutes for the deletion of ~100 amino acids present in the ancestral luxB gene product (Fig. 2). Similarly, the other two binding sites, which are located near the N-termini of the homodimer, also feature important residues that have been added during the functional divergence from LuxB (e.g., Trp4, Tyr6 and Tyr221, Fig. 2). A close-up of the structural comparison of the interface binding site (Fig. 3) shows substantial movement of amino acid side chains that interact with the ribitylphosphate side

chain attached to N(10) of the isoalloxazine ring. These amino acids form hydrogen bonds to C2'(OH) (Lys84) and C4'(OH) (Thr81) as well as a salt bridge and two hydrogen bonds to the phosphate group (Lys61 and Thr77 + Ser78, respectively). In addition, Tyr14 flips into the binding site to interact with the isoalloxazine ring system in a π -stacking fashion and Lys87 as well as Tyr88 coordinate the negatively charged myristic acid carboxylate group. In contrast to these pronounced changes near the polar regions of the myrFMN ligand, the apolar alkyl chain of the myristic acid is predominantly embedded in a pre-organized binding pocket with rather small spatial adjustments of all surrounding amino acid side chains excluding Leu62, which is part of the rearranged loop region described above and substantially changes position to accommodate the myristyl side chain (Fig. 3B).

Interestingly, the two myrFMN binding sites that are found near the N-termini (Fig. 4) are distinct from the interface binding sites by having fewer interactions between amino acid side chains and the ribitylphosphate side chain [11] or in other words, the ribitylphosphate side chain appears less involved in binding interactions to the protein in the N-terminal binding site. In fact, only one salt bridge is formed between the phosphate group and the N-terminal amino group (Fig. 4A). Closer inspection of the apo- and holo-protein structure at the N-terminal binding sites reveals that other contacts appear to play

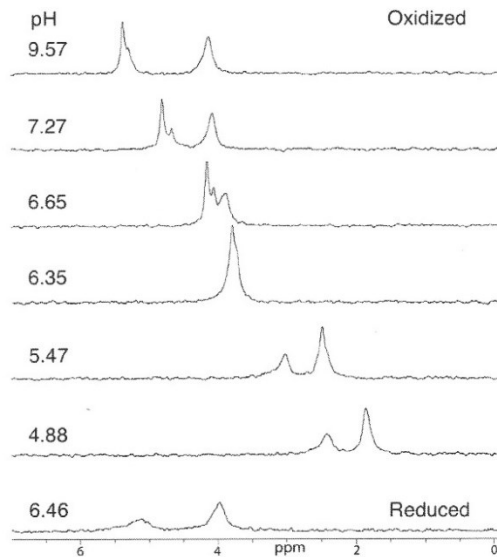


Fig. 5. ^{31}P -NMR spectra of LuxF isolated from *P. leognathi* S1 at various pH. ^{31}P -NMR spectra were recorded at the pH values indicated. The bottom spectrum was recorded under reducing conditions.

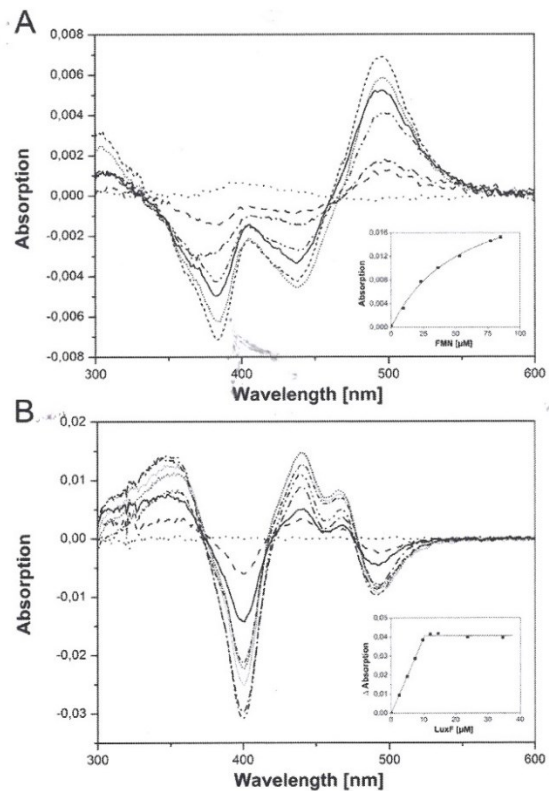


Fig. 6. Titration of apo-LuxF with FMN (panel A) and myrFMN (panel B) as monitored by UV/Vis differential absorption spectroscopy. (A) 50 μM apo-LuxF was titrated with 2.5 mM FMN in tandem cuvettes at 25 °C and absorption spectra was recorded after each addition from 300 to 600 nm. Data points in the insert were fitted to a hyperbolic equation yielding a K_d of 50 μM . (B) 20 μM myrFMN was titrated with 450 μM apo-LuxF in tandem cuvettes at 25 °C and absorption spectra was recorded after each addition from 300 to 600 nm. Based on the sharp titration endpoint, only a stoichiometry of four molecules of myrFMN per LuxF-homodimer could be calculated.

a role in accommodating the myrFMN: Most notably, the stacking of the isoalloxazine ring system between residues Trp4 and Tyr221 appears to be an important determinant of this binding site due to the evolutionary divergence of the corresponding sequence elements from LuxB (Fig. 2). In addition, the imidazole ring of His179 swings by ca. 90° to accommodate the isoalloxazine ring in the binding site (Fig. 4A) and Leu178 moves closer to the edge of the benzene moiety of the isoalloxazine ring. Also, the carboxyl group of the myristyl residue forms a salt-bridge to the guanidinium group of Arg217, which is already in place in apo-LuxF and just moves slightly to interact with the carboxyl group. However, apart from Leu178 there is no strong conservation of these amino acids in LuxF homologs (Fig. 2) suggesting that their role in myrFMN binding might only be marginal. Similar to observations for the interface binding site, the hydrophobic channel that holds the apolar part of the myristyl moiety is essentially preformed by several conserved residues and seems to undergo only slight adjustments upon binding of myrFMN (Fig. 4B). Some of the important hydrophobic residues are significantly different to amino acids at the corresponding positions of the LuxB ancestor (e.g., Phe 174, Leu178 and Val181), suggesting that the hydrophobic binding pocket also significantly contributes to efficient binding of myrFMN.

In summary, the two structurally different binding sites apparently employ common strategies to accommodate the apolar moiety of myrFMN in a hydrophobic tunnel, to bind the carboxylate of the myristic acid via salt bridges and to interact with the isoalloxazine ring system via π -stacking. Interestingly, the stacking interactions with the isoalloxazine ring system are induced upon myrFMN binding at the interface (Tyr14) but are already preformed at the N-terminal binding site (Trp4 and Tyr221). In contrast to the overall similarities of myrFMN binding, interactions with the polar ribitylphosphate chain are much more pronounced for the interface binding sites, suggesting that myrFMN binds more strongly at the interface site.

Some more detailed information regarding flavin binding was obtained by ^{31}P NMR spectroscopy. At pH 7.27 there are two main peaks observed resonating at 4.1 ppm and 4.8 ppm and a smaller one at 4.7 ppm. Deconvolution of the spectrum revealed that the peak at 4.1 ppm accounts for 49% of the total intensity while the smaller peak at 4.8 ppm accounts for 35%. The origin of the small peak at 4.7 ppm (16%) remains unassigned. The line width of the peak at 4.1 and 4.8 ppm is 22 Hz and 9 Hz, respectively (determined under proton decoupling conditions). The line widths strongly indicate that the two phosphate groups of the two flavins in the protein experience a different environment and/or mobility. Additions of incremental amounts of Mn^{2+} to the preparation revealed that the peak at 4.8 ppm broadens somewhat faster than the peak at 4.1 ppm. These data, in combination with the line widths, very strongly indicate that the peak at 4.8 ppm can be assigned to the phosphate group of the flavin located at the interface of the protein. Conversely the peak at 4.1 ppm is assigned to the flavin located close to the surface at the N-terminal binding site. This interpretation is in full agreement with the X-ray data (see above). The accessibility of the two phosphate groups bound to the protein prompted us to undertake a pH-dependent study of the ^{31}P NMR spectra (Fig. 5). For the high and low field peak a pK_a value of 6.3 and 6.0, respectively, was determined (data not shown). The current ^{31}P NMR data of the protein show very unusual features as compared to those of flavoproteins of similar sizes, e.g., flavodoxins [27] as none show a pH-dependency or bulk solvent accessibility. In the two-electron reduced state the two peaks appear at 4.0 ppm and 5.3 ppm at pH 6.46 (Fig. 5, bottom spectrum). The downfield shifts of the resonances observed upon reduction were also found in other FMN-containing proteins [27]. The increase in line width of the lowfield peak can be ascribed to conformational changes at the phosphate site and/or a more restricted mobility of the phosphate group as compared to those in the oxidized state.

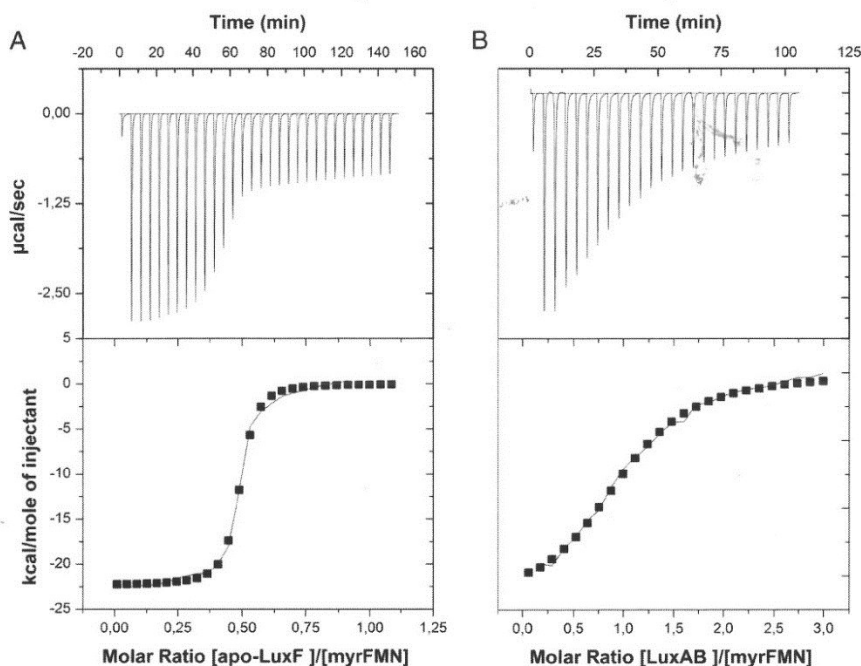


Fig. 7. Determination of dissociation constants by isothermal titration calorimetry. (A) The measurement shows the titration of 45 μM myrFMN with recombinant apo-LuxF (300 μM in 20 mM Tris-buffer, containing 100 mM NaCl, pH 8 at 25 °C). (B) The measurement shows the titration of 45 μM myrFMN with recombinant luciferase (450 μM in 45 mM Tris-buffer, 40 mM MES, containing 20 mM L-malic acid, pH 8 at 25 °C).

3.3. Binding of FMN and myrFMN to apo-LuxF

To evaluate the binding capacity of isolated apo-LuxF we performed difference titration experiments with FMN and myrFMN isolated from *P. leiognathi* S1 (for isolation of myrFMN see Materials & Methods). Primarily, we investigated the binding of FMN to apo-LuxF with increasing FMN concentration. The concentration dependence yielded a K_d of $\approx 50 \mu\text{M}$ for the binding of FMN to apo-LuxF (Fig. 6, panel A). Furthermore, we observed the absorption changes in the spectrum of myrFMN, as a function of LuxF concentration. In contrast to FMN, myrFMN bound much more tightly to apo-LuxF as indicated by the sharp titration end point (Fig. 6, panel B and insert). Therefore, we used isothermal microcalorimetry (ITC) to determine the dissociation constant for the binding of myrFMN to apo-LuxF. With the ITC, a single binding isotherm was

obtained for the titrations with FMN (data not shown) and myrFMN (Fig. 7, panel A) indicating that the two binding sites are thermodynamically indistinguishable. Hence, isotherms were fitted to a single binding site model, yielding dissociation constants of $\approx 25 \mu\text{M}$ for FMN and $80 \pm 20 \text{ nM}$ for myrFMN, respectively.

3.4. Binding of myrFMN to photobacterial luciferase

In parallel microcalorimetry experiments, myrFMN was titrated with recombinant luciferase (*luxAB* from *P. leiognathi* S1) (Fig. 7, panel B). This yielded a dissociation constant of $4.0 \pm 0.4 \mu\text{M}$ (three independent ITC measurements). Thus binding of myrFMN to luciferase is 50-fold weaker than to apo-LuxF. In a similar experiment recombinant β -homodimer of *P. leiognathi* luciferase was titrated with myrFMN. No binding was

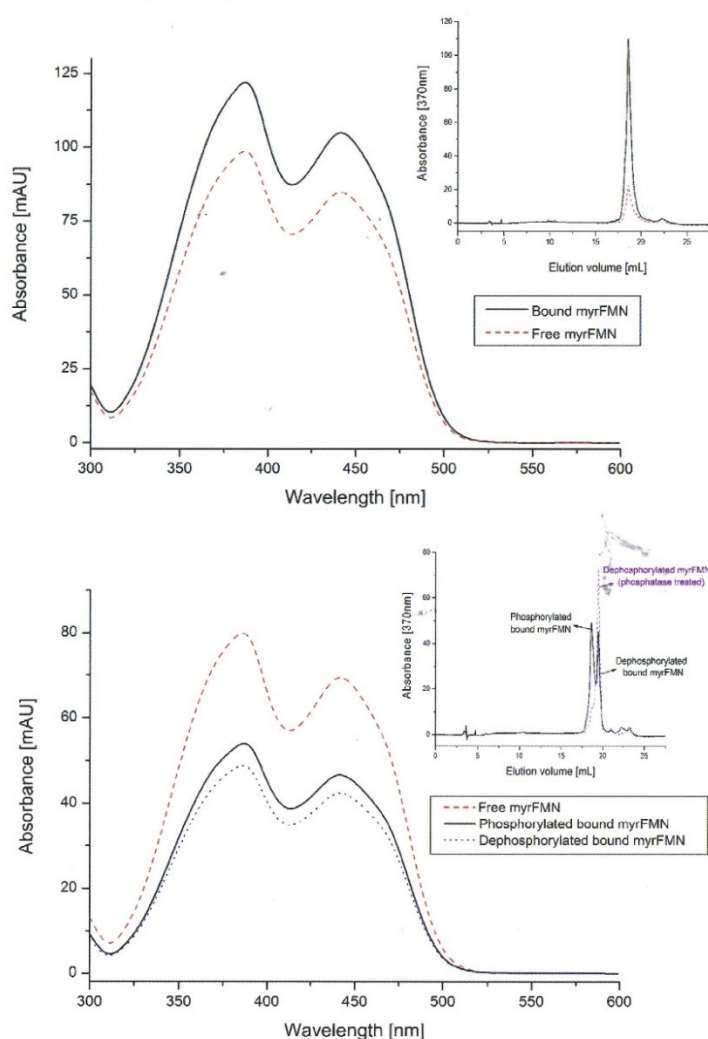


Fig. 8. Identification of myrFMN scavenged by apo-LuxF from *P. leiognathi* S1 (top panel) and TH1 (bottom panel). Top panel, UV/Vis absorption spectrum of the free myrFMN (red dashed line) and bound myrFMN (black solid line). Insert shows the chromatograms from HPLC analysis. A similar analysis using *P. leiognathi* TH1 is shown in the bottom panel: UV/Vis absorption spectrum of free myrFMN (red dashed line) and bound myrFMN (black solid line and blue dotted line, representing the phosphorylated and dephosphorylated form of myrFMN). myrFMN isolated from the bound fraction was further treated with phosphatase resulting in a shift from 18 ml to 19.5 ml elution volume. The insert shows the HPLC trace of myrFMN isolated from the bound fraction before (black solid line featuring two peaks) and after phosphatase treatment (violet dashed line with a single peak at 19.5 ml elution volume).

observed in this case indicating that the β -homodimer does not bind myrFMN (data not shown).

3.5. Screening several species of Photobacteria with apo-LuxF

Tight binding of myrFMN to recombinant apo-LuxF was exploited to monitor its occurrence in several bioluminescent marine bacteria (see Materials & methods). This analysis was performed in two ways: we incubated the supernatant of cell extracts with recombinant apo-LuxF to scavenge the free myrFMN. Furthermore, after scavenging free myrFMN, we precipitated all the proteins of the cell extract using 4 M guanidinium hydrochloride. This led to the release of any protein-bound myrFMN (from LuxF and possibly luciferase) and then the analysis was repeated. In each case, the histidine-tagged LuxF was isolated by affinity chromatography and myrFMN was then released by acid precipitation from the purified recombinant LuxF and the supernatant was subjected to HPLC analysis. As shown in Fig. 8, myrFMN was clearly detectable in the untreated supernatant of crude extracts (free myrFMN) as well as in the acid-treated fraction (bound myrFMN). Furthermore our analysis showed that the majority of myrFMN was in the bound fraction, i.e., bound to either LuxF or luciferase.

The highest amount of myrFMN was found in *P. leiognathi* S1 and TH1. However, trace amounts were also detected in all other photobacterial strains analyzed in our study (Fig. 9). Because the composition of the *lux*-operon was not clear for TH1 we performed colony PCR with *luxF* specific primers to check for its presence (see Experimental procedures). As expected a PCR product with the calculated size of ~680 bp was obtained for *P. leiognathi* S1, ATCC 27561 and svers.1.1 but not for ATCC 25521 and ATCC 25587 (Fig. 9, insert). In addition, a PCR product was obtained for strain TH1 indicating the presence of *luxF*. To further substantiate the presence of *luxF* in TH1, the PCR product was sequenced and compared with known *luxF* sequences (Fig. 2). The PCR product obtained for TH1 is highly similar to previously reported *luxF* sequences and thus confirms the presence of *luxF* in this strain.

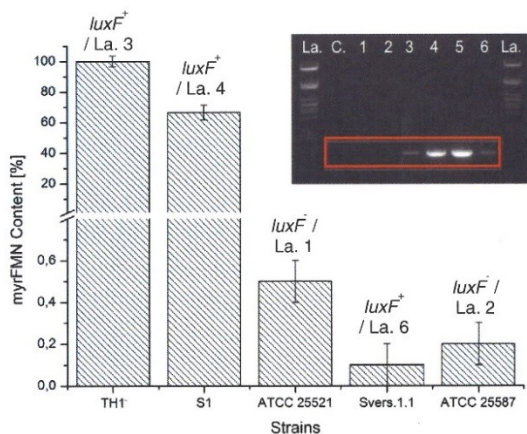


Fig. 9. Occurrence of myrFMN in photobacterial species. Total amount of myrFMN isolated from the cells grown in liquid culture. TH1 produced the highest amount of myrFMN and was set to 100%. The strains TH1, S1 and svers.1.1 are *luxF*⁺ and the two strains ATCC 25521 and ATCC 25587 are *luxF*⁻. The analysis was carried out in triplicate. Insert shows the analysis of different *P. leiognathi* strains for the presence of *luxF* in the *lux*-operon. Shown are the results from colony PCR with common primers for *luxF* (see Experimental procedures). Lanes were loaded with the following samples: La., λ /PstI ladder; C., sterile control (sample contains H₂O instead of DNA); 1, ATCC 25521; 2 ATCC 25587; 3, TH1; 4, *P. leiognathi* S1; 5, ATCC 27561 and 6, svers.1.1.

4. Discussion

The generation of 6-(3'-(*R*)-myristyl)-FMN (myrFMN) in some species of *Photobacteria* is a largely unexplored phenomenon in bacterial bioluminescence. According to a current hypothesis, myrFMN is produced in a side-reaction of luciferase and LuxF functions as a scavenger to prevent its inhibition (Scheme 1) [11]. Although this appears to be a plausible explanation, solid experimental evidence is limited to a study of the affinity and inhibitory effect of myrFMN on luciferase from *V. harveyi* [16]. However, the relationship between the occurrence of *luxF* and the generation of myrFMN remained to be analyzed. Therefore, we set out to study the binding properties of apo-LuxF because despite the availability of a three-dimensional structure of holo-LuxF [10–12] nothing was known about the ligand binding specificity and affinity of the protein. Similarly, binding of myrFMN to photobacterial luciferase was not investigated in any detail yet. Furthermore, we were interested whether the generation of myrFMN is linked to the presence of *luxF* in the *lux* operon. To address these questions we established the recombinant production of LuxF and luciferase by expressing *luxF* and *luxAB* from *P. leiognathi* S1, respectively, in *E. coli* host cells. To assess the binding specificity and affinity of LuxF, we performed difference absorption titrations with FMN and myrFMN isolated from *P. leiognathi* S1 (see Experimental procedures). These experiments showed that both flavins bind to recombinant apo-LuxF albeit with different affinities (Fig. 6). In the case of myrFMN the sharp titration endpoint suggested binding in the low micromolar range and therefore accurate determination of the dissociation constant was achieved by ITC (Fig. 7). These measurements yielded dissociation constants of $\approx 25 \mu\text{M}$ and 80 nM for FMN and myrFMN, respectively, indicating that the myristic acid moiety substantially contributes to the binding energy. Interestingly, the two distinct binding sites appear to be fairly similar in their affinity to myrFMN and FMN since the binding isotherm could be fitted to a single site-binding model despite the differences seen in ³¹P-NMR spectroscopy. Similarly, the spectral changes observed in difference absorption spectroscopy proceeded with a single set of isosbestic points again indicating that the two sites provide similar environments with similar binding affinities.

The hypothetical role of LuxF as a scavenger for myrFMN was supported by ITC measurements with recombinant luciferase (LuxAB). The dissociation constant for binding of myrFMN to luciferase is ca. 50 times higher and thus enables LuxF to trap myrFMN efficiently to prevent inhibition of luciferase. Interestingly, a homodimer of the β -subunit of luciferase is not capable of binding myrFMN indicating that the β -subunit lacks both types of binding sites found in LuxF despite their suspected evolutionary relationship (i.e., *luxF* has arisen by gene duplication from *luxB*). Multiple sequence alignment shows that LuxF from different photobacterial strains possess conserved amino acids in both binding sites. Interestingly, these are not present in LuxB indicating that evolutionary neo-functionalization required major changes in the length and composition of the duplicated gene. In the same vein, LuxF shows a deletion of almost 100 amino acids as compared to the LuxB sequence with most of the amino acids conserved in both LuxF and LuxB are mainly important in the structural backbone of the protein.

Crystals obtained with recombinant LuxF were colorless and this led to the conclusion that LuxF was isolated in an unliganded form, i.e., as an apo-protein. This was not unexpected since *E. coli* lacks the genes *luxAB* encoding luciferase, which is held responsible for the generation of myrFMN. On the other hand, this initial observation also indicated that other naturally occurring flavin derivatives, such as riboflavin, FMN and FAD, do not bind (tightly) to LuxF. This was confirmed for FMN (as the most likely candidate to bind to apo-LuxF), which exhibits a dissociation constant in the range of 25–50 μM and is thus 300–600 fold higher than for myrFMN.

Structural analysis by X-ray crystallography confirmed that the four binding sites in the LuxF dimer were not occupied. The overall topology

of apo-LuxF is nearly identical to the previously reported (holo-) LuxF structure (RMSD of 1.2 Å, Fig. 1). Differences are seen mainly in the interface binding pocket where loops are reorganized to enable contacts between amino acid side chains and the N(10)-ribitylphosphate chain of myrFMN, e.g., formation of contacts to Tyr14 and Lys61 (Fig. 3). On the other hand, the changes observed in the other binding site near the N-terminus involve reorientation of amino acid side chains to form additional contacts (e.g., Arg217 and the carboxyl group of the myristic acid) or to accommodate the dimethylbenzene moiety of the isoalloxazine moiety (e.g., His179). Hence, LuxF provides two preorganized binding pockets, which are only slightly rearranged in the course of myrFMN binding.

Having demonstrated that recombinant apo-LuxF tightly binds myrFMN we exploited this property to analyze different bioluminescent species for their myrFMN content. This revealed that myrFMN occurs in all strains regardless of the presence of *luxF* in the *lux*-operon. This finding rules out that LuxF is the source of myrFMN as speculated earlier [28]. In the strongest producers of myrFMN, TH1 and S1, we found that a detectable fraction of myrFMN occurred free in the cell indicating that its production outruns the biosynthesis of the scavenger protein LuxF.

Acknowledgments

We like to thank Profs. Chaiyen, Mahidol University, and Paul Dunlap, University of Michigan, for the generous gift of *P. leiognathi* TH1 and ATCC 25521, ATCC 25587, ATCC 27561 and svers.1.1, respectively. We also appreciate the help of Jakov Ivkovic for his support with the HPLC-MS analysis of isolated myrFMN samples.

References

- [1] J.W. Hastings, J. Spudich, G. Malnic, The influence of aldehyde chain length upon the relative quantum yield of the bioluminescent reaction of *Achromobacter fischeri*, *J. Biol. Chem.* 238 (1963) 3100–3105.
- [2] S. Ulitzur, J.W. Hastings, Evidence for tetradecanal as the natural aldehyde in bacterial bioluminescence, *Proc. Natl. Acad. Sci. U. S. A.* 76 (1979) 265–267.
- [3] M. Kurfurst, S. Ghisla, J.W. Hastings, Characterization and postulated structure of the primary emitter in the bacterial luciferase reaction, *Proc. Natl. Acad. Sci. U. S. A.* 81 (1984) 2990–2994.
- [4] X. Li, D.C. Chow, S.C. Tu, Thermodynamic analysis of the binding of oxidized and reduced FMN cofactor to *Vibrio harveyi* NADPH-FMN oxidoreductase FRP apoenzyme, *Biochemistry* 45 (2006) 14781–14787.
- [5] S. Nijvipakul, J. Wongratana, C. Suadee, B. Entsch, D.P. Ballou, P. Chaiyen, LuxG is a functioning flavin reductase for bacterial luminescence, *J. Bacteriol.* 190 (2008) 1531–1538.
- [6] E.A. Meighen, Bacterial bioluminescence: organization, regulation, and application of the lux genes, *FASEB J.* 7 (1993) 1016–1022.
- [7] C.Y. Lee, R.B. Sztitner, E.A. Meighen, The lux genes of the luminous bacterial symbiont, *Photobacterium leiognathi*, of the ponyfish. Nucleotide sequence, difference in gene organization, and high expression in mutant *Escherichia coli*, *Eur. J. Biochem.* 201 (1991) 161–167.
- [8] R.R. Soly, J.A. Mancini, S.R. Ferri, M. Boylan, E.A. Meighen, A new lux gene in bioluminescent bacteria codes for a protein homologous to the bacterial luciferase subunits, *Biochem. Biophys. Res. Commun.* 155 (1988) 351–358.
- [9] J.A. Mancini, M. Boylan, R.R. Soly, A.F. Graham, E.A. Meighen, Cloning and expression of the *Photobacterium phosphoreum* luminescence system demonstrates a unique lux gene organization, *J. Biol. Chem.* 263 (1988) 14308–14314.
- [10] S.A. Moore, M.N. James, Common structural features of the luxF protein and the subunits of bacterial luciferase: evidence for a (beta alpha)8 fold in luciferase, *Protein Sci.* 3 (1994) 1914–1926.
- [11] S.A. Moore, M.N. James, D.J. O’Kane, J. Lee, Crystal structure of a flavoprotein related to the subunits of bacterial luciferase, *EMBO J.* 12 (1993) 1767–1774.
- [12] S.A. Moore, M.N. James, Structural refinement of the non-fluorescent flavoprotein from *Photobacterium leiognathi* at 1.60 Å resolution, *J. Mol. Biol.* 249 (1995) 195–214.
- [13] A.A. Raibekas, Green flavoprotein from *P. leiognathi*: purification, characterization and identification as the product of the lux G(N) gene, *J. Biolumin. Chemilumin.* 6 (1991) 169–176.
- [14] S. Kasai, Preparation of P-flavin-bound and P-flavin-free luciferase and P-flavin-bound beta-subunit of luciferase from *Photobacterium phosphoreum*, *J. Biochem.* 115 (1994) 670–674.
- [15] J.W. Hastings, C.J. Potrikus, S.C. Gupta, M. Kurfurst, J.C. Makemson, Biochemistry and physiology of bioluminescent bacteria, *Adv. Microb. Physiol.* 26 (1985) 235–291.
- [16] C.J. Wei, B. Lei, S.C. Tu, Characterization of the binding of *Photobacterium phosphoreum* P-flavin by *Vibrio harveyi* luciferase, *Arch. Biochem. Biophys.* 396 (2001) 199–206.
- [17] B.A. Illarionov, V.M. Blinov, A.P. Donchenko, M.V. Protopopova, V.A. Karginov, N.P. Mertvetsov, J.I. Gitelson, Isolation of bioluminescent functions from *Photobacterium leiognathi*: analysis of luxA, luxB, luxG and neighboring genes, *Gene* 86 (1990) 89–94.
- [18] B.A. Illarionov, M.V. Protopopova, V.A. Karginov, N.P. Mertvetsov, J.I. Gitelson, Nucleotide sequence of part of *Photobacterium leiognathi* lux region, *Nucleic Acids Res.* 16 (1988) 9855.
- [19] S.C. Gill, P.H. von Hippel, Calculation of protein extinction coefficients from amino acid sequence data, *Anal. Biochem.* 182 (1989) 319–326.
- [20] W. Kabsch, Integration, scaling, space-group assignment and post-refinement, *Acta Crystallogr.* 66 (2010) 133–144.
- [21] A.J. McCoy, R.W. Grosse-Kunstleve, P.D. Adams, M.D. Winn, L.C. Storoni, R.J. Read, Phaser crystallographic software, *J. Appl. Crystallogr.* 40 (2007) 658–674.
- [22] P. Emsley, B. Lohkamp, W.G. Scott, K. Cowtan, Features and development of coot, *Acta Crystallogr. D66* (2010) 486–501.
- [23] P.D. Adams, P.V. Afonine, G. Bunkoczi, V.B. Chen, I.W. Davis, N. Echols, J.J. Headd, L.-W. Hung, G.J. Kapral, R.W. Grosse-Kunstleve, A.J. McCoy, N.W. Moriarty, R. Oeffner, R.J. Read, D.C. Richardson, J.S. Richardson, T.C. Terwilliger, P.H. Zwart, PHENIX: a comprehensive Python-based system for macromolecular structure solution, *Acta Crystallogr. D66* (2010) 213–221.
- [24] G.J. Kleywegt, A.T. Brunger, Checking your imagination: applications of the free R value, *Structure* 4 (1996) 897–904.
- [25] D. O’Kane, J. Vervoort, F. Müller, J. Lee, Purification and characterization of an unusual non-fluorescent flavoprotein from *Photobacterium leiognathi*, in: D.E.M. Edmondson, D. B. (Eds.), *Flavins and Flavoproteins*, Walter de Gruyter, Berlin, New York 1987, pp. 641–645.
- [26] E. Krissinel, K. Henrick, Inference of macromolecular assemblies from crystalline state, *J. Mol. Biol.* 372 (2007) 774–797.
- [27] F. Müller, Nuclear magnetic resonance studies on flavoproteins, in: F. Müller (Ed.), *Chemistry and Biochemistry of Flavoproteins*, vol. III, CRC Press, Boca Raton, Ann Arbor, London 1992, pp. 557–595.
- [28] D.J. O’Kane, D.C. Prasher, Evolutionary origins of bacterial bioluminescence, *Mol. Microbiol.* 6 (1992) 443–449.

Chapter 2

Synthesis of α , β -unsaturated aldehydes as potential substrates for bacterial luciferases

Eveline Brodl^a, Jakov Ivkovic^{b,1}, Chaitanya R. Tabib^a, Rolf Breinbauer^b and Peter Macheroux^{a,*}

^aGraz University of Technology, Institute of Biochemistry, Petersgasse 12/2, 8010 Graz, Austria

^bGraz University of Technology, Institute of Organic Chemistry, Stremayrgasse 9, 8010 Graz, Austria

¹current affiliation: University of Lund, Kemikum, Center for Analysis and Synthesis, Naturvetarvägen 14, 22100 Lund, Sweden.

*Corresponding author at present address: Graz University of Technology, Petersgasse 12/2, A-8010 Graz, Austria. Tel.: +43 3168736450. Email address: peter.macheroux@tugraz.at

Keywords: luciferase; bacterial bioluminescence; α , β -unsaturated aldehydes

Abbreviations: DIBALH: diisobutylaluminum hydride; DMAP: 4-(dimethylamino)-pyridine; DMF: *N,N*-dimethylformamide; DCM: dichloromethane; THF: tetrahydrofuran

Author Contributions:

Jl and EB designed and synthesized all the substrates (except C14 which was commercially purchased). CRT and EB expressed and purified all proteins and cofactors. CRT designed the experiments, performed the assays for the aldehyde chain length vs light emission correlation and the test of saturated vs unsaturated aldehydes with different luciferases. EB analyzed the results for both the experiments and made the figures. CRT, EB, IV, RB and PM wrote the manuscript.

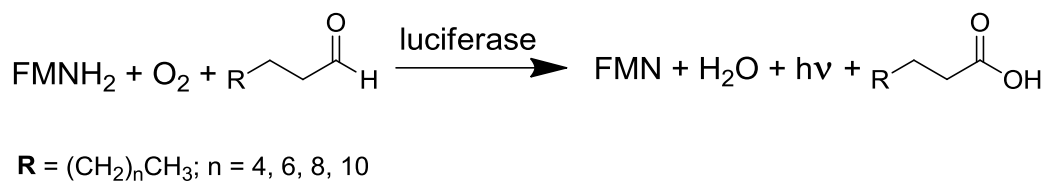
2.1 Abstract

Bacterial luciferase catalyzes the monooxygenation of long-chain aldehydes such as tetradecanal to the corresponding acid accompanied by light emission with a maximum at 490 nm. In this study even numbered aldehydes with eight, ten, twelve and fourteen carbon atoms were compared with analogs having a double bond at the α , β -position. These α , β -unsaturated aldehydes were synthesized in three steps and were examined as potential substrates *in vitro*. The luciferase of *Photobacterium leiognathi* was found to convert these analogs and showed a reduced but significant bioluminescence activity compared to tetradecanal. This study showed the trend that aldehydes, both saturated and unsaturated, with longer chain lengths had higher activity in terms of bioluminescence than shorter chain lengths. The maximal light intensity of (*E*)-tetradec-2-enal was approximately half with luciferase of *P. leiognathi*, compared to tetradecanal. Luciferases of *Vibrio harveyi* and *Aliivibrio fischeri* accepted these newly synthesized substrates but light emission dropped drastically compared to saturated aldehydes. The onset and the decay rate of bioluminescence were much slower, when using unsaturated substrates, indicating a kinetic effect. As a result the duration of the light emission is doubled. These results suggest that the substrate scope of bacterial luciferases is broader than previously reported.

2.2 Introduction

The “cold-light” phenomenon - the enzymatic production of light commonly known as bioluminescence - can be found in prokaryotes and eukaryotes.¹ The involvement of long-chain aliphatic aldehydes as substrates in bacterial bioluminescence has been known since 1953 when various chain lengths of the substrates were investigated by Strehler and Cormier.^{2,3} In the 1960s, the role of these potential substrates was analyzed concerning the reaction velocity, the initial maximal intensity and the decay of luminescence.^{4,5} In 1963 Spudich and Hastings tested the first unsaturated aldehyde, 2-decenal, and postulated complete inactivity with this substrate.⁶ Despite these experiments, it was not clear if the aldehyde substrates have a catalytic function or are consumed in the reaction. Cormier *et al.* were the first to prove that long-chain aldehydes were definitely required for light production.⁷ It took another nine years to identify tetradecanal as the “natural” substrate for bacterial bioluminescence in 1978 by Ulitzur and Hastings.⁸ By now it is known, that the

luciferase catalyzes the monooxygenation of long-chain aliphatic aldehydes to the corresponding acids employing reduced flavin mononucleotide (FMNH₂) as redox cofactor (Scheme 1).¹



Scheme 1: General reaction of bacterial bioluminescence.

The initial step of the reaction is the binding of reduced FMN to luciferase. The enzyme-FMNH₂ complex reacts with molecular oxygen to form flavin-4a-hydroperoxide. This enzyme-FMNHOOH complex subsequently reacts with a long chain aliphatic aldehyde to form a highly stable intermediate. Its slow decay results in the oxidation of the aldehyde to the corresponding acid and the free energy released during this reaction populates an excited state flavin-4a-hydroxide, which in turn serves as the light emitting molecule.⁹

Bacterial luciferases are heterodimeric enzymes consisting of an α -subunit and a β -subunit. The two subunits have a sequence identity of approximately 32 % and have evolved from a common ancestor.¹⁰ The active site of the enzyme is exclusively on the α -subunit and also distant from the subunit interface. The exact role of the β -subunit is not clear, but deletion or mutation of this subunit reveals less or complete loss of activity. A mutation of β Tyr151, for instance, has a negative effect on FMNH₂ binding. It seems that the β -subunit is responsible for high quantum yield and protein stability.^{10, 11}

Only two crystal structures of bacterial luciferases have been reported, where one of them elucidates the structure of the apo-LuxAB of *Vibrio harveyi*^{10, 12} and the other one reveals the luciferase/flavin complex.¹¹ In the latter crystal structure, the product FMN is bound to the luciferase of *V. harveyi*. The isoalloxazine ring of the flavin shows a planar conformation and is held in place by mainly backbone contacts. The amino acids involved in the binding of the 5' phosphate are Arg107, Arg125, Glu175, Ser176 and Thr179 (Figure 1).^{11, 13} Both structures designate a TIM barrel fold ($\beta\alpha$)₈ for the enzyme. Both subunits have a loop between the β -strand 7 and α -helix 7. The α -subunit, in contrast to the β -subunit, has 29 additional amino acids and a stretch of disordered residues from Lys283 to Arg290. This loop region is the most conserved region of the luciferase sequence. It is highly protease-labile, but binding of FMN

or polyvalent anions can prevent proteolytic inactivation.^{10, 11} Complete deletion of the loop results in reduction of total quantum yield by two orders of magnitude. It was hypothesized that the mobile loop has a lid-gating mechanism similar to other TIM-barrel enzymes.¹⁴ This loop is in close proximity to the active center and seems to undergo conformational changes from an open or semi open state to a closed state after flavin binding and before reaction with oxygen.^{10, 11, 14}

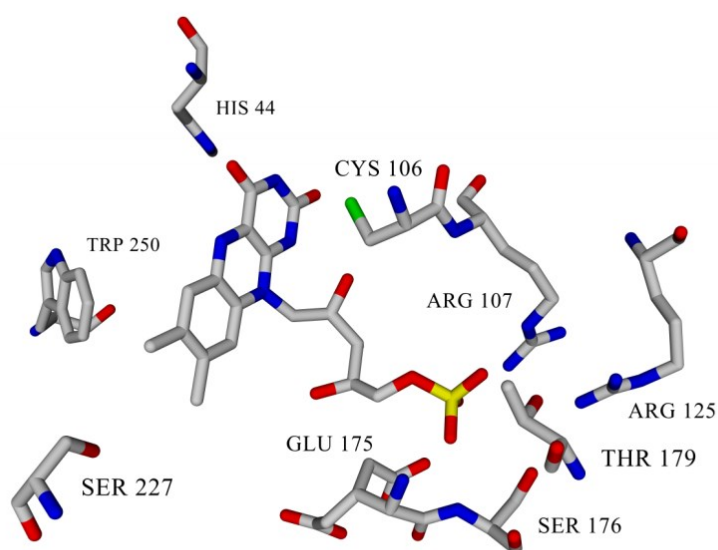


Figure 1: Graphical representation of FMN bound to luciferase of *V. harveyi*. Based on the crystal structure¹¹, FMN and a few key residues discussed in the text are depicted in stick confirmation with according labelling. General color code is used for the atoms. Residues Arg107, Arg125, Glu175, Ser176 and Thr179 are responsible for binding of the 5' phosphate group of FMN. His44, Ser227 and Trp250 might have a role in substrate binding and interaction.

Currently, structural information on the spatial arrangement of FMN and the aldehyde substrate in the active site is lacking, however various mutagenesis and modelling studies were performed in the last years. It was assumed that the flavin binding pocket is large enough to accommodate FMNH₂, O₂ and long chain aldehydes.¹⁵ In particular, two amino acids, Cys106 and Ser227, have attracted interest, because their exchange substantially affected enzymatic activity. The former amino acid apparently plays an important catalytic role as alkylation of its reactive thiol led to inactivation of the luciferase (Figure 1).^{10, 11} In addition it was found that the Cys106Val variant exhibits decreased aldehyde utilization and reduced stability of the flavin-4a-hydroperoxide intermediate.¹³ On the other hand, replacement of Ser227 to phenylalanine in the α -subunit led to a steric effect in the well-characterized mutant

AK-20 (Figure 1). Generally, replacement of Ser227 by large aromatic amino acids led to a 10-fold decreased binding affinity for aldehyde, smaller amino acids, e.g. alanine had no influence.^{10, 16} Modelling studies suggest that the bioluminescent reaction occurs on the *si*-face of the isoalloxazine ring facing the amino acid His44 (Figure 1). The distance of the C4a atom of flavin and N δ atom of His44 is approximately 7 Å. This leaves enough space for functional groups of the intermediates (peroxide, hydroxide) and aldehyde binding. Additionally a spacious cavity is formed at this position, which is surrounded by hydrophobic residues. Among those residues is Trp250, which was suggested to interact with the aldehyde substrate (Figure 1).^{13, 17} Despite this analysis the exact structure of bacterial luciferases in complex with FMNH₂ and aldehyde substrate is still unknown and prompts speculations about the reaction mechanism as well as the substrate scope.

In this study, α , β -unsaturated aldehydes with chain lengths of eight, ten, twelve and fourteen carbon atoms were synthesized. To investigate the mechanism of bacterial bioluminescence, the luciferases of *Photobacterium leiognathi*, *Vibrio harveyi* and *Aliivibrio fischeri* were chosen as model systems to test these potential substrates and analyze the substrate specificity of bacterial luciferases.

2.3 Materials and Methods

2.3.1 General experimental information

All commercially available reagents and solvents were purchased from Sigma-Aldrich, Alfa Aesar, Fisher Scientific, Acros Organics, Roth or VWR, and were used without further purification if not stated otherwise. When it was required, non-dry solvents were distilled before use. If reactions were performed under inert conditions, e.g. exclusion of water, oxygen or both, all experiments were carried out using established Schlenk techniques. Herein solvents were dried and/or degassed with common methods and afterwards stored under inert gas atmosphere (argon or N₂) over molecular sieves. In some cases, when explicitly mentioned, dry solvents were received from the listed suppliers. DCM (EtOH stabilized) was distilled first over P₄O₁₀ to remove the stabilizer and then over CaH₂ under argon atmosphere and stored over 4 Å molecular sieves in an amber-colored 1000 mL Schlenk bottle.

All reactions were stirred with Teflon-coated magnetic stirring bars. Molecular sieves (Sigma Aldrich, beads with 8-12 mesh) were activated in a round-bottom flask with a gas-inlet adapter by heating them carefully in a heating mantle for approximately 12 h under high vacuum until complete dryness was obtained. These activated molecular sieves were stored at room temperature under argon atmosphere.

Temperatures were measured externally if not otherwise stated. Reactions that were carried out at -78 °C were cooled by keeping the reaction vessel immersed in a properly sized Dewar vessel containing acetone/dry ice.

Analytical thin layer chromatography (TLC) was carried out on Merck TLC silica gel 60 F254 aluminum sheets and spots were visualized by UV light ($\lambda = 254$ and/or 366 nm) or by staining with iodide, cerium ammonium molybdate (2.0 g $\text{Ce}(\text{SO}_4)_2$, 50.0 g $(\text{NH}_4)_6\text{Mo}_7\text{O}_{24}$ and 50 mL conc. H_2SO_4 in 400 mL water) (CAM) or potassium permanganate (0.3 g KMnO_4 , 20 g K_2CO_3 , 5 mL 5 % aqueous NaOH in 300 mL H_2O) followed by the development of the stains in the heat. Flash column chromatography was performed on silica gel 0.035-0.070 mm, 60 Å (Acros Organics). A 30 to 100 fold excess of silica gel was used with respect to the amount of dry crude product, depending on the separation problem. The dimensions of the column were selected in such a way that the required amount of silica gel formed a pad between 10 cm and 25 cm. The column was equilibrated first with the solvent or solvent mixture, and the crude product diluted with the eluent was applied onto the top of the silica pad. In case when the crude product was insoluble in the eluent, the sample was dissolved in an appropriate solvent (EtOAc or DCM), and the equal amount of diatomaceous earth was added, followed by removal of the solvent under reduced pressure and drying the sample in vacuum, which was then directly loaded onto the top of the silica pad. The mobile phase was forced through the column using a rubber bulb pump.

2.3.2 General procedure GP-1 (Synthesis of α , β -unsaturated ethyl esters)

In a 100 mL single neck round-bottom flask equipped with a magnetic stir bar, 4-(dimethylamino)pyridine (122 mg, 1.00 mmol, 0.10 eq), mono-ethyl malonate (2.36 mL, 20.0 mmol, 2.0 eq) and saturated alkyl aldehyde (10.0 mmol, 1.0 eq) were dissolved in DMF (50 mL). The reaction mixture was stirred at room temperature for 42 h. Subsequently, the mixture was diluted with diethyl ether (50 mL), washed with saturated aqueous NH_4Cl (50 mL), saturated aqueous NaHCO_3 (50 mL), water (50 mL), and concentrated under reduced

pressure. Flash chromatography (SiO₂, 5 % EtOAc in cyclohexane) afforded the desired unsaturated ethyl ester as a colorless liquid.

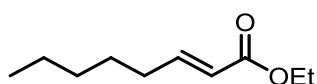
2.3.3 General procedure GP-2 (Synthesis of allyl alcohols)

In a nitrogen-purged 100 mL Schlenk tube equipped with a magnetic stir bar, unsaturated ethyl ester (4.5 mmol, 1.0 eq) was dissolved in dry dichloromethane (18 mL), the vessel was sealed with a glass stopper and cooled to -78 °C in an acetone/dry ice bath. 1.0 M solution of diisobutylaluminum hydride in hexanes (10.8 mL, 10.8 mmol, 2.4 eq) was added dropwise via a syringe and a septum throughout 10 min. The reaction was stirred at -78 °C until TLC indicated quantitative conversion (3 h). The reaction mixture was quenched by the dropwise addition of MeOH (1 mL). Subsequently, the cooling bath was removed, saturated aqueous potassium sodium tartrate solution (18 mL) was added, and the mixture was stirred vigorously for 2 h. After phase separation the aqueous layer was extracted with dichloromethane (10 mL). The combined organic layers were dried over anhydrous Na₂SO₄ and concentrated under reduced pressure. Flash chromatography (SiO₂, 20 % EtOAc in cyclohexane) afforded the desired allyl alcohol as a colorless liquid.

2.3.4 General procedure GP-3 (Synthesis of α , β -unsaturated aldehydes)

In a nitrogen-purged 10 mL Schlenk tube equipped with a magnetic stir bar, manganese(IV) oxide (494 mg, 5.0 mmol, 5.0 eq) and activated 4 Å molecular sieves were suspended in dry dichloromethane (4 mL). Allyl alcohol (1.0 mmol, 1.0 eq) was dissolved in dry dichloromethane (3.3 mL), added to the mixture in the Schlenk tube, which was sealed with a glass stopper. After stirring the mixture overnight at room temperature the dark brown reaction mixture was filtered through a compressed pad of diatomaceous earth. The pad was washed with dichloromethane (2 mL), and the filtrate was concentrated under reduced pressure. Flash chromatography (SiO₂, 10 % EtOAc in cyclohexane) afforded the desired unsaturated aldehyde as a pale yellow liquid.

2.3.5 Ethyl (*E*)-oct-2-enoate (3d)



Unsaturated ester **3d** was synthesized and isolated according to the general procedure GP-1 and its stated stoichiometry.

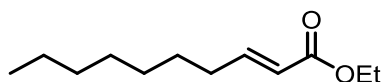
Yield: 940 mg (5.52 mmol, 55 %), colorless liquid.

R_f = 0.35 (cyclohexane/EtOAc 40:1 (v/v); staining: KMnO₄).

¹H NMR (300 MHz, CDCl₃) δ = 6.97 (dt, ³J = 15.6 Hz, ³J = 7.0 Hz, 1H), 5.81 (d, ³J = 15.6 Hz, 1H), 4.18 (q, ³J = 7.1 Hz, 2H), 2.25–2.14 (m, 2H), 1.52–1.40 (m, 2H), 1.36–1.25 (m, 7H), 0.82 (t, ³J = 6.7 Hz, 3H) ppm.

¹³C NMR (75 MHz, CDCl₃) δ = 166.9 (s, 1C), 149.6 (s, 1C), 121.4 (s, 1C), 60.2 (s, 1C), 32.3 (s, 1C), 31.4 (s, 1C), 27.8 (s, 1C), 22.6 (s, 1C), 14.4 (s, 1C), 14.1 (s, 1C) ppm.

2.3.6 Ethyl (*E*)-dec-2-enoate (**3c**)



Unsaturated ester **3c** was synthesized and isolated according to the general procedure GP-1 and its stated stoichiometry.

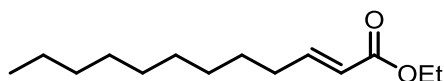
Yield: 1.480 g (7.46 mmol, 75 %), colorless liquid.

R_f = 0.35 (cyclohexane/EtOAc 40:1 (v/v); staining: KMnO₄).

¹H NMR (300 MHz, CDCl₃) δ = 6.96 (dt, ³J = 15.6 Hz, ³J = 7.0 Hz, 1H), 5.80 (d, ³J = 15.6 Hz, 1H), 4.18 (q, ³J = 7.1 Hz, 2H), 2.26–2.12 (m, 2H), 1.51–1.39 (m, 2H), 1.35–1.21 (m, 11H), 0.88 (t, ³J = 6.7 Hz, 3H) ppm.

¹³C NMR (75 MHz, CDCl₃) δ = 166.9 (s, 1C), 149.6 (s, 1C), 121.4 (s, 1C), 60.3 (s, 1C), 32.3 (s, 1C), 31.9 (s, 1C), 29.3 (s, 1C), 29.2 (s, 1C), 28.2 (s, 1C), 22.8 (s, 1C), 14.4 (s, 1C), 14.2 (s, 1C) ppm.

2.3.7 Ethyl (*E*)-dodec-2-enoate (**3b**)



Unsaturated ester **3b** was synthesized and isolated according to the general procedure GP-1 and its stated stoichiometry.

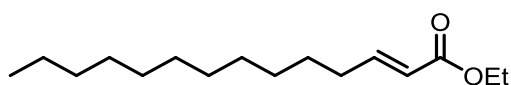
Yield: 1.235 g (5.46 mmol, 55 %), colorless liquid.

R_f = 0.36 (cyclohexane/EtOAc 40:1 (v/v); staining: KMnO₄).

¹H NMR (300 MHz, CDCl₃) δ = 6.96 (dt, ³J = 15.6 Hz, ³J = 7.0 Hz, 1H), 5.80 (d, ³J = 15.6 Hz, 1H), 4.18 (q, ³J = 7.1 Hz, 2H), 2.25–2.13 (m, 2H), 1.51–1.39 (m, 2H), 1.35–1.21 (m, 15H), 0.88 (t, ³J = 6.7 Hz, 3H) ppm.

¹³C NMR (75 MHz, CDCl₃) δ = 166.9 (s, 1C), 149.6 (s, 1C), 121.3 (s, 1C), 60.2 (s, 1C), 32.3 (s, 1C), 32.0 (s, 1C), 29.6 (s, 1C), 29.5 (s, 1C), 29.4 (s, 1C), 29.3 (s, 1C), 28.2 (s, 1C), 22.8 (s, 1C), 14.4 (s, 1C), 14.2 (s, 1C) ppm.

2.3.8 Ethyl (*E*)-tetradec-2-enoate (**3a**)



Unsaturated ester **3a** was synthesized and isolated according to the general procedure GP-1 and its stated stoichiometry.

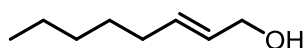
Yield: 1.733 g (6.81 mmol, 68 %), colorless liquid.

R_f = 0.38 (cyclohexane/EtOAc 40:1 (v/v); staining: KMnO₄).

¹H NMR (300 MHz, CDCl₃) δ = 6.96 (dt, ³J = 15.6 Hz, ³J = 7.0 Hz, 1H), 5.80 (d, ³J = 15.6 Hz, 1H), 4.17 (q, ³J = 7.1 Hz, 2H), 2.25–2.12 (m, 2H), 1.51–1.38 (m, 2H), 1.35–1.21 (m, 19H), 0.87 (t, ³J = 6.7 Hz, 3H) ppm.

¹³C NMR (75 MHz, CDCl₃) δ = 166.9 (s, 1C), 149.6 (s, 1C), 121.3 (s, 1C), 60.2 (s, 1C), 32.3 (s, 1C), 32.0 (s, 1C), 29.8 (m, 2C), 29.7 (s, 1C), 29.5 (s, 1C), 29.4 (s, 1C), 29.3 (s, 1C), 28.2 (s, 1C), 22.8 (s, 1C), 14.4 (s, 1C), 14.2 (s, 1C) ppm.

2.3.9 (*E*)-Oct-2-en-1-ol (**4d**)



Allyl alcohol **4d** was synthesized and isolated according to the general procedure GP-2 and its stated stoichiometry.

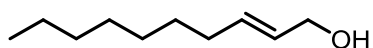
Yield: 449 mg (3.50 mmol, 78 %), colorless liquid.

R_f = 0.57 (cyclohexane/EtOAc 9:1 (v/v); staining: KMnO₄).

^1H NMR (300 MHz, CDCl_3) δ = 5.77–5.54 (m, 2H), 4.08 (br s, 2H), 2.03 (dt, 3J = 6.9 Hz, 3J = 6.6 Hz, 2H), 1.45–1.19 (m, 7H), 0.88 (t, 3J = 6.7 Hz, 3H) ppm.

^{13}C NMR (75 MHz, CDCl_3) δ = 133.8 (s, 1C), 129.0 (s, 1C), 64.0 (s, 1C), 32.3 (s, 1C), 31.5 (s, 1C), 29.0 (s, 1C), 22.7 (s, 1C), 14.2 (s, 1C) ppm.

2.3.10 (*E*)-Dec-2-en-1-ol (**4c**)



Allyl alcohol **4c** was synthesized and isolated according to the general procedure GP-2 and its stated stoichiometry.

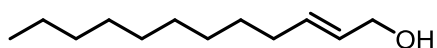
Yield: 605 mg (3.87 mmol, 86 %), colorless liquid.

R_f = 0.57 (cyclohexane/EtOAc 9:1 (v/v); staining: KMnO_4).

^1H NMR (300 MHz, CDCl_3) δ = 5.77–5.55 (m, 2H), 4.07 (br s, 2H), 2.03 (dt, 3J = 6.9 Hz, 3J = 6.5 Hz, 2H), 1.46–1.17 (m, 11H), 0.88 (t, 3J = 6.7 Hz, 3H) ppm.

^{13}C NMR (75 MHz, CDCl_3) δ = 133.7 (s, 1C), 129.0 (s, 1C), 64.0 (s, 1C), 32.3 (s, 1C), 32.0 (s, 1C), 29.3 (s, 3C), 22.8 (s, 1C), 14.2 (s, 1C) ppm.

2.3.11 (*E*)-Dodec-2-en-1-ol (**4b**)



Allyl alcohol **4b** was synthesized and isolated according to the general procedure GP-2 and its stated stoichiometry.

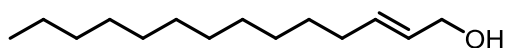
Yield: 617 mg (3.35 mmol, 74 %), colorless liquid.

R_f = 0.57 (cyclohexane/EtOAc 9:1 (v/v); staining: KMnO_4).

^1H NMR (300 MHz, CDCl_3) δ = 5.77–5.56 (m, 2H), 4.08 (br s, 2H), 2.03 (dt, 3J = 6.9 Hz, 3J = 6.6 Hz, 2H), 1.41–1.18 (m, 15H), 0.88 (t, 3J = 6.7 Hz, 3H) ppm.

^{13}C NMR (75 MHz, CDCl_3) δ = 133.8 (s, 1C), 129.0 (s, 1C), 64.0 (s, 1C), 32.4 (s, 1C), 32.1 (s, 1C), 29.8–29.6 (m, 2C), 29.5 (s, 1C), 29.4–29.2 (m, 2C), 22.8 (s, 1C), 14.3 (s, 1C) ppm.

2.3.12 (*E*)-Tetradec-2-en-1-ol (**4a**)



Allyl alcohol **4a** was synthesized and isolated according to the general procedure GP-2 and its stated stoichiometry.

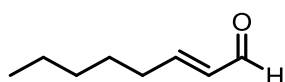
Yield: 641 mg (3.02 mmol, 67 %), colorless liquid.

R_f = 0.57 (cyclohexane/EtOAc 9:1 (v/v); staining: KMnO₄).

¹H NMR (300 MHz, CDCl₃) δ = 5.77–5.56 (m, 2H), 4.08 (br s, 2H), 2.03 (dt, ³J = 6.9 Hz, ³J = 6.6 Hz, 2H), 1.36–1.17 (m, 19H), 0.88 (t, ³J = 6.7 Hz, 3H) ppm.

¹³C NMR (75 MHz, CDCl₃) δ = 133.8 (s, 1C), 129.0 (s, 1C), 64.0 (s, 1C), 32.4 (s, 1C), 32.1 (s, 1C), 29.9–29.7 (m, 3C), 29.7 (s, 1C), 29.5 (s, 1C), 29.4–29.2 (m, 2C), 22.8 (s, 1C), 14.3 (s, 1C) ppm.

2.3.13 (*E*)-Oct-2-enal (**5d**)



Unsaturated aldehyde **5d** was synthesized and isolated according to the general procedure GP-3 and its stated stoichiometry.

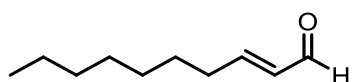
Yield: 103 mg (0.816 mmol, 82 %), pale yellow liquid.

R_f = 0.37 (cyclohexane/EtOAc 9:1 (v/v); staining: KMnO₄).

¹H NMR (300 MHz, CDCl₃) δ = 9.50 (d, ³J = 7.9 Hz, 1H), 6.86 (dt, ³J = 15.6 Hz, ³J = 6.9 Hz, 1H), 6.11 (dd, ³J = 15.6 Hz, ³J = 7.9 Hz, 1H), 2.33 (dt, ³J = 7.2 Hz, ³J = 7.2 Hz, 2H), 1.58–1.42 (m, 2H), 1.37–1.26 (m, 4H), 0.98–0.85 (m, 3H) ppm.

¹³C NMR (75 MHz, CDCl₃) δ = 194.3 (s, 1C), 159.2 (s, 1C), 133.1 (s, 1C), 32.8 (s, 1C), 31.4 (s, 1C), 27.7 (s, 1C), 22.5 (s, 1C), 14.1 (s, 1C) ppm.

2.3.14 (*E*)-Dec-2-enal (**5c**)



Unsaturated aldehyde **5c** was synthesized and isolated according to the general procedure GP-3 and its stated stoichiometry.

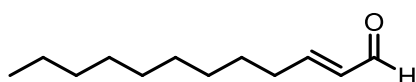
Yield: 122 mg (0.791 mmol, 79 %), pale yellow liquid.

R_f = 0.37 (cyclohexane/EtOAc 9:1 (v/v); staining: KMnO₄).

¹H NMR (300 MHz, CDCl₃) δ = 9.51 (d, ³J = 7.9 Hz, 1H), 6.85 (dt, ³J = 15.6 Hz, ³J = 6.9 Hz, 1H), 6.11 (dd, ³J = 15.6 Hz, ³J = 7.9 Hz, 1H), 2.33 (dt, ³J = 7.2 Hz, ³J = 7.2 Hz, 2H), 1.57–1.44 (m, 2H), 1.40–1.19 (m, 8H), 0.88 (t, ³J = 6.7 Hz, 3H) ppm.

¹³C NMR (75 MHz, CDCl₃) δ = 194.2 (s, 1C), 159.2 (s, 1C), 133.1 (s, 1C), 32.9 (s, 1C), 31.8 (s, 1C), 29.2 (s, 1C), 29.1 (s, 1C), 28.0 (s, 1C), 22.8 (s, 1C), 14.2 (s, 1C) ppm.

2.3.15 (*E*)-Dodec-2-enal (**5b**)



Unsaturated aldehyde **5b** was synthesized and isolated according to the general procedure GP-3 and its stated stoichiometry.

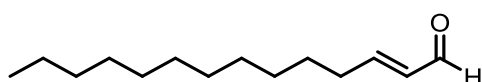
Yield: 136 mg (0.746 mmol, 75 %), pale yellow liquid.

R_f = 0.38 (cyclohexane/EtOAc 9:1 (v/v); staining: KMnO₄).

¹H NMR (300 MHz, CDCl₃) δ = 9.50 (d, ³J = 7.9 Hz, 1H), 6.85 (dt, ³J = 15.6 Hz, ³J = 6.9 Hz, 1H), 6.11 (dd, ³J = 15.6 Hz, ³J = 7.9 Hz, 1H), 2.33 (dt, ³J = 7.2 Hz, ³J = 7.2 Hz, 2H), 1.57–1.43 (m, 2H), 1.39–1.18 (m, 12H), 0.88 (t, ³J = 6.7 Hz, 3H) ppm.

¹³C NMR (75 MHz, CDCl₃) δ = 194.3 (s, 1C), 159.2 (s, 1C), 133.1 (s, 1C), 32.9 (s, 1C), 32.0 (s, 1C), 29.6 (s, 1C), 29.5 (s, 1C), 29.4 (s, 1C), 29.3 (s, 1C), 28.0 (s, 1C), 22.8 (s, 1C), 14.2 (s, 1C) ppm.

2.3.16 (*E*)-tetradec-2-enal (**5a**)



Unsaturated aldehyde **5a** was synthesized and isolated according to the general procedure GP-3 and its stated stoichiometry.

Yield: 159 mg (0.756 mmol, 76 %), pale yellow liquid.

$R_f = 0.40$ (cyclohexane/EtOAc 9:1 (v/v); staining: KMnO_4).

^1H NMR (300 MHz, CDCl_3) $\delta = 9.50$ (d, $^3J = 7.8$ Hz, 1H), 6.85 (dt, $^3J = 15.6$ Hz, $^3J = 6.9$ Hz, 1H), 6.11 (dd, $^3J = 15.6$ Hz, $^3J = 7.9$ Hz, 1H), 2.33 (dt, $^3J = 7.2$ Hz, $^3J = 7.2$ Hz, 2H), 1.57–1.44 (m, 2H), 1.38–1.20 (m, 16H), 0.88 (t, $^3J = 6.7$ Hz, 3H) ppm.

^{13}C NMR (75 MHz, CDCl_3) $\delta = 194.3$ (s, 1C), 159.2 (s, 1C), 133.1 (s, 1C), 32.9 (s, 1C), 32.0 (s, 1C), 29.8 (s, 2C), 29.6 (s, 1C), 29.5–29.4 (m, 2C), 29.3 (s, 1C), 28.0 (s, 1C), 22.8 (s, 1C), 14.2 (s, 1C) ppm.

2.3.17 Instrumentation

UV/Vis absorption spectra were recorded with a Specord 210 spectrophotometer (Analytic Jena, Jena, Germany). The light emission was measured by a Berthold Technologies Centro LB 960 microplate Luminometer with Mikro Win version 4.16. Gel filtration was performed using a Superdex-200 column (prep grade XK 16/100; GE Healthcare) with an Äktaexplorer 100 Pharmacia Biotech (GE Healthcare).

^1H -, ^{13}C -NMR spectra were recorded on a Bruker AVANCE III 300 spectrometer (^1H : 300.36 MHz; ^{13}C : 75.53 MHz). Chemical shifts were referenced to the residual proton and carbon signal of the deuterated solvent, respectively (CDCl_3 : $\delta = 7.26$ ppm (^1H), 77.16 ppm (^{13}C)). Signal multiplicities are abbreviated as s (singlet), bs (broad singlet), d (doublet), dd (doublet of doublet), t (triplet), q (quadruplet), p (pentet) and m (multiplet). Deuterated solvents for nuclear resonance spectroscopy were purchased from Euriso-top®.

2.3.18 Design, expression and purification of recombinant His-tagged proteins

LuxAB from *Photobacterium leiognathi* (ATCC 27561; PL_LuxAB) and YcnD from *Bacillus subtilis* were cloned into pET21a vector and transformed into *E. coli* BL21 (DE3) strain for expression as described previously.^{18, 19} LuxAB from *Vibrio harveyi* (ATCC 14126; VH_LuxAB) and *Aliivibrio fischeri* (ATCC 7744; AF_LuxAB) were cloned similarly. The genes for VH_LuxAB and AF_LuxAB were integrated into pET24b vector and transformed into *E. coli* Rosetta strain. Both constructs had an additional C-terminal octa-histidine tag. Heterologous expression cultures were grown at 37 °C in LB media containing kanamycin (50 $\mu\text{g}/\text{mL}$) and chloramphenicol (20 $\mu\text{g}/\text{mL}$) as selection markers until an OD (600 nm) of 0.6 was reached.

The expression was induced with 0.1 mM IPTG and cells were further grown at 20 °C for 16 h. Cells were harvested by centrifugation (4400 g, 10 min, 4 °C) and the wet cell pellets were stored at -20 °C. The cell pellets were suspended in lysis buffer (50 mM NaH₂PO₄, 300 mM NaCl, 10 mM imidazole, pH 8), lysed by addition of lysozyme and sonication and after centrifugation the clear supernatant was loaded on 5 mL HisTrap FF/HP columns (GE Healthcare) for purification via Ni-NTA affinity chromatography. The columns were washed with wash buffer (50 mM NaH₂PO₄, 300 mM NaCl, 20 mM imidazole, pH 8) and the purified protein fractions were gained with elution buffer (50 mM NaH₂PO₄, 300 mM NaCl, 300 mM imidazole, pH 8). After concentrating and buffer exchange to 45 mM Tris-buffer containing 40 mM MES and 20 mM L-malic acid pH 8, a subsequent gel filtration using a Superdex-200 column was performed. The concentration of the various proteins was determined spectrophotometrically at 280 nm or at 450 nm using the extinction coefficients 82,335 M⁻¹ cm⁻¹ (PL_LuxAB), 84,230 M⁻¹ cm⁻¹ (VH_LuxAB), 83,200 M⁻¹ cm⁻¹ (AF_LuxAB) and 12,190 M⁻¹ cm⁻¹ (YcnD).

2.3.19 *In vitro* assay

The *in vitro* assay was performed in 96 well white assay plates. For the assay all enzymes and substrates were prepared and/or diluted in 100 mM potassium phosphate buffer pH 7. The reaction mixture contained the enzyme luciferase with either 50 nM for *P. leiognathi* or 200 nM for *V. harveyi* or *A. fischeri*, respectively. YcnD and FMN were adjusted to 1.5 fold of the luciferase concentration, respectively. Additionally 500 nM NADPH and the substrate-buffer suspension were added to make up the final volume of 250 µL. The tested substrates include even chain length (8 to 14 carbon atoms) saturated and unsaturated aldehydes, respectively. Due to the relatively low solubility of aldehydes in water, concentrated aldehyde suspensions were obtained by adding 5 µL of the substrate to 10 mL of the reaction buffer, respectively (Supplementary Data).⁴ The reaction was started by injecting NADPH to the reaction mixture (after a delay of 5 seconds) and the readings were subsequently taken every 0.01th of a second for a total of 90 seconds. The light was measured using the luminometer. The light emission was recorded as emission counts. The area under the curve was taken for calculation of the percentage and the total light emission of luciferase with tetradecanal (**6a**) as substrate was considered as 100 %. The data was calculated to 100 nM of luciferase concentration to compare the results with each other. The values for the conversion of

luciferase of *P. leiognathi* are shown by means \pm SD of seven individual measurements for the saturated aldehydes and four individual measurements for the unsaturated aldehydes, respectively. The values for the conversion of luciferase of *V. harveyi* and *A. fischeri* are shown by means \pm SD of four individual measurements, respectively.

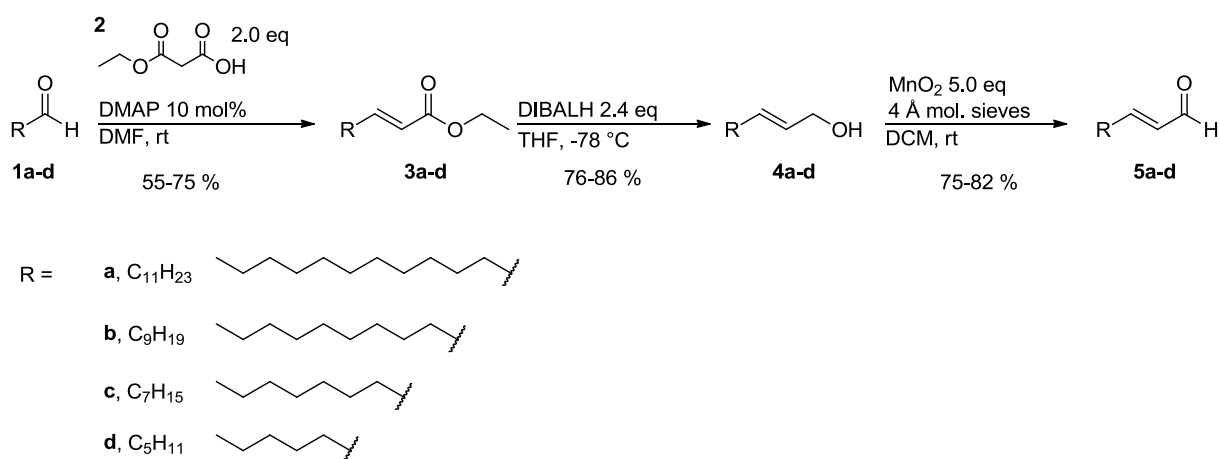
2.3.20 Molecular docking

In silico molecular docking studies were performed using Yasara Structure 13.9.8.²⁰ The crystal structure of the luciferase/flavin complex of *Vibrio harveyi* was retrieved from the Protein Data Bank (PDB entry: 3FGC). Structure preparation and all following experiments were performed within Yasara Structure 13.9.8. All the crystallographic water molecules and the β -subunit of the luciferase were removed before molecular docking. Missing hydrogens were added to the molecules by using the clean mode of Yasara.

For the docking experiments the oxidized flavin structure was modified to the flavin-4a-hydroperoxide intermediate. Therefore the additional hydrogens and the two oxygens were attached to the molecule and refined by energy minimization using AMBER99 force field, while fixing Lys283 and Arg290 which connect the luciferase backbone with an unstructured and therefore missing loop.¹¹ The resulting crystal structure was utilized for docking the substrate molecules (**5a-d**, **6a-d**) in flexible mode into the rigid receptor using the plugin Autodock Vina in Yasara Structure 13.9.8.^{21,22} The docking simulation cell was set to 15 Å around the flavin-4a-hydroperoxide intermediate and 500 docking runs with an RMSD cutoff of 2 Å were performed. The docked conformations for each substrate (**5a-d**, **6a-d**) were ranked according to the distance between the C1 atom of the substrate molecule and the terminal oxygen atom of the hydroperoxide functional group. The best-ranked docking pose for each substrate (**5a-d**, **6a-d**) was analyzed in Yasara Structure 13.9.8.

2.4 Results

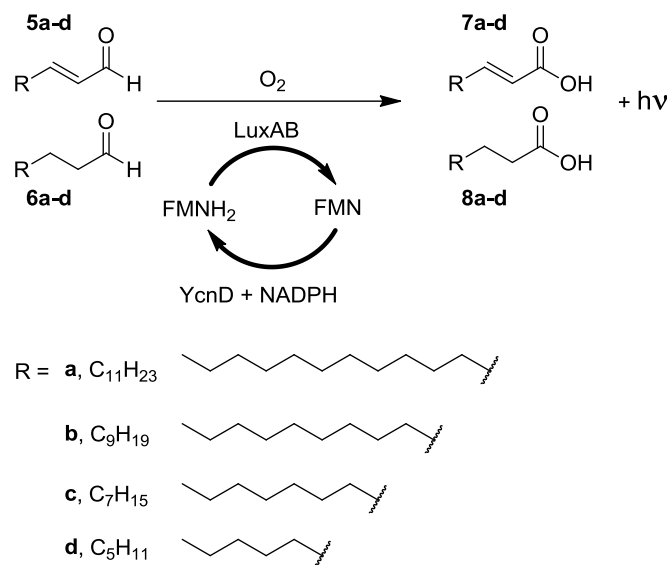
To obtain new insights into the activity and selectivity of luciferases, unsaturated aldehydes with various chain lengths were synthesized and analyzed. The substrate synthesis was carried out in three steps (Scheme 2). The α , β -unsaturated aldehydes were synthesized starting from commercially available saturated aldehydes with two carbons less in chain length. The starting aldehydes **1a-d** were subjected to a DMAP-catalyzed Knoevenagel condensation with monoethyl malonate (**2**) to obtain the corresponding unsaturated esters **3a-d**.²³ **3a-d** were reduced to the corresponding allyl alcohols **4a-d** using 1.2 equivalents diisobutylaluminum hydride (DIBALH) in DCM at -78 °C and were subsequently oxidized with manganese(IV) oxide (MnO₂) to afford the desired α , β -unsaturated aldehydes **5a-d**.



Scheme 2: Synthesis route for aliphatic, unsaturated aldehydes with different chain lengths (C8-C14). Using DMAP-catalyzed Knoevenagel condensation the starting aldehydes **1a-d** were converted to the unsaturated ethyl esters **3a-d**, which were reduced to the corresponding allyl alcohols **4a-d** and were finally oxidized to the α , β -unsaturated aldehydes **5a-d**. The exact equivalents, solvents and temperature conditions are given and the yield for each step is given as percentage.

To test the newly synthesized substrates, an *in vitro* assay was developed (Scheme 3). Briefly, 50 nM recombinant luciferase of *P. leiognathi* (LuxAB) was used in a reaction mixture with 100 mM potassium phosphate buffer pH 7, 75 nM FMN, 75 nM YcnD, 500 nM NADPH and substrate-buffer suspensions of **5a-d** and **6a-d** (see Materials and Methods). YcnD, an NADPH-dependent oxidoreductase from *Bacillus subtilis*, reduces FMN to provide the cosubstrate FMNH₂.¹⁹ The luciferase then oxidizes the various substrates to their corresponding acids using the enzyme-bound flavin-4a-hydroperoxide with concomitant emission of light. The

photons, emitted during this reaction, were collected by a luminometer for 90 seconds and the areas under the light emission curve were compared to tetradecanal (**6a**).



Scheme 3: Schematic representation of the *in vitro* assay. The synthesized unsaturated aldehydes **5a-d**, as well as the four saturated aldehydes **6a-d**, were investigated in an *in vitro* assay. The oxidation reaction catalyzed by 50 nM luciferase (LuxAB), employing molecular oxygen (O₂) and reduced FMN (FMNH₂), results in long-chain aliphatic acids **7a-d** and **8a-d** and the emission of light (hν). For the reduced FMN a recycling system was established using the NADPH-dependent oxidoreductase YcnD from *Bacillus subtilis*. The light emission is measured by a luminometer and subsequently converted to total light emission in per cent for comparison and analysis.

As expected, tetradecanal (**6a**) showed the highest light emission and was set to 100 %. The other aldehydes showed lower activity with the luciferase (Figure 1). In the case of dodecanal (**6b**), decanal (**6c**) and (*E*)-tetradec-2-enal (**5a**), light emission was greater than 50 % in comparison to tetradecanal (**6a**). Octanal (**6d**) exhibited the lowest yield of the saturated aldehydes. The unsaturated aldehyde substrates **5b-d**, however, resulted in yields below 10 %. Comparing saturated aldehydes with each other, substrates with longer chain length emit more light than those with shorter chain length and therefore are apparently better substrates for luciferase. This tendency was already observed earlier^{5,24}, however a clear comparison and definite values were not reported. The same tendency was found for the unsaturated aldehydes, where total light emission decreases with shorter chain length. Thus saturated and unsaturated aldehydes exhibit a similar chain length dependency but are clearly accepted as substrates for bacterial luciferase.

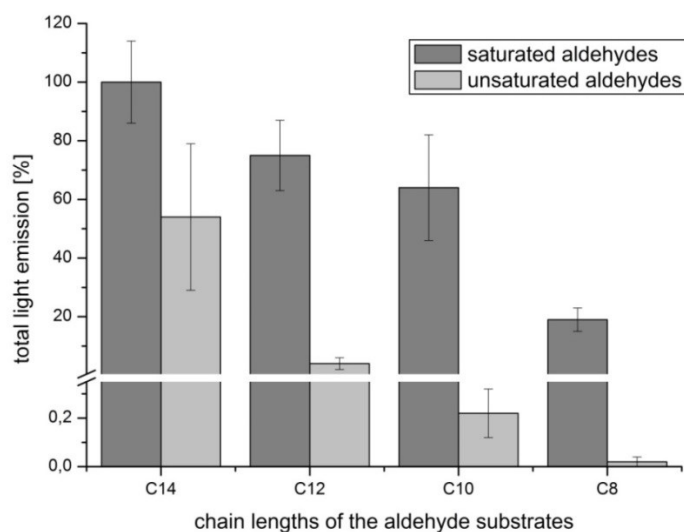


Figure 2: Comparison of saturated and unsaturated aldehydes as potential substrates for the luciferase of *P. leiognathi*. The conversion of unsaturated aldehydes **5a-d** (light grey) and saturated aldehydes **6a-d** (dark grey) by the luciferase during the *in vitro* assay (Scheme 3) can be determined by the total light emission of the reaction measured by the luminometer. The counts of the light emission were converted to percent. The total light emission (as percentage) was plotted against the substrates (here differentiated by their chain lengths). The production of light by the conversion of tetradecanal (**6a**) was set to 100 %. The values are shown by means \pm SD of seven individual measurements for the saturated aldehydes and four individual measurements for the unsaturated aldehydes, respectively.

Next, we analyzed the time course of light emission for unsaturated and saturated aldehydes. As an example, the kinetics of light emission with tetradecanal (**6a**) and (*E*)-tetradec-2-enal (**5a**) as substrates are shown in Figure 2. Generally, the onset as well as the decay of the light emission is faster with saturated aldehydes. In the case of **6a** a maximum light emission is reached after ca. 7 s whereas light emission with **5a** peaks at ca. 10 s. On the other hand, light emission lasted much longer for the unsaturated aldehyde **5a** than for the saturated aldehyde **6a**. A similar kinetic behavior was observed for all other saturated/unsaturated aldehyde pairs. This result indicates that the rate-limiting step leading to the population of the excited state luciferin (presumably the flavin-4a-hydroxide²⁵) is slowed down when unsaturated aldehydes are used as substrates.

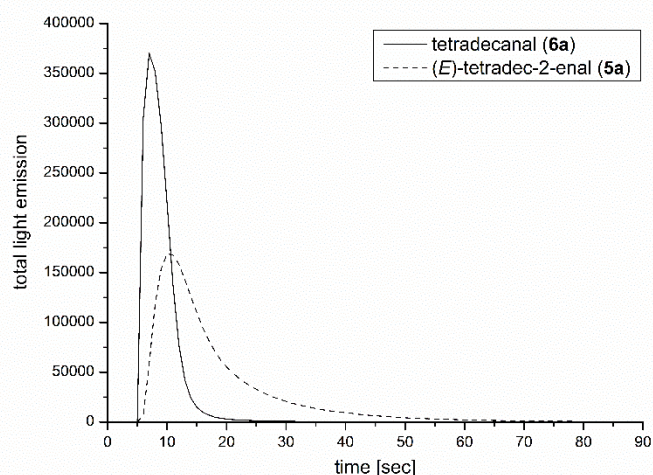


Figure 3: Time course of the total light emission of tetradecanal (6a) and (E)-tetradec-2-enal (5a). The light emission during the conversion of the substrates tetradecanal (6a, solid line) and (E)-tetradec-2-enal (5a, dashed line) was measured as a function of time by the luminometer. The counts of light emission were plotted against the time (in seconds). This is a representative figure of a single measurement.

Tetradecanal (6a) and (E)-tetradec-2-enal (5a) were chosen as substrates for the *in vitro* assay with luciferases from different genera (*P. leiognathi*, *V. harveyi*, *A. fischeri*) as depicted in Figure 3. The assay conditions were adopted for *V. harveyi* and *A. fischeri*. For the latter, a luciferase concentration of 200 nM was used and the concentrations for FMN and YcnD were set to 300 nM, respectively. Because light emission was highest with the luciferase from *P. leiognathi* it was used as a reference point, i.e. set to 100%. *V. harveyi* and *A. fischeri* accepted both substrates but showed a much lower activity than *P. leiognathi*. This was expected as *in vivo* analysis of the light emission of various strains showed already this tendency (to be reported elsewhere). Comparison of these two substrates with various luciferases confirms the previous results by depicting a decline of light emission with unsaturated aldehydes. Nevertheless, (E)-tetradec-2-enal (5a) is a substrate for various bacterial luciferases.

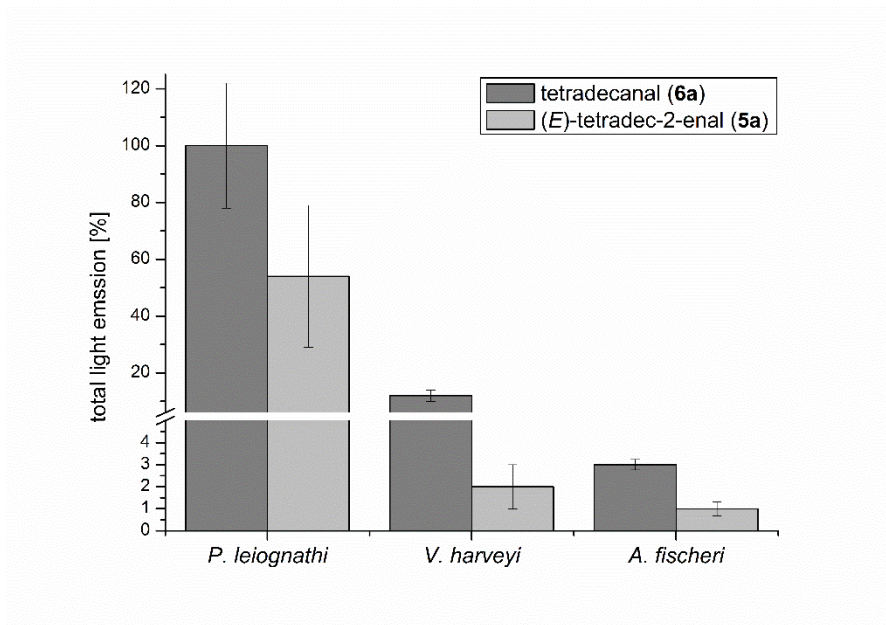


Figure 4: Conversion of tetradecanal (6a) and (E)-tetradec-2-enal (5a) by luciferases from *P. leiognathi*, *V. harveyi* and *A. fischeri*. Three luciferases of different genera were compared with each other by analyzing the total light emission (as percentage) during conversion of the two potential substrates tetradecanal (6a, dark grey) and (E)-tetradec-2-enal (5a, light grey) in *in vitro* assays. The values are shown by means \pm SD of four individual measurements, respectively.

2.5 Discussion

Four different compounds, namely (E)-tetradec-2-enal (5a), (E)-dodec-2-enal (5b), (E)-dec-2-enal (5c) and (E)-oct-2-enal (5d), were successfully synthesized and analyzed as potential substrates for recombinant luciferases from three different genera. Spudich and Hastings postulated in 1963 that 2-decenal (referring to (E)-dec-2-enal (5c)) is completely inactive in the production of light with the luciferase of *Achromobacter fischeri*. On the contrary, this compound was found to be a potent competitive inhibitor in the bioluminescent reaction. Strangely enough, they have reported similar quantum yields for the reaction with saturated and unsaturated substrate.⁶ Thus it was assumed that all α , β -unsaturated aldehydes exert an inhibitory effect and were therefore not considered as possible substrates. In contrast to that, we show here that unsaturated aldehydes are accepted as substrates by various recombinant luciferases from the genera *Photobacterium*, *Vibrio* and *Aliivibrio*, although the light emission yield was lower with the unsaturated aldehydes.

In light of our observations, the previously observed inhibitory effect⁶ seems to be a kinetic one. The reaction velocity is strongly influenced by the various substrates, which was clearly

shown by the time course of the light emission (Figure 2). Unfortunately, substrate-buffer suspensions had to be used for the assays; therefore it was not possible to conduct more detailed kinetic measurements. Studies with organic co-solvents were attempted, but led to denaturation of the luciferases (data not shown). The solubility of the aldehydes corresponds to the aldehyde chain length according to molar solubility values (Supplementary Data). Octanal (**6d**), for instance, should presumably give better results than tetradecanal (**6a**), as its solubility in aqueous buffer is higher. However, the reverse dependency was observed, as aldehydes with longer chain length are more efficient in light emission in our *in vitro* assay system.

As mentioned in the introduction, structural information on the active site of luciferase is still scarce in particular in regard of the positioning of the aldehyde substrate. Current mechanistic considerations are based on the crystal structure of luciferase of *V. harveyi* with bound FMN.¹¹ Modelling studies suggested several amino acids that may play an important role for binding or interacting with the aldehyde substrate, as for example His44 and Trp250. Additionally, a spacious hydrophobic cavity was postulated as potential substrate binding position.¹³ Nevertheless, a structure of the ternary complex of luciferase, FMNH₂ and aldehyde is still lacking leading to speculations concerning substrate binding and the reaction mechanism.

To evaluate whether the binding of the substrate within the active site might influence the enzyme activity and maximal light intensity, a preliminary docking study was performed. Based on the crystal structure with bound FMN¹¹, the intermediate state of flavin-4a-hydroperoxide was predicted and the various substrates were docked into the active site. After energy minimization, the structure with the flavin-4a-hydroperoxide in the active site was used for further docking studies with the substrates used in this study, *i. e.* **5a-d** and **6a-d**. The docking results obtained with the saturated and unsaturated aldehydes indicate similar distances of the C1 atom of the respective aldehyde and the distal oxygen atom of the flavin-4a-hydroperoxide (Supplementary Data).

In Figure 4, an overlay of the two docking results with the substrates tetradecanal (**6a**) and (*E*)-tetradec-2-enal (**5a**) is depicted. It appears that the two substrates **5a** and **6a** adopt similar conformations and orientations, except for the position of the oxygen atom of the aldehyde

that points in opposite directions. The distance between the C1 of the aldehyde and the distal oxygen of the flavin intermediate is around 3.6-3.7 Å (Supplementary Data).

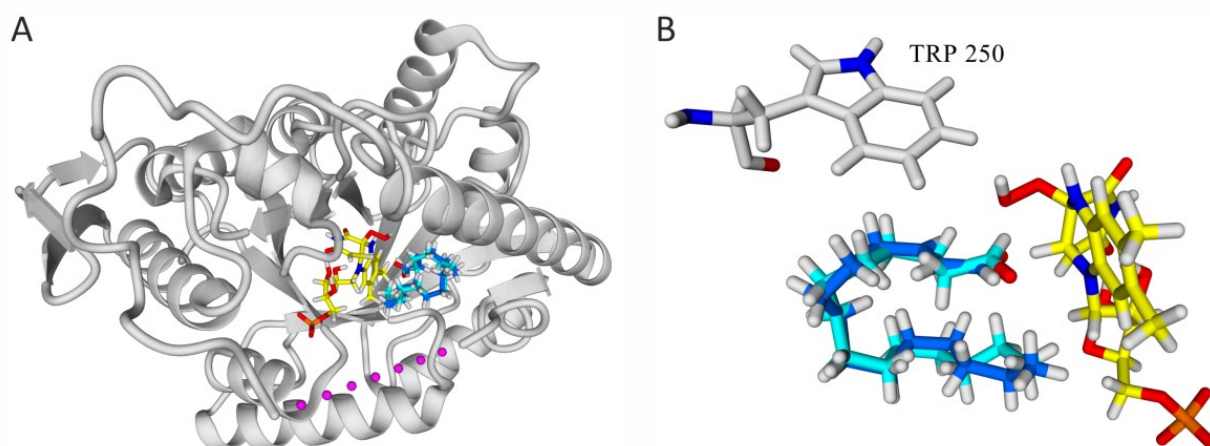


Figure 4: Docking of tetradecanal (6a) and (*E*)-tetradec-2-enal (5a) into the active site of the luciferase of *V. harveyi* with bound flavin-4a-hydroperoxide intermediate. **A:** Crystal structure of the α -subunit of the luciferase of *V. harveyi* with modelled flavin-4a-hydroperoxide intermediate is depicted in yellow. The unstructured loop is displayed as pink dots. The two substrates tetradecanal (**6a**, cyan) and (*E*)-tetradec-2-enal (**5a**, blue) are docked into the active site of the luciferase. **B:** Zoom into the active site and overlay of tetradecanal (**6a**, cyan) and (*E*)-tetradec-2-enal (**5a**, blue). The flavin-4a-hydroperoxide intermediate (yellow) is in close proximity to the substrates **6a** and **5a**, having a distance between the distal oxygen of flavin-4a-hydroperoxide to C1 of 3,637 Å and 3,740 Å, respectively.

Thus our docking results support our experimental findings that unsaturated aldehydes are accepted substrates and indicate that luciferases have a broader substrate range as previously assumed. The different orientation observed for the aldehyde function may be a first hint why unsaturated aldehydes show a substantial difference in kinetics as compared to their saturated counterparts. The hydrophobic pocket, lined for example by Trp250 (Figure 4) within the active site does not allow binding of bulkier or larger substrates, however, replacement of amino acids in the active site of luciferase may help to engineer the putative substrate binding pocket for other aldehyde substrates. Clearly, further structural and computational methods need to be applied to enhance our understanding of the mechanism and substrate scope of bacterial luciferases.

2.6 Conclusion

Bacterial bioluminescence is a fascinating phenomenon and the structure-function relationships responsible for the population of an excited state remains a scientific challenge even after decades of research. Here, we have demonstrated that the scope of substrates utilized by bacterial luciferases is not as limited as previously thought. In this study, the α , β -unsaturated aldehydes with chain length of 8, 10, 12 and 14 carbon atoms were synthesized in a three step synthesis approach. To elucidate the conversion of these potential substrates, an *in vitro* assay was developed. The four synthesized, unsaturated aldehydes **5a-d**, as well as their saturated analogs **6a-d** were analyzed with luciferases from three different genera (*P. leiognathi*, *V. harveyi*, *A. fischeri*). The results indicate, that all of them are accepted by the enzymes and show reasonable to low light emission. Comparing the different potential substrates, tetradecanal (**6a**) exhibits the highest light emission yield, while three other substrates (**5a**, **6b**, **6c**) reached only about 54-75 % of the best performing tetradecanal (**6a**). This study comprises the first comparison of these eight aldehydes (**5a-d**, **6a-d**) as substrates for bacterial luciferases. Having a closer look at the time course of light emission, the different kinetics in the onset as well as decay of light emission for tetradecanal (**6a**) and (*E*)-tetradec-2-enal (**5a**) were evident. Also, we have shown that luciferases from other bioluminescent bacteria show a similar pattern with regard to yield and kinetics of light emission. In summary, all eight substrates **5a-d** and **6a-d** were accepted by the luciferase leading to the conclusion that further investigations on substrate specificity and compatibility will lead to new insights in to bacterial bioluminescence.

2.7 Acknowledgments

This work was supported by the Austrian “Fonds zur Förderung der wissenschaftlichen Forschung” (FWF) to PM (P24189) and the PhD program “DK Molecular Enzymology” to PM and RB (W901). We would like to thank Johannes Niederhauser and Dr. Grit Straganz (Graz University of Technology) for their help with molecular docking experiments using Yasara.

2.8 References

- (1) Dunlap, P. In *Encyclopedia of Microbiology*; Schaechter, M., Ed.; Elsevier: Oxford, 2009; pp 45–61.
- (2) Strehler, B. L. *J. Am. Chem. Soc. USA* **1953**, *75*, 1264.
- (3) Strehler, B. L.; Cormier, M. J. *Arch. Biochem. Biophys.* **1953**, *47*, 16–33.
- (4) Hastings, J. W.; Gibson, Q. H. *J. Biol. Chem.* **1963**, *238* (7), 2537–2554.
- (5) Hastings, J. W.; Spudich, J.; Malnic, G. J. *Biol. Chem.* **1963**, *238* (9), 3100–3105.
- (6) Spudich, J.; Hastings, J. W. *J. Biol. Chem.* **1963**, *238* (9), 3106–3108.
- (7) Cormier, M. J.; Eley, M.; Abe, S.; Nakano, Y. *Photochem. Photobiol.* **1969**, *9*, 351–358.
- (8) Ulitzur, S.; Hastings, J. W. *Proc. Natl. Acad. Sci. USA* **1979**, *76* (1), 265–267.
- (9) Dunlap, P. In *Bioluminescence: Fundamentals and Applications in Biotechnology - Volume 1*; Thouand, G., Marks, R., Eds.; Springer Berlin Heidelberg: Berlin, Heidelberg, 2014; Vol. 144, pp 37–64.
- (10) Fisher, A. J.; Raushel, F. M.; Baldwin, T. O.; Rayment, I. *Biochemistry* **1995**, *34*, 6581–6586.
- (11) Campbell, Z. T.; Weichsel, A.; Montfort, W. R.; Baldwin, T. O. *Biochemistry* **2009**, *48* (26), 6085–6094.
- (12) Fisher, A. J.; Thompson, T. B.; Thoden, J. B.; Baldwin, T. O.; Rayment, I. *J. Biol. Chem.* **1996**, *271* (36), 21956–21968.
- (13) Lin, L. Y.-C.; Sulea, T.; Szittner, R.; Vassilyev, V.; Purisima, E. O.; Meighen, E. A. *Protein Sci.* **2001**, *10* (8), 1563–1571.
- (14) Campbell, Z. T.; Baldwin, T. O.; Miyashita, O. *Biophys. J.* **2010**, *99* (12), 4012–4019.
- (15) Baldwin, T. O.; Christopher, J. A.; Raushel, F. M.; Sinclair, J. F.; Ziegler, M. M.; Fisher, A. J.; Rayment, I. *Curr. Opin. Struct. Biol.* **1995**, *5*, 798–809.
- (16) Chen, L. H.; Baldwin, T. O. *Biochemistry* **1989**, *28*, 2684–2689.
- (17) Li, Z.; Meighen, E. A. *Biochemistry* **1995**, *34*, 15084–15090.
- (18) Bergner, T.; Tabib, C. R.; Winkler, A.; Stipsits, S.; Kayser, H.; Lee, J.; Malthouse, J. P.; Mayhew, S.; Müller, F.; Gruber, K.; Macheroux, P. *Biochim. Biophys. Acta BBA - Proteins Proteomics* **2015**, *1854* (10), 1466–1475.
- (19) Morokutti, A.; Lyskowski, A.; Sollner, S.; Pointner, E.; Fitzpatrick, T. B.; Kratky, C.; Gruber, K.; Macheroux, P. *Biochemistry* **2005**, *44* (42), 13724–13733.
- (20) de Groot, B. L.; van Aalten, D. M. F.; Scheek, R. M.; Amadei, A.; Vriend, G.; Berendsen, H. J. C. *Proteins Struct. Funct. Genet.* **1997**, *29*, 240–251.
- (21) Morris, G. M.; Goodsell, D. S.; Halliday, R. S.; Huey, R.; Hart, W. E.; Belew, R. K.; Olson, A. J. *J. Comput. Chem.* **1998**, *19* (14), 1639–1662.
- (22) Trott, O.; Olson, A. J. *J. Comput. Chem.* **2009**, NA – NA.
- (23) List, B.; Doehring, A.; Fonseca, M. T. H.; Wobser, K.; van Thienen, H.; Torres, R. R.; Galilea, P. L. *Adv. Synth. Catal.* **2005**, *347* (11–13), 1558–1560.
- (24) Strehler, B. L.; Cormier, M. J. *J. Biol. Chem.* **1954**, *211*, 213–225.
- (25) Kurfürst, M.; Ghisla, S.; Hastings, J. W. *Proc. Natl. Acad. Sci. USA* **1984**, *81*, 2990–2994.

2.9 Highlights

- α , β -unsaturated aldehydes were synthesized in a three-step approach
- (un-)saturated aldehydes were investigated as potential substrates for luciferases
- saturated aldehydes showed higher light emission than unsaturated aldehydes
- light emission increases with longer aldehyde chain length, i.e. C14>C12>C10>C8
- unsaturated aldehydes display slower kinetics of light emission

2.10 Supplementary Data

Table S.1: List of used substrates for the *in vitro* assay. Substrate names, numbers, molecular formula, molecular weight and density are listed together with the calculated μmol s used in the substrate-buffer suspension and their molar solubility.

Substrate	Molecular formula	Molecular weight (g/mol)	Density (g/cm ³) (20°C, 760 Torr)	Moles (μmol)	Molar solubility [mol/L] (pH 7, 25°C)
tetradecanal (6a)	C ₁₄ H ₂₈ O	212.37	0.826	19.4	3.7E-5
(<i>E</i>)-tetradec-2-enal (5a)	C ₁₄ H ₂₆ O	210.36	0.839	19.9	1.0E-4
dodecanal (6b)	C ₁₂ H ₂₄ O	184.32	0.823	22.3	1.8E-4
(<i>E</i>)-dodec-2-enal (5b)	C ₁₂ H ₂₂ O	182.30	0.837	23.0	5.2E-4
decanal (6c)	C ₁₀ H ₂₀ O	156.27	0.818	26.2	9.8E-4
(<i>E</i>)-dec-2-enal (5c)	C ₁₀ H ₁₈ O	154.25	0.835	27.1	2.8E-3
octanal (6d)	C ₈ H ₁₆ O	128.21	0.811	31.6	5.4E-3
(<i>E</i>)-oct-2-enal (5d)	C ₈ H ₁₄ O	126.20	0.832	33.0	0.015

Table S.2: Results of the total light emission of the eight substrates investigated *in vitro*. List of eight aldehydes with structure, name and number that were analyzed with the luciferase of *P. leiognathi* in an *in vitro* assay. Their total light emission was measured and calculated in per cent, thereby setting the result of tetradecanal (**6a**) to 100 %.

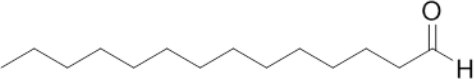
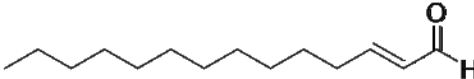
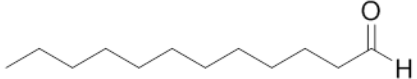
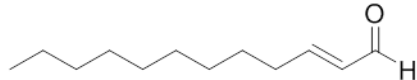
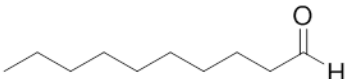
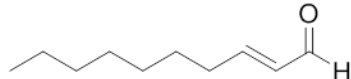
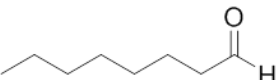
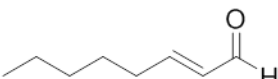
Number	Substrate		total light emission [%]
6a	tetradecanal		100
5a	(<i>E</i>)-tetradec-2-enal		54
6b	dodecanal		75
5b	(<i>E</i>)-dodec-2-enal		4
6c	decanal		64
5c	(<i>E</i>)-dec-2-enal		0,22
6d	octanal		19
5d	(<i>E</i>)-oct-2-enal		0,02

Figure S.1: ^1H and ^{13}C NMR spectra of ethyl (*E*)-oct-2-enoate (3d)

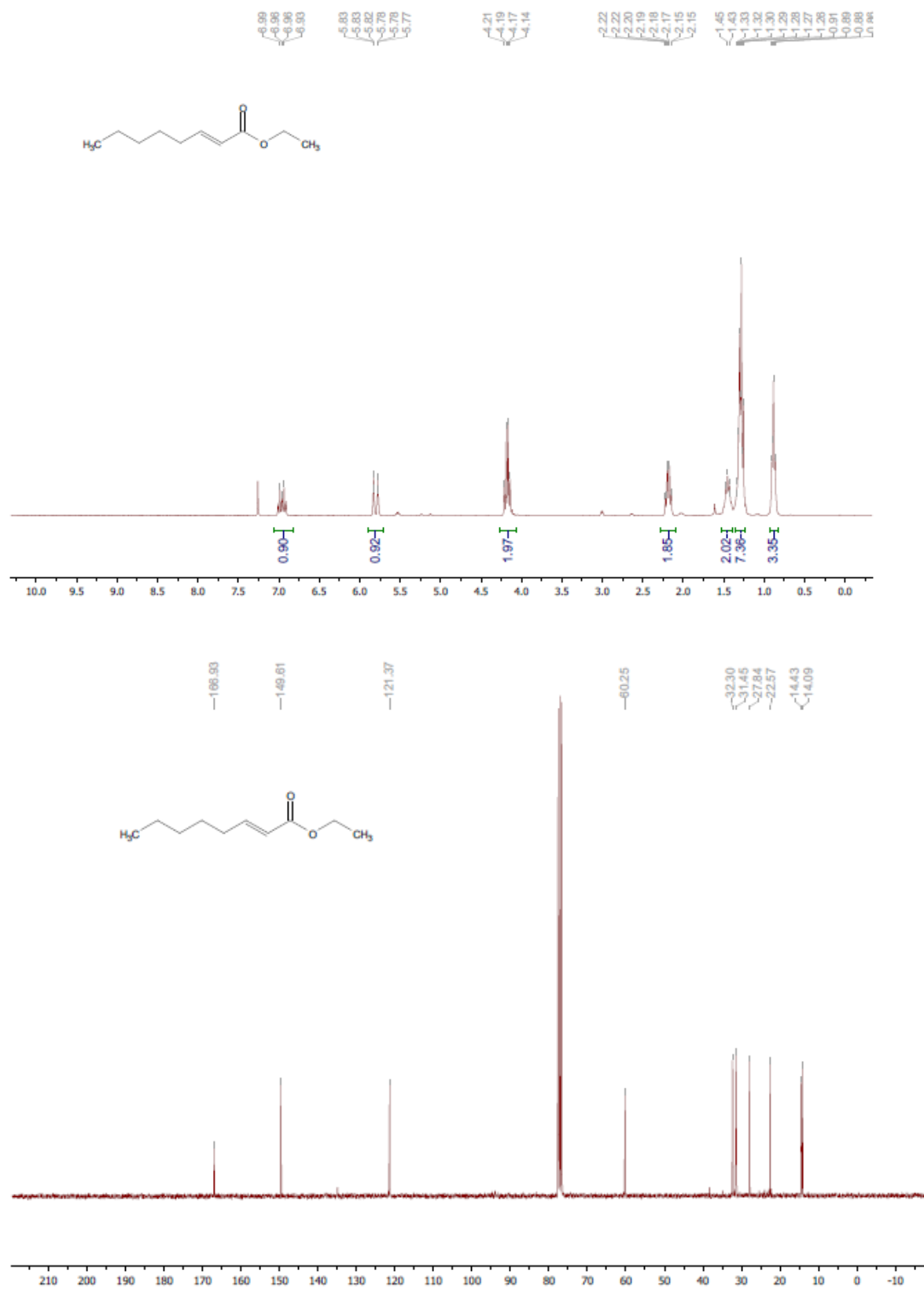


Figure S.2: ^1H and ^{13}C NMR spectra of ethyl (*E*)-dec-2-enoate (3c)

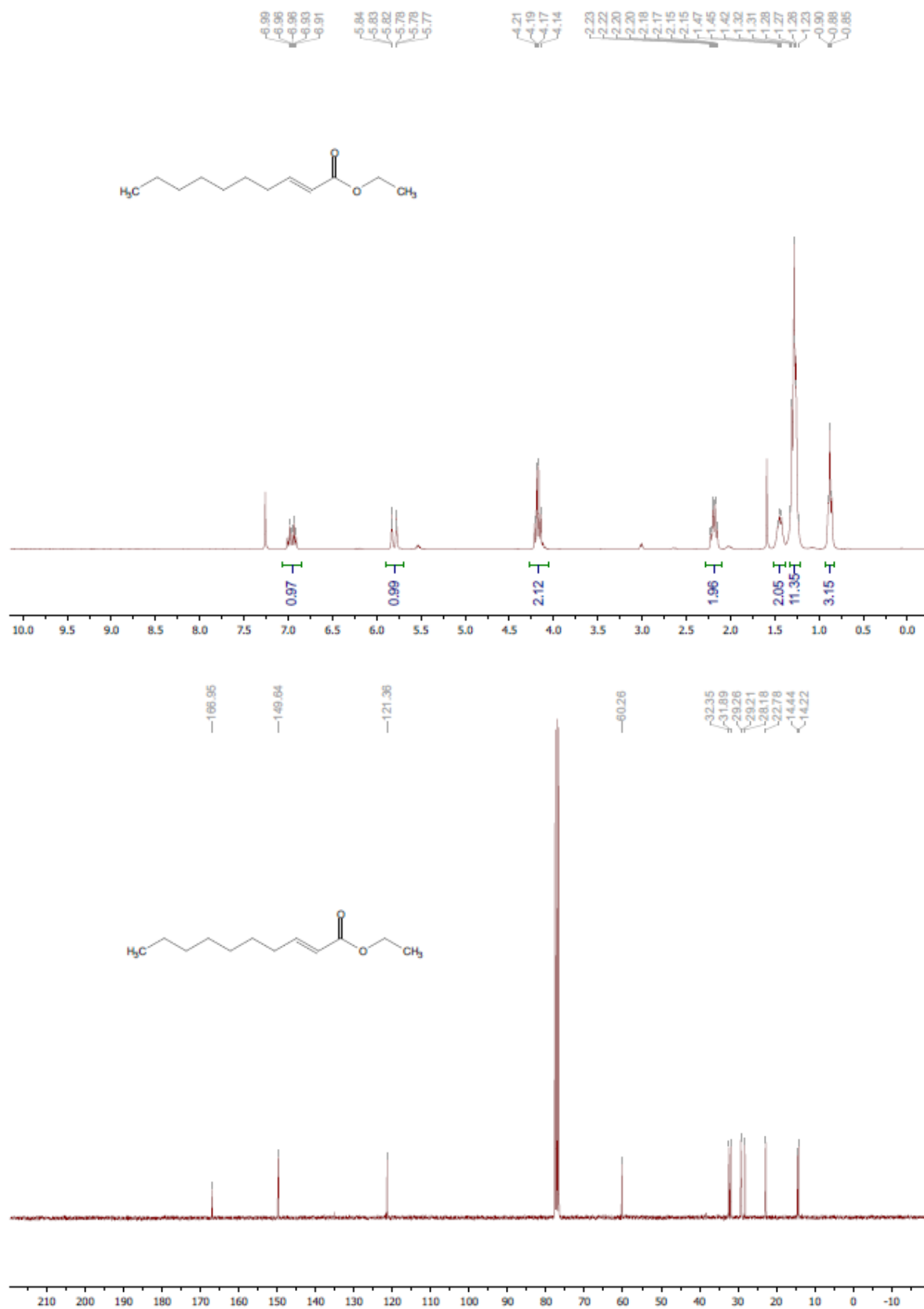


Figure S.3: ^1H and ^{13}C NMR spectra of ethyl (*E*)-dodec-2-enoate (3b)

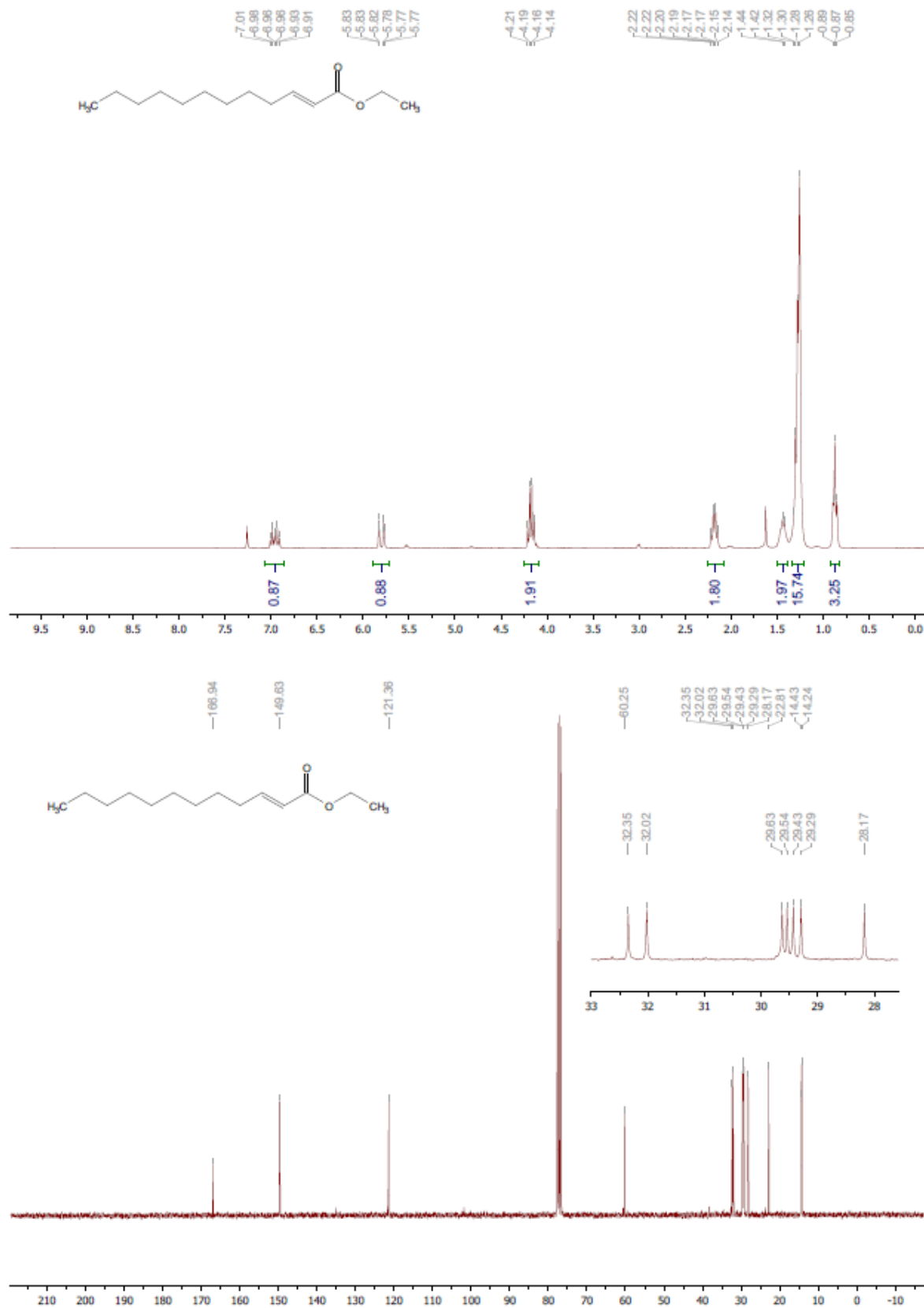


Figure S.4: ^1H and ^{13}C NMR spectra of ethyl (*E*)-tetradec-2-enoate (3a)

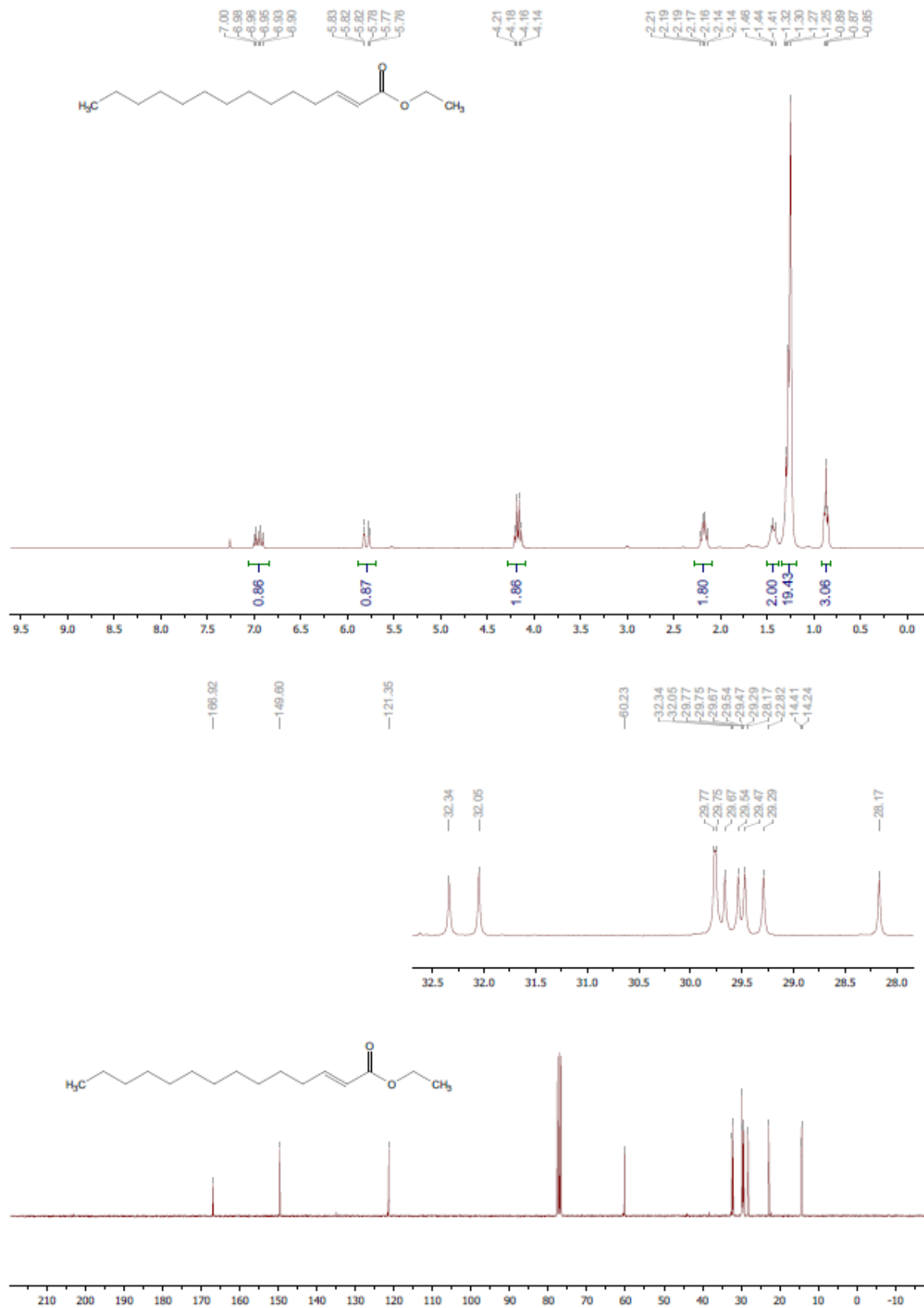


Figure S.5: ^1H and ^{13}C NMR spectra of ethyl (*E*)-oct-2-en-1-ol (4d)

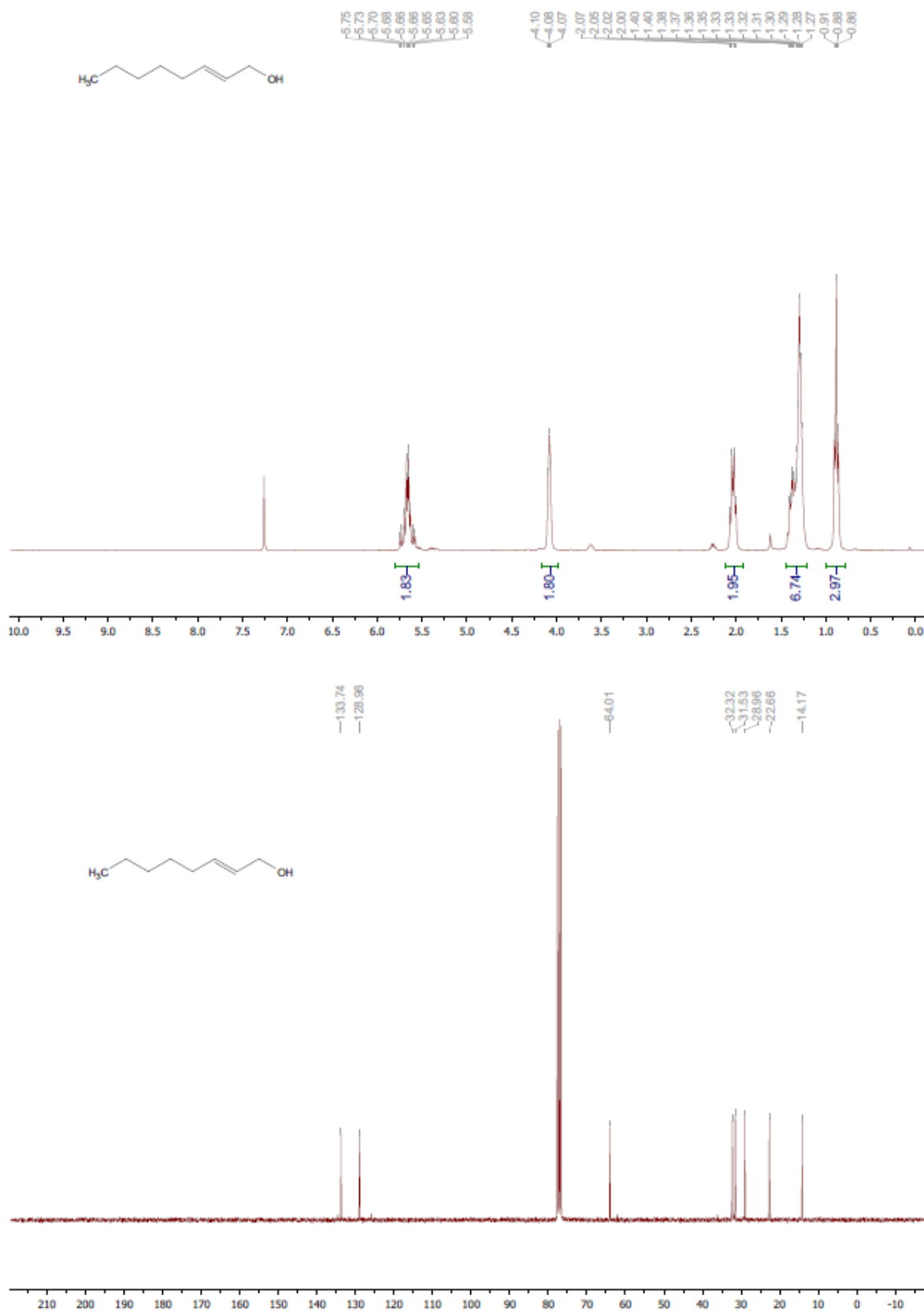


Figure S.6: ^1H and ^{13}C NMR spectra of ethyl (*E*)-dec-2-en-1-ol (4c)

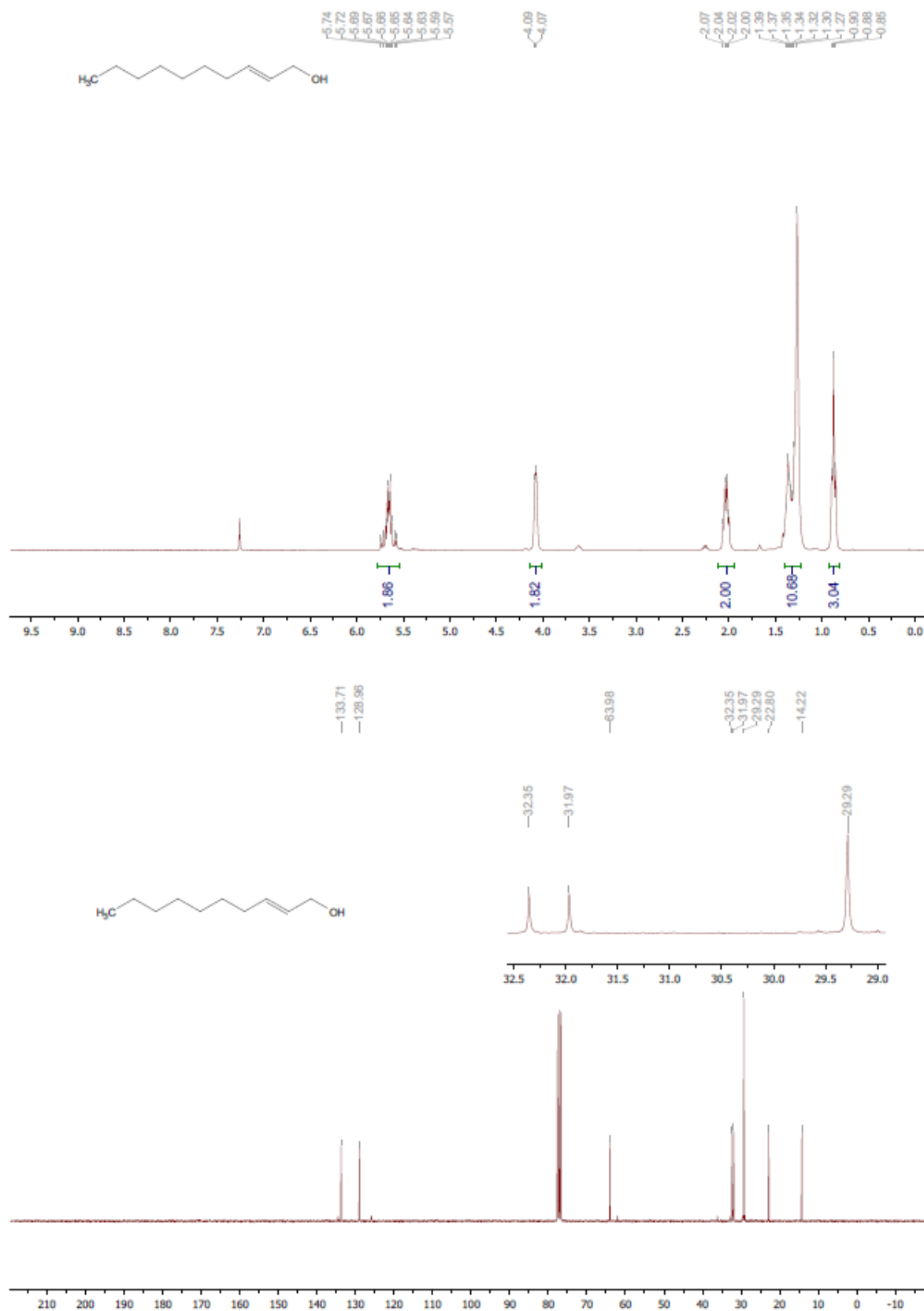


Figure S.7: ^1H and ^{13}C NMR spectra of ethyl (*E*)-dodec-2-en-1-ol (4b)

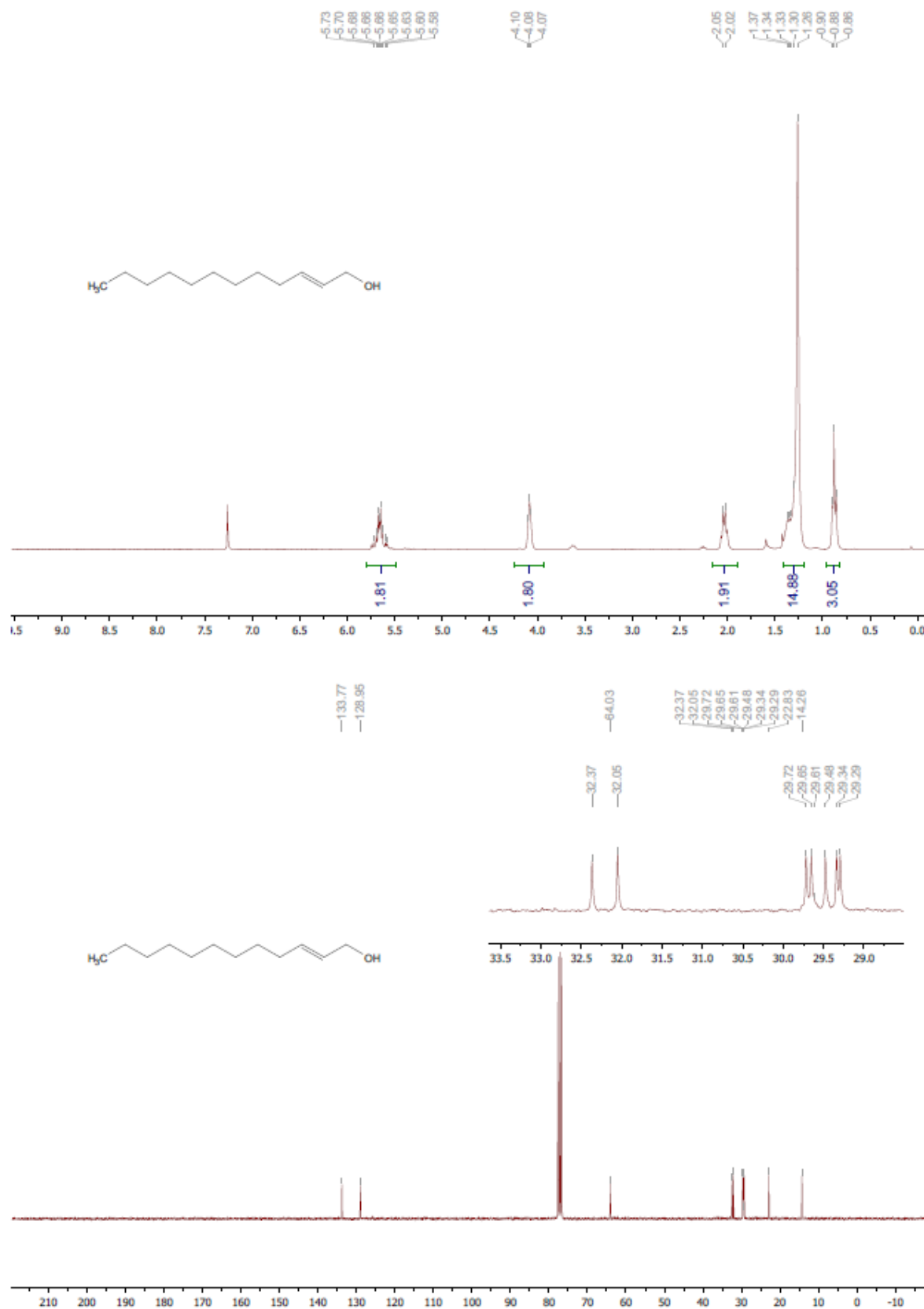


Figure S.8: ^1H and ^{13}C NMR spectra of ethyl (*E*)-tetradec-2-en-1-ol (4a)

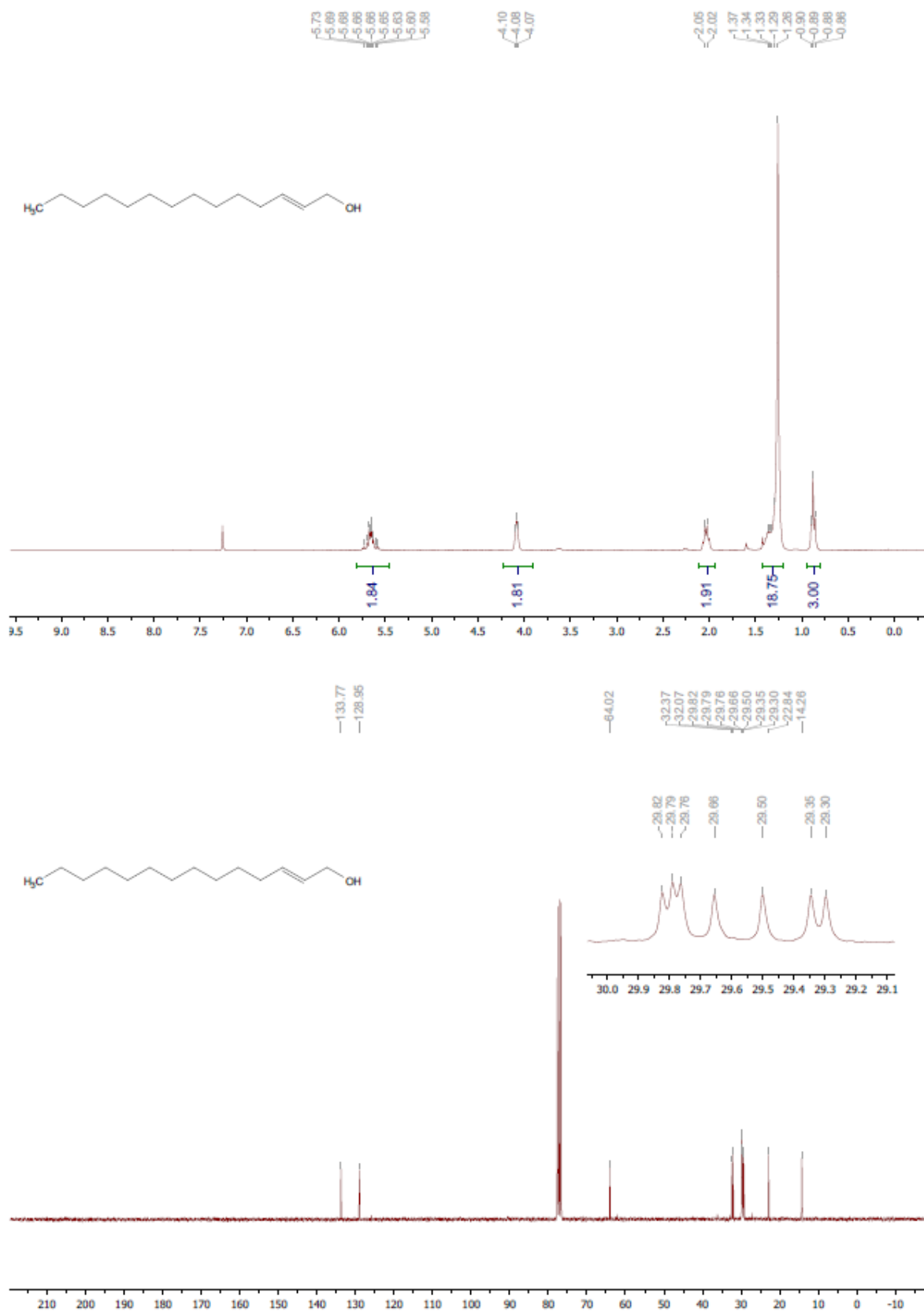


Figure S.9: ^1H and ^{13}C NMR spectra of (*E*)-oct-2-enal (5d)

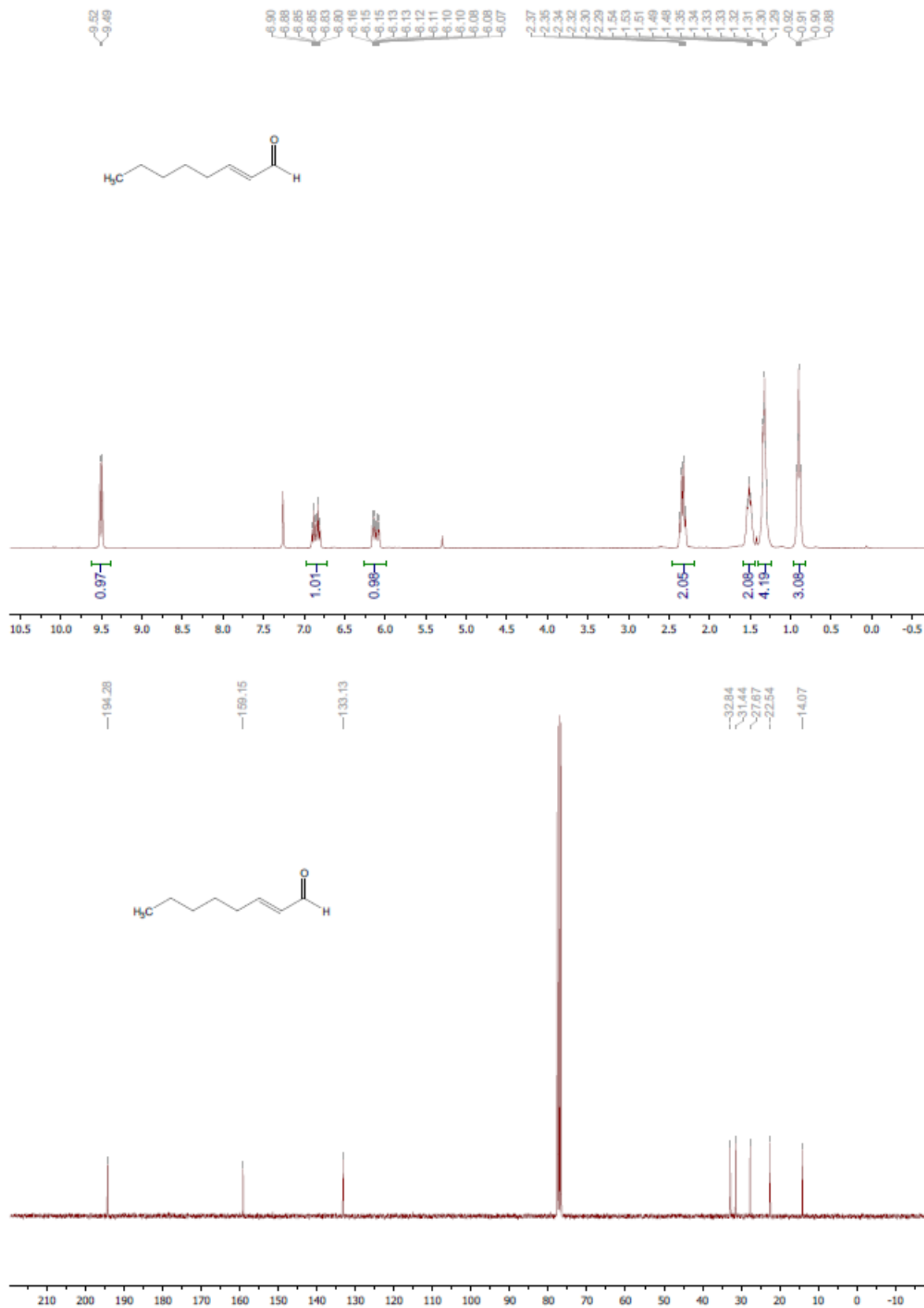


Figure S.10: ^1H and ^{13}C NMR spectra of (*E*)-dec-2-enal (5c)

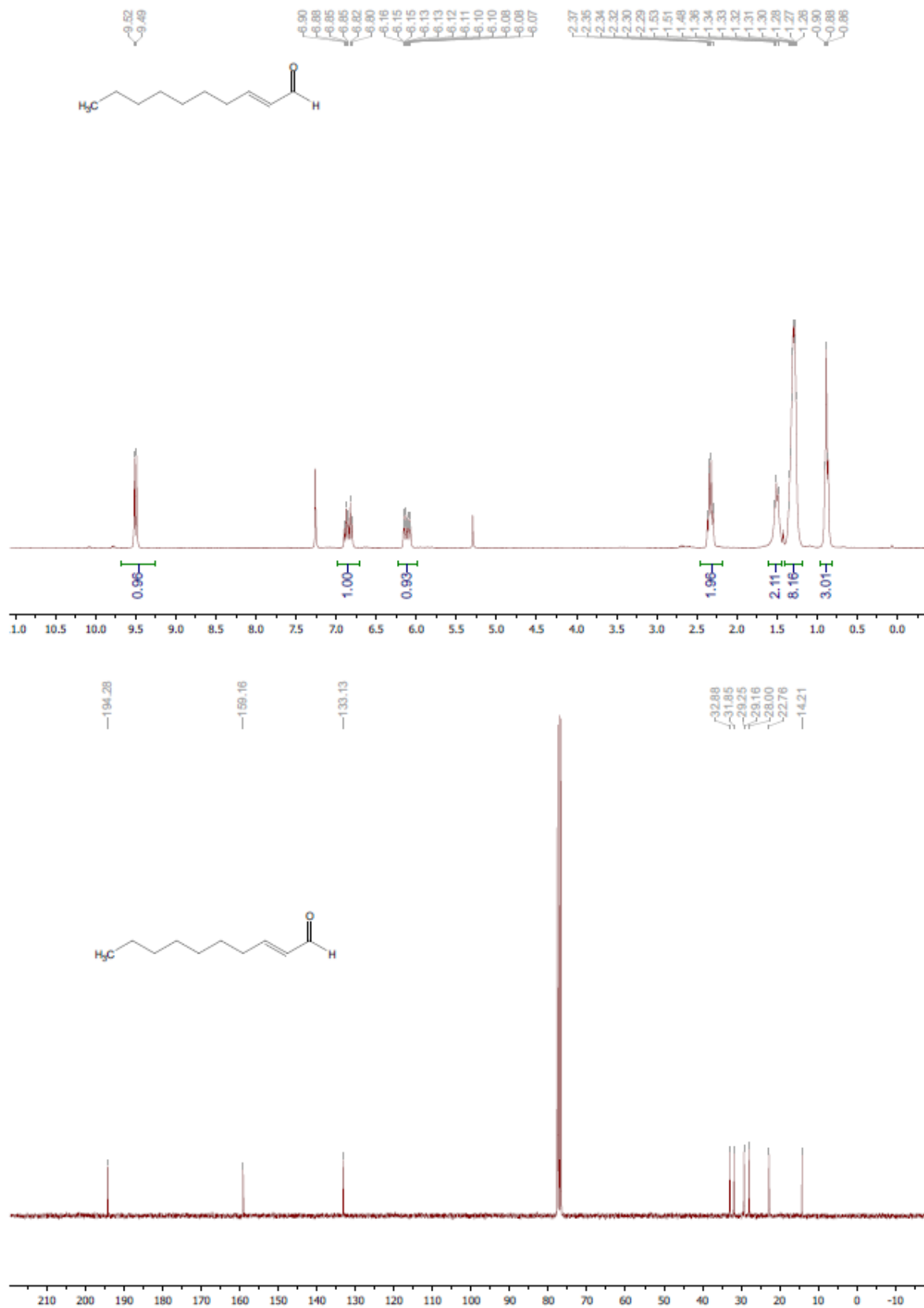


Figure S.11: ^1H and ^{13}C NMR spectra of (*E*)-dodec-2-enal (5b)

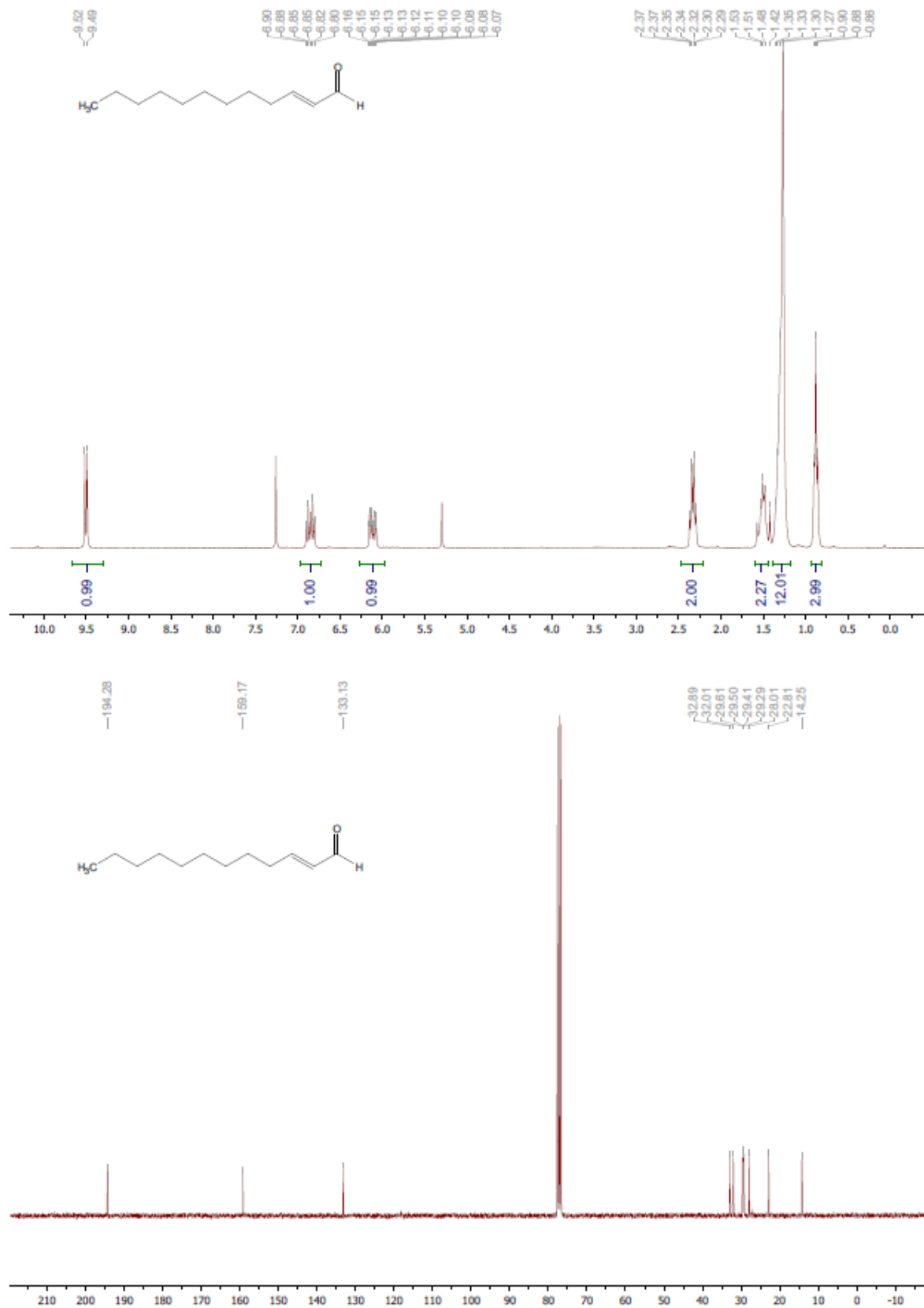


Figure S.12: ^1H and ^{13}C NMR spectra of (*E*)-tetradec-2-enal (5a)

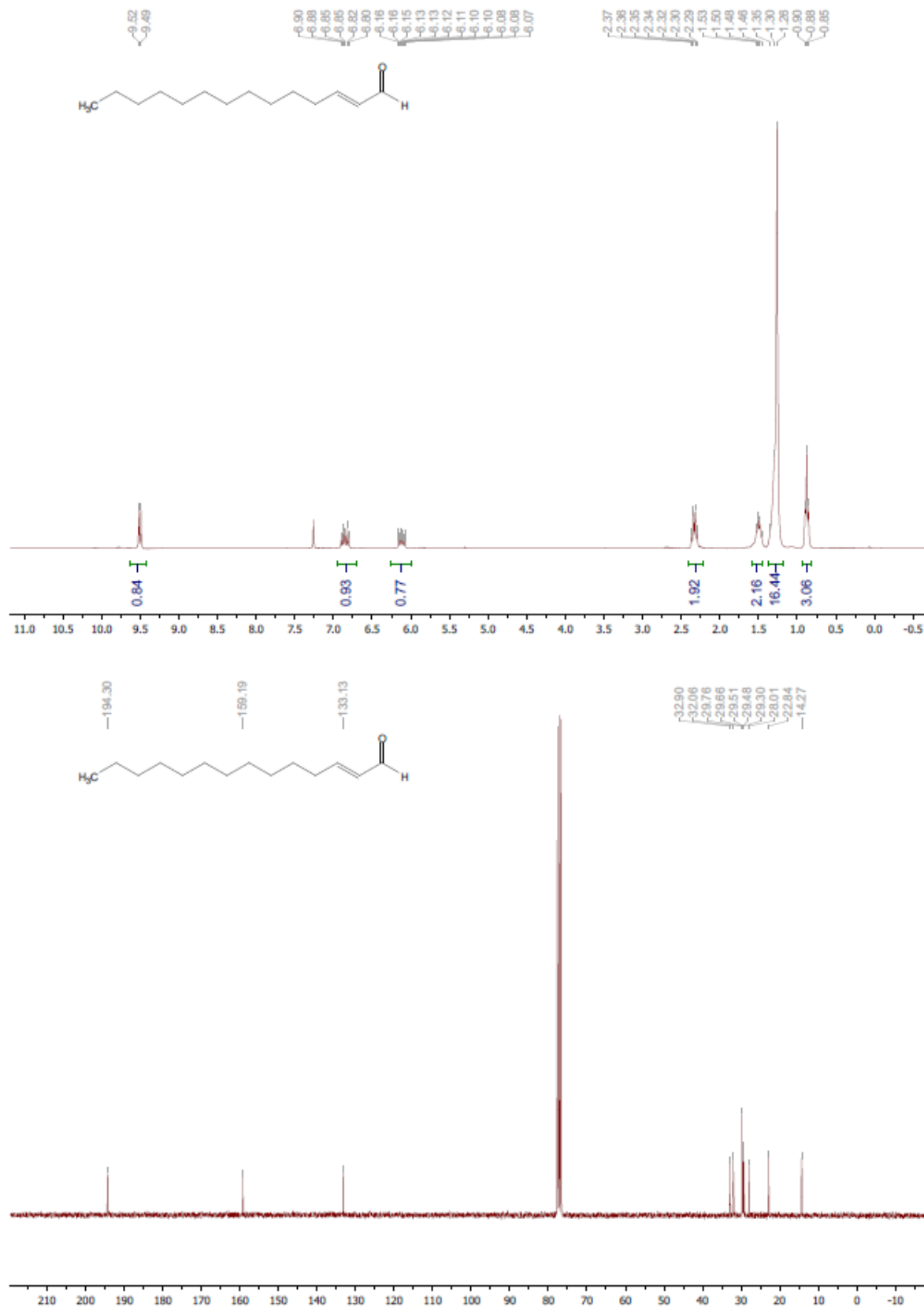


Figure S.13: Overlay of the molecular docking of octanal (6d, shown in cyan) and (*E*)-oct-2-enal (5d, shown in blue) into the active site of the luciferase of *Vibrio harveyi* with the flavin-4a-hydroperoxide intermediate (depicted in yellow). Additionally Trp250 is represented in the graph. The usual color code was applied, where oxygen is red, nitrogen is blue and phosphate is orange.

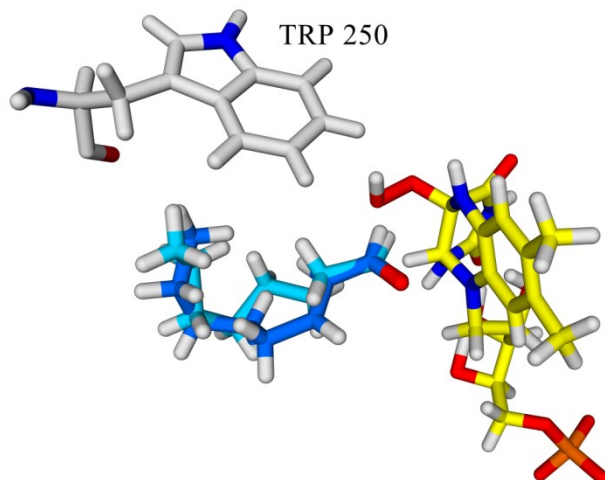


Figure S.14: Overlay of the molecular docking of decanal (6c, shown in cyan) and (*E*)-dec-2-enal (5c, shown in blue) into the active site of the luciferase of *Vibrio harveyi* with the flavin-4a-hydroperoxide intermediate (depicted in yellow). Additionally Trp250 is represented in the graph. The usual color code was applied, where oxygen is red, nitrogen is blue and phosphate is orange.

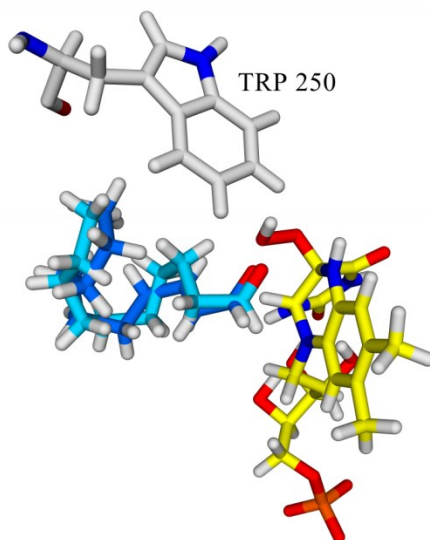


Figure S.15: Overlay of the molecular docking of dodecanal (6b, shown in cyan) and (*E*)-dodec-2-enal (5b, shown in blue) into the active site of the luciferase of *Vibrio harveyi* with the flavin-4a-hydroperoxide intermediate (depicted in yellow). Additionally Trp250 is represented in the graph. The usual color code was applied, where oxygen is red, nitrogen is blue and phosphate is orange.

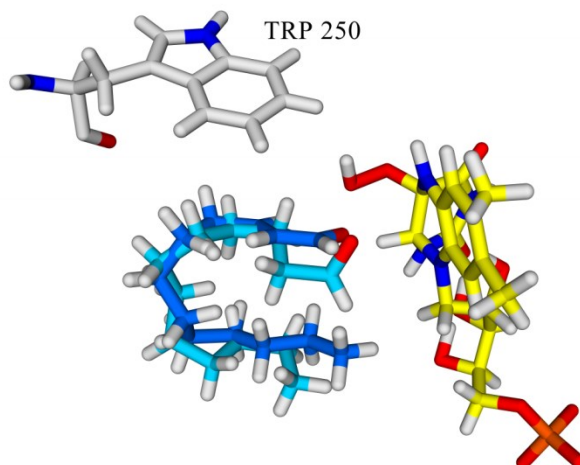
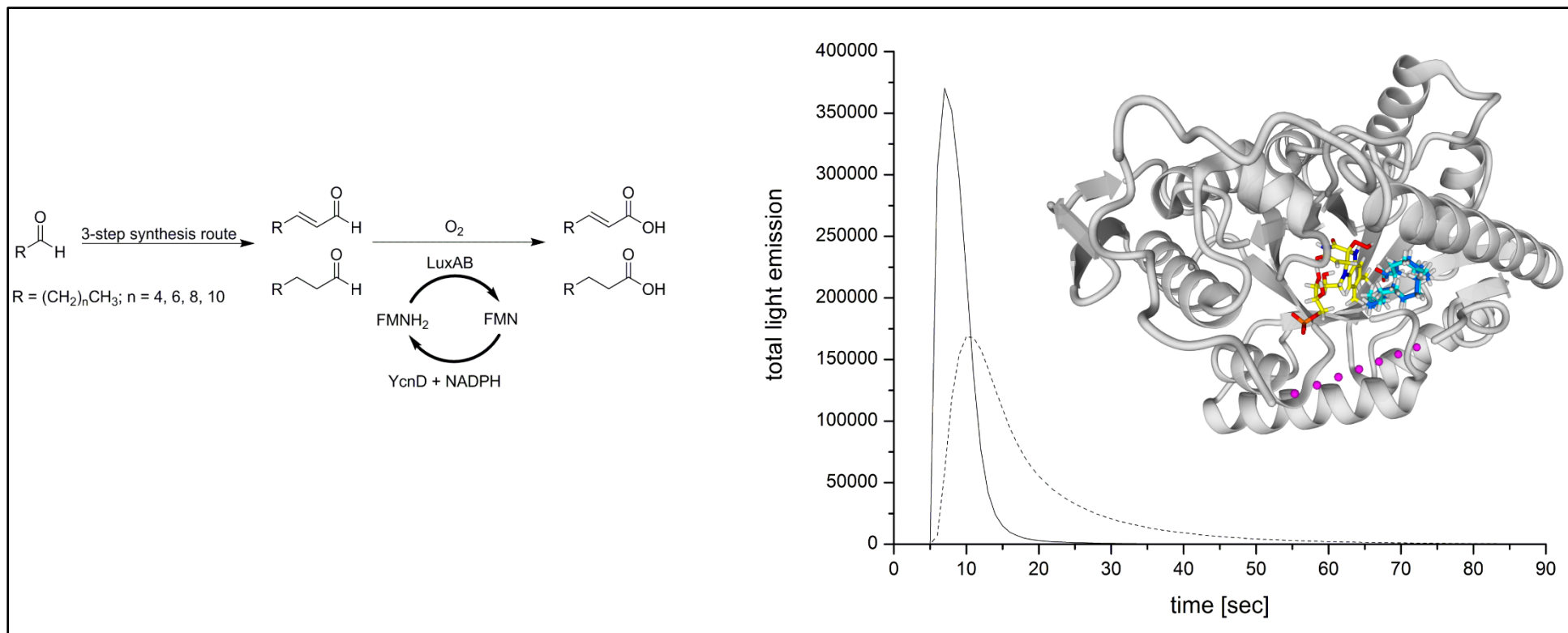


Table S.3: Evaluated distances of the C1 atom of the respective aldehyde substrate 5a-d and 6a-d to the distal oxygen atom of the flavin-4a-hydroperoxide intermediate given in angstrom.

	Substrate	distance O-C1 [Å]
6a	tetradecanal	3,637
5a	(<i>E</i>)-tetradec-2-enal	3,740
6b	dodecanal	4,696
5b	(<i>E</i>)-dodec-2-enal	3,751
6c	decanal	3,711
5c	(<i>E</i>)-dec-2-enal	3,708
6d	octanal	3,572
5d	(<i>E</i>)-oct-2-enal	3,577

2.11 Graphical abstract



Chapter 3

Generation of myristylated FMN by luciferase supports a radical mechanism for bacterial bioluminescence

Chaitanya R. Tabib*, Eveline Brodl* and Peter Macheroux⁺

Graz University of Technology, Institute of Biochemistry, Graz, Austria

*these authors contributed equally to this work

+To whom correspondence should be addressed:

Correspondence:

Prof. Dr. Peter Macheroux, Graz University of Technology, Institute of Biochemistry,
Petersgasse 12/II, A-8010 Graz, Austria;

Tel.: +43-316-873 6450;

Fax: +43-316-873-6952;

Email: peter.macheroux@tugraz.at

Keywords: Myristylated FMN, bacterial bioluminescence, CIEEL mechanism, enzyme cascade, inhibition, *in vitro* assay.

Running title: *Occurrence and generation of myrFMN*

3.1 Abstract

The genes responsible for the light production in bioluminescent bacteria, are present as an operon, *luxCDABEG*. Many strains of *Photobacteria* also carry an extra gene, termed *luxF*. X-ray crystallographic analysis of LuxF revealed the presence of four flavin derivatives, *i.e.* 6-(3'-(*R*)-myristyl) FMN non-covalently bound to the homodimer. In the present study, we exploited the binding of myrFMN to recombinant apo-LuxF to explore the occurrence of myrFMN in various bioluminescent bacteria. MyrFMN was detected in all bacterial strains tested including *Vibrio* and *Aliivibrio* indicating that it is more widely occurring in bioluminescent bacteria than previously assumed. We also show that the apo-LuxF captures myrFMN and thereby relieves the inhibitory effect on luciferase activity. Thus our results provide further support for the hypothesis that LuxF serves as a scavenger of myrFMN in bioluminescent bacteria. However, the source of myrFMN remained obscure. In order to address this issue we have established a cofactor regeneration enzyme-catalyzed cascade reaction that supports luciferase activity *in vitro* for up to three days. This approach enabled to unambiguously demonstrate by UV-Vis absorption spectroscopy and mass spectrometry that myrFMN is generated in the bacterial bioluminescent reaction. Based on this finding we postulate a reaction mechanism for myrFMN generation that is compatible with the proposed radical mechanism for the luciferase reaction.

3.2 Introduction

Riboflavin, also known as vitamin B₂, serves as a precursor for the synthesis of FAD and FMN, which share the same structural backbone, the isoalloxazine ring (Macheroux *et al.*, 2011). Flavoenzymes use either FMN or FAD to carry out a plethora of redox reactions that mostly revolve around the activation of dioxygen and the handling of one-electron or two-electron transfer reactions (Massey, 1994; Teufel *et al.*, 2016; Joosten *et al.*, 2007). A prominent example for the utilization of dioxygen is the bacterial luciferase, which catalyzes the oxidation of long-chain fatty aldehydes to their corresponding fatty acids, *e.g.* tetradecanal to myristic acid (Scheme 1).

In the course of the reaction, reduced FMN reacts with dioxygen to the FMN-4a-hydroperoxide, which subsequently reacts with the aldehyde to the FMN-4a-peroxyhemiacetal. The collapse of this intermediate generates the FMN-4a-hydroxide in an

excited state, which relaxes to the ground state by emission of light centered at 490 nm. (Ulitzur *et al.*, 1979; Kurfurst *et al.*, 1984). Detailed studies on the reaction mechanism led to the suggestion that a radical mechanism, such as the chemically-induced electron exchange luminescence (“CIEEL”) mechanism, is responsible for the population of the excited state (Eckstein *et al.*, 1993). For details see “Discussion”.

The enzymes involved in bacterial bioluminescence are arranged in the form of an operon, with the typical gene organization being *luxCDABEG* as in *Photobacterium leiognathi* ATCC 25521 (Meighen, 1991). The *luxAB* genes encode for the heterodimeric protein luciferase consisting of a 40 kDa α -subunit and a 37 kDa β -subunit. The aldehyde required for the reaction is formed by a multi-enzyme complex consisting of a reductase (*luxC*), a transferase (*luxD*) and a synthetase (*luxE*). In addition, a NADH-dependent FMN reductase is encoded by *luxG* providing reduced FMN to the luciferase (Hastings *et al.*, 1969; Boylan *et al.*, 1985; Nijvipakul *et al.*, 2008). In many photobacterial strains (like TH1, S1 and ATCC 27561) an extra gene ‘*luxF*’ was found in the operon inserted between *luxB* and *luxE* resulting in the new order, *luxCDABFEG* (Lee *et al.*, 1991; Dunlap, 2009; Bergner *et al.*, 2015). Interestingly, large quantities of LuxF were found in these bacteria. LuxF exists as a homodimer and shows an α/β barrel fold, similar to the β -subunit of the bacterial luciferase, and therefore has presumably arisen by gene duplication of *luxB* (Moore *et al.*, 1994). The exact role of LuxF is not yet known, however it was hypothesized that the main function of LuxF is the binding of myristylated FMN (myrFMN), which is presumably a side product of the luciferase reaction. MyrFMN is thought to bind sufficiently tight in the active site of luciferase to inhibit the bioluminescent reaction (Moore *et al.*, 1995). In fact, Wei and coworkers could demonstrate the inhibiting effect of myrFMN on the luciferase from *Vibrio harveyi* (Wei *et al.*, 2001).

The generation of myrFMN in the marine bacterial strains is a largely unexplored phenomenon. In our previous report, we have reported a method to isolate myrFMN from *Photobacterium leiognathi* S1 (Bergner *et al.*, 2015). Using isolated and purified myrFMN we showed that it binds to recombinant apo-LuxF ($K_d = 80$ nM) fifty times more tightly than to luciferase from *Photobacterium leiognathi* ($K_d = 4$ μ M) by using isothermal titration calorimetry. This tight binding to LuxF is clearly due to the large hydrophobic surface area of the myristyl group, which is deeply buried in each binding site. As a consequence, it is extremely difficult to remove the bound flavin derivative from LuxF and therefore harsh

denaturing conditions are required to extract myrFMN from LuxF, as described previously (Bergner *et al.*, 2015). Therefore, this tight binding of myrFMN to recombinant apo-LuxF was exploited to explore its occurrence in various bioluminescent bacterial strains (*luxF*⁺ and *luxF*⁻) of *Photobacteria*. This analysis showed that myrFMN is present in all photobacterial strains tested, suggesting that its production is independent of the occurrence of *luxF*.

To better understand the occurrence and generation of myrFMN, we were interested in the relationship of bioluminescence intensity and the production of myrFMN in different bioluminescent bacterial genera, *i.e.* *Aliivibrio*, *Vibrio* and *Photobacteria*. These experiments suggested that total light production in bacteria correlates to myrFMN production and thus indicated that myrFMN is directly generated in the luciferase reaction. This insight prompted us to establish an enzyme driven cofactor regeneration system that sustains *in vitro* light emission for up to three days. We then utilized the apo-LuxF scavenging method to enrich and isolate any myrFMN produced in the experiment. This approach enabled us finally to unambiguously demonstrate that myrFMN is formed in the luciferase reaction.

3.3 Experimental procedures

3.3.1 Chemicals

Tetradecanal, IPTG, FMN, NADPH, glucose and all buffer components were from Chemos GmbH, Sigma-Aldrich, Peqlab and Roth. All these chemicals were used directly without further purifications. GDH (glucose dehydrogenase) was a gift from Dr. Wolfgang Kroutil, University of Graz.

3.3.2 Instrumentation

UV-Vis absorption spectra were recorded using a Specord 205/210 spectrophotometer (Analytic Jena, Jena, Germany). Both, *in vivo* (bacterial bioluminescence) and *in vitro* light emission (single and multiple turnover reactions), were measured using a Centro LB960 microplate luminometer (Berthold Technologies, Bad Wildbach, Germany). All protein purifications were primarily performed using a 5 mL HisTrap FF affinity column (GE Healthcare, UK) and later applied to a HiLoad 16/600 Superdex 200 prep grade gel filtration column on an ÄKTAexplorer 100 Pharmacia Biotech (GE Healthcare life sciences, UK).

HPLC analysis was performed with a semi-preparative Dionex UltiMate 3000 equipped with a Dionex UltiMate Diode Array Detector. Separation over an Atlantis dC18 (4.6 x 250 mm, 5 μ m) column (Waters) was achieved using a gradient of 0.1 % TFA in water and acetonitrile at 25 °C and 1 mL/min flow rate starting from 0 % acetonitrile to 95 % within 20 min, holding 95 % for 5 min and going down to 0 % within 5 min and holding 0 % for another 10 min. For determination of the peaks the wavelengths at 280, 370 and 450 nm were used, respectively. For evaluation of the results, up to four references were measured having the following retention times and wavelength maxima: FAD: t_R = 9.1 min; Maxima: 372/447 nm; FMN: t_R = 9.8 min; Maxima: 371/446 nm; Riboflavin: t_R = 10.4 min; Maxima: 370/445 nm; myrFMN: t_R = 18.7 min; Maxima: 386/442 nm. Fractions were collected by time from 18.0 to 24.0 min and fraction tubes were changed every 15 seconds. Those fractions containing myrFMN, according to the analysis at 370 nm, were combined and dried under reduced pressure. This sample was dissolved in MeOH for HPLC-MS analysis.

HPLC-MS analysis was performed on an Agilent Technologies 1200 Series system equipped with a MWD SL multiple wavelength detector (deuterium lamp, 190-400 nm) and with a single quadrupole LCMS detector using electrospray ionization source (ESI). The samples were separated over an Agilent Poroshell 120 SB-C18 (3 x 100 mm, 2.7 μ m) column using the same gradient as mentioned above but with 0.01 % FA in water and acetonitrile at 25 °C and 0.5 mL/min flow rate. Determination of the peaks was achieved by analyzing the chromatograms at 210, 280, 370 and 450 nm, respectively and by using the mass spectrometer.

A negative ESI-Scan mode from m/z 100 to 800 was used to evaluate all the peaks and corresponding masses. The application "extracted ion chromatogram" of the HPLC-MS software ChemStation was utilized for linking the peaks with the m/z values 601 (dephosphorylated 6'-(3'-(*R*)-myristyl FMN; $C_{31}H_{45}N_4O_8^-$; exact mass 601.31)) and 681 (phosphorylated 6'-(3'-(*R*)-myristyl FMN; $C_{31}H_{46}N_4O_{11}P^-$; exact mass 681.29)). By using this function one defined m/z value (in this case 601 or 681) is searched within the negative ESI-Scan mode from m/z 100 to 800 and drawn as separate chromatogram by the program.

3.3.3 Bioluminescent bacterial strains

The following bacterial strains were selected for our study: TH1, S1, ATCC 27561, ATCC 25521 and ATCC 25587 from genus *Photobacterium leiognathi*; ATCC 14126 from genus *Vibrio harveyi* and ATCC 7744 from genus *Aliivibrio fischeri*. Only TH1, S1 and ATCC 27561 contained *luxF* as reported previously (Bergner *et al.*, 2015). The bacteria were cultivated in 1 L flasks with 200 mL of 246-SWC media (246-Sea water culture). The cells were grown at 25 °C with 130 rpm shaking for optimal aeration.

3.3.4 Cloning, expression and purification of various proteins

Expression and purification of LuxAB and LuxF from *P. leiognathi* ATCC 27561 and of YcnD from *B. subtilis* was performed as described previously (Bergner *et al.*, 2015; Morokutti *et al.*, 2005). The protein concentrations were calculated using the molar extinction coefficients 82335 M⁻¹cm⁻¹ (*P. leiognathi* LuxAB) and 26025 M⁻¹cm⁻¹ (LuxF) at 280 nm and 12190 M⁻¹cm⁻¹ (YcnD) at 450 nm, respectively.

Based on the DNA sequence available, a synthetic gene for LuxAB (from *V. harveyi* ATCC 14126 and *A. fischeri* ATCC 7744) was designed with a C-terminal octa-histidine tag and optimised for *E. coli* codon usage. The gene was then sub-cloned into a pET24b vector (Kan^R) and transformed into *E. coli* Rosetta strain (Cmp^R) for heterologous expression. The cells containing the construct were grown in LB media with kanamycin (50 µg mL⁻¹) and chloramphenicol (20 µg mL⁻¹) at 37 °C to an OD₆₀₀ of ~0.6. The protein expression was then induced by addition of 0.1 mM IPTG and the cells were further grown for 16 hours at 20°C. The cells were then harvested by centrifugation (7000 g, 10 min, at 4 °C) and the wet cell pellets were stored at -20 °C until further use. The proteins were purified similar to the photobacterial luciferase as reported previously (Bergner *et al.*, 2015). The protein concentrations were calculated using the molar extinction coefficients 84230 M⁻¹ cm⁻¹ (*V. harveyi* LuxAB) and 83200 M⁻¹ cm⁻¹ (*A. fischeri* LuxAB) at 280 nm.

3.3.5 Analysis of bacterial strains for light emission vs myrFMN content

Assays were performed using the 96 well white assay plates. Light emission was measured using the luminometer. The OD of the cells was obtained by absorption measurements using an UV-Vis spectrophotometer at 660 nm (instead of 600 nm) to exclude the interference of artefacts due to bioluminescence.

To measure the light emission, 100 µl of cells were pipetted into each well of the assay plate and after an initial delay of 1 second and rapid mixing of the plate for 0.1 second, the reading was taken for 1 second total time. The readings were taken for 24 hours with time intervals 30/60 minutes. The light intensity (counts) at each time point was plotted. For comparison, the following bioluminescent bacterial strains were taken into consideration: *P. leiognathi* TH1, S1, ATCC 27561, ATCC 25587 and ATCC 25521; *V. harveyi* ATCC 14126; *A. fischeri* ATCC 7744.

For the quantification of myrFMN content, 10 g of wet cell pellet was taken for each strain mentioned above. The extraction of myrFMN *in vivo*, using recombinant apo-LuxF was performed precisely as described previously (Bergner *et al.*, 2015). The isolated product was analyzed with HPLC.

3.3.6 Inhibition assay

In this assay, the light emitted by the enzyme luciferase was measured using the luminometer. The assay was performed in 96 well black assay plates using 100 mM potassium phosphate buffer with 300 mM NaCl, pH 7 as reaction buffer.

The reaction mixture contained 200 nM luciferase, 300 nM YcnD, 300 nM FMN, 500 nM NADPH and the substrate-buffer suspension in the reaction buffer to make up the final volume to 250 µL [due to the low solubility of aldehyde in the buffer, concentrated aldehyde suspensions were obtained by mixing 5 µL of aldehyde with 10 mL of buffer using ultrasonication]. Apo-LuxF was used in excess concentrations (up to 100 µM) as a scavenger for myrFMN. The reactions were started by injecting NADPH to the master mix (after a delay of 5 seconds) and the readings were subsequently taken every second for 90 seconds total time.

Pure myrFMN sample in a concentration gradient from 0 to 50 μM was used as the inhibitor in this assay (extracted and purified as reported previously in Bergner *et al.*, 2015; the concentration of myrFMN was calculated using the extinction coefficient (ϵ) at 396 nm = $11350 \text{ M}^{-1} \text{ cm}^{-1}$. Three different sub-assay conditions were used to observe the inhibitory effect on the luciferase activity: First, in the absence of LuxF; second, in the presence of LuxF from the beginning of the reaction; and lastly when LuxF is added at a later stage of the reaction (after 90 seconds). All three conditions were tested for increasing myrFMN concentrations. Light emission was plotted against myrFMN concentration. The control reactions without myrFMN in each condition were considered as 100 %.

3.3.7 In vitro multiple turnover reaction

All enzymes and cofactors were diluted and prepared in 100 mM potassium phosphate buffer pH 7. For the multiple turnover reactions the following components and concentrations were used: 100 μM LuxAB, 150 μM FMN, 150 μM YcnD, 2 mM NADPH, 200 mg GDH (lyophilized powder), 1 M glucose and 100 μl substrate-buffer solution. Due to low solubility of aldehydes in water, a substrate-buffer solution was obtained by adding 40 μL of tetradecanal to a mixture of 1900 μL reaction buffer and 100 μL Triton X. This led to complete solubility of the substrate. All components were mixed to a final volume of 25 mL in a 50 mL enzyme reactor. The reaction was started by the addition of LuxAB and stirred at 4 $^{\circ}\text{C}$ for a maximum of 72 hours. After six hours reaction time, 200 μM BSA was added to stabilize the enzymes.

For the workup, three main steps were performed analog to the extraction of myrFMN *in vivo* (Bergner *et al.*, 2015). The reactions were stopped by adding 2.5 g guanidine-HCl and dropwise concentrated HCl to lower the pH to ~ 2 . Three consecutive extractions were made with 15 mL each of an organic mixture of ethyl acetate:butanol (1:1). The organic phase was separated by centrifugation (4566 g at 4 $^{\circ}\text{C}$ for 30 min) and the collected, unified organic layers were dried in a vacuum evaporator at 56 $^{\circ}\text{C}$ under reduced pressure. The residual powder was dissolved in 20 mL lysis buffer (50 mM NaH_2PO_4 , 300 mM NaCl, 10 mM imidazole, pH 8) and incubated with excess of recombinant histidine-tagged apo-LuxF for 30 minutes in the dark. The apo-LuxF with bound myrFMN was loaded on a 1 mL HisTrap FF/HP column (GE Healthcare) for purification. The column was washed with wash buffer (50 mM NaH_2PO_4 , 300 mM NaCl, 20 mM imidazole, pH 8) and the fractions were eluted with elution buffer (50 mM NaH_2PO_4 ,

300 mM NaCl, 300 mM imidazole, pH 8). The eluent fractions were pooled and concentrated to 500 μ L. As a final purification step organic extraction was repeated again in small scale as described above. The dried samples were analyzed by HPLC.

3.4 Results

3.4.1 Analysis of bacterial strains for light emission and myrFMN content

In a previous study we have shown that 6-(3'-(*R*)-myristyl)-FMN (myrFMN) is generated by various bacteria in the genera *Photobacterium* and does not correlate with the presence of *luxF*, a gene encoding a protein that specifically binds myrFMN (Bergner *et al.*, 2015). However, it remained unclear how myrFMN is generated and whether it affects the capability of bacteria to produce light. In order to address these issues we have monitored the total light emission of various bioluminescent species and finally isolated myrFMN from the same bacterial cultures exploiting the high affinity of recombinant apo-LuxF as previously demonstrated (Bergner *et al.*, 2015). The extraction protocol as described in materials and methods was designed to ensure that protein-bound myrFMN is released and thus becomes available for re-binding to the added recombinant apo-LuxF. The scavenged myrFMN was then co-purified with the histidine-tagged LuxF by means of affinity chromatography and eventually released from the purified protein for quantification via HPLC. The results of the total light emission and myrFMN determination in seven different bioluminescent marine bacteria are summarized in Figure 1. The highest total light emission and myrFMN content were found in *P. leiognathi* TH1 (this was set to 100 % for further comparison) followed by strains S1 and 27561, respectively. However, only trace amounts of myrFMN were detected in strains 25521 and 25587. It was also tested if myrFMN production is confined to the genus *Photobacteria* or also occurs in other genera, *i.e.* *Aliivibrio* and *Vibrio*. As is evident from Figure 1, the presence of myrFMN was demonstrated for *A. fischeri* and *V. harveyi* albeit in very small amounts in the case of the former species. These strains also produce less than 2 % of light compared to the best light-emitting strain TH1. Thus our results clearly indicate that generation of myrFMN occurs ubiquitously in bioluminescent bacteria and is not confined to *Photobacteria*. The presence of myrFMN extracted from the strains TH1 and S1 were further confirmed by HPLC-MS (supplementary data). The amounts of myrFMN isolated from the other strains were below the detection limit for MS and therefore were not analysed in further detail. Furthermore, our findings show that myrFMN production and total light emission correlate suggesting that myrFMN is generated in the chemical processes leading to light emission, *i.e.* the oxidation of tetradecanal by bacterial luciferase. Interestingly, the best light emitters, *i.e.* *P. leiognathi* strains TH1, S1 and 27561 possess the *luxF* gene and thus produce LuxF, which

may protect bacterial luciferase by scavenging myrFMN. In fact, we could recently demonstrate binding of myrFMN to photobacterial luciferase (Bergner *et al.*, 2015), however, it remained to be shown whether binding of myrFMN affects the activity of the enzyme.

3.4.2 Inhibition of luciferase by myrFMN

Therefore we set up an inhibition assay to evaluate the effect of myrFMN on the luciferase-catalyzed reaction. Briefly, purified myrFMN from *P. leiognathi* S1 was used in increasing concentrations (0 – 50 μM) in an assay with luciferase (200 nM) and other required components as mentioned in materials and methods. The light emission over a period of 90 seconds was recorded. In Figure 2A, it was shown that as the concentration of myrFMN increased, the intensity of light emitted decreased (reaction 1 - black filled squares). A decrease in light emission indicates inhibition of luciferase activity as the active site is obstructed by myrFMN and prevents binding of FMNH_2 . However, addition of recombinant apo-LuxF to the same reaction (after a primary cycle of 90 seconds) scavenged myrFMN and thus allowed binding of FMNH_2 to be used in the bioluminescent reaction (reaction 1 + LuxF - red filled circles). In an additional reaction that more closely mimicked the situation *in vivo*, LuxF was added prior to initiating the reaction (reaction 2 - blue filled triangles). Increased light emission is observed at each concentration compared to the other two experiments suggesting that LuxF scavenged myrFMN before it bound to the luciferase in agreement with the 10-fold higher affinity to LuxF. This is also reflected by the IC_{50} for the inhibition as shown in Figure 2B. The concentration of myrFMN required to reduce the light emission to 50 % is approximately 2 μM , very close to the reported dissociation constant of myrFMN of 4 μM (Bergner *et al.*, 2015). However, to inhibit 50 % of the luciferase activity in the presence of LuxF, a 6-fold higher concentration ($\sim 11 \mu\text{M}$) of myrFMN is required, thus demonstrating the protective effect of LuxF on the bioluminescent reaction.

3.4.3 In vitro multiple turnover reaction

These findings point toward a direct link between light emission and myrFMN generation and thus we endeavored to provide direct proof that myrFMN is produced during the luciferase-catalyzed monooxygenation of long-chain fatty aldehydes. Toward this goal, we developed an

in vitro multiple turnover assay using the luciferase from *P. leiognathi*. This was achieved by coupling the bioluminescent reaction to YcnD, an oxidoreductase from *Bacillus subtilis* (Morokutti *et al.*, 2005) and glucose dehydrogenase (GDH). YcnD reduces FMN at the expense of NADPH and thus provides FMNH₂, which is stoichiometrically consumed in the luciferase-catalyzed reaction. On the other hand, GDH regenerates NADPH from NADP by oxidizing D-glucose, which is added at a concentration to ensure prolonged luciferase activity (Scheme 2). Detailed reaction conditions and reagent concentrations are described in materials and methods.

The reactions were started by the addition of luciferase resulting in intense light emission, clearly visible in the darkroom. The light intensity decreased over time and the reactions were stopped when light emission ceased (typically after ca. 72 h). After quenching the reaction, recombinant apo-LuxF was employed as before to isolate any myrFMN produced during multiple luciferase turnovers. Recombinant histidine-tagged LuxF incubated with the reaction mixture was then extracted by affinity chromatography and bound ligands were released by acid treatment and analyzed by a semi-preparative HPLC. As shown in Figure 3, the main compound released from LuxF has a retention time identical to an authentic myrFMN sample isolated from *P. leiognathi* S1 ($t_R = 18.8$ min). Moreover, the UV-Vis absorption spectrum is identical to the reference with absorption maxima at 386 and 441 nm (Figure 3, insert). MyrFMN samples were combined and dried under reduced pressure. The isolated and purified myrFMN was then subjected to HPLC-MS analysis using an Agilent Poroshell 120 SB-C18 column. Due to the usage of that column, the retention time of the myrFMN peak shifted to 14.2 minutes (Figure 4A). Phosphorylated and dephosphorylated myrFMN have exact molecular masses of 681.29 and 601.31, respectively, and therefore a negative ESI scan mode from 100-800 m/z was used. The extracted ion chromatogram (XIC) at m/z 681 showed a distinct peak at the same retention time as the chromatogram at 370 nm, verifying the result (Figure 4B). The mass spectrum confirms the formation of myrFMN (Figure 4B, insert) showing a distinct peak at m/z 681.3. Thus the retention time observed in the HPLC system, the UV-Vis absorption properties and the determined mass of the isolated compound clearly show that myrFMN is generated in a luciferase multiple turnover reaction system.

3.5 Discussion

In our previous studies, we focussed on the binding of myrFMN to LuxF and luciferase from *P. leiognathi* S1 (Bergner *et al.*, 2015). We have shown that myrFMN binds to LuxF and luciferase with a K_d of 80 nM and 4 μ M, respectively. Using this strong affinity towards LuxF, we showed that myrFMN is present in all photobacterial strains tested, irrespective of the presence or absence of *luxF*. In an extension of this work, we have demonstrated here that myrFMN is also produced in *Vibrio* and *Aliivibrio*. Furthermore, a quantitative analysis of light emission and myrFMN production showed a positive correlation suggesting that myrFMN is indeed generated as a consequence of luciferase activity (Figure 1). Interestingly, the best emitting strains, *i.e.* TH1, S1 and ATCC 27561, were those featuring *luxF* prompting the question whether LuxF is prerequisite to high and sustained luciferase activity *in vivo*. To address this question, we have conducted a series of *in vitro* luciferase assays to probe the potential of LuxF to relieve the inhibitory effect of myrFMN on luciferase activity. As shown in Figure 2, the presence of LuxF, tested in different experimental set-ups, unequivocally rescues luciferase activity in the presence of myrFMN and shifts the inhibition constant of myrFMN, as expressed by the IC_{50} , to higher concentrations. The IC_{50} of $\sim 2 \mu$ M, as deduced in Figure 2, is similar to the K_d of myrFMN to luciferase reported earlier, *i.e.* $K_d = 4 \mu$ M (Bergner *et al.*, 2015), which in turn is similar to the binding constant of FMNH₂ to luciferase, *i.e.* $K_d = 0.8 \mu$ M (Meighen *et al.*, 1971). Therefore, our results are in accordance with the relative affinities of myrFMN to LuxF and luciferase, respectively (Bergner *et al.*, 2015). The fact that preincubation with LuxF, mimicking the *in vivo* situation, leads to a substantially higher luciferase activity also suggests that dissociation of myrFMN from luciferase is a slow process compared to the binding to LuxF. The obtained results clearly indicate a direct link between the formation of myrFMN and the luciferase catalyzed reaction. To provide a direct proof for this hypothesis, we designed an *in vitro* multi-enzyme, cofactor recycling system that sustained the luciferase reaction for at least 48-72 hours. This allowed us to isolate sufficient material for chromatographic, spectroscopic and mass spectrometric analysis and clearly provided evidence that myrFMN is produced in the *in vitro* luciferase reaction. This is the first direct experimental proof that myrFMN is formed in the luciferase catalyzed reaction.

3.5.1 Proposed mechanism for myrFMN formation

The demonstration that myrFMN is produced in the luciferase reaction invites the question how myrFMN generation can be rationalized based on the mechanism for the light-emitting process. It was shown that bacterial luciferase forms a stable FMN-4a-hydroperoxide intermediate, which subsequently reacts with the aldehyde substrate to form a FMN-4a-peroxyhemiacetal (Macheroux *et al.*, 1993; Kurfurst *et al.*, 1984; Eberhard *et al.*, 1972). The decomposition of this intermediate is the most critical step because it eventually leads to the population of the excited state of the FMN-4a-hydroxide intermediate (Scheme 3). The currently preferred models to explain the population of an excited-state FMN-4a-hydroxide are based on a radical mechanism, such as the chemically initiated electron exchange luminescence (CIEEL) process (Eckstein *et al.*, 1993; Tu, 2013). In this mechanism the decomposition of the FMN-4a-peroxyhemiacetal is initiated by the transfer of an electron from the N5 position of the flavin to the distal oxygen atom of the peroxyhemiacetal (Scheme 3). This triggers the cleavage of the O-O bond and the generation of an alkoxy radical. At this stage the proton from the C-1 carbon is abstracted and the resulting anionic radical transfers an electron back to the FMN-4a-hydroxy cation radical (Scheme 3, top line). This process is accompanied by the population of the excited state of the FMN-4a-hydroxide, which acts as the light-emitting luciferin.

Based on this radical mechanism we propose that the alkoxy radical rearranges to the carbon radical, as shown in Scheme 3, which then recombines with the FMN-4a-hydroxide radical cation to form a covalent bond between the C-3 carbon of the aldehyde and the C-6 carbon of the isoalloxazine ring. Rearomatization and cleavage of water will then lead to the formation of the flavin adduct. It should be noted that this leads to the formation of the myristylaldehyde linked to the flavin rather than myristic acid. Because aldehydes are prone to oxidation, we assume that this may occur spontaneously after formation of the flavin adduct. It is important to emphasize that this model rationalizes how a rather unreactive saturated carbon atom is activated to form a covalent carbon-carbon bond. Because no other mechanism put forward for the luciferase catalysed reaction has the potential to explain the formation of myrFMN, its very occurrence supports a radical mechanism for the luciferase reaction.

Given the very low yield of myrFMN obtained after up to 3 days of turnover *in vitro* we assume that the bioluminescent reaction efficiently outruns the formation of the side product. Nevertheless our data show that bacterial strains that are capable of producing LuxF produce significantly more light apparently because LuxF scavenges myrFMN and thereby prevents the inhibition of the luciferase. Therefore, the creation of *luxF*, presumably by gene duplication of *luxB*, was an important evolutionary invention that provided an enormous advantage over other bioluminescent bacteria.

3.6 References

- Bergner, T., Tabib, C.R., Winkler, A., Stipsits, S., Kayer, H., Lee, J., *et al.*, (2015) Structural and biochemical properties of LuxF from *Photobacterium leiognathi*. *Biochim Biophys Acta* **1854**, 1466-1475.
- Boylan, M., Graham, A.F., and Meighen, E.A., (1985) Functional identification of the fatty acid reductase components encoded in the luminescence operon of *Vibrio fischeri*. *J Bacteriol* **163**:1186-90.
- Dunlap, P.V., (2009) Bioluminescence, microbial, *Encyclopedia of Microbiology*, 3rd edition. Elsevier, Oxford; In M. Schaechter (ed.), pp 45-61.
- Eberhard, A., and Hastings, J. W., (1972) A postulated mechanism for the bioluminescent oxidation of reduced flavin mononucleotide. *Biochem Biophys Res Commun* **47**, 348-353.
- Eckstein, J. W., Hastings, J. W., and Ghisla, S., (1993) Mechanism of bacterial bioluminescence: 4a,5-dihydroflavin analogs as models for luciferase hydroperoxide intermediates and the effect of substituents at the 8-position of flavin on luciferase kinetics. *Biochemistry* **32**, 404-411.
- Hastings, J.W., Weber, K., Friedland, J., Eberhard, A., Mitchell, G.W., and Gunsalus, A., (1969) Structurally distinct bacterial luciferases. *Biochemistry* **8**:4681-9.
- Joosten, V., and van Berkel, W. J, (2007). Flavoenzymes. *Curr Opin Chem Biol* **11**, 195-202.
- Kurfurst, M., Ghisla, S., and Hastings, J. W., (1984) Characterization and postulated structure of the primary emitter in the bacterial luciferase reaction. *Proc Natl Acad Sci U S A* **81**: 2990-2994.
- Lee, C. Y., Szittner R. B., and Meighen E. A., (1991) The lux genes of the luminous bacterial symbiont, *Photobacterium leiognathi*, of the ponyfish. Nucleotide sequence, difference in gene organization, and high expression in mutant *Escherichia coli*. *Eur J Biochem* **201**: 161-167.
- Macheroux, P., Ghisla, S., and Hastings, J. W., (1993) Spectral detection of an intermediate preceding the excited state in the bacterial luciferase reaction. *Biochemistry* **32**, 14183-14186.
- Macheroux, P., Kappes, B., and Ealick, S. E, (2011). Flavogenomics - A genomic and structural view of flavin-dependent proteins. *FEBS J* **278**, 2625-2634.
- Massey, V., (1994) Activation of molecular oxygen by flavins and flavoproteins. *J Biol Chem* **269**, 22459-22462.

Meighen, E. A., (1991) Molecular biology of bacterial bioluminescence. *Microbiol Rev* **55**, 123-142.

Meighen, E.A., and Hastings, J.W., (1971) Binding site determination from kinetic data. Reduced flavin mononucleotide binding to bacterial luciferase. *J Biol Chem* **246**:7666-74.

Moore, S. A., and James, M. N. G., (1994) Common structural features of the luxF protein and the subunits of bacterial luciferase: Evidence for a ($\beta\alpha$)₈ fold in luciferase. *Protein Sci* **3**, 1914-1926.

Moore, S.A., and James, M. N. G., (1995) Structural refinement of the non-fluorescent flavoprotein from *Photobacterium leiognathi* at 1.60 Å resolution. *J Mol Biol* **249**, 195–214.

Morokutti, A., Lyskowski, A., Sollner, S., Pointner, E., Fitzpatrick, T.B., Kratky, C., *et al.*, (2005) Structure and function of YcnD from *Bacillus subtilis*, a flavin-containing oxidoreductase. *Biochemistry* **44**:13724-33.

Nijvipakul, S., Wongratana J., Suadee C., Entsch B., Ballou D. P., and Chaiyen P., (2008) LuxG is a functioning flavin reductase for bacterial luminescence. *J Bacteriol* **190**: 1531-1538.

Tu, S-C., (2013) Mechanisms of bacterial luciferase and related flavin reductases. *In Handbook of flavoproteins*. Hille, R., Miller, S.M., and Palfey, B. (eds). Berlin: De Gruyter, pp. 101-118.

Teufel, R., Agarwal, V., and Moore, B.S., (2016) Unusual flavoenzyme catalysis in marine bacteria. *Curr Opin Chem Biol* **31**:31-9.

Ulitzur, S., and Hastings, J. W., (1979) Evidence for tetradecanal as the natural aldehyde in bacterial bioluminescence. *Proc Natl Acad Sci U S A* **76**: 265-267.

Wei, C.J., Lei, B., and Tu, S.C., (2001) Characterization of the binding of *Photobacterium phosphoreum* P-flavin by *Vibrio harveyi* Luciferase. *Arch Biochem Biophys* **396**:199-206.

3.7 Acknowledgements

This work was supported by the Austrian “Fonds zur Förderung der wissenschaftlichen Forschung” (FWF) to PM (P24189) and the PhD program “DK Molecular Enzymology” to PM (W901). We want to thank Dr. Wolfgang Kroutil, Institute of Organic and Bioorganic Chemistry, University of Graz, for providing us with GDH (glucose dehydrogenase). We would also like to thank Dr. Rolf Breinbauer, Institute of Organic Chemistry, Graz University of Technology, for providing us the HPLC-MS machine.

3.8 Author contributions

CRT and EB expressed and purified all proteins and cofactors. CRT designed the experiments, performed the assays and analyzed the data for the myrFMN vs light correlation in bacterial strains and determined the IC_{50} for the inhibition assays. CRT and EB designed and performed the *in vitro* multiple turnover assays. EB analyzed the results for *in vitro* assays via HPLC. EB further confirmed the cofactor molecule on HPLC-MS. CRT, EB and PM wrote the manuscript.

3.9 Figure legends

Figure 1: Correlation between light emission and myrFMN content: different bacterial strains compared for their light emission and myrFMN content. *Photobacterium leiognathi* TH1 exhibited maximum bioluminescence as well as produced maximum myrFMN (was set to 100 % for further comparison). It was subsequently followed by the S1 strain which we used as a reference strain. Nevertheless, trace amounts were also detected in all other tested photobacterial strains (ATCC 27561, ATCC 25521 and ATCC 25587). Furthermore, the last columns evidently show detectable amounts of light emission and myrFMN content in *V. harveyi* ATCC 14126 and *A. fischeri* ATCC 7744.

Figure 2: The Inhibition assays: Figure **2A** demonstrates inhibition of luciferase activity with increasing concentration of myrFMN. It is seen that as myrFMN concentration increases, the light emission decreases (reaction 1 - filled square). However, addition of LuxF to the same reaction (after primary cycle of 90 seconds) scavenges myrFMN allowing FMNH₂ to follow the normal reaction and produce light (reaction 1 + LuxF - filled round). A third condition, mimicking the *in vivo* situation, shows the inhibition effect of myrFMN in the presence of LuxF from the beginning of the reaction (reaction 2 - filled triangle). The peak maximum was plotted at each time point measured. Figure **2B** clearly shows the concentration of myrFMN at which luciferase still emits 50 % of light (IC₅₀), which is approximately 1.7 μM. However, to inhibit 50 % of the luciferase activity in the presence of LuxF, 6 fold higher concentration of myrFMN is required (~11 μM), thus demonstrating the scavenging behavior of LuxF.

Figure 3: HPLC chromatograms of the myrFMN reference and the sample of the *in vitro* assay with the corresponding absorption spectra. After workup the sample of the *in vitro* assay (black line) was measured by HPLC with UV-Vis detection and compared to the reference sample of myrFMN (red line). The retention time for both samples is 18.8 minutes. The insert shows the overlay of the absorption spectra of the reference (red line) and the sample (black line) with the maxima of 386 nm and 441 nm.

Figure 4: HPLC-MS measurement of the isolated myrFMN sample of the *in vitro* assay. **A:** HPLC chromatogram at 370 nm with a retention time of 14.2 minutes for the isolated and purified myrFMN sample. **B:** Extracted Ion Chromatogram (XIC) of m/z 681 in negative ESI mode. **B, insert:** MS-Spectrum at the retention time of 14.2 minutes corresponds to myrFMN with m/z 681 [M-H]⁻.

3.10 Scheme legends

Scheme 1: General reaction scheme for bacterial bioluminescence. Schematic representation of the luciferase catalyzed reaction, demonstrating the conversion of a long chain aldehyde (chain length from C8-C14) to the corresponding carboxylic acid where a FMNH₂ and an O₂ molecule are consumed in the process. Visible luminescence is emitted with a maximum at 490 nm.

Scheme 2: Schematic representation of the multiple turnover *in vitro* assay. The luciferase employs molecular oxygen (O₂) and reduced FMN (FMNH₂) in order to oxidize, in this case, tetradecanal to tetradecanoic acid. For the reduced FMN a recycling system was established using the NADPH-dependent oxidoreductase YcnD from *Bacillus subtilis*. To recycle NADPH, glucose dehydrogenase (GDH) was applied.

Scheme 3: Proposed mechanism for myrFMN formation: In the scheme above is shown the CIEEL (Chemically initiated electron exchange luminescence) mechanism for the luciferase catalyzed bioluminescence reaction. The reaction is initiated by the transfer of an electron from the N5 position of the flavin to the distal oxygen atom of the peroxide moiety. During the normal course of the reaction, the O-O bond cleavage leads to the formation of a radical anion, which transfers the electron back to the flavin generating an excited state of the flavin-4a-hydroxide. This excited state intermediate further goes on to emit light with a maximum at 490 nm. The mechanism we propose, for the formation of myrFMN suggests that a hydrogen rearrangement of the alkoxy radical leads to a C-3-carbon radical moiety. This then combines with the flavin-4a-hydroxide radical cation to form the covalent bond between the

C-3 carbon of the aldehyde and the C-6 carbon of the isoalloxazine ring. After rearomatization and release of water, our stipulated product myrFMN is formed.

3.11 Figures

Figure 1

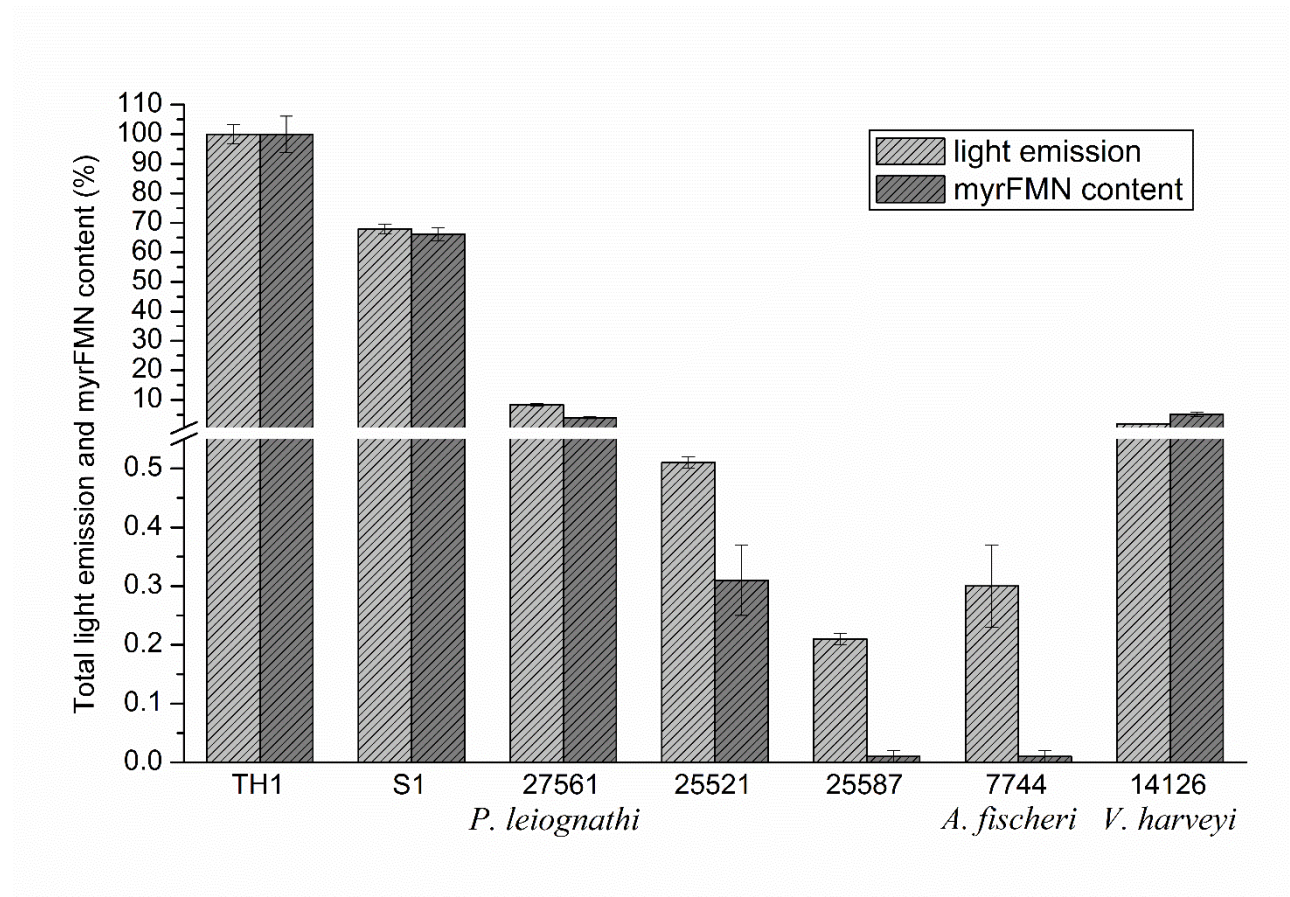


Figure 2

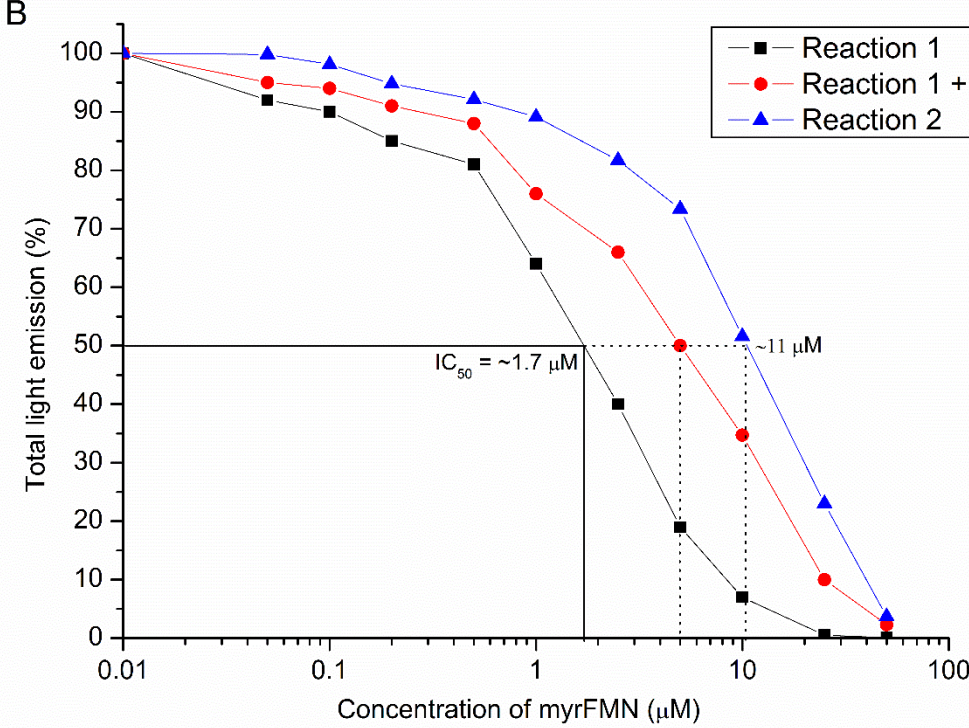
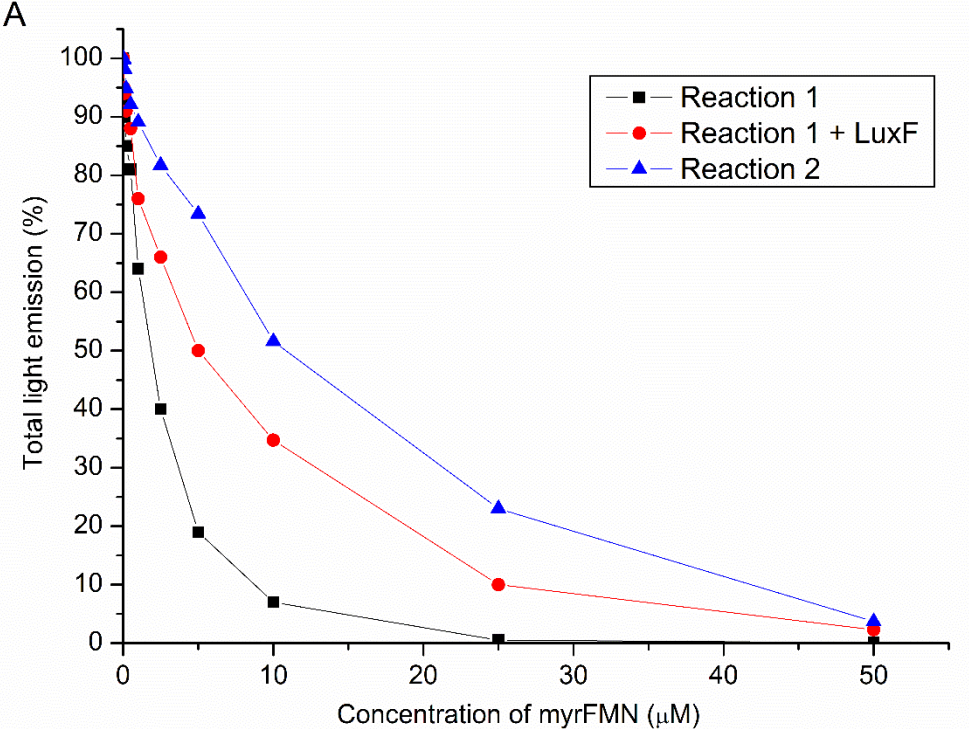


Figure 3

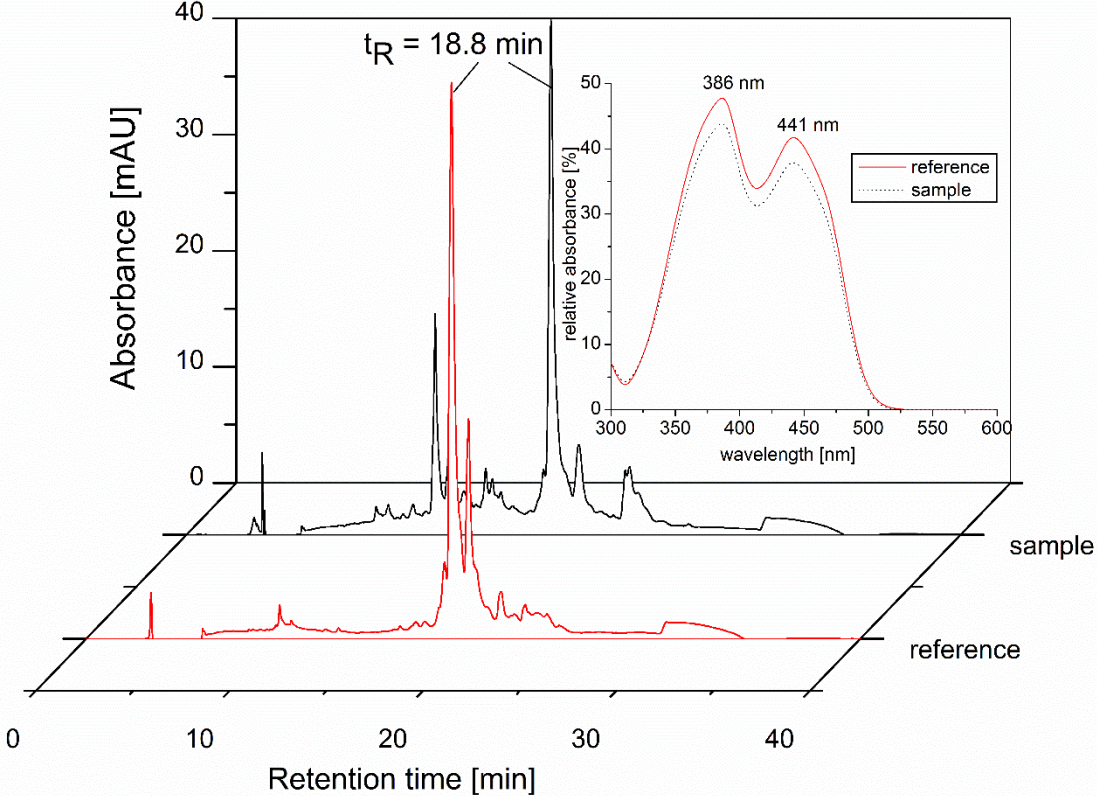
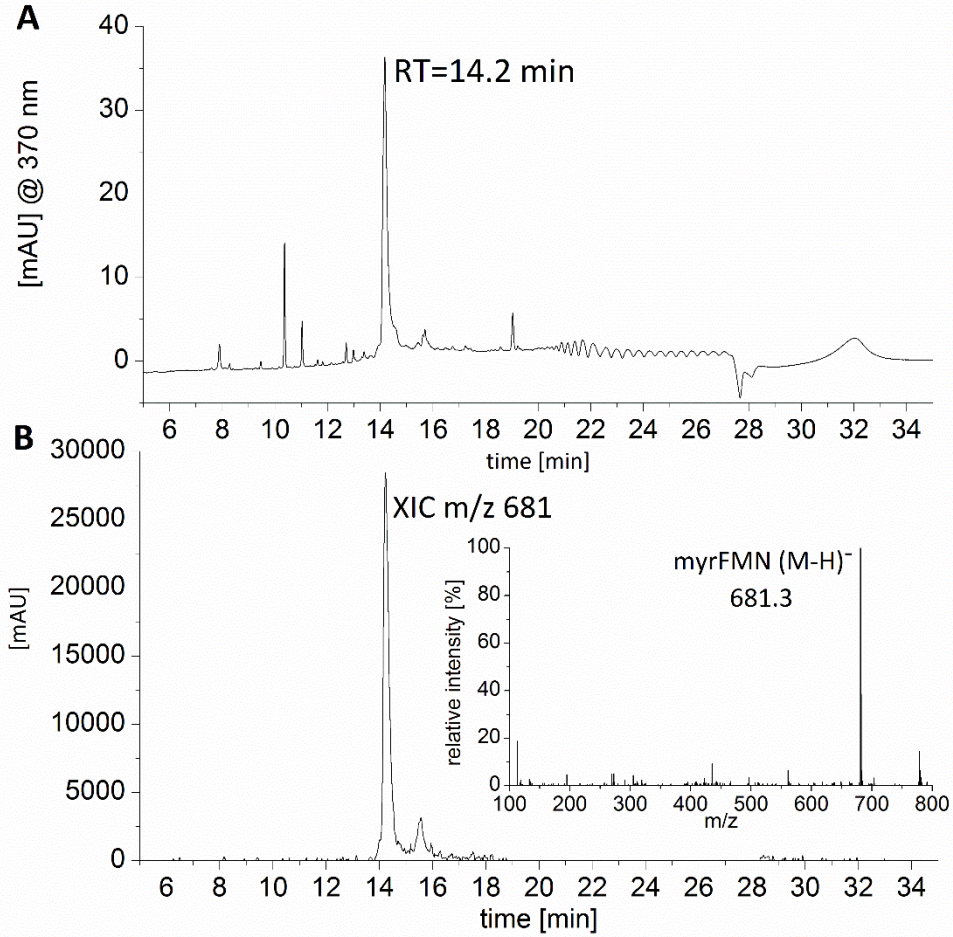
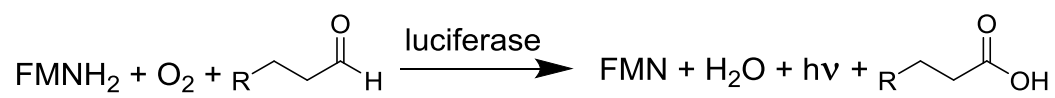


Figure 4



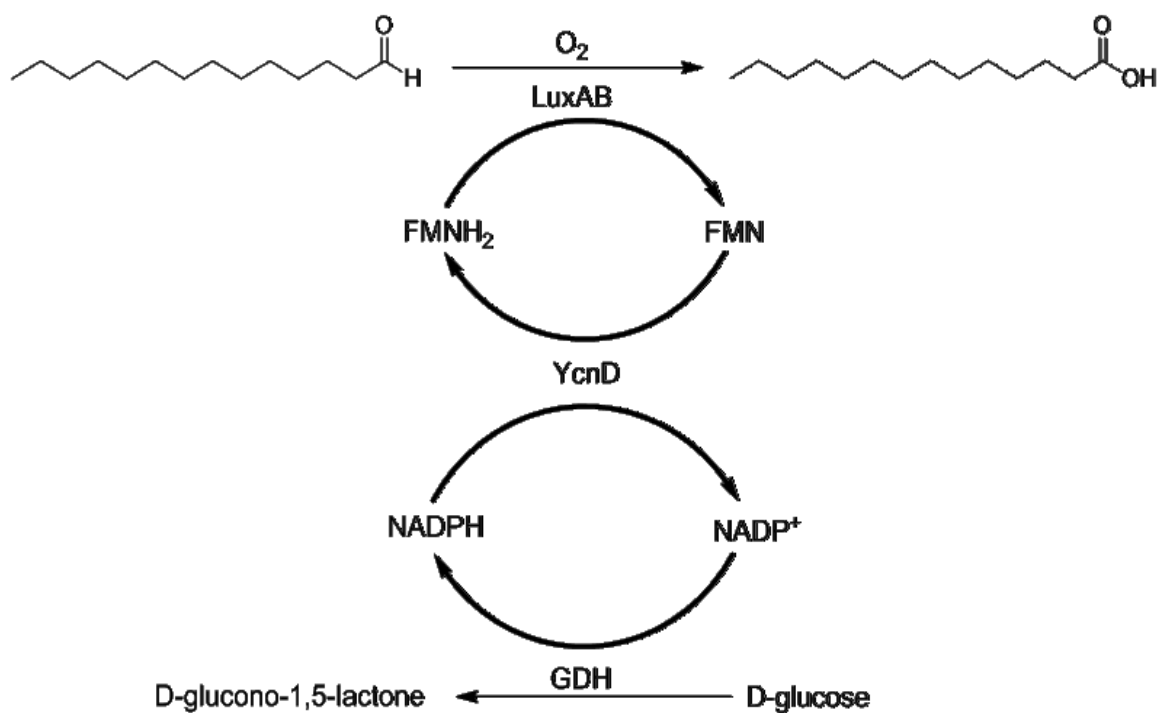
3.12 Schemes

Scheme 1

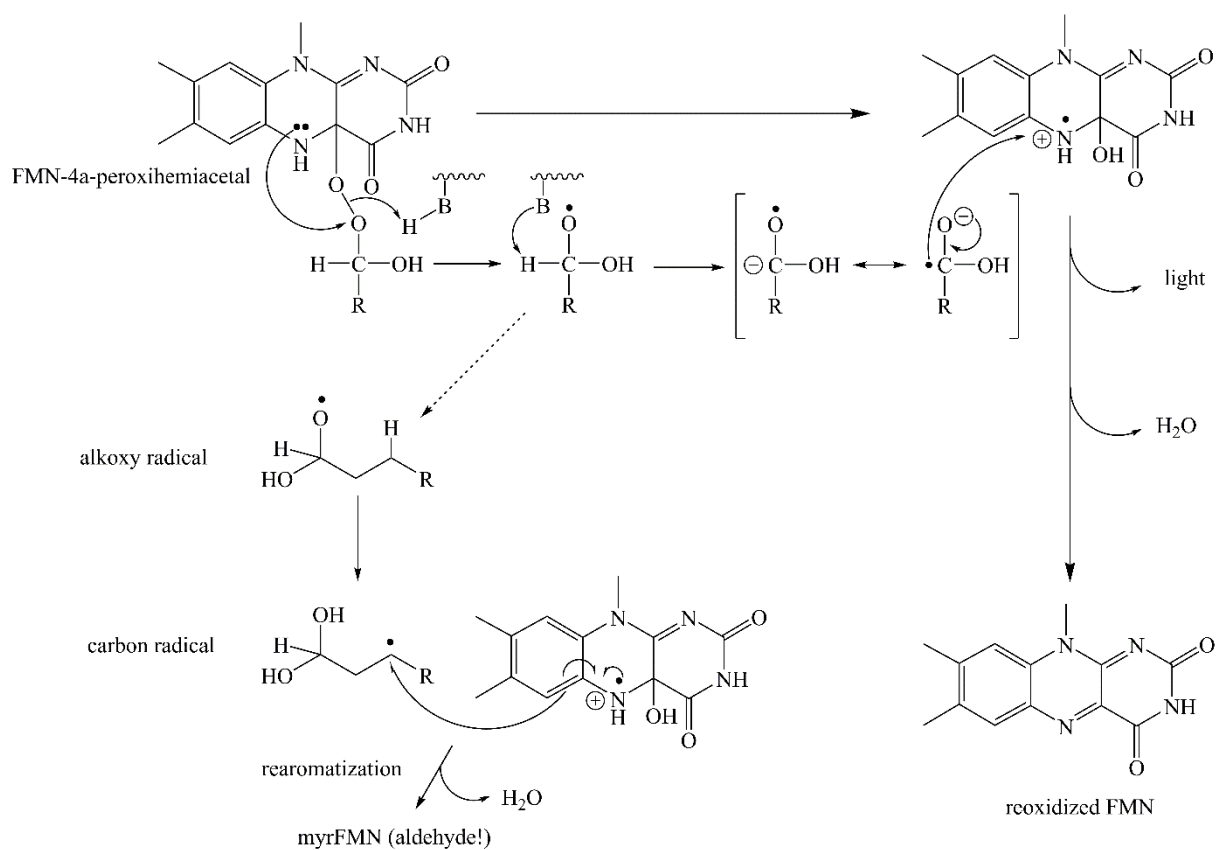


$\text{R} = (\text{CH}_2)_n\text{CH}_3$; $n = 4, 6, 8, 10$

Scheme 2



Scheme 3



3.13 Supplementary data

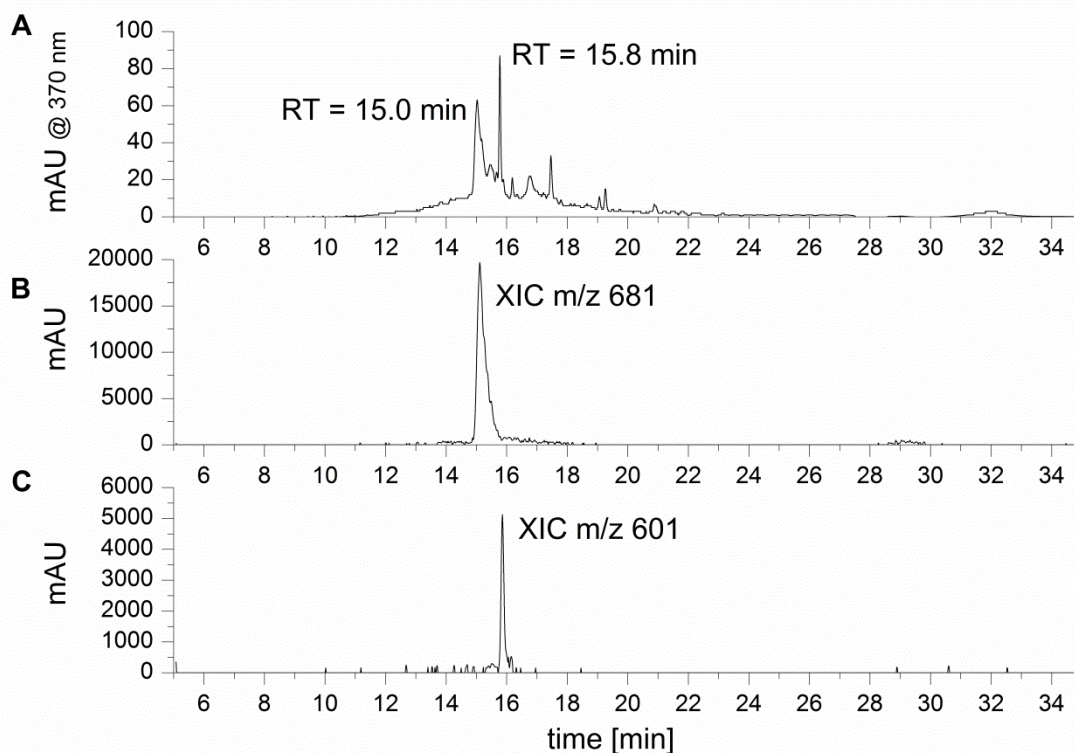


Figure 1_SupplInfo: HPLC-MS measurement of the isolated myrFMN sample of *Photobacterium leiognathi* S1. A: HPLC chromatogram at 370 nm with a retention time of 15.0 and 15.8 minutes for the isolated and purified myrFMN sample. **B:** Extracted Ion Chromatogram (XIC) of m/z 681 in negative ESI mode. **C:** Extracted Ion Chromatogram (XIC) of m/z 601 in negative ESI mode.

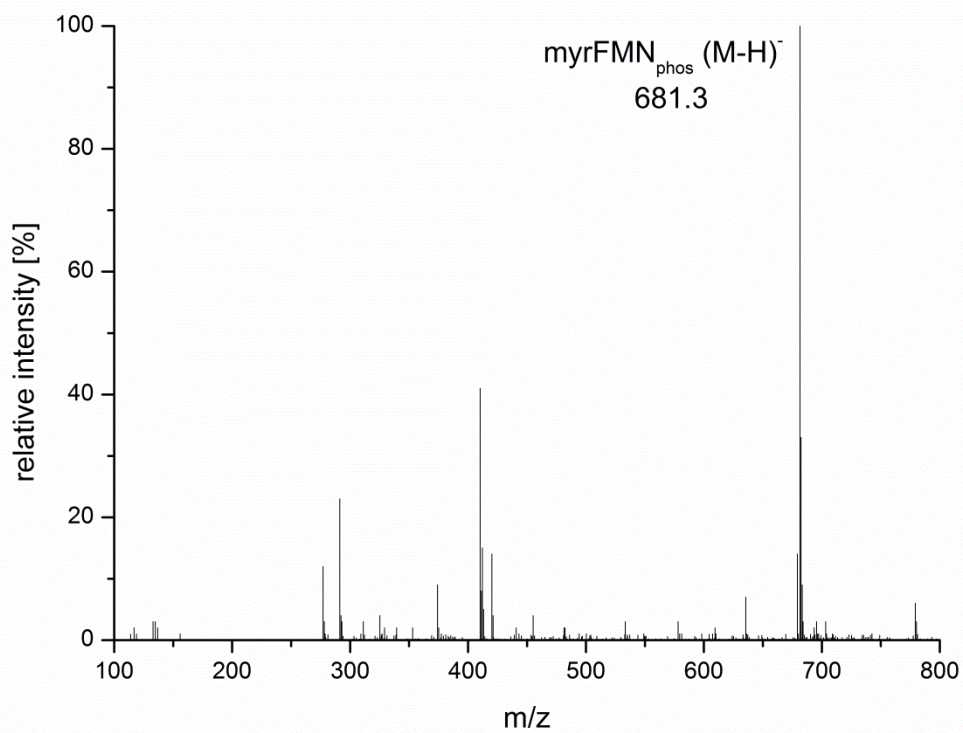


Figure 2_SupplInfo: MS-Spectrum at the retention time of 15.0 minutes corresponds to the phosphorylated myrFMN with m/z 681.3 [M-H]⁻.

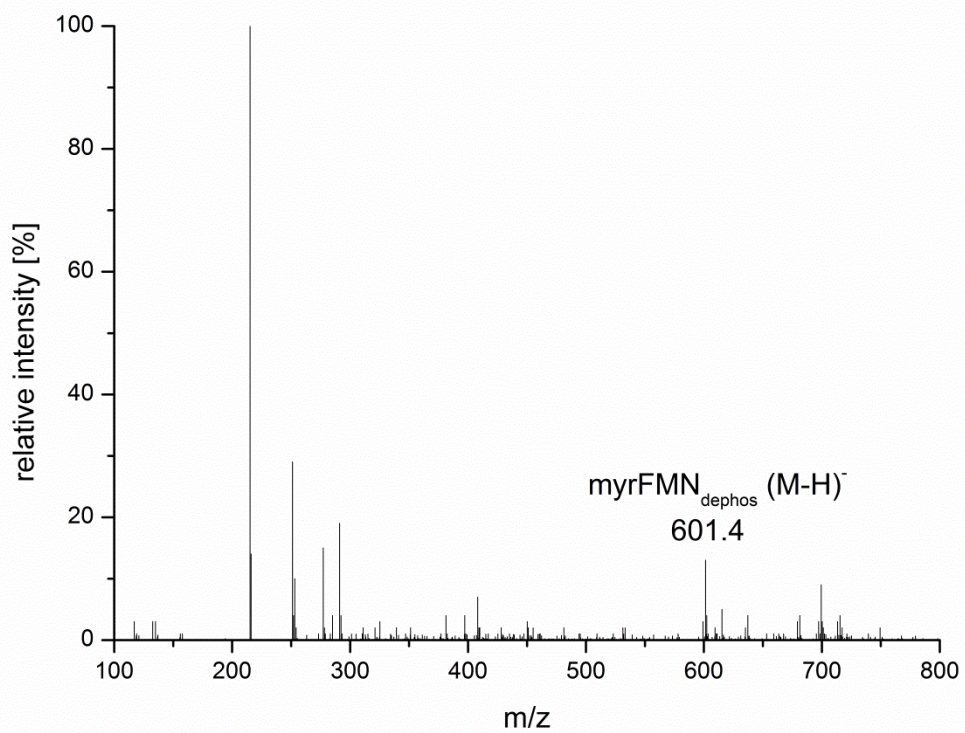


Figure 3_SupplInfo: MS-Spectrum at the retention time of 15.8 minutes corresponds to the dephosphorylated myrFMN with m/z 601.4 [M-H]⁻.

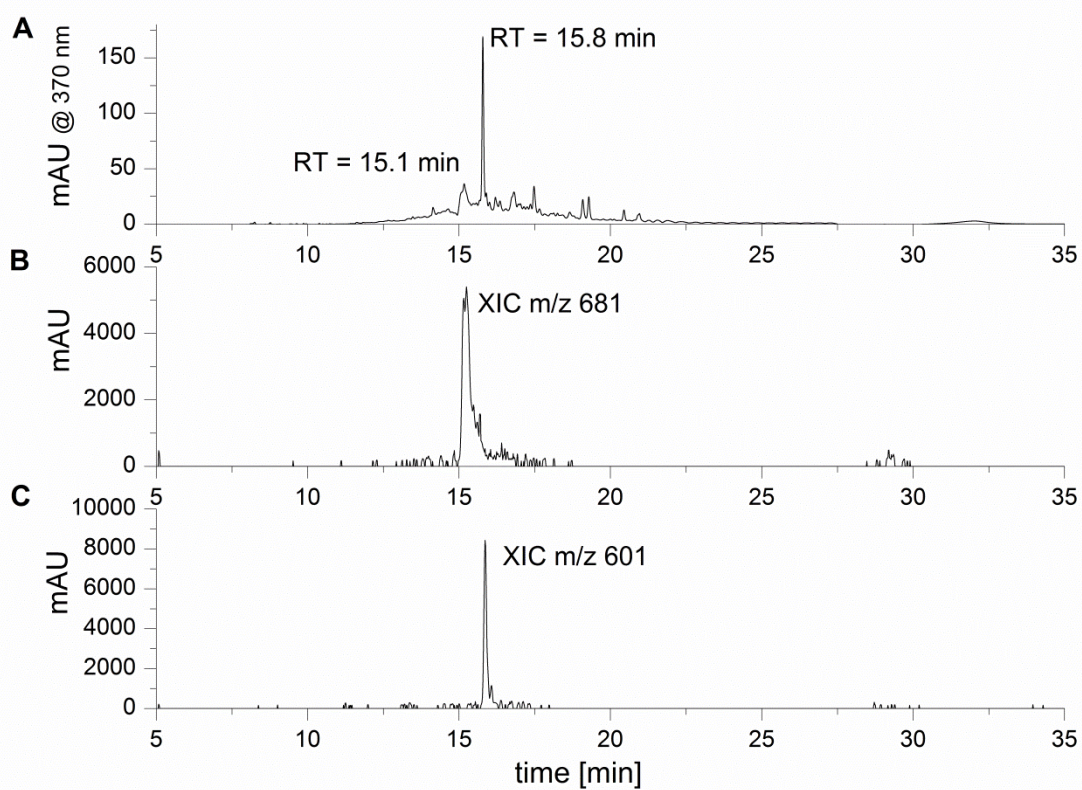


Figure 4_SupplInfo: HPLC-MS measurement of the isolated myrFMN sample of *Photobacterium leiognathi* TH1. **A:** HPLC chromatogram at 370 nm with a retention time of 15.1 and 15.8 minutes for the isolated and purified myrFMN sample. **B:** Extracted Ion Chromatogram (XIC) of m/z 681 in negative ESI mode. **C:** Extracted Ion Chromatogram (XIC) of m/z 601 in negative ESI mode.

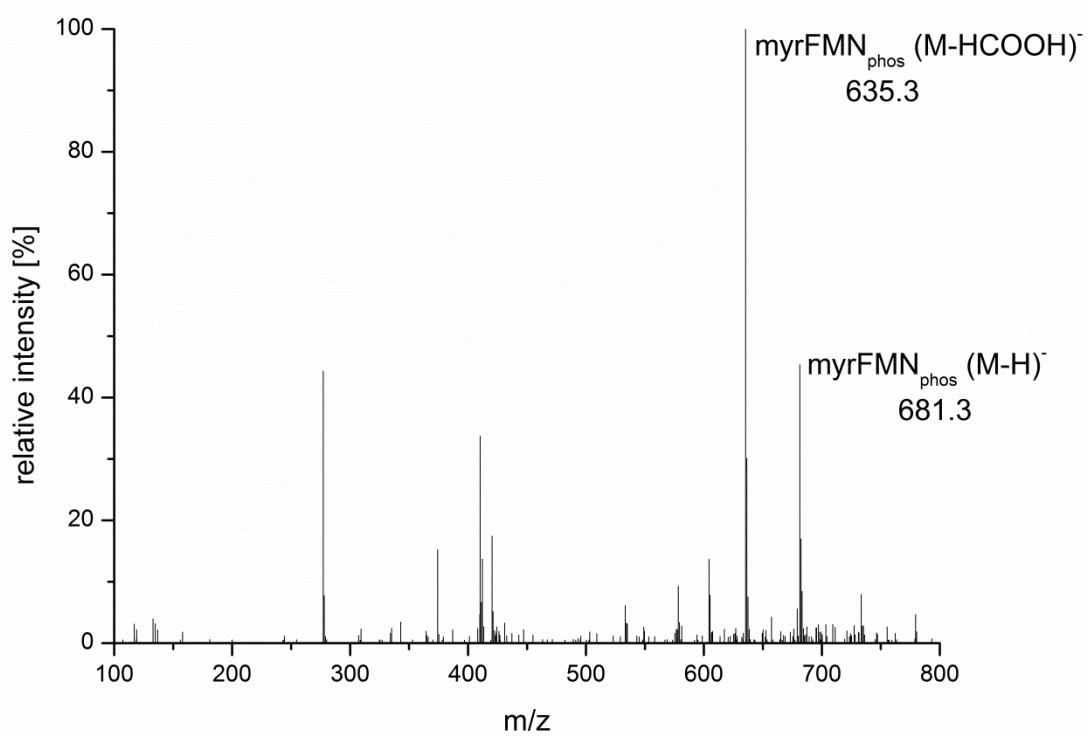


Figure 5_SupplInfo: MS-Spectrum at the retention time of 15.1 minutes corresponds to the phosphorylated myrFMN with m/z 681.3 [M-H]⁻ and to one main fragment with m/z 635.3 [M-HCCOH]⁻.

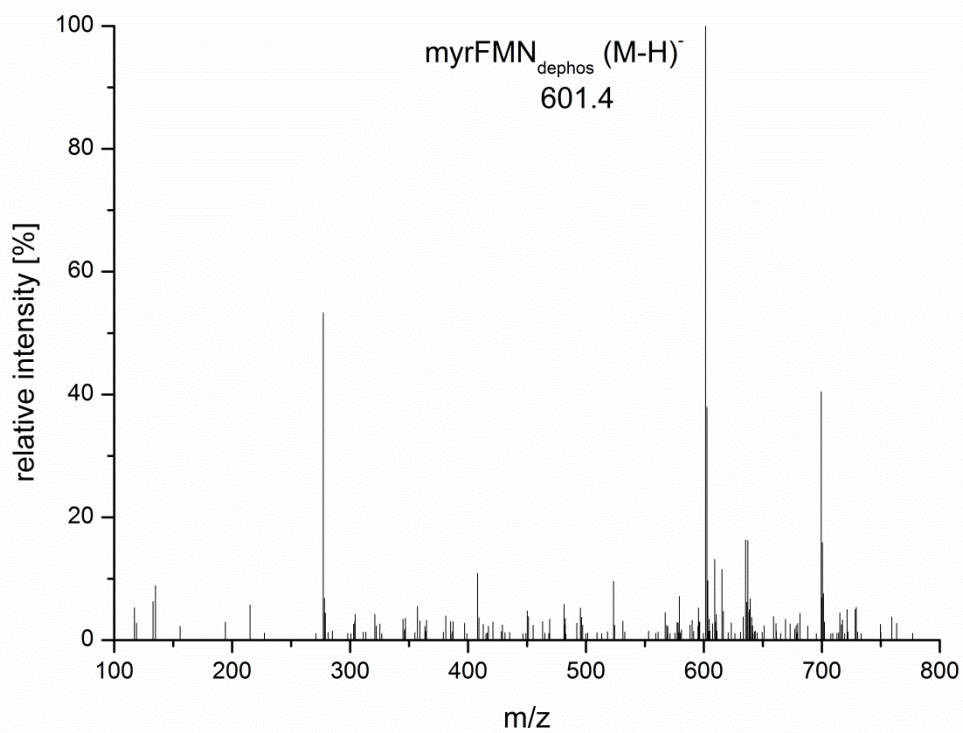
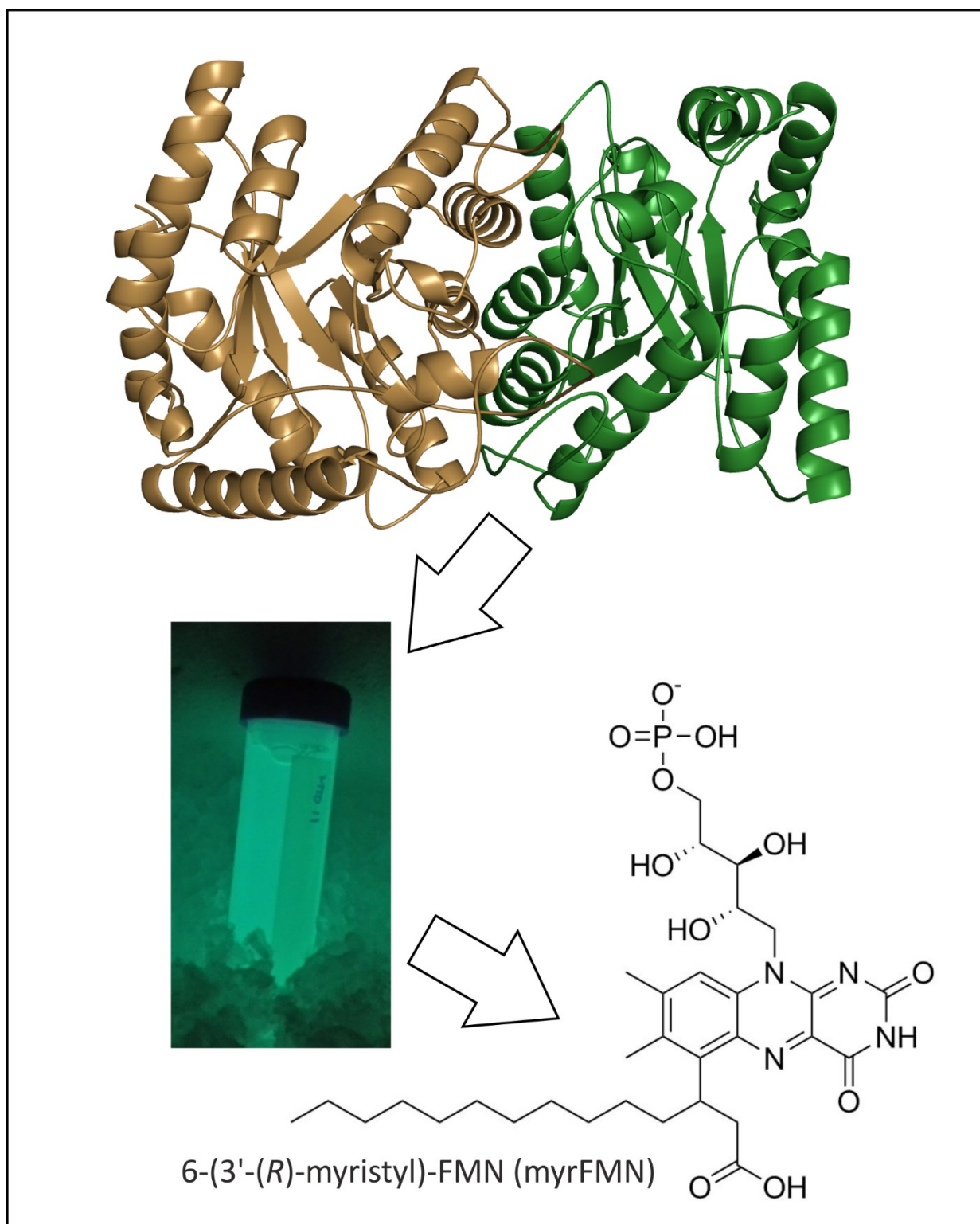


Figure 6_SupplInfo: MS-Spectrum at the retention time of 15.8 minutes corresponds to the dephosphorylated myrFMN with m/z 601.4 [M-H]⁻.

3.14 Graphical abstract



Abbreviated summary

Myristylated FMN, a flavin derivative with a unique structure, where the C3 atom of tetradecanoic acid is bound to the C6 atom of the isoalloxazine ring, is formed during the bacterial bioluminescence reaction. This formation catalyzed by the bacterial luciferase supports the radical formation theory via the CIEEL mechanism.

Chapter 4

Mutagenic study of cysteine residues on the structural stability and enzymatic behavior of bacterial luciferase

Andrea Marianne Friedrich, Chaitanya Tabib, Eveline Brodl, Silvia Wallner and Peter Macheroux

Graz University of Technology, Graz, Austria

Keywords: Bacterial luciferase, site directed mutagenesis, Thermofluor,

4.1 Abstract

Bioluminescence is a natural phenomenon in living organisms, which involves enzymatic catalysis of a substrate to pass through a series of intermediates of different energies to finally form the product with light emission in visible range. This reaction is found in organisms ranging from bacteria to insects, fish and fungi and is utilized for vital functions from defense to reproduction. All luminous bacteria known today are assigned to γ -proteobacteria, namely to the genera *Vibrio*, *Aliivibrio* and *Photobacterium*.

The genes required for light emission in luminescent bacteria are organized in the so called “*lux*-operon”. Two of these genes encode for the bacterial luciferase (*luxAB*), the enzyme that catalyzes the reaction. The heterodimeric flavin monooxygenase LuxAB mediates the oxidation of reduced flavin mononucleotide (FMNH₂) and a long-chain aliphatic aldehyde (RCHO) by O₂ to produce the respective acid (RCOOH) and the blue-green light (~490 nm).

This enzyme is relatively unstable and commonly loses its activity at room temperature because of structural changes resulting in the loss its enzymatic applications. Improving the stability of proteins is a main goal in many biochemical and industrial applications. Different approaches are applied to increase the stability of the bacterial luciferase; the main topic of this study is to test the protein by replacing the reactive, easily oxidisable cysteines (C170, C242, C306, C465, C501, and C519) on the surface of the protein to serines using site-directed mutagenesis.

After over-expression of the variants in *E. coli* BL21*, the proteins were purified via affinity chromatography and gel filtration. The mutants were verified by MALDI-TOF-MS. The proteins were further tested if the site-directed mutagenesis on LuxAB has an impact on the yield of emitted light (luminometer measurements), thus the enzymatic activity and how it affects the melting temperature of each protein variant (Thermofluor experiments). The immediate results showed that four out of six luciferases (C306S, C465S, C501S and C519S) were completely denatured from the beginning and were not able to catalyze the light emitting reaction with high yield. C170S and C242S had similar characteristics compared to the wild type that is still unsurpassed in both enzymatic activity and stability.

4.2 Introduction

Bioluminescence is a natural phenomenon which was first scientifically discovered in the 1880s¹ and is found in several different major groups ranging from organisms like fungi, fish, insects, bacteria, etc. where visible light is emitted due to a chemical reaction. Algae, archaea and higher eukaryotes such as mammals, birds, amphibians, and plants are not known to be luminescent. The ability to produce light has evolved as a defense mechanism, alluring prey and hosts or for communication like attracting appropriate mates for successful reproduction.² Today, bioluminescence reactions are an essential tool in many biomedical and industrial applications such as measuring ATP which indicates living cells or tracing biological intracellular processes by using Ca^{2+} -sensitive photoproteins e.g. aequorin derived from a jellyfish.³

The *lux* operon contains all genes in bacteria that encode for the proteins necessary for producing bioluminescence. The operon usually consists of *luxCDABE* but is differently organized in various species and strains.⁴ Bacterial luminescence requires at least the enzymes luciferase (LuxAB), NADPH-dependent acyl protein reductase (LuxC), acyl transferase (LuxD), ATP-dependent acyl protein-synthetase (LuxE)⁵ and a flavin reductase (LuxG).⁶ LuxAB binds FMNH₂ and molecular oxygen to mediate the oxidation of the aldehyde (RCHO) leading in the production of light with a maxima at 490 nm (green-blue) and H₂O (Figure 1).¹

The heterodimeric bacterial luciferase, a flavin monooxygenase, consists of a α -subunit LuxA (40 kDa) and a β -subunit LuxB (37 kDa).¹ With regard to the domain structures it folds into an α/β domain which consists of eight central parallel β -sheets surrounded by the same number of α -helices. This structural form is called a TIM barrel ($[\beta/\alpha]_8$). The axis of the two barrels corresponding to LuxA and LuxB is arranged with a rotation of 80° and a translation of 34 Å, whereas the overall dimensions of the whole protein are ca. 75 Å x 45 Å x 40 Å. Alignment of the amino acid sequence of the α - with the β -subunit demonstrates that they share 32% sequence identity. LuxB lacks 31 amino acid residues which are present in the α -subunit. Due to the homology there should be at least one active site in each subunit, but it is assumed that only LuxA holds the catalytic center. Therefore the whole enzyme is able to bind just one reduced FMN at the time in the bioluminescence reaction.⁷ The subunits of LuxAB do not show a luminescent activity as monomers or homodimers.^{8,9}

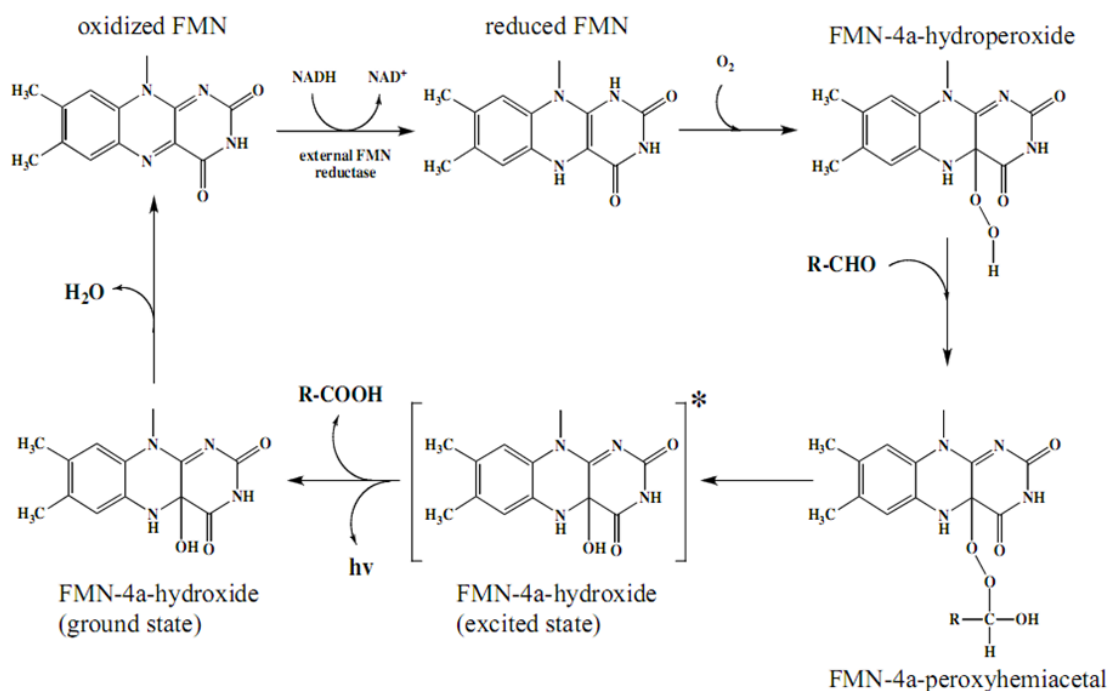


Figure 1: Mechanism of the bacterial bioluminescence reaction catalyzed by LuxAB.

4.2.1 Homology model

Homology modelling is used if no three-dimensional structure of the target protein is available. For that purpose an experimentally determined 3D-structure of a protein of a related family is used as a template together with the amino acid sequence of the target protein. Therefore a sequence identity of at least 30% is required.¹⁰ In this thesis the LuxAB amino acid sequence derived from *Photobacterium leiognathi* ATCC 27561 is used to build the model using the available luciferase structure from *Vibrio harveyi* (PDB: 1brl¹¹) as template.

According to the homology model the cysteines on the surface (green; C170S, C465S and C519S) and those which might be facing the surface (red; C242S, C306S and C501S) are replaced to serines for this study. All cysteines on the inside of the structure are not marked and stay non-mutated (C7, C59, C229 and C488). The subunit LuxA (dark-grey) consists of 354 and LuxB (light-grey) of 326 amino acids (Figure 2).

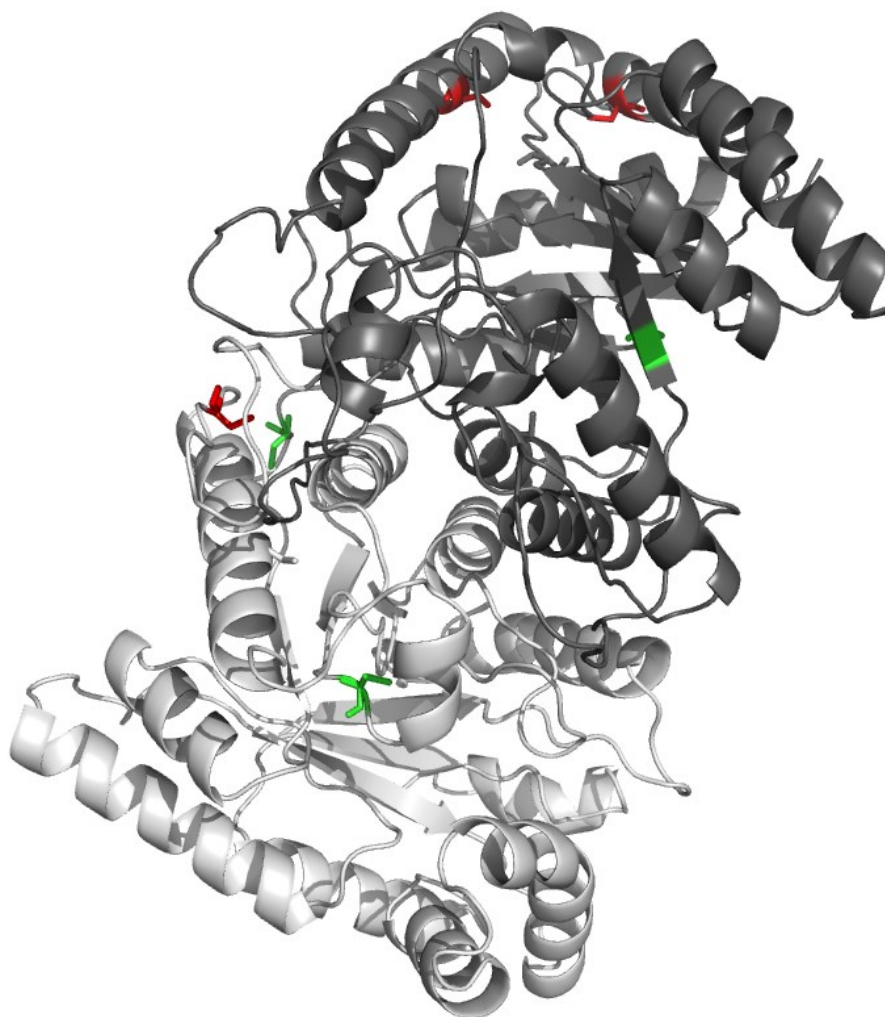


Figure 2: Homology model of the bacterial luciferase. Cysteines on the surface of *P. leiognathi* LuxAB (green; C170S, C465S and C519S) and those which might be facing the surface (red; C242S, C306S and C501S) are marked.

4.3 Materials and methods

4.3.1 Cloning and expression of luciferase variants

With PCR based site-directed mutagenesis, single mutations on the *luxAB* WT gene (from *Photobacterium leiognathi* ATCC 27561) were created. The clones were confirmed with sequencing and transformed into *E. coli* BL21* strain for expression. All the variants were expressed and purified similar to the procedure for the LuxAB WT protein as mentioned previously.¹² All the buffers for the purification and assays were prepared as mentioned below. The concentration of the proteins were determined via UV/VIS-spectroscopy at 280 nm using the extinction coefficient, $\epsilon = 82\,335 \text{ l mol}^{-1} \text{ cm}^{-1}$; MGW = 79908 g mol⁻¹).

4.3.2 Matrix-assisted laser desorption/ionization time-of-flight mass spectrometry (MALDI-TOF MS)

The sample preparation, all measurements and also the analysis of the results follow the standard protocols of MALDI-TOF MS. The protein samples have to be treated with Iodoacetamide for reducing as well as alkylating the cysteine residues. Due to proteolytic digestion with trypsin fragments with 500-6000 Da are generated. A calibration has to be done by the use of the organic molecule PEG. In addition the shift of the mass-to-charge ratio has to be corrected by co-introducing the analyte with ACTH.

4.3.3 Thermofluor stability check

For detection of the T_m for all the proteins in this study (LuxAB WT and six variants), the protein concentration was normalized to approximately 10 mg ml⁻¹ with assay buffer and the SYPRO Orange dye was 1:500 diluted with ddH₂O. To 2.5 µl protein, 2.5 µl diluted dye and in total 20 µl of the different buffer conditions were added. Every reaction was performed in triplicates.

Each measurement started at 20 °C, lasted 5 s and then the temperature was increased by 0.5 °C step, up to 95 °C final temperature.

Reagents/buffers used for testing in Thermofluor:

- ddH₂O
- Storage buffer: 50 mM L-Malic acid, 25 mM MES, 25 mM Tris (pH 8.0)
- KH₂PO₄ + K₂HPO₄: 100 mM (pH 7.0)
- KH₂PO₄ + KOH: 200 mM (pH 5.0 / 6.0 / 7.0 / 8.0 / 9.0)
- NaH₂PO₄ + NaOH: 200 mM (pH 5.0 / 6.0 / 7.0 / 8.0 / 9.0)
- HEPES + KOH: 200 mM (pH 5.2 / 6.0 / 7.0 / 8.0 / 9.0)
- Tris/HCl + NaOH: 200 mM (pH 5.0 / 6.0 / 7.0 / 8.0 / 9.0)
- NaCl: 0.2 M / 0.5 M / 0.6 M / 1.2 M / 2 M / 2.5 M
- KCl: 0.2 M / 0.5 M / 0.6 M / 1 M / 1.2 M / 2 M
- KH₂PO₄ + KOH 200 mM (pH 7.0) + NaCl 0.2 M / 0.5 M / 0.6 M / 1.2 M / 2 M / 2.5 M
- KH₂PO₄ + KOH 200 mM (pH 7.0) + KCl 0.2 M / 0.5 M / 0.6 M / 1 M / 1.2 M / 2 M
- NaH₂PO₄ + NaOH 200 mM (pH 7.0) + NaCl 0.2 M / 0.5 M / 0.6 M / 1.2 M / 2 M / 2.5 M
- NaH₂PO₄ + NaOH 200 mM (pH 7.0) + KCl 0.2 M / 0.5 M / 0.6 M / 1 M / 1.2 M / 2 M

4.3.4 Enzyme activity assay

This method is applied for detection of bioluminescence by measuring the counts of photons produced per second. A master mix with 890 μ l assay buffer, 50 μ l saturated C14 aldehyde, 300 nM FMN, 300 nM YcnD and 200 nM LuxAB was prepared. Everything had to be kept on ice except the saturated C14 aldehyde. A white assay 96 well plate was used for measurements. The master mix was divided by four and approximately 240 μ l were pipetted in each well. Care had to be taken that the four filled wells were as far away of each other as possible so that the independent measurements could not interact. Each measurement was started after an initial delay of 5 s per plate and later 3 s before the NADPH (500 nM/10 μ l) was injected. Light was recorded 0.01th of every second and the whole read time took 90 s. The assays were performed in triplicates.

4.4 Results and discussion

4.4.1 Cloning and expression of luciferase variants

The mutant constructs were extracted and sequenced. By the use of sequence alignment tools, the sequences obtained were compared against the wild type luciferase, the mutagenesis were confirmed (as shown below). The cysteine-codons (TGT) at the amino acid positions 170, 306, 465, 501, and 519 were exchanged to serine-codons (TCT). Also at position 242 the cysteine (TGC) was replaced by a serine (AGC).

WT_LuxAB	5' -CCCTACT TGT ATGACAG-3'	517
C170S_2.T7prom	5' -CCCTACT TCT ATGACAG-3'	540

WT_LuxAB	5' -AAGTGTC TGC CGTGACTTCCTATCAAAC TGGTA -3'	749
C242S_1.T7prom	5' -AAGTGTC AGC CGTGACTTCCTATCAAAC TGGTA -3'	780

WT_LuxAB	5' -TGAAAAA TGT ATTGAAATTAT-3'	929
C306S_9.T7prom	5' -TGAAAAA TCT ATTGAAATTAT-3'	960

WT_LuxAB	5' -AAGTGAT TGT GTTAGTG-3'	1450
C465S_1.T7term	5' -AAGTGAT TCT GTTAGTG-3'	351

WT_LuxAB	5' -CAACTACT TGT TATGCGAAT-3'	1560
C501S_6.T7term	5' -CAACTACT TCT TATGCGAAT-3'	462

WT_LuxAB	5' -CCCACACT TGT ATTAGTAAAGAAAAC-3'	1620
C519S_6.T7term	5' -CCCACACT TCT ATTAGTAAAGAAAAC-3'	534

After the successful sequencing results, expression of all mutated luciferases were checked in *E. coli* BL21*. All induced samples showed a much higher amount of protein at approximately 40 kDa (Figure 3). These bands are presumably originated from the expression of the two subunits, LuxA and LuxB, compared to the uninduced protein extracts.

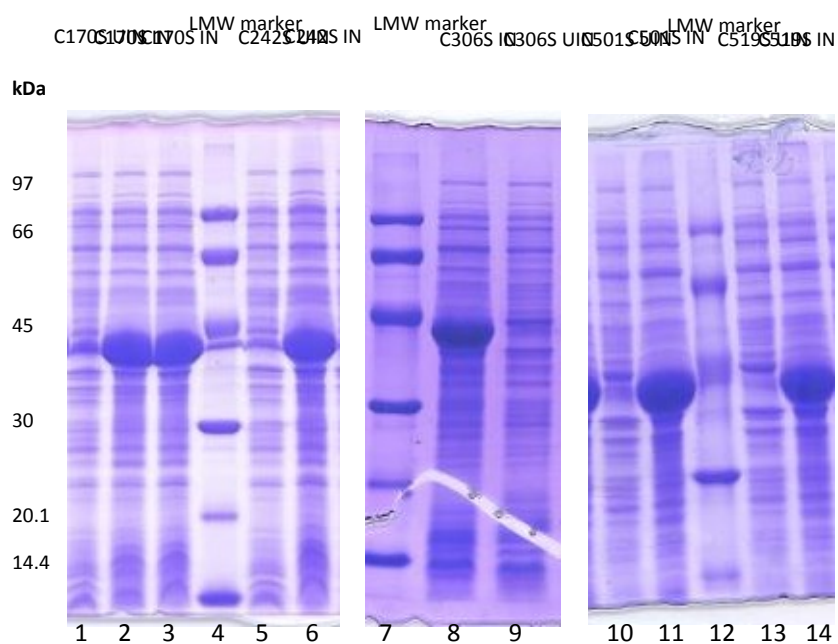


Figure 3: Comparison between uninduced and induced expression of all mutated LuxABs. The uninduced variants are abbreviated with UIN and the induced ones with IN. All induced samples (lanes 2, 3, 6, 8, 11 and 14) showed a much higher protein yield at 40 kDa than each uninduced control (lanes 1, 5, 9, 10 and 13). A low molecular weight standard (LMW marker, lanes 4, 7 and 12) was used.

The protein was purified using the His-affinity chromatography and size exclusion-gel filtration chromatography. The protein yields after each purification were calculated as shown in the table below (Table 1).

Table 1. Total yield of LuxAB WT and mutated luciferases after all purification steps. The expression of all luciferases could be performed. *E. coli* BL21* cells with protein expressed were harvested and the protein was purified via his-tag chromatography and in further step with gel filtration chromatography. The volume of media used, cell mass obtained, protein concentration and the yield of total protein (LuxAB) was calculated.

Name	Medium	Cell pellet	Concentration		Total protein
LuxAB WT	15 * 800 ml	75.4 g	1.2 μ M	96.0 mg/ml	722.1 mg
LuxAB C170S	5 * 800 ml	20.4 g	1.9 μ M	151 mg/ml	378.8 mg
LuxAB C242S	5 * 800 ml	25.2 g	1.3 μ M	104 mg/ml	104.7 mg
LuxAB C306S	5 * 800 ml	25.2 g	0.15 μ M	11.9 mg/ml	17.79 mg
LuxAB C465S	5 * 800 ml	28.5 g	0.39 μ M	31.1 mg/ml	46.57 mg
LuxAB C501S	5 * 800 ml	23.6 g	0.099 μ M	7.91 mg/ml	10.28 mg
LuxAB C519S	5 * 800 ml	23.5 g	0.13 μ M	10.5 mg/ml	5.236 mg

4.4.2 Verification of the luciferases with MALDI-TOF MS

With MALDI-TOF MS it could be confirmed, on one hand that every purified protein sample was in fact a luciferase and on the other that each one contained the desired mutation.

For this purpose nine significant mass-peaks of the wild type (3317.69 Da, 1922.07 Da, 1766.91 Da, 1634.77 Da, 1316.64 Da, 1167.61 Da, 949.46 Da, 872.39 Da and 819.47 Da) were selected in order to check whether these were also present in the mutants. Here the maximum deviation to the wild type was not more than 0.2 Da. Furthermore, each LuxAB-variant had to represent a single different mass-peak due to the exchange of cysteine to serine compared to LuxAB WT. These were based on the proteolytic digestion with trypsin at 2036.99 Da (C170S), 648.33 Da (C242S), 858.50 Da (C306S), 2096.99 Da (C465S), 4040.76 Da (C501S) and 1095.62 Da (C519S). All peaks invariably existed without mass deviation.

4.4.3 Determination of the T_m of LuxAB WT and variant LuxAB with Thermofluor experiments

With Thermofluor measurements, it was possible to compare the behavior of the pure luciferase variants with the wild type for different conditions. These experiments showed whether any of the cysteine to serine mutation impacted positively on the stability of the protein.

All Thermofluor results of the luciferases are represented just by their specific melting temperature under different conditions if existing. In order to interpret the data, the melting curves must be included in the considerations.

Table 2. Melting temperature of the luciferases under different conditions. Empty boxes are not tested. The results of treatment with Tris/HCl + NaOH 200 mM at various pH are not shown because LuxAB is not compatible with this buffer in general.

Conditions		Melting temperature [°C]						
		WT	C170S	C242S	C306S	C465S	C501S	C519S
ddH ₂ O		40.5	39.5	39.0		-		-
Storage buffer	pH 8.0	40.0	38.5	39.0	-	-	-	-
KH ₂ PO ₄ + K ₂ HPO ₄		42.5	40.5			-		-
KH ₂ PO ₄ + KOH	pH 5.0	-						
	pH 6.0	-						
	pH 7.0	45.5	44.0			-		-
	pH 8.0	42.0	37.5			-		-
	pH 9.0	35.5						
NaH ₂ PO ₄ + NaOH	pH 5.0	-						
	pH 6.0	-						
	pH 7.0	44.5	43.0			-		-
	pH 8.0	41.0	37.0			-		-
	pH 9.0	36.0						
HEPES + KOH	pH 5.2	-						
	pH 6.0	-						
	pH 7.0	41.5						
	pH 8.0	39.5						
	pH 9.0	34.5						
NaCl	0.2 M	41.0						
	0.5 M	42.5						
	0.6 M	42.0						
	1.2 M	43.0						
	2.0 M	44.5						
	2.5 M	46.5						
Conditions		Melting temperature [°C]						
		WT	C170S	C242S	C306S	C501S	C501S	C519S
KCl	0.2 M	40.5						
	0.5 M	42.0						

	0.6 M	42.0						
	1.0 M	42.0						
	1.2 M	42.0						
	2.0 M	44.5						
KH ₂ PO ₄ + KOH (pH 7.0) + NaCl	0.2 M	42.5						
	0.5 M	43.0						
	0.6 M	43.5						
	1.2 M	-						
	2.0 M	48.0						
	2.5 M	-						
KH ₂ PO ₄ + KOH (pH 7.0) + KCl	0.2 M	42.5						
	0.5 M	42.5						
	0.6 M	42.5						
	1.0 M	44.0						
	1.2 M	45.0						
	2.0 M	44.5						
NaH ₂ PO ₄ + NaOH (pH 7.0) + NaCl	0.2 M	42.5						
	0.5 M	44.0	42.0	43.5	-	-	-	-
	0.6 M	43.0						
	1.2 M	45.5	43.0	44.5	-	-	-	-
	2.0 M	47.5	44.5	45.0	-	-	-	-
	2.5 M	47.5						
NaH ₂ PO ₄ + NaOH (pH 7.0) + KCl	0.2 M	42.0						
	0.5 M	44.0						
	0.6 M	44.0						
	1.0 M	44.5						
	1.2 M	44.0						
	2.0 M	46.5						

As seen in the above table, LuxAB WT was in general best compatible with all buffers at pH 7.0 except Tris/HCl + NaOH 200 mM pH 5.0 – 9.0, where the protein was immediately structurally denatured. The greatest stability was achieved in the buffers NaH₂PO₄ + NaOH 200 mM pH 7.0 (T_m = 44.5 °C) and KH₂PO₄ + KOH 200 mM pH 7.0 (T_m = 45.5 °C), followed by KH₂PO₄ + K₂HPO₄ 100 mM pH 7.0 (T_m = 42.5 °C) as well as HEPES + KOH 200 mM pH 7.0 (T_m = 41.5 °C) and water

($T_m = 40.5\text{ }^\circ\text{C}$). The lowest melting temperatures appeared surprisingly under conditions with the standard buffer which is used for LuxAB experiments ($T_m = 40.0\text{ }^\circ\text{C}$). However this buffer system is best suitable for storage of the protein and hence used (Table 2).

It also could be observed that the stability of the wild type luciferase increased with the concentration of salt (NaCl and KCl), although the protein showed continuously a better tolerance with NaCl than KCl. Based on these results, the two most appropriate buffers ($\text{NaH}_2\text{PO}_4 + \text{NaOH}$ 200 mM pH 7.0 and $\text{KH}_2\text{PO}_4 + \text{KOH}$ 200 mM pH 7.0) were mixed in each case with NaCl and KCl in increasing concentrations (Table 2).

Therefore, the greatest stability could be observed in $\text{NaH}_2\text{PO}_4 + \text{NaOH}$ 200 mM pH 7.0 + 2 M NaCl ($T_m = 47.5\text{ }^\circ\text{C}$) although a higher melting temperature was observed in $\text{KH}_2\text{PO}_4 + \text{KOH}$ 200 mM pH 7.0 + 2 M NaCl ($T_m = 48.0\text{ }^\circ\text{C}$). It seemed that LuxAB WT doesn't like treatment with different kind of ions ($\text{KH}_2\text{PO}_4 + \text{KOH}$ 200 mM pH 7.0 + 2 M NaCl ($T_m = 48.0\text{ }^\circ\text{C}$), $\text{KH}_2\text{PO}_4 + \text{KOH}$ 200 mM pH 7.0 + 0.2 M NaCl ($T_m = 42.5\text{ }^\circ\text{C}$)). There was also no good stability seen in $\text{KH}_2\text{PO}_4 + \text{KOH}$ 200 mM pH 7.0 + 0.2 M KCl ($T_m = 42.5\text{ }^\circ\text{C}$), as well as in $\text{KH}_2\text{PO}_4 + \text{KOH}$ 200 mM pH 7.0 + 2 M KCl ($T_m = 44.5\text{ }^\circ\text{C}$), $\text{NaH}_2\text{PO}_4 + \text{NaOH}$ 200 mM pH 7.0 + 0.2 M NaCl ($T_m = 42.5\text{ }^\circ\text{C}$) and $\text{NaH}_2\text{PO}_4 + \text{NaOH}$ 200 mM pH 7.0 + 0.2 M KCl ($T_m = 42.0\text{ }^\circ\text{C}$). But by the use of $\text{NaH}_2\text{PO}_4 + \text{NaOH}$ 200 mM pH 7.0 + 2 M KCl ($T_m = 46.5\text{ }^\circ\text{C}$) a good stability was observed (Table 2).

From all the Thermofluor experiments with the wild type, apparently the buffer which is most suitable is $\text{NaH}_2\text{PO}_4 + \text{NaOH}$ 200 mM pH 7.0 + 2 M NaCl. However it is not suitable for freezing proteins under high salt concentrations, because due to the huge variation in temperature the pH changes and would denature the protein immediately, thus making it no longer useable for further tests. Therefore, although the storage buffer resulted a low T_m of LuxAB WT, it is suited for freezing the protein to stay under stable conditions (Table 2).

Then the melting temperatures of all mutated luciferases were determined under the treatment with the storage buffer and $\text{NaH}_2\text{PO}_4 + \text{NaOH}$ 200 mM pH 7.0 with different concentrations of NaCl. With LuxAB C170S a melting temperature of $38.5\text{ }^\circ\text{C}$ and with C242S, $39.0\text{ }^\circ\text{C}$ was observed (LuxAB WT, $T_m = 40.0\text{ }^\circ\text{C}$). In NaH_2PO_4 that contained 0.5 M NaCl, C170S and C242S showed also a lower T_m compared to the wild type ($T_m = 44.0\text{ }^\circ\text{C}$) with T_m $42.0\text{ }^\circ\text{C}$ and $43.5\text{ }^\circ\text{C}$ respectively. The same behavior of these two mutants could be pointed out while increasing the NaCl concentration till 2 M - 2.5 M. Half of LuxAB C170S denatured at $44.5\text{ }^\circ\text{C}$

and of LuxAB C242S at 45.0 °C (dark-blue). The wild type also showed here a higher temperature stability ($T_m = 47.5$ °C) (Table 2).

For LuxAB C306S, C465S, C501S and C519S, no melting temperatures could be determined suggesting that the mutants may have structurally denatured and do not form an active conformation of the protein. All the raw data graphs are shown in the supplementary section later (Supplementary figure S1-4).

4.4.4 Determining the activity of LuxAB WT and variants by measuring the bioluminescence

The light produced by the luciferase in an *in vitro* assay was measured to test its activity. For this purpose the luminometer counts all photons which impinge the connected detector. The resulting readings were plotted and the area under the curve integrated which represents the produced amount of bioluminescence. The produced bioluminescence of the wild type amounted to $4.06 \times 10^6 \pm 179159$ counts and decreased approximately by half for LuxAB C170S ($2.37 \times 10^6 \pm 256140$ counts) followed by a 4-fold decrease for LuxAB C242S ($1.80 \times 10^6 \pm 212518$ counts). Almost no bioluminescence was produced by LuxAB C306S (16180 ± 5550), C465S (34110 ± 2605), C519S (28792 ± 1033) and especially C501S (3370 ± 45) as shown below (Figure 4).

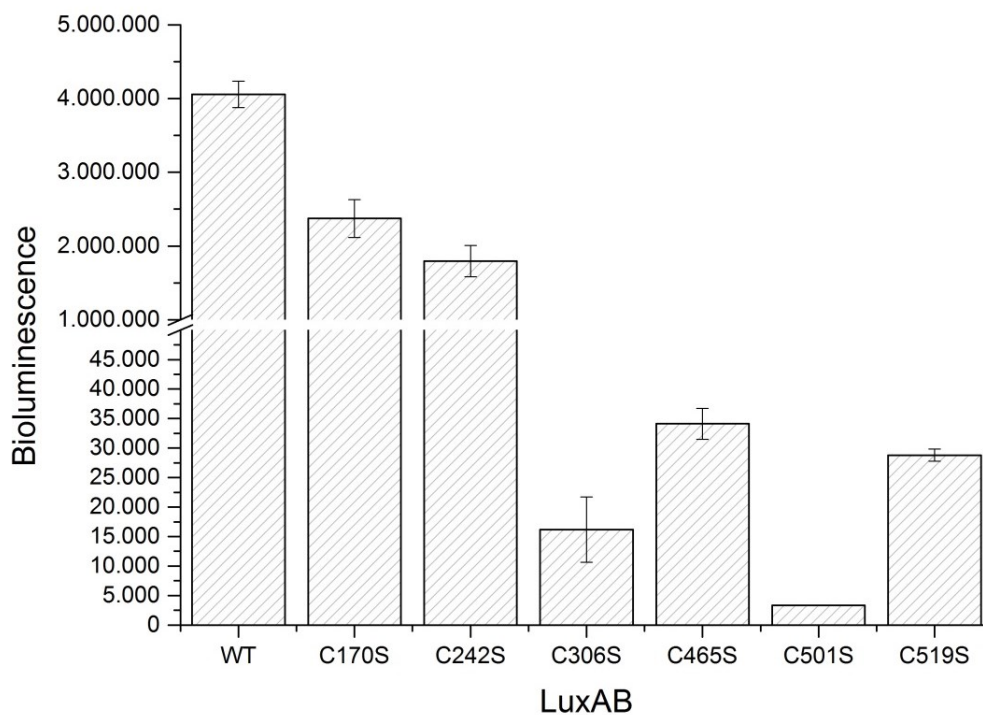


Figure 4: The enzymatic activity measured by the amount of produced bioluminescence for LuxAB WT in comparison with the variant luciferases.

4.5 Conclusions

Luciferase is relatively unstable and commonly loses its activity at room temperature because of structural changes resulting in the loss of its enzymatic functions. Improving the stability of proteins is a main goal in many biochemical and industrial applications. Different approaches are applied to increase the stability of the bacterial luciferase; the main topic of this study is to test the protein by replacing the reactive, easily oxidisable cysteines (C170, C242, C306, C465, C501, and C519) on the surface of the protein to serines using site-directed mutagenesis.

After over-expression of the variants in *E. coli* BL21*, the protein was purified via affinity chromatography and gel filtration. The mutants were verified by MALDI-TOF-MS. The protein was further tested if the site-directed mutagenesis on LuxAB has an impact on the yield of emitted light (luminometer measurements), thus the enzymatic activity and how it affects the melting temperature of each protein variant (Thermofluor experiments). The immediate results showed that four out of six luciferases (C306S, C465S, C501S and C519S) were completely denatured from the beginning and were not able to catalyze the light emitting reaction with high yield. C170S and C242S had similar characteristics compared to the wild type that is still unsurpassed in both enzymatic activity and stability.

In summary it could be shown that exchanging of cysteines to serine has neither improved the protein stability nor does it help in any folding changes that enhance the enzymatic activity. On the contrary the proteins exhibited rather premature denaturation or less functioning. Only mutations C170S and C242S impaired the enzyme compared to wild type not as strong as the other mutations (C306S, C465S, C501S and C519S) and the stability and the enzymatic behavior were relatively similar.

4.6 Supplementary data

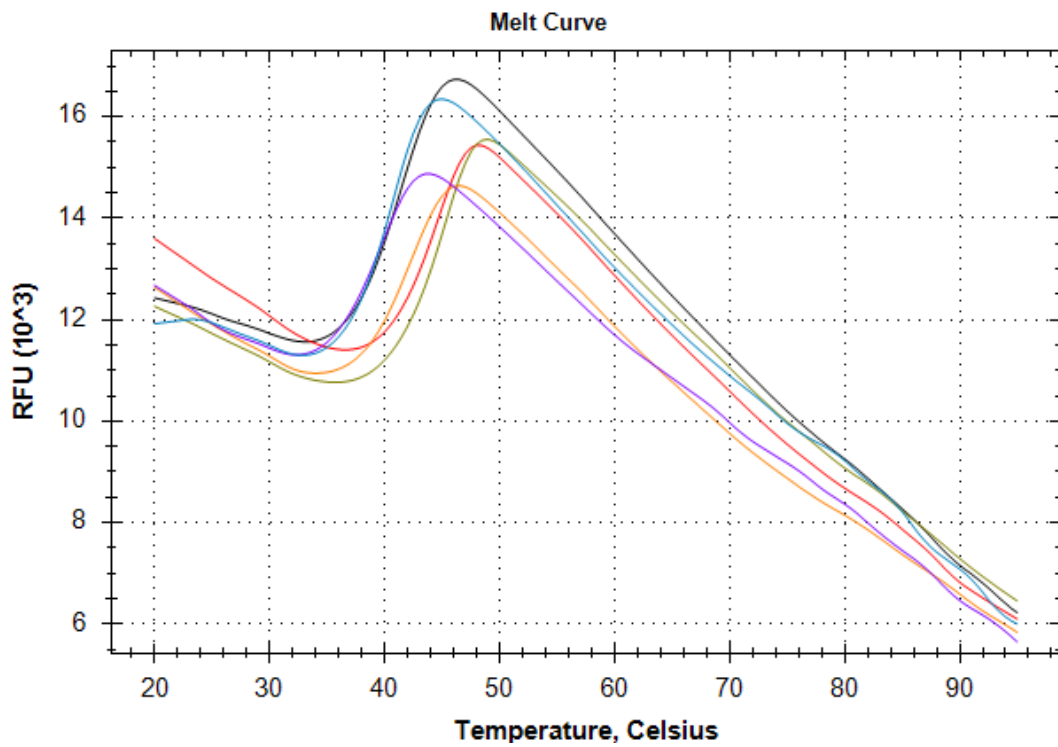


Figure S1: Melt curves of LuxAB WT under the influence of different buffer systems. The greatest stability was observed in the buffers NaH₂PO₄ + NaOH 200 mM pH 7.0 (red, T_m = 44.5 °C) and KH₂PO₄ + KOH 200 mM pH 7.0 (olive, T_m = 45.5 °C), followed by KH₂PO₄ + K₂HPO₄ 100 mM pH 7.0 (orange, T_m = 42.5 °C) as well as HEPES + KOH 200 mM pH 7.0 (black, T_m = 41.5 °C) and ddH₂O (blue, T_m = 40.5 °C). The storage buffer (purple, T_m = 40.0 °C) is the least suitable in this comparison.

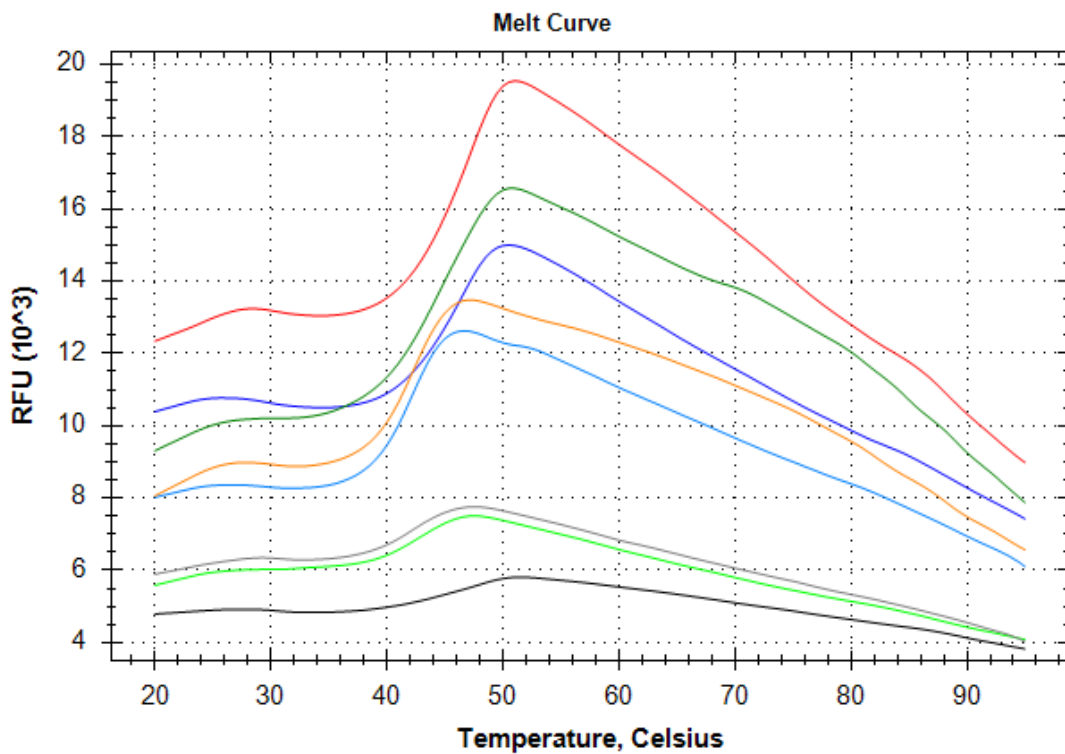


Figure S2: Melt curves of LuxAB WT in presence of different concentrations of salts. The luciferase is present in NaH₂PO₄ + NaOH 200 mM pH 7.0 or KH₂PO₄ + KOH 200 mM pH 7.0 with increasing concentration of NaCl and KCl, respectively. LuxAB WT is most stable in NaH₂PO₄ + NaOH 200 mM pH 7.0 + 2 M NaCl (red, T_m = 47.5 °C) but also stable in NaH₂PO₄ + NaOH 200 mM pH 7.0 + 2 M KCl (dark-blue, T_m = 46.5 °C) as well as KH₂PO₄ + KOH 200 mM pH 7.0 + 2 M KCl (dark-green, T_m = 44.5 °C), NaH₂PO₄ + NaOH 200 mM pH 7.0 + 0.2 M NaCl (orange, T_m = 42.5 °C) and NaH₂PO₄ + NaOH 200 mM pH 7.0 + 0.2 M KCl (light-blue, T_m = 42.0 °C). LuxAB did not like the treatment with KH₂PO₄ + KOH 200 mM pH 7.0 + 2 M NaCl (black, T_m = 48.0 °C), KH₂PO₄ + KOH 200 mM pH 7.0 + 0.2 M NaCl (grey, T_m = 42.5 °C) and also with KH₂PO₄ + KOH 200 mM pH 7.0 + 0.2 M KCl (light-green, T_m = 42.5 °C).

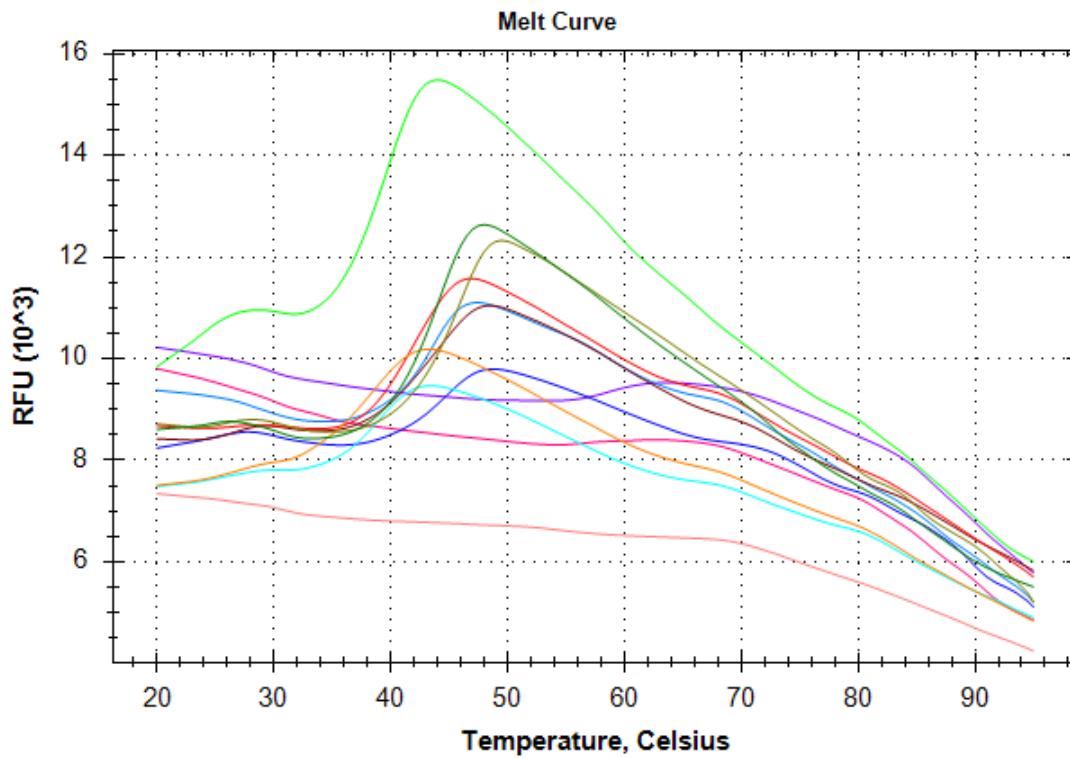


Figure S3: Melt curves of LuxAB C170S, C242S and C306S compared to the wild type. LuxAB C306S (salmon, pink and purple) was completely denatured therefore no T_m could be detected. LuxAB C170S when tested with storage buffer, a melting temperature of 38.5 °C (orange) was observed and with the mutant C242S, 39.0 °C (turquoise) could be achieved (LuxAB WT, T_m = 40.0 °C, light-green). C170S and C242S showed also a lower T_m compared to the wild type (dark-green (T_m = 44.0 °C) and olive (T_m = 47.5 °C)) in NaH₂PO₄ + NaOH 200 mM pH 7.0 + 0.5 M (dark-green, red and light-blue) and 2 M NaCl (olive, brown and dark-blue). Half of LuxAB C170S denatured at 42.0 °C (red) and 44.5 °C (brown), respectively and of LuxAB C242S at 43.5 °C (light-blue) and 45.0 °C (dark-blue), respectively.

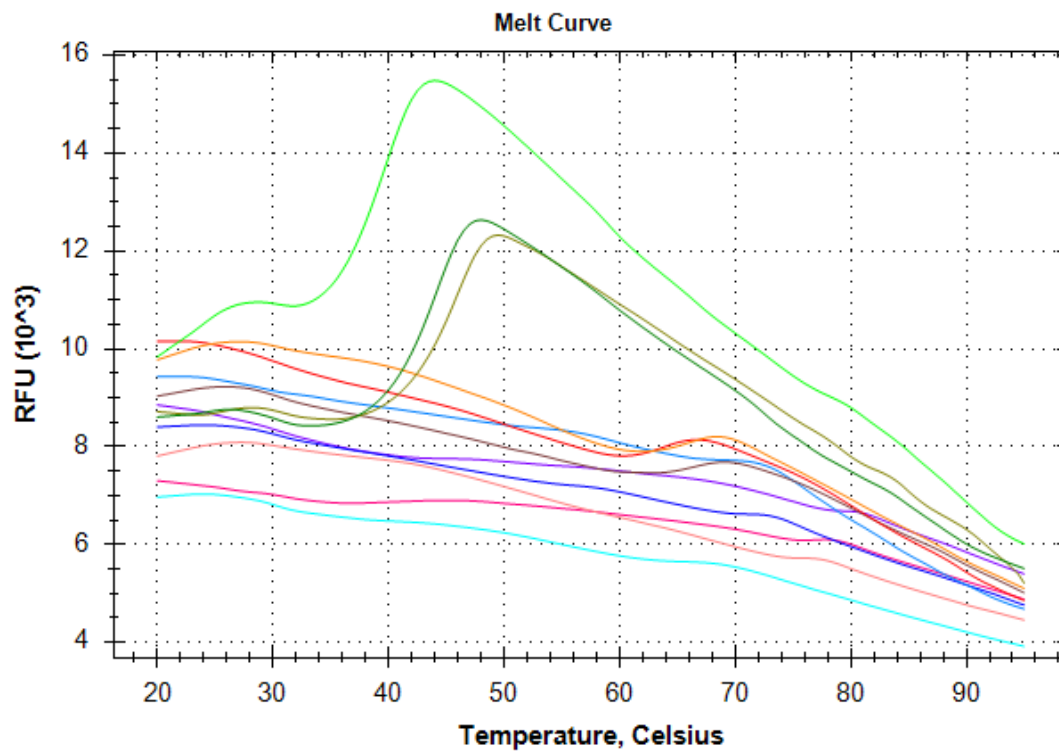


Figure S4: Melt curves of LuxAB C465S, C501S and C519S compared to the wild type. LuxAB C465S (orange, red and brown), C501S (turquoise, light- and dark-blue) and C519S (salmon, pink and purple) were all completely denatured right from the beginning of the measurement under all conditions. Orange, turquoise and salmon shows the protein dissolved in storage buffer; red, light-blue and pink represents $\text{NaH}_2\text{PO}_4 + \text{NaOH}$ 200 mM pH 7.0 + 0.5 M NaCl; brown, dark-blue and purple $\text{NaH}_2\text{PO}_4 + \text{NaOH}$ 200 mM pH 7.0 + 2 M NaCl. For comparison LuxAB WT is shown in light-green (storage buffer, $T_m = 40.0^\circ\text{C}$), dark-green ($\text{NaH}_2\text{PO}_4 + \text{NaOH}$ 200 mM pH 7.0 + 0.5 M NaCl, $T_m = 44.0^\circ\text{C}$) and olive ($\text{NaH}_2\text{PO}_4 + \text{NaOH}$ 200 mM pH 7.0 + 2 M NaCl, $T_m = 47.5^\circ\text{C}$).

4.7 References

1. Dunlap, P.V., (2009) Bioluminescence, microbial, *Encyclopedia of Microbiology*, 3rd edition. Elsevier, Oxford; In M. Schaechter (ed.), pp 45-61.
2. Haddock, S.N.D., Moline, M.A., and Case, J.F., (2010) Bioluminescence in the sea. *Ann Rev Mar Sci* **2**:443-93.
3. Shimomura, O., Johnson, F.H., and Saiga, Y. (1962) Extraction, purification and properties of aequorin, a bioluminescent protein from the luminous hydromedusan, *Aequorea*. *J Cell Comp Physiol* **59**:223-39.
4. Meighen, E. A., (1991) Molecular biology of bacterial bioluminescence. *Microbiol Rev* **55**, 123-142.
5. Boylan, M., Graham, A.F., and Meighen, E.A., (1985) Functional identification of the fatty acid reductase components encoded in the luminescence operon of *Vibrio fischeri*. *J Bacteriol* **163**:1186-90.
6. Nijvipakul, S., Wongratana J., Suadee C., Entsch B., Ballou D. P., and Chaiyen P., (2008) LuxG is a functioning flavin reductase for bacterial luminescence. *J Bacteriol* **190**: 1531-1538.
7. Baldwin, T.O., Christopher, J.A., Raushel, F.M., Sinclair, J.F., Ziegler, M.M., Fisher, A.J., and Rayment, I., (1995) Structure of bacterial luciferase. *Curr Opin Struct Biol* **5**:798-809.
8. Tanner, J.J., Miller, M.D., Wilson, K.S., Tu, S.C., and Krause, K.L., (1997) Structure of bacterial luciferase beta 2 homodimer: implications for flavin binding. *Biochemistry* **36**:665-72.
9. Thoden, J.B., Holden, H.M., Fisher, A.J., Sinclair, J.F., Wesenberg, G., Baldwin, T.O., and Rayment, I., (1997) Structure of the beta 2 homodimer of bacterial luciferase from *Vibrio harveyi*: X-ray analysis of a kinetic protein folding trap. *Protein Sci* **6**:13-23.
10. Bordoli, L., Kiefer, F., Arnold, K., Benkert, P., Battey, J., and Schwede, T., (2009) Protein structure homology modeling using SWISS-MODEL workspace. *Nat Protoc* **4**:1-13.
11. Fisher, A.J., Raushel, F.M., Baldwin, T.O., and Rayment, I., (1995) Three-dimensional structure of bacterial luciferase from *Vibrio harveyi* at 2.4 Å resolution. *Biochemistry* **34**:6581-6.
12. Bergner, T., Tabib, C.R., Winkler, A., Stipsits, S., Kayer, H., Lee, J., *et al.*, (2015) Structural and biochemical properties of LuxF from *Photobacterium leiognathi*. *Biochim Biophys Acta*, **1854**, 1466-1475.

Chapter 5

Generation of *luxAB*, *luxF* and *luxABF* knockouts in photobacterial strains

Chaitanya R. Tabib, Silvia Wallner and Peter Macheroux

Graz University of Technology, Graz, Austria

Keywords: *lux* operon, Type IV secretion system, knockouts

5.1 Introduction

The *lux* operon consists of the genes responsible for the enzymatic production of light in living cells, also known as Bioluminescence. The operon mainly consists of six genes, *luxCDABEG*, however, there are plenty of genes flanking this operon, which in some way play a role in bioluminescence.¹ More details on the genes and their roles have been already discussed in the last few chapters. Here in this chapter, we will discuss the operon from *Photobacterium leiognathi* ATCC 27561, with a gene order *luxCDABFEG*. The gene *luxAB* encodes for the bacterial luciferase, *luxCDE* for the fatty acid synthetase complex and *luxG* for the flavin reductase.^{2, 3} During the reaction, the luciferase (LuxAB-heterodimeric protein) catalyses the oxidation of an aldehyde substrate to its corresponding acid product. In the course of the reaction a reduced flavin reacts with molecular oxygen (O₂) and goes through a series of intermediate states, and before getting oxidised it goes to an excited energy state and relaxes back to ground state with the release of the energy in the form of light in blue-green range ($\lambda_{\max} = 490 \text{ nm}$).^{4, 5}

Within this luminescence reaction is an interesting flavin adduct (myrFMN or 6-(3'-(*R*)-myristyl) FMN), which is formed. Primary investigations showed myrFMN bound to LuxF in the crystal structure of this holoenzyme.⁶ Therefore, it was hypothesised that the presence of LuxF is required for the production of myrFMN. We, in our 1st publication, show a method we developed to extract this adduct from bacterial cells in pure form, to perform few binding experiments with luciferase and LuxF. Binding affinities indicated that myrFMN has 50 times higher affinity towards LuxF than to the luciferase ($K_d = 80 \text{ nM}$ for LuxF and $K_d = 4 \text{ }\mu\text{M}$ for luciferase). Exploiting this property of LuxF, we used this protein to screen for myrFMN in all bioluminescent bacterial strains we had. The results have clearly shown that myrFMN is present in all bioluminescent bacterial strains tested, independent of the presence or absence of LuxF.⁷

Therefore, we wanted to investigate the mechanism for the production of myrFMN *in vivo*, in the presence and absence of LuxF and luciferase. If myrFMN is produced in the luciferase reaction and LuxF is scavenging it away, then knockout out these genes (one protein at a time – as shown in the cartoon below) would give significant information on myrFMN production.

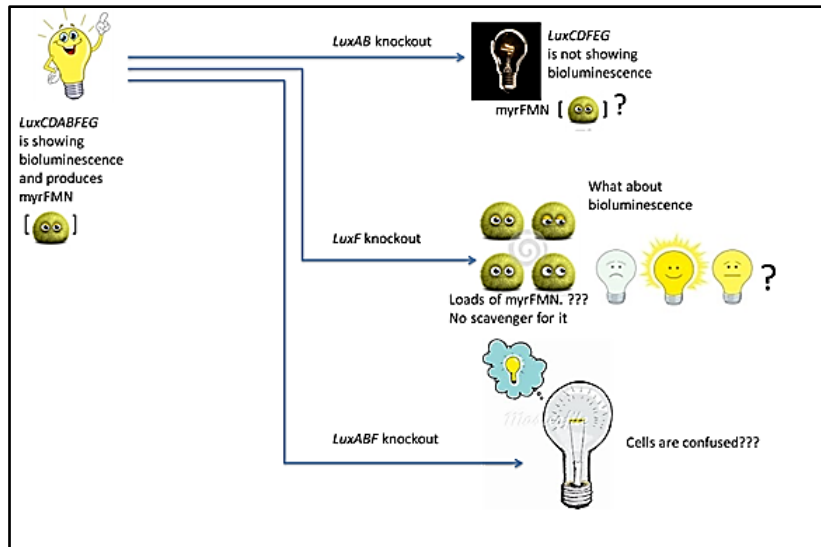


Figure 1: Three scenarios that could have helped us understand the mechanism of myrFMN production. Scenario 1: *luxAB* knockout, thus no light should be produced and so in principle no myrFMN has to be produced. Scenario 2: *luxF* knockout, thus there should be a huge accumulation of myrFMN in the cells thus inhibiting the luciferase reaction and so the light production. Scenario 3: *luxABF* knockout, should have basically similar effects like the *luxAB* knockout, however if myrFMN was to be found in scenario 1, this scenario would have helped investigating the role of LuxF in myrFMN production.

A knockout strategy using ‘type IV secretion system’ was followed.

5.1.1 Type IV secretion system (T4SSs)

Bacteria are known to have several methods to secrete genetic material or proteins using macromolecular assemblies.⁸ The Type IV secretion system (T4SSs) is very versatile as it can exchange both DNA and proteins. Thus these systems have played a significant role in evolving prokaryotic genome. The process of transfer of DNA from one cell to another using T4SSs is called ‘conjugation’. Such conjugation systems are present in both Gram positive and Gram negative bacteria. Most T4SSs consist of three main substructures: one is the cell pili that helps to contact the neighbouring cell, the second is the transport channel that conducts the substrate transfer across the cell envelop and lastly the type IV coupling protein, which acts as a receptor at the cytoplasmic entrance.⁹

To initiate a DNA transfer to the host cells, a donor cell and a conjugative plasmid are required. Generally, the conjugative plasmids encode for all the proteins, which are essential for their successful translocation to recipient cells. The genetic material required to be incorporated into the host cell should be cloned on the conjugative plasmid with correct translation frame

for incorporation. Delivery of necessary genetic material with complementary flanking regions into recipient cells leads to its integration into the host chromosome through recombination.

5.2 Aim of this study

The primary goal was to construct conjugative plasmids with an antibiotic cassette, flanked with the *lux* genes to generate specific knockouts. As explained in Figure 1, two different proteins were aimed to be knocked out from the bacterial genome. To achieve this, the flanking regions were to be pcr amplified from the bacterial genome.

The final aim was to use the conjugative plasmids in the T4SSs to generate knockouts in *Photobacteria leiognathi*.

5.3 Experiments and setups:

5.3.1 Preparation of constructs in conjugative plasmids

The construction of these plasmids were planned as follows:

Step 1: Primers were designed to amplify the overhangs from the bacterial genomic DNA. The overhangs were around 1kb long on each side of the antibiotic cassette. (Shown in Supplementary figure 2-5)

Primer names	Primer sequences
LuxAB 25521 US Fwd	5'-GGCGCAGAATTCGTCTCGGTGAAAATCGAACAGACTCGTTATCTTGAGG-3'
LuxAB 25521 US Rev	5'-GGTAGCGGATCCGGTAAGTACTATTTAGACACTAGCCAATACGCGATCAGC-3'
LuxAB 25521 DS Fwd	5'-GCGGGCGGATCCGTGCAGATCCTTACACTGCCATTTATAAATTAATAAGGG-3'
LuxAB 25521 DS Rev	5'-GTACGGTCTAGAGAATTCGATTAAGCCCTGCTTTTATTTTCAGGCTCGTGCC-3'
LuxAB 27561 US Fwd	5'-GGCGCAGAATTCATGAAAAATACTCAAACCTCTGCACCTATTGATCACATG-3'
LuxAB 27561 US Rev	5'-GGCAGCGGATCCGCCAAATTTTATTATCTTTTCTTTTGATGACTTGAATAGG-3'
LuxAB 27561 DS Fwd	5'-GGCAGCGGATCCATGACAAAATGGAATTATGGCGTCTTCTTCC-3'
LuxAB 27561 DS Rev	5'-GTACGGTCTAGAGAATTCGGCGCTGAAGCGATCTGGTCCCATATTCACC-3'
LuxF 27561 US Fwd	5'-GGTGCAGAATTCGTGGCGCCATACCTAAAAGATCCGAAATAAACTGCCAC-3'
LuxF 27561 US Rev	5'-GGCAGCGGATCCGGAAGAAGACGCCATAATTCATTTTGTCAT-3'
LuxABF 27561 DS Fwd	5'-GGTATCGGATCCATTGTCATTATTAATGGCAGTGTGGCTTCTTACGCTGCC-3'
Lux ABF 27561 DS Rev	5'-GTACGGTCTAGAGAATTCAGTCCTGTTGCTTATTTCAAGCTGGTCGCCATCG-3'
Primers for Chloramphenicol cassette from pACYC184 plasmid	
Chlo_Fwd:	5'-GGCAGCGGATCCATGGAGAAAAAATCACTGGATATACCACCG-3'
Chlo_Rev:	5'-GAATAAGGATCCTTACGCCCGCCCTGCCACTC-3'

[LuxAB 25521 US Fwd: means to say the primer is the forward direction for the Up Stream sequence of the LuxAB in ATCC 25521 strain. Similarly 'DS' stands for Down Stream and 'Rev' stands for Reverse direction primer]

Step 2: The upstream and downstream regions were cloned in pMS119EH vector using EcoRI/BamHI for US and BamHI/XbaI for DS. Later, the chloramphenicol cassette was inserted between the upstream and the downstream regions using BamHI. (The resulting constructs are as shown in supplementary figure 1-5)

Step 3: Cut the pRL27 vector with EcoRI to get rid of all the transposases. (Shown in Supplementary figure 6)

Step 4: The construct "Upstream-Chloramphenicol-Downstream" was cut by EcoRI enzyme to sub clone it into the conjugation vector, pRL27. (The resulting constructs are as shown in supplementary figure 7)

Step 5: The pRL27_constructs were transformed in the donor cells (*E. coli* BW20767 strain) via chemical transformation (heat-shock method).

Step 6: The conjugation procedure was implemented on the system. (The procedure is as shown in Scheme 1)

5.3.2 Plasmids and strains used

The plasmids used in this study were:

- pRL27_Kan[®] (50µg/ml)

Plasmid pRL27 is a transposon delivery vector that carries a mini-Tn5 cassette encoding kanamycin resistance, a transposase gene and the oriT of RP4. The transposase is hyperactive in many Gram-negative hosts. Therefore, the transposition events are several magnitudes higher than obtained with the mini-Tn5 series of de Lorenzo and co-workers. Plasmid pRL27 was found to be perfectly suited for mutagenesis in many clinical isolates of *E. coli*. Donor cells can be counter-selected by plating of mating mixtures on minimal medium.¹⁰

- BW20767_no antibiotic resistance

This is the host strain for the conjugative plasmid pRL27. [RP4–2-Tc::Mu-1 kan::Tn7 integrant leu-63::IS10 recA1 zbf-5 creB510 hsdR17 endA1 thi uidA (ΔMlul)::pir+]¹¹

- pMS119EH_Amp[®] (100µg/ml)

This is a Ptac expression vector.¹²

- *Photobacterium leiognathi* (ATCC 27561 – LuxF⁺; ATCC 25521 – LuxF⁻ strain)

5.3.3 Principle underlying usage of these plasmid/strains

The pRL27 is a low-copy, transferable suicide plasmid. Suicide plasmids carry a R6K replicon that is pir-dependent for replication. Without the pir-gene encoded protein present in the host cell (which is not expressed by the pRL27 plasmid), this plasmid cannot replicate and will be eventually lost. Therefore, it is necessary to use a host strain (e.g. BW20767), where the pir gene is integrated in the chromosome to stably work with pRL27 and all its derivatives. The photobacterial strain has no pir gene and will not allow replication of pRL27. Thus it makes sure there is no free pRL27 derivative in the strain but only integrates are screened for.

There are two methods to introduce the pRL27 construct into the host strain:

1.) Electroporation: Not a very efficient method.

2.) T4SSs: The pRL27 derivatives are mobilized from your host to your strain of interest via a Type IV secretion system. This is achieved through the RP4 origin of transfer on the pRL27 plasmid (a piece of DNA that gets recognized and cleaved by specific enzymes leading to the mobilization of the whole pRL27) and a Type IV secretion system that is encoded in the host strain. Mobilization is more efficient than electroporation.

Scheme 1: Protocol for Transposon Mutagenesis (adapted and modified from Schneiditz *et al.*, 2014)¹³. The miniTn5 delivery vector pRL27 carrying the construct (27561 AB/F/ABF; 25521 AB knockout flanking sequences + Chloramphenicol cassette) was introduced to *P. leiognathi* via conjugation transfer from BW20767 λ pir donor cells.

The donor and the recipient strains were incubated overnight in 5ml LB medium under selective conditions (*pRL27 knockout constructs with 50 mg/ml kanamycin in LB at 37 °C; Photobacteria in 246 media with no antibiotic at 25 °C*)

↓
1 ml of each ONC was used to inoculate 100 ml fresh medium (----same as above----)

↓
These cultures were incubated for 1 h at respective temperatures of growth

↓
Then the donor and recipient cells were mixed in a ratio 1:10, normalised to $\sim 0.5 * 10^7$ cfu of the donor strain

↓
The cell mixture was harvested via centrifugation at 4000rpm/10min/RT

↓
The pellet was suspended in 50-100 μ l **PBS** and applied to a **sterile cellulose acetate filter (0.45 μ m pore size; Millipore)**

↓
The filter was placed on a **LB agar plate and incubated at 25 °C for 6 h (incubation time can be changed)**

↓
Bacteria were removed from the filter and suspended in 1ml PBS

↓
Cells were plated on selective agar plate containing **35 mg/ml Chloramphenicol**

↓
Screen for colonies by colony PCR or Bioluminescence

5.4 Results

The knockout construct was successfully cloned into the conjugation vector pRL27. The donor cells with the correct construct were screened for kanamycin resistance. The right donor cells were chosen and stored as glycerol stocks for conjugation experiments.

Donor cells carrying all four different constructs were tested with the specific bacterial host strains (ATCC 27561 & 25521) at different conditions as summarised below. Unfortunately, no colonies were seen on any of the plates with Chloramphenicol (1, 2, 5, 10, 20µg).

5.4.1 Different conditions tested

1. Literature survey and experimental check for antibiotic sensitivity of *Photobacterium* (photobacterial strains contain R – plasmids!!)
2. Cloning principle checked for:
 - pRL27 vector
 - BW20767 *E. coli* strain
 - pMS119EH vector
3. Tested the protocol from Schneditz's PNAS paper. (Protocol as in Scheme 1)
 - Different time points for incubation (1 h, 2 h, 6 h, 18 h, 36 h)
 - Different dilutions
 - Colony PCR to screen for Chlo and Kan cassette in colonies plated on 'no antibiotic' plates
4. Other alternative controls:
 - pRL27 in BW20767 (Kanamycin-40)
 - pRL27 in BM25142 (Kanamycin-40) (different donor strain)
 - pAR106 vector (Chloramphenicol-10, RP4 backbone, insertion cassette cat-P A1/04/03 – gfpmut3b*-T0) (different conjugation plasmid)
 - pAR177 vector (Kanamycin-40, Replicon and OriT of RSF1010; pTET-GFP fusion broad host range) (different conjugated plasmid)
5. Electroporation
 - Different protocols for preparation of electro-competent cells
 - Different concentrations of insert (1, 2, 5, 10, 20µg)
 - Double strand DNA transformed, circular pRL27 vector/pMS119EH vector & pACYC184 as control
 - Different protocols for electric pulse (standard, EC1 and EC2)
 - O/N and 36 hrs incubation at 25°C

- *E. coli* taken as control
6. Chemical transformation (heat shock method)
- CaCl₂ method of competent cells preparation
 - 5µg DNA taken
 - Double strand insert, whole pRL27 vector, whole pMS119EH vector & pACYC184 as control
 - *E. coli* taken as control
 - O/N and 36 hrs incubation at 25`C

5.5 Conclusion

5.5.1 Possible reasons for DNA not being taken up by *Photobacteria*

1. Photobacterial strains were found to contain R – plasmids, which are generally huge (100 – 150 kb) plasmids that contain resistance markers for almost all antibiotics. These plasmids help the bacteria to survive antibiotic attacks. Also, the R – plasmids are RP4 type of plasmids (RP4 plasmids are conjugative plasmids which transfer the genetic materials to other host cells). Therefore, it's difficult to know if the donor cells (BW20767) and the photobacterial cells are even transferring any genetic material or not.
2. The second problem could be that *E. coli* does not prefer 25 °C for conjugation. However, all the conjugations have to be performed at this temperature because *Photobacterium* doesn't grow above 27 °C. Thus the temperature difference could be hindering the conjugation process.
3. Lastly, It was also observed during the experiments that *Photobacterium* when incubated with *E. coli* doesn't shine (instantly forms dark mutant for reasons unknown). This makes it difficult to screen these cells via colony PCR when grown without antibiotic.

5.5.2 Alternative experimental approaches to investigate production of myrFMN

1. *In vitro* multi-enzyme cascade reaction with cofactor recycling (described in chapter 3)
2. Heterologous expression of the whole *lux* operon in *E. coli* (experiments ongoing)

Table 1: Results for the conjugation experiments performed at different concentrations and different incubation time points.

18 hrs	Pure culture conjugated								
25521		100µl	Light						
	LB	Less lawn	Yes						
	246	Lawn	Yes						
	246 + AMP	Less Lawn	Yes						
	246 + KAN	Lesser Lawn	Yes						
	246 + CHLO	None	-						
BW20767		100µl							
	LB	Lawn	-						
	246	Lawn	-						
	246 + AMP	None	-						
	246 + KAN	None	-						
	246 + CHLO	None	-						
pRL27		100µl							
	LB	Lawn	-						
	246	Lawn	-						
	246 + AMP	None	-						
	246 + KAN	Lawn	-						
	246 + CHLO	None	-						
pRL27 + Const		100µl							
	LB	Lawn	-						
	246	Lawn	-						
	246 + AMP	None	-						
	246 + KAN	Lawn	-						
	246 + CHLO	None	-						

18 hrs		1:1 (1 OD:1 OD)								E:P
25521		100µl	Light	10 ⁻¹	Light	10 ⁻²	Light	10 ⁻³	Light	
	LB									
	246									
	246 + AMP									
	246 + KAN									
	246 + CHLO									
	246 + C + A									
BW20767 + 21										
	LB									
	246	Lawn	Yes	Lawn	Yes	1000s	Yes	~1000	Yes	
	246 + AMP	10000s	Yes	1000s	Yes	1000s	Yes	~1000	Yes	
	246 + KAN									
	246 + CHLO	No	No	No	No	No	No	No	No	
	246 + C + A									
pRL27 + 21										
	LB									
	246	Lawn	Yes	Lawn	Yes	Lawn	Yes	1000	Yes	
	246 + AMP	Lawn	Yes	1000s	Yes	No	No	No	No	
	246 + KAN	Lawn	Yes	Lawn	Yes	1000s	Yes	~400	Yes	
	246 + CHLO	No	No	No	No	No	No	No	No	
	246 + C + A									
pRL27 + Const + 21										
	LB									
	246	Lawn	Yes	Lawn	Yes	1000s	Yes	~100	Yes	
	246 + AMP	10000s	Yes	No	No	No	No	No	No	
	246 + KAN									
	246 + CHLO	No	No	No	No	No	No	No	No	
	246 + C + A	No	No	No	No	No	No	No	No	

18 hrs		1:10 (0.1 OD:1 OD)								E:P
25521		100µl	Light	10 ⁻¹	Light	10 ⁻²	Light	10 ⁻³	Light	
	LB									
	246									
	246 + AMP									
	246 + KAN									
	246 + CHLO									
	246 + C + A									
BW20767 + 21										
	LB									
	246	Lawn	Yes	Lawn	Yes	Lawn	Yes	1000s	Yes	
	246 + AMP	Lawn	Yes	~1000	Yes	~100	Yes	No	No	
	246 + KAN									
	246 + CHLO	No	No	No	No	No	No	No	No	
	246 + C + A									
pRL27 + 21										
	LB									
	246	Lawn	Yes	Lawn	Yes	Lawn	Yes	Lawn	Yes	
	246 + AMP	Lawn	Yes	10000s	Yes	-	-	1000s	Yes	
	246 + KAN	Lawn	Yes	Lawn	Yes	Lawn	Yes	1000s	Yes	
	246 + CHLO	No	No	No	No	No	No	No	No	
	246 + C + A									
pRL27 + Const + 21										
	LB									
	246	Lawn	Yes	Lawn	Yes	1000s	Yes	~100	Yes	
	246 + AMP	Lawn	Yes	1000s	Yes	~1000	Yes	No	No	
	246 + KAN									
	246 + CHLO	No	No	No	No	No	No	No	No	
	246 + C + A	No	No	No	No	No	No	No	No	

18 hrs		1:100 (0.01 OD:1 OD)								E:P
25521		100µl	Light	10 ⁻¹	Light	10 ⁻²	Light	10 ⁻³	Light	
	LB									
	246									
	246 + AMP									
	246 + KAN									
	246 + CHLO									
	246 + C + A									
BW20767 + 21										
	LB									
	246	Lawn	Yes	Lawn	Yes	Lawn	Yes	1000s	Yes	
	246 + AMP	Lawn	Yes	1000s	Yes	No	No	No	No	
	246 + KAN									
	246 + CHLO	No	No	No	No	No	No	No	No	
	246 + C + A									
pRL27 + 21										
	LB									
	246	Lawn	Yes	Lawn	Yes	Lawn	Yes	~10000	Yes	
	246 + AMP	Lawn	Yes	~Lawn	Yes	1000s	Yes	~1000	Yes	
	246 + KAN	Lawn	Yes	~Lawn	Yes	Lawn	Yes	1000s	Yes	
	246 + CHLO	No	No	No	No	No	No	No	No	
	246 + C + A									
pRL27 + Const + 21										
	LB									
	246	Lawn	Yes	Lawn	Yes	Lawn	Yes	~Lawn	Yes	
	246 + AMP	Lawn	Yes	~10000	No	No	No	No	No	
	246 + KAN									
	246 + CHLO	No	No	No	No	No	No	No	No	
	246 + C + A	No	No	No	No	No	No	No	No	

36 hrs		Pure culture conjugated							
25521		100µl	Light						
	LB	Lawn	Yes						
	246	Lawn	Yes						
	246 + AMP	Lawn	No						
	246 + KAN	Lawn	No						
	246 + CHLO	None	-						
BW20767		100µl							
	LB	Lawn	-						
	246	Lawn	-						
	246 + AMP	None	-						
	246 + KAN	None	-						
	246 + CHLO	None	-						
pRL27		100µl							
	LB	Lawn	-						
	246	Lawn	-						
	246 + AMP	None	-						
	246 + KAN	Lawn	-						
	246 + CHLO	None	-						
pRL27 + Const		100µl							
	LB	Lawn	-						
	246	Lawn	-						
	246 + AMP	None	-						
	246 + KAN	Lawn	-						
	246 + CHLO	None	-						

36 hrs		1:1								E:P
25521		100μl	Light	10⁻¹	Light	10⁻²	Light	10⁻³	Light	
	LB									
	246									
	246 + AMP									
	246 + KAN									
	246 + CHLO									
	246 + C + A									
BW20767 + 21										
	LB									
	246	Lawn	No	Lawn	No	~Lawn	Yes	~1000	Yes	
	246 + AMP	10000s	Yes	1000s	Yes	1000s	Yes	~1000	No	
	246 + KAN									
	246 + CHLO	No	No	No	No	No	No	No	No	
	246 + C + A									
pRL27 + 21										
	LB									
	246	Lawn	Yes	Lawn	Yes	Lawn	Yes	Lawn	Yes	
	246 + AMP	Lawn	Yes	1000s	Yes	No	No	No	No	
	246 + KAN	Lawn	No	Lawn	Yes	1000s	Yes	~1000	Yes	
	246 + CHLO	No	No	No	No	No	No	No	No	
	246 + C + A									
pRL27 + Const + 21										
	LB									
	246	Lawn	Yes	Lawn	Yes	10000s	Yes	~500	Yes	
	246 + AMP	Lawn	Yes	~1000	Yes	No	No	No	No	
	246 + KAN									
	246 + CHLO	No	No	No	No	No	No	No	No	
	246 + C + A	No	No	No	No	No	No	No	No	

36 hrs		1:10								E:P
25521		100µl	Light	10 ⁻¹	Light	10 ⁻²	Light	10 ⁻³	Light	
	LB									
	246									
	246 + AMP									
	246 + KAN									
	246 + CHLO									
	246 + C + A									
BW20767 + 21										
	LB									
	246	Lawn	Yes	Lawn	Yes	Lawn	Yes	~Lawn	Yes	
	246 + AMP	Lawn	Yes	~10000	Yes	~1000	Yes	No	No	
	246 + KAN									
	246 + CHLO	No	No	No	No	No	No	No	No	
	246 + C + A									
pRL27 + 21										
	LB									
	246	Lawn	No	Lawn	No	Lawn	Yes	Lawn	Yes	
	246 + AMP	Lawn	Yes	10000s	Yes	1000s	Yes	1000s	Yes	
	246 + KAN	Lawn	No	Lawn	Yes	Lawn	No	1000s	Yes	
	246 + CHLO	No	No	No	No	No	No	No	No	
	246 + C + A									
pRL27 + Const + 21										
	LB									
	246	Lawn	No	Lawn	No	Lawn	No	Lawn	No	
	246 + AMP	Lawn	Yes	Lawn	Yes	~1000	Yes	No	No	
	246 + KAN									
	246 + CHLO	No	No	No	No	No	No	No	No	
	246 + C + A	No	No	No	No	No	No	No	No	

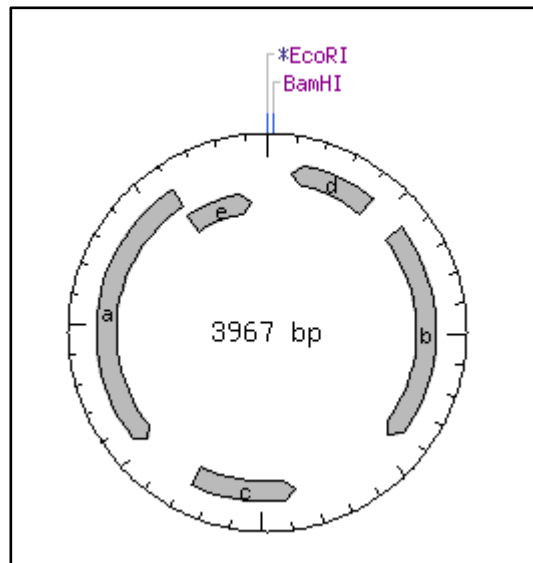
36 hrs		1:100								E:P
25521		100μl	Light	10⁻¹	Light	10⁻²	Light	10⁻³	Light	
	LB									
	246									
	246 + AMP									
	246 + KAN									
	246 + CHLO									
	246 + C + A									
BW20767 + 21										
	LB									
	246	Lawn	No	Lawn	No	Lawn	No	Lawn	No	
	246 + AMP	Lawn	No	10000s	Yes	1000s	Yes	~1000	No	
	246 + KAN									
	246 + CHLO	No	No	No	No	No	No	No	No	
	246 + C + A									
pRL27 + 21										
	LB									
	246	Lawn	No	Lawn	No	Lawn	No	Lawn	Yes	
	246 + AMP	Lawn	No	Lawn	Yes	10000s	Yes	10000s	Yes	
	246 + KAN	Lawn	Yes	Lawn	Yes	Lawn	Yes	10000s	Yes	
	246 + CHLO	No	No	No	No	No	No	No	No	
	246 + C + A									
pRL27 + Const + 21										
	LB									
	246	Lawn	No	Lawn	No	Lawn	No	~Lawn	Yes	
	246 + AMP	Lawn	Yes	Lawn	Yes	1000s	Yes	100s	No	
	246 + KAN									
	246 + CHLO	No	No	No	No	No	No	No	No	
	246 + C + A	No	No	No	No	No	No	No	No	

5.5 References

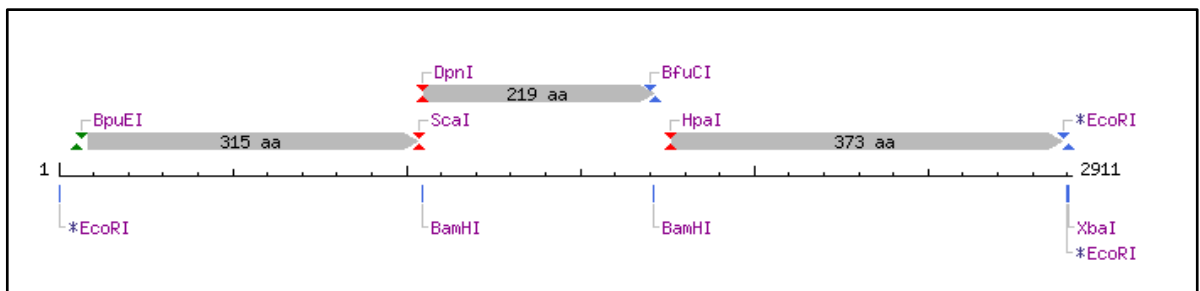
1. Meighen, E. A., (1991) Molecular biology of bacterial bioluminescence. *Microbiol Rev* **55**, 123-142.
2. Boylan, M., Graham, A.F., and Meighen, E.A., (1985) Functional identification of the fatty acid reductase components encoded in the luminescence operon of *Vibrio fischeri*. *J Bacteriol* **163**:1186-90.
3. Nijvipakul, S., Wongratana J., Suadee C., Entsch B., Ballou D. P., and Chaiyen P., (2008) LuxG is a functioning flavin reductase for bacterial luminescence. *J Bacteriol* **190**: 1531-1538.
4. Ulitzur, S., and Hastings, J. W., (1979) Evidence for tetradecanal as the natural aldehyde in bacterial bioluminescence. *Proc Natl Acad Sci U S A* **76**: 265-267.
5. Kurfurst, M., Ghisla, S., and Hastings, J. W., (1984) Characterization and postulated structure of the primary emitter in the bacterial luciferase reaction. *Proc Natl Acad Sci U S A* **81**: 2990-2994.
6. Moore, S.A., and James, M. N. G., (1995) Structural refinement of the non-fluorescent flavoprotein from *Photobacterium leiognathi* at 1.60 Å resolution. *J Mol Biol* **249**, 195–214.
7. Bergner, T., Tabib, C.R., Winkler, A., Stipsits, S., Kayer, H., Lee, J., *et al.*, (2015) Structural and biochemical properties of LuxF from *Photobacterium leiognathi*. *Biochim Biophys Acta* **1854**, 1466-1475.
8. Costa, T.R., Felisberto-Rodrigues, C., Meir, A., Prevost, M.S., Redzej, A., Trokter, M., and Waksman, G., (2015) Secretion systems in Gram-negative bacteria: structural and mechanistic insights. *Nat Rev Microbiol* **13**:343-59.
9. Zechner, E.L., Lang, S., and Schildbach, J.F., (2012) Assembly and mechanisms of bacterial type IV secretion machines. *Philos Trans R Soc Lond B Biol Sci* **367**:1073-87.
10. Larsen, R.A., Wilson, M.M., Guss, A.M., and Metcalf, W.W., (2002) Genetic analysis of pigment biosynthesis in *Xanthobacter autotrophicus* Py2 using a new, highly efficient transposon mutagenesis system that is functional in a wide variety of bacteria. *Arch Microbiol* **178**:193-201.
11. Metcalf, W.W., Jiang, W., Daniels, L.L., Kim, S.K., Haldimann, A., and Wanner, B.L., (1996) Conditionally replicative and conjugative plasmids carrying *lacZ* alpha for cloning, mutagenesis, and allele replacement in bacteria. *Plasmid* **35**:1-13.
12. Strack, B., Lessl, M., Calendar, R., and Lanka, E., (1992) A common sequence motif, -E-G-Y-A-T-A-, identified within the primase domains of plasmid-encoded I- and P-type DNA primases and the alpha protein of the *Escherichia coli* satellite phage P4. *J Biol Chem* **267**:13062-72.
13. Schneditz, G., Rentner, J., Roier, S., Pletz, J., Herzog, K.A., Bückner, R, *et al.*, (2014) *Proc Natl Acad Sci U S A* **111**:13181-6.

5.6 Supplementary figures:

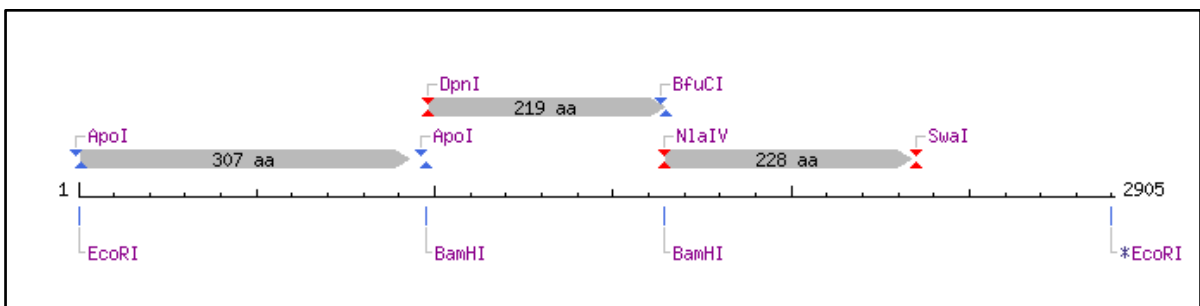
1. pMS119EH vector map: Used to clone the constructs



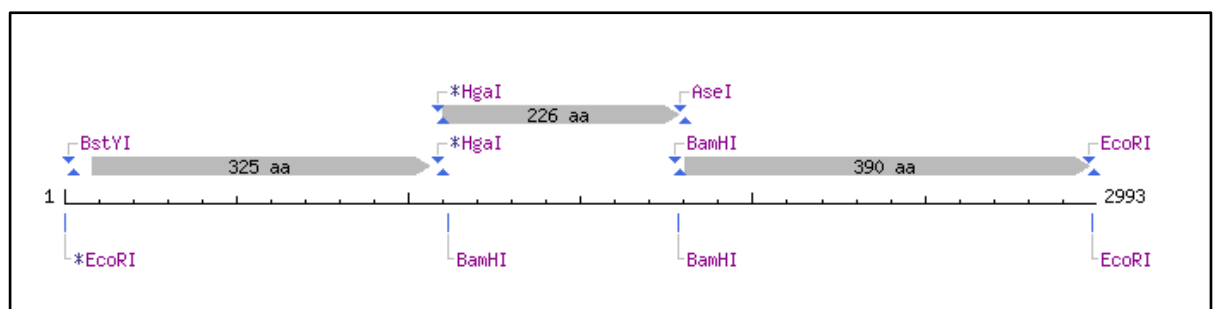
2. ATCC 25521 LuxAB US + Chlo + DS knockout construct



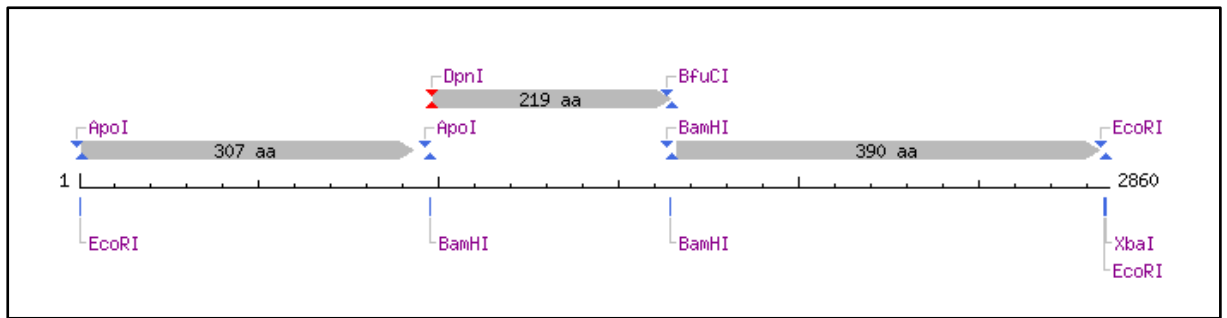
3. ATCC 27561 LuxAB US + Chlo + DS knockout construct



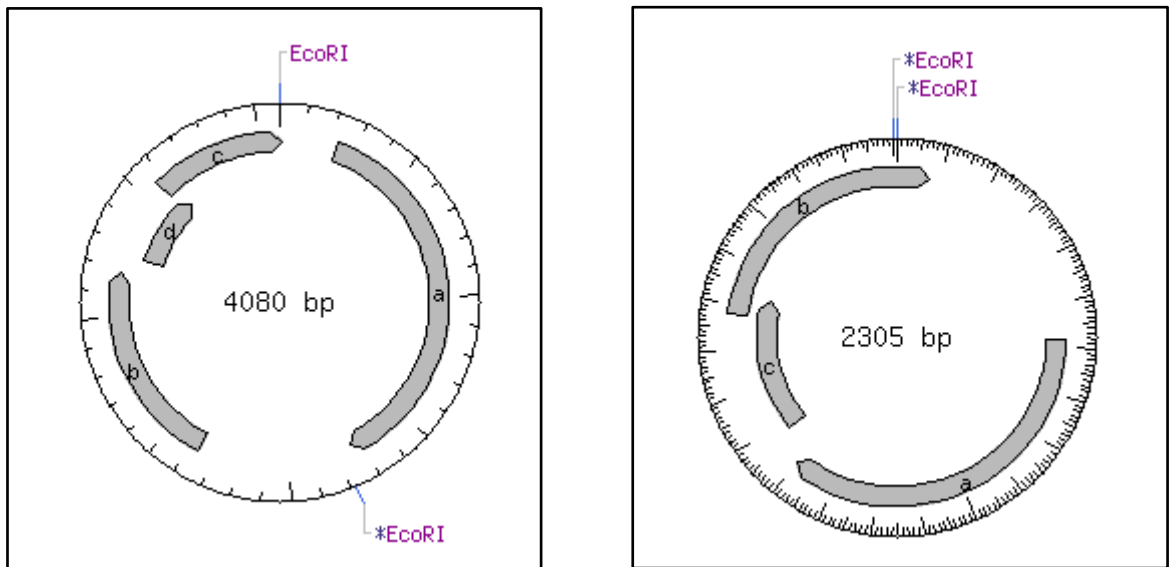
4. ATCC 27561 LuxF US + Chlo + DS knockout construct



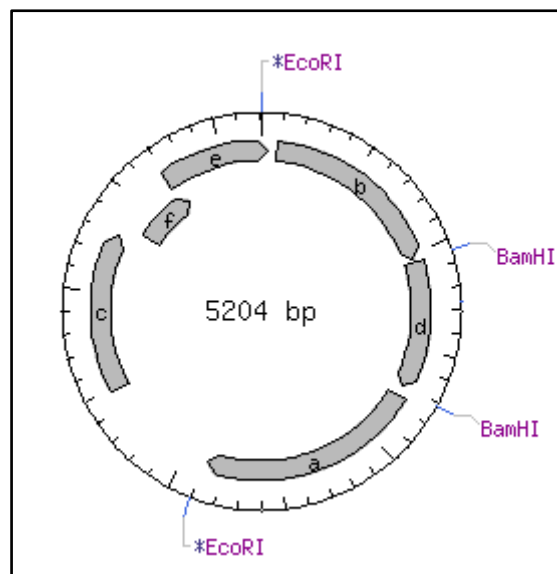
5. ATCC 27561 LuxABF US + Chlo + DS knockout construct



6. pRL27 vector before and after cutting with EcoRI



7. pRL27_LuxAB/F/ABF US + Chlo + DS knockout construct (after cloning each of these constructs into pRL27)



Appendix

Abbreviations

<i>A. fischeri</i> or AF	<i>Aliivibrio fischeri</i>
Abs	Absorbance
Amp [®]	Ampicillin resistance
ATP	Adenosine triphosphate
CIEEL	Chemically initiated electron exchange luminescence
Chlo [®]	Chloramphenicol resistance
DNA	Deoxyribonucleic acid
ddH ₂ O	Double distilled sterile water
<i>E. coli</i>	<i>Escherichia coli</i>
FMN	Flavin mononucleotide
FMNH ₂	Reduced flavin mononucleotide
FAD	Flavin adenine dinucleotide
GDH	Glucose dehydrogenase
GFP	Green fluorescence protein
6xHis-tag	Hexa histidine-tag
HCl	Hydrochloric acid
HPLC	High Performance Liquid Chromatography
IC ⁵⁰	Inhibition constant
IPTG	isopropyl β-D-1-thiogalactopyranoside
ITC	Isothermal titration calorimetry
Kan [®]	Kanamycin resistance
K _d	Dissociation constant
LB medium	Luria-bertani broth
LMW	Low molecular weight standard
MALDI	Matrix-assisted laser desorption/ionization mass spectrometry
MyrFMN	6-(3'-(R)-myristyl) FMN
NADPH	Nicotinamide adenine dinucleotide phosphate
O ₂	Molecular oxygen
<i>P. leiognathi</i> or PL	<i>Photobacterium leiognathi</i>
rpm	revolutions per minute

T_m	melting temperature
<i>V. harveyi</i> or <i>VH</i>	Vibrio harveyi
WT	Wildtype

Curriculum Vitae

Curriculum Vitae

Name **Chaitanya R Tabib, MSc**
Address Institute of Biochemistry
Petersgasse 12/II, 8010 Graz, Austria
Mobile (+43) 660 5118005
Email **chaitanya.tabib@student.tugraz.at**
chaitanya.tabib@gmail.com
Date/place of birth 23/12/1985, Ranebennur, Karnataka, India
Nationality **Indian**
Marital status Married



Education

2012-present **PhD** – Natural sciences (**Thesis title:** Biochemistry and Microbiology of *Photobacterial* bioluminescence; **Supervisor:** Prof. Dr. Peter Macheroux) at Institute of Biochemistry, Graz University of Technology, Graz, Austria
2008-2012 **Research Fellow (RF)** under the supervision of Prof. D N Rao at Department of Biochemistry, Indian Institute of Science (IISc), Bangalore, India
2006-2008 **MSc** - Biochemistry at Sri Bhagwan Mahaveer Jain College, Bangalore, India
2003-2006 **BSc** - Biotechnology at JSS College, Karnatak University, Dharwad, India

Publications

- **Tabib CR***, Brodl E*, Macheroux P (2016): Generation of myristylated FMN by luciferase supports a radical mechanism for bacterial bioluminescence; (**manuscript under preparation**) (* - *Co-first authors*)
- Brodl E, Ivkovic J, **Tabib CR**, Breinbauer R, Macheroux P (2016): Synthesis of α , β -unsaturated aldehydes as potential substrates for bacterial luciferases; (**manuscript submitted to Bioorganic & Medicinal Chemistry**)
- Bergner T*, **Tabib CR***, Winkler A, Stipsits S, Kayer H, Lee J, Malthouse JP, Mayhew S, Müller F, Gruber K, Macheroux P (2015): Structural and biochemical properties of LuxF from *Photobacterium leiognathi*; **Biochim-Biophys Acta**, 1854, 1466-1475. (* - *Co-first authors*)
- Namadurai S, Jain D, Kulkarni DS, **Tabib CR**, Friedhoff P, Rao DN, Nair DT (2010): The C-Terminal Domain of the MutL Homolog from *Neisseria gonorrhoeae* Forms an Inverted Homodimer; **PLoS ONE** 5(10): e13726.

Experimental skills

Molecular Biology Gene manipulation suited for cloning, over-expression, mutagenesis, and sequencing; PCR; analysis of DNA-protein and protein-protein interactions.
Biochemistry Recombinant protein expression and purification, flavin dependent protein chemistry, enzyme kinetics, HPLC, Isothermal titration calorimetry (ITC), Thermofluor, Dynamic light scattering (DLS), circular dichroism (CD), western blot and raising polyclonal antibodies in rabbit.
Microbiology Generation of knockouts in bacteria, preparation of chemical and electro competent cells and electroporation, cultivation using fermenters, microbial techniques and replica plating, blue-white screening, maintenance of subcultures, plaque assays and preparation of phage lysates.

Chaitanya Tabib, MSc || Graz University of Technology, Graz, Austria || chaitanya.tabib@student.tugraz.at || +43 6605118005

Computer skills	Microsoft Office, Windows and MAC OS X, working experience on bioinformatics tools and programs like PyMOL, Modeller, ClustalW, Procheck, ChemDraw, CorelDraw and Origin 7.0
Academic awards	"Award for Inventors: From Science to Innovation" achievement award by Graz University of Technology (11/ 2015) Qualified for Senior Research Fellow (SRF) post under CSIR, India (09/2010) Qualified in GATE (Graduate Aptitude Test in Engineering), India (02/2009)
Language skills	Mother tongue: Kannada English (proficient), Hindi and Marathi (fluent) German (beginner)
Membership	Society of Biological Chemists (SBC, India) – Lifetime member
Strength and skills	Good presentation and communication skills, a team player, perseverance in given task, good at literature survey, adaptability and presence of mind
Hobbies	Numismatics, philately, travelling, reading, listening to music, solving puzzles and playing games (strategic board games and cricket)

Scientific Presentations and Conferences

Oral:

- **14th DocDay:** NAWI Graz Doctoral School Molecular Biosciences and Biotechnology (07/2015)
- **Graduate Seminar:** DK Molecular Enzymology Doctoral program (05/2014 & 05/2015)

Poster:

- **8th OxiZymes:** meeting in Wageningen, The Netherlands (07/2016)
- **Gordon Research Seminar and Conference (GRS & GRC):** "Enzymes, Coenzymes & Metabolic Pathways" in Waterville Valley, NH 03215 United States (07/2015)
- **12th & 15th DocDay:** NAWI Graz Doctoral School Molecular Biosciences and Biotechnology (07/2014 & 02/2016)
- **18th International Society for Bioluminescence and Chemiluminescence Symposium: ISBC conference** in Uppsala, Sweden (06/2014)
- Enzyme mechanisms by biological systems: **EMBO conference** in Manchester, UK (06/2014)
- Mechanisms in Biology: **38th FEBS congress** in Saint Petersburg, Russia (07/2013)
- Enzymes and Signals: **Joint DK research summit**, Graz (12/2012)
- 79th annual meet of the **SBC** at Indian Institute of Science (IISc), Bangalore, India (12/2010)

References

- **Prof. Dr. Peter Macheroux**, peter.macheroux@tugraz.at, +43 316 8736450 (Head of the Institute, Institute of Biochemistry, Graz University of Technology, Austria)
- **Prof. Dr. Ellen Zechner**, ellen.zechner@uni-graz.at, +43 316 3805624 (Head of the DK Molecular Enzymology, Institute of Molecular Biosciences, Karl Franzens Universität Graz, Austria)
- **Prof. Desirazu N. Rao**, dnrao@biochem.iisc.ernet.in, +91 944 9566659 (Department of Biochemistry, Indian Institute of Science (IISc), Bangalore 560012, India)

Graz, Austria

Date:

Chaitanya R Tabib

Chaitanya Tabib, MSc || Graz University of Technology, Graz, Austria || chaitanya.tabib@student.tugraz.at || +43 6605118005